LA DISPARITÉ MORPHOLOGIQUE ET LA RADIATION ÉVOLUTIVE DES GNATHOSTOMES BASAUX

Thèse présentée

dans le cadre du programme de doctorat en biologie

en vue de l'obtention du grade de Philosophiæ doctor

PAR

© OLIVIA VANHAESEBROUCKE

Juin 2026

Composition du jury :

Céline Audet, présidente du jury, Université du Québec à Rimouski (ISMER)

Richard Cloutier, directeur de recherche, Université du Québec à Rimouski

David Deslauriers, examinateur interne, Université du Québec à Rimouski (ISMER)

Tetsuto Miyashita, examinateur externe, University of Ottawa, Musée canadien de la nature

Dépôt initial le 2 Avril 2026 Dépôt final le 16 Juin 2026

UNIVERSITÉ DU QUÉBEC À RIMOUSKI
Service de la bibliothèque

Avertissement

La diffusion de ce mémoire ou de cette thèse se fait dans le respect des droits de son auteur, qui a signé le formulaire « *Autorisation de reproduire et de diffuser un rapport, un mémoire ou une thèse* ». En signant ce formulaire, l'auteur concède à l'Université du Québec à Rimouski une licence non exclusive d'utilisation et de publication de la totalité ou d'une partie importante de son travail de recherche pour des fins pédagogiques et non commerciales. Plus précisément, l'auteur autorise l'Université du Québec à Rimouski à reproduire, diffuser, prêter, distribuer ou vendre des copies de son travail de recherche à des fins non commerciales sur quelque support que ce soit, y compris Internet. Cette licence et cette autorisation n'entraînent pas une renonciation de la part de l'auteur à ses droits moraux ni à ses droits de propriété intellectuelle. Sauf entente contraire, l'auteur conserve la liberté de diffuser et de commercialiser ou non ce travail dont il possède un exemplaire.

Deep roots are not reached by the frost – Les racines profondes ne sont pas atteintes par le gel.

J.R.R. Tolkien, The Fellowship of the Ring

Knowledge is the wing wherewith we fly to heaven – La connaissance est l'aile qui nous permet de voler jusqu'au ciel.

W. Shakespeare, Henry VI

To know that we know what we know, and to know that we do not know what we do not know, that is true knowledge – Savoir ce que l'on sait et savoir ce que l'on ne sait pas : voilà le vrai savoir.

Confucius, Analectes

Avant de commencer cette thèse, je souhaite reconnaître la diversité des peuples autochtones à travers le monde, sur les territoires traditionnels desquels provient une partie du matériel qui a servi dans ce projet de recherche. Je tiens tout particulièrement à souligner la diversité des peuples autochtones sur le territoire que nous appelons aujourd'hui le Canada et à reconnaître les contributions essentielles de ces peuples dans chaque région où nous vivons, travaillons et étudions. Il est important de poursuivre nos efforts vers une réconciliation véritable et de continuer à approfondir notre compréhension de ces enjeux.

L'Université du Québec à Rimouski se situe à la jonction des territoires traditionnels non cédés de plusieurs Premières Nations. Je souhaite remercier tout particulièrement la Nation Wolastoqiyik Wahsipekuk, qui occupait ce territoire avant le contact et dont la communauté de Cacouna est la plus proche de Rimouski. Je suis reconnaissante d'avoir eu l'occasion d'étudier et de mener mes recherches sur ces terres. Je souhaite également reconnaître la Nation mi'kmaq, sur le territoire de laquelle se trouve Miguasha, situé dans le septième district, Gespegewa'gi, du Mi'gma'gi, au bord du Mawipoqtapei, connu sous le nom de baie des Chaleurs, où j'ai eu à plusieurs reprises l'occasion de me rendre dans le cadre de mon doctorat.

Cette thèse est le résultat de plusieurs années dédiées à une passion pour la science. J'aimerais prendre un moment pour reconnaître non seulement les terres sur lesquelles nous nous trouvons, mais aussi l'importante contribution des savoirs autochtones à notre compréhension du monde naturel.

Reconnaître les territoires traditionnels sur lesquels nous vivons et travaillons n'est qu'un début. C'est un petit, mais important, pas qui nous rappelle l'importance d'en apprendre davantage sur les peuples autochtones de ces régions. Considérer et reconnaître leur histoire, leur culture, leurs savoirs et leur souveraineté nous rappelle que nous pouvons tous contribuer au processus de réconciliation.

REMERCIEMENTS

Je tiens à remercier l'Université du Québec à Rimouski, dont les murs ont été ma maison pour les dix dernières années, de m'avoir offert un environnement de travail stimulant qui m'a permis de m'épanouir en tant que personne et en tant que chercheuse. Je remercie les membres du SAPS notamment Émilie et Martin pour leur bonne humeur et leur énergie débordante lors des cours de groupe, qui ont grandement participé à maintenir ma santé mentale tout au long du doctorat. Je remercie également les Fonds de Recherche du Québec pour le soutien financier accordé à mon projet, sans lequel cette recherche n'aurait pas été possible, ainsi que mon comité d'évaluation, la Prof. Céline Audet et le Prof. David Deslauriers, et plus particulièrement le Prof. Tetsuto Miyashita qui m'a conseillé tout au long de ce doctorat. Je tiens finalement à remercier chaleureusement Richard Cloutier, qui m'a ouvert les portes de son laboratoire dès mon baccalauréat et qui m'a transmis sa passion pour la paléontologie, les poissons, l'enseignement et la science en général. J'ai beaucoup appris à tes côtés, Richard, et je te suis profondément reconnaissante pour tout ce temps passé avec toi.

Bien que mon nom figure sur la première page de cette thèse, ce projet représente plus que mon seul travail. Il représente le soutien inconditionnel que mon entourage m'a apporté. Tout d'abord, Olivier Larouche, qui m'a ramassée à la petite cuillère bien des fois et sans qui je ne serais jamais allée au bout. Tu as toujours été là pour moi et je ne pourrais jamais assez te remercier de ce que tu m'as apporté par ta gentillesse, ton écoute et ta bienveillance. Merci à toutes les personnes du laboratoire, qui ont fait de cet endroit un cocon toujours chaleureux, empreint de rires et de moments partagés. Vous êtes bien plus que des collègues de travail, vous êtes des amis ! Merci à mes amis – que dis-je, ma famille du Québec – Guillaume, Fred, Juliette, Philippe, Manue, Pauline, Félicia, Alice, Chio, Laurianne, Richard, Laurent, Marie, Valentine, de m'avoir accompagnée et soutenue à travers toutes ces années. Je n'oublierai jamais les instants que nous avons partagés, les éclats de rire comme les petites larmes, et surtout votre amitié précieuse qui m'a tant portée. Enfin, merci à toute ma famille, mamie, papy, et en particulier Thomas, d'avoir traversé avec moi les moments les plus stressants de

cette aventure et de m'avoir soutenue sans faille. Je n'ai pas toujours été facile, et pourtant, tu as été un pilier constant, et pour cela je t'en suis profondément reconnaissante.

Pour finir, je souhaite vous remercier, vous, papou, mamounette et gugule, vous avez été mon roc depuis toujours. La vie n'a pas toujours été facile et vous avez toujours été là pour me relever. Vous avez cru en la petite fille qui voulait étudier au Québec et même si je sais que ça a été dur pour vous, vous m'avez laissée partir à l'autre bout de la planète pour réaliser mon rêve. Même si un océan nous a séparés pendant les dernières années, notre petite famille est restée toujours aussi soudée et unie. Je ne pourrais jamais assez vous remercier d'être là. Je vous aime.

RÉSUMÉ

L'histoire des vertébrés a été marquée par d'importantes innovations ayant joué un rôle central dans le succès évolutif de ce clade, telles que l'apparition de l'os endochondral ou de l'œuf amniotique. L'origine de la mâchoire constitue un tournant majeur de l'histoire évolutive des vertébrés. Les vertébrés à mâchoires, appelés gnathostomes, représentent aujourd'hui 99 % des vertébrés actuels. Ils seraient apparus durant l'Ordovicien moyen (470 – 458,4 Ma) avant de connaitre d'importantes périodes de diversification durant le Dévonien (419,2 – 358,9 Ma) et le Carbonifère (358,9 – 298,9 Ma) alors que l'environnement aquatique connaît des changements biogéochimiques majeurs impactant fortement la structure de ces écosystèmes. Cette période de transition entre le Dévonien et le Carbonifère constitue une des cinq extinctions massives de l'histoire de la Terre. De tels changements environnementaux ont participé à l'apparition de clades incroyablement diversifiés aujourd'hui tels que les téléostéens (~ 30 000 espèces), les lézards (~ 10 000 espèces) et les oiseaux (~ 11 000 espèces). Lors de ces événements évolutifs, appelés « radiations évolutives », une augmentation rapide du taux de spéciation est associée à une augmentation de la disparité morphologique et écologique des espèces. Bien que la diversification des premiers vertébrés à mâchoires et leur succès évolutif aient été l'objet de nombreuses études, les radiations évolutives potentielles à leur origine n'ont jamais été proprement investiguées. Cette thèse propose donc une approche intégrative alliant une étude approfondie de la disparité morphologique, de la diversification écologique, ainsi que de mécanismes évolutifs sous-jacents, notamment la modularité, afin de caractériser les grandes étapes de diversification des lignées de gnathostomes basaux durant le Dévonien et le Carbonifère.

Nous avons commencé par documenter les variations de la disparité morphologique des ostéichthyens basaux au cours du temps dont les deux lignées principales (les actinoptérygiens et les sarcoptérygiens) ont connu des trajectoires évolutives opposées lors de la crise de la fin du Dévonien. Les sarcoptérygiens présentaient une première augmentation de leur disparité morphologique au Dévonien moyen, accompagnant leur diversification taxonomique, suivie d'un important déclin lors de la crise. Leur récupération durant le Carbonifère inférieur (Mississippien) serait liée à la diversification de lignées survivantes, notamment des cœlacanthes, associées à la réémergence des récifs coraliens. Chez les actinoptérygiens, la disparité crânienne augmente progressivement à la fin du Dévonien et se maintient malgré la crise, avant de connaitre un premier maximum lors du Carbonifère inférieur. Cette augmentation de la disparité morphologique du crâne accompagne leur première grande diversification taxonomique et précède leur diversification morphologique postcrânienne. Cette dynamique suggère une radiation adaptative trophique, marquée par l'apparition de nouveaux morphotypes et de stratégies d'alimentation variées.

Nous avons ensuite investigué les patrons d'intégration morphologique et de modularité crânienne chez les actinoptérygiens basaux afin de tester l'existence de plusieurs modules morpho-fonctionnels, et d'évaluer le rôle possible de ces processus dans la diversification du groupe. Cette analyse a permis de supporter la radiation adaptative trophique proposée en suggérant une organisation modulaire du crâne et notamment la présence d'un module mâchoire. Bien que le crâne apparaisse globalement intégré, la quasi-indépendance de cette région pourrait expliquer sa grande variation morphologique. La modularité de la mâchoire aurait ainsi facilité l'exploration de nouvelles niches écologiques tout en maintenant une fonctionnalité globale efficace.

Enfin, nous avons exploré les changements de la répartition écologique des gnathostomes basaux dans différents habitats aquatiques au cours du temps. Nous avons observé une distribution hétérogène dans l'espace fonctionnel des différents groupes et un important chevauchement de l'assemblage de « placodermes » du Dévonien et des chondrichthyens du Carbonifère. Cela pourrait refléter un remplacement écologique des espèces éteintes lors des crises de la fin du Dévonien par les lignées survivantes, dont le comportement écologique opportuniste aurait grandement participé à leur rapide diversification.

Cette étude aura participé à la caractérisation d'un moment clé de l'histoire des vertébrés, à savoir l'apparition de la mâchoire. La radiation évolutive putative associée à cet événement reçoit ici un important soutien en venant confirmer l'existence de radiations à l'origine de la diversification des différents groupes de gnathostomes. Nous avons détecté des patrons d'augmentation de la diversité taxonomique associée à des augmentations de la disparité morphologique et écologique chez les actinoptérygiens, les sarcoptérygiens et les chondrichthyens, constituant le patron caractéristique d'une radiation.

Mots-clés : Morphométrie géométrique ; Poissons paléozoïques ; Radiation adaptative ; Extinction massive; Disparité fonctionnelle ; Modularité variationnelle ; Macroévolution ; Écomorphologie ; Paléoenvironnement

ABSTRACT

The history of vertebrates has been marked by major innovations that each played a central role in the evolutionary success of this clade, such as the emergence of endochondral bone and the amniotic egg. The origin of jaws represents a major turning point in vertebrate evolutionary history. Jawed vertebrates, known as "gnathostomes," now account for 99% of extant vertebrates. They are thought to have appeared during the Middle Ordovician (470 – 458.4 Ma), before undergoing major diversification phases during the Devonian (419.2 – 358.9 Ma) and Carboniferous (358.9 – 298.9 Ma), at a time when aquatic environments experienced significant biogeochemical changes that profoundly affected ecosystem structure. The transition between the Devonian and Carboniferous corresponds to one of the five mass extinctions in Earth's history. Environmental changes of such extent contributed to the emergence of highly diverse extant clades, such as teleosts (~30,000 species), lizards (~10,000 species), and birds (~11,000 species). During these evolutionary events, known as "evolutionary radiations," a rapid increase in speciation rates is associated with increased morphological and ecological disparities. Although the diversification of early jawed vertebrates and their evolutionary success have been widely studied, putative evolutionary radiations at their origin have never been properly investigated. Therefore, this thesis proposes an integrative approach combining a study of morphological disparity, ecological diversification, and underlying evolutionary mechanisms – especially modularity – to characterize the major stages of diversification in early gnathostome lineages during the Devonian and the Carboniferous.

I first documented temporal variations in the morphological disparity of osteichthyans, whose two main lineages followed different evolutionary trajectories during the end-Devonian crises. Sarcopterygians exhibited an initial increase in morphological disparity during the Middle Devonian, accompanying their taxonomic diversification, followed by a marked decline during the crisis. Their recovery in the Carboniferous appears to be linked to the diversification of surviving lineages, especially coelacanths, in association with the re-emergence of reef ecosystems. In actinopterygians, cranial disparity gradually increased toward the end of the Devonian and was maintained despite the crisis, before reaching a first maximum in the Early Carboniferous. This increase in cranial morphological disparity coincided with their first major taxonomic diversification and preceded their postcranial morphological diversification. This pattern suggests a trophic adaptive radiation, marked by the emergence of new morphotypes and diverse feeding strategies.

I then investigated patterns of morphological integration and cranial modularity in early actinopterygians to test the existence of morpho-functional modules and to assess the potential role of these processes in the group diversification. This analysis supports the proposed trophic adaptive radiation by indicating a modular organization of the skull, particularly the presence of a jaw module. Although the skull appears globally integrated, the quasi-independence of this region may explain its high morphological variation. Jaw

modularity may thus have facilitated the exploration of new ecological niches while maintaining overall functional efficiency.

Finally, I explored changes in the ecological distribution of early gnathostomes across different aquatic habitats through time. I observed a heterogeneous distribution of groups within functional space and a substantial overlap between Devonian "placoderm" assemblages and Carboniferous chondrichthyans. This may reflect an ecological replacement of species lost during the end-Devonian crisis by surviving lineages, whose rapid diversification may have been facilitated by opportunistic ecological behaviour.

This study overall contributes to characterising a key moment in vertebrate history – the emergence of jaws. The putative evolutionary radiation associated with this event is strongly supported here, confirming radiations at the origin of the different groups of gnathostome diversification. I identified patterns of increasing taxonomic diversity associated with rising morphological and ecological disparity in actinopterygians, sarcopterygians, and chondrichthyans, consistent with the characteristic patterns of evolutionary radiations.

Keywords: Geometric morphometrics; Paleozoic fish; Adaptive radiation; Mass extinction; Functional disparity; Variational modularity; Macroevolution; Ecomorphology; Paleoenvironment

TABLE DES MATIÈRES

REMERCIEMENTS X

RÉSUMÉ XIII

ABSTRACT XV

TABLE DES MATIÈRES XXV

LISTES DES FIGURES XXX

INTRODUCTION GÉNÉRALE 1

1. LES RADIATIONS ÉVOLUTIVES : RADIATION ADAPTATIVE OU NON-ADAPTATIVE, LÀ EST LA QUESTION 2
2. LA DISPARITÉ MORPHOLOGIQUE ET LA DIVERSITÉ TAXONOMIQUE : COMMENT LEURS PATRONS PEUVENT ÊTRE RÉVÉLATEURS DE TRAJECTOIRES ÉVOLUTIVES ? 7
3. LA MODULARITÉ : UN POTENTIEL MOTEUR BIOLOGIQUE À L'ÉVOLUTION 10
4. LES GNATHOSTOMES BASAUX : UNE BRÈVE HISTOIRE DE LEUR ÉVOLUTION 13
    - 4.1. Les "placodermes" : les poissons cuirassés du passé 14
    - 4.2. Les "acanthodiens" : les poissons armés d'épines 16
    - 4.3. Les chondrichthyens : les poissons au squelette de cartilage 17
    - 4.4. Les ostéichthyens : les poissons tout en os 18
5. LA TRANSITION SILURIEN-DÉVONIEN-CARBONIFÈRE : LES MONTAGNES RUSSES ÉCOLOGIQUES 20
6. LE REGISTRE FOSSILE : LA VÉRITABLE MACHINE À REMONTER LE TEMPS 25
7. OBJECTIFS SPÉCIFIQUES ET ORGANISATION DE LA THÈSE 26

CHAPITRE 1 LA DISPARITÉ MORPHOLOGIQUE ET LA RADIATION ÉVOLUTIVE DES ACTINOPTÉRYGIENS BASAUX AU TRAVERS DE LA CRISE DU DÉVONIEN-CARBONIFÈRE 31

1.1 RÉSUMÉ EN FRANÇAIS DU PREMIER ARTICLE 31

1.2 MORPHOLOGICAL DISPARITY AND EVOLUTIONARY RADIATION OF EARLY ACTINOPTERYGIANS THROUGH THE DEVONIAN-CARBONIFEROUS CRISIS 33
ABSTRACT 33
1. INTRODUCTION 34
2. MATERIAL AND METHODS
2.1. Taxonomic Diversity 36
2.2. Morphological and Palaeogeographical Dataset 36
2.3. Landmarking Scheme 37
2.4. Morphological Disparity Analyses 39
3. RESULTS 40
3.1. Body Shape Disparity 40
3.2. Cranial Shape Disparity 43
3.3. Early Actinopterygian Taxonomic Diversity and Morphological Disparity Variation Through Time 45
3.4. Palaeogeographical Distribution of Early Actinopterygians 46
4. DISCUSSION 47
4.1. Body Shape Disparity Explained by Locomotory Properties and Ecological Opportunities 48
4.2. Skull Shape Disparity Explained by Feeding Strategies and Ecological Opportunities 49
4.3. Is There an Early Adaptive Radiation of Actinopterygians? 50
5. CONCLUSION 52
6. REFERENCES 53

CHAPITRE 2 LA DISPARITÉ MORPHOLOGIQUE DES SARCOPTÉRYGIENS BASAUX AU TRAVERS DE LA CRISE DU DÉVONIEN-CARBONIFÈRE 63
2.1 RÉSUMÉ EN FRANÇAIS DU DEUXIÈME ARTICLE 63
2.2 EARLY SARCOPTERYGIAN MORPHOLOGICAL DISPARITY THROUGH THE DEVONIAN-CARBONIFEROUS CRISIS 65
ABSTRACT 65

1. INTRODUCTION 66
2. METHODS 67
2.1. Taxonomic Diversity 67
2.2. Morphological Dataset 67
2.3. Landmarking Scheme 70
2.4. Morphological Disparity Analyses 71
2.5. Lagerstätte Effect 72
3. RESULTS 73
3.1. Body Shape Disparity 73
3.2. Cheek Disparity 75
3.3. Skull Roof Disparity 79
3.4. Early Sarcopterygian Diversity and Morphological Disparity Variation Through Time 80
3.5. Lagerstätte Effect 81
4. DISCUSSION 81
4.1. Devonian Environmental Changes Influenced the Early Diversification of Sarcopterygians 82
4.2. The Aquatic Habitats Influenced Cheek Disparity 83
4.3. Shared Ancestry Influenced Skull Roof Disparity 85
4.4. Post-Crisis Ecological Opportunities Influenced Body Shape Disparity 86
5. CONCLUSION 88
6. REFERENCES 89

CHAPITRE 3 MODULARITÉ VARIATIONNELLE DES ACTINOPTÉRYGIENS BASAUX : LES UNITÉS STRUCTURALES DU CRÂNE DES POISSONS DU PALÉOZOÏQUE 97
3.1 RÉSUMÉ EN FRANÇAIS DU DEUXIÈME ARTICLE 97
3.2 VARIATIONAL MODULARITY OF EARLY ACTINOPTERYGIANS: THE BUILDING BLOCKS OF PALEOZOIC FISH HEAD 99
ABSTRACT 99

1. INTRODUCTION 100
2. MATERIAL AND METHODS 102
2.1. Taxonomic Diversity 102
2.2. Morphological Dataset 103
2.3. Landmarking Scheme 105
2.4. Modular *a priori* hypotheses 106
2.5. Morphological Integration and Modularity Tests 106
3. RESULTS 108
4. DISCUSSION 110
4.1. The Actinopterygian Skull: A Modular Organisation as Driver for Morphological Disparity 110
4.2. Disparity in Modularity Analyses and Future Investigations 112
5. CONCLUSION 113
6. REFERENCES 114

CHAPITRE 4 L'ÉCOMORPHOLOGIE DES GNATHOSTOMES DU SILURIEN AU CARBONIFÈRE ET LA DYNAMIQUE D'ÉCOMORPHOESPACES PARTAGÉS ET INNOVANTS 121
4.1 RESUME EN FRANÇAIS DU DEUXIEME ARTICLE 121
4.2 ECOMORPHOLOGY OF JAWED VERTEBRATES DURING THE SILURIAN-CARBONIFEROUS AND THE DYNAMICS OF SHARED AND INNOVATIVE ECOMORPHOSPACES 123
ABSTRACT 124
1. INTRODUCTION
2. MATERIAL AND METHODS 126
2.1.Taxonomic Diversity 126
2.2. Morphological Dataset 128
2.3. Data Transformations 128
2.4. Non-Multidimensional Scaling 129
2.5. Trait-Spaces 130

3. RESULTS 131
3.1. Early Jawed Vertebrate Taxonomic Diversity 131
3.2. Ecomorphospaces: Patterns of Habitat Occupation 132
3.3. Functional Diversity of Early Jawed Vertebrates 133
4. DISCUSSION 136
4.1. “Placoderms” and the Loss of Devonian Functional Richness 139
4.2. Chondrichthyans: from Generalists to Specialists 139
4.3. Actinopterygians: Taxonomic Diversification with Functional Redundancy 140
4.4. Sarcopterygians: Between Generalists and Extreme Specialists 141
4.5. The Devonian-Carboniferous Functional Turnover 141
4.6. Ecological Reorganisation and Faunal Replacement 142
4.7. Limitations and Future Investigation 142
5. CONCLUSION 143
6. REFERENCES 145

CONCLUSION GÉNÉRALE 153
LA DISPARITÉ MORPHOLOGIQUE ET LA RADIATION ÉVOLUTIVE DES GNATHOSTOMES BASAUX 153
PORTÉE DE L’ÉTUDE, LIMITES ET PERSPECTIVES 159

ANNEXE I : CHARTE CHRONOSTRATIGRAPHIQUE INTERNATIONALE (DEPUIS INTERNATIONAL COMMISSION ON STRATIGRAPHY) 165
ANNEXE II : SUPPLEMENTARY INFORMATION FOR CHAPTER I 166
ANNEXE III : SUPPLEMENTARY INFORMATION FOR CHAPTER II 207
ANNEXE IV : SUPPLEMENTARY INFORMATION FOR CHAPTER III 239
ANNEXE V : SUPPLEMENTARY INFORMATION FOR CHAPTER IV 259
RÉFÉRENCES BIBLIOGRAPHIQUES 287

LISTE DES FIGURES

Figure 1. Représentation des deux principaux types de radiation évolutive. 5

Figure 2. Représentation des différents descripteurs morphologiques utilisés dans l'étude de la disparité morphologique. 8

Figure 3. Représentation schématique de la modularité. 11

Figure 4. Phylogénie simplifiée des gnathostomes basaux. Issue de la figure 3 de Brazeau et Friedman (2015). 14

Figure 5. Boucliers céphalique et thoracique du "placoderme" *Bothriolepis canadensis* Whiteaves (Devonien Supérieur). Credit photo: Fossiilid.info 15

Figure 6. "Acanthodien" *Ptomacanthus anglicus* Miles (Dévonien Inférieur). Issue de la figure 2 dans Brazeau 2012. 16

Figure 7.Chondrichthyen *Phoebodus saidselachus* Frey et al. (Dévonien Supérieur). Issue de la figure 1 dans Frey et al. 2019. 18

Figure 8. Larve du cœlacanthe (Ostéichthyens, sarcoptérygien) *Rhabdoderma exiguum* Eastman (Carbonifère Supérieur). Crédit photo : Marie Boirot et Olivia Vanhaesebroucke 19

Figure 9. Diversité des grands groupes de gnathostomes à la fin du Dévonien et au début du Carbonifère. Adaptée de Sallan et Coates 2010. 22

Figure 10. Variation de l'abondance des récifs et de leur composition durant le Dévonien Supérieur et le Mississippien. Adaptée de Yao et al. 2020. 24

INTRODUCTION GÉNÉRALE

L'histoire des vertébrés a été marquée par d'importantes innovations, ayant joué un rôle central dans le succès évolutif de ce clade, telles que l'apparition de l'os endochondral (Brazeau et al. 2020) ou encore de l'œuf amniotique (Starck et al. 2021). L'origine de la mâchoire constitue, elle aussi, un tournant majeur de l'histoire évolutive des vertébrés. Aujourd'hui, les vertébrés à mâchoires, appelés aussi « gnathostomes », représentent 99 % des vertébrés vivants. Ils seraient apparus durant l'Ordovicien moyen (470 – 458,4 Ma) (Johanson et al. 2019; Sansom et al. 2012) et se sont diversifiés durant le Dévonien (419,2 – 358,9 Ma) et le Carbonifère (358,9 – 298,9 Ma) (Annexe I) (Coates 2009; M. Zhu et al. 2009) occupant alors une grande diversité d'habitats (Frey et al. 2019; Sallan et Friedman 2012; Young 2010). Au même moment, l'environnement aquatique connaît des changements biogéochimiques majeurs (*p. ex.* apparition des premières forêts, refroidissement global, crise de la biodiversité) qui entraînent un bouleversement de la structure de ces écosystèmes (Aretz et al. 2021; Bridge et al. 2022; Carmichael et al. 2019; Kaiser et al. 2016). Le milieu du Paléozoïque constitue ainsi une ère cruciale dans l'histoire des vertébrés.

La diversification des premiers vertébrés à mâchoires et leur succès évolutif subséquent ont été l'objet de nombreuses études. Ils ont été associés à des changements climatiques (Qu et al. 2010), des changements écologiques (Klug et al. 2010) et même à des innovations clés telles que l'apparition de la mâchoire (Brazeau et Friedman 2015) ou encore l'apparition de la ceinture pelvienne (Zhu et al. 2012). Toutefois, une question demeure : peut-on vraiment qualifier cette diversification de "radiation évolutive" ?

1. Les radiations évolutives : Radiation adaptative ou non-adaptative, là est la question.

Les radiations évolutives sont un des processus évolutifs les plus fascinants. Elles sont caractérisées par une augmentation rapide du taux de diversification (*c.-à-d.* la différence entre le taux de spéciation et le taux d'extinction des espèces) et une augmentation de la disparité morphologique et de la diversité écologique des espèces (Simpson 1953).

Au cours des dernières décennies, les radiations évolutives étaient souvent appelées « radiations adaptatives » (Simpson 1953; Schluter 2000) et depuis la publication de l'Origine des espèces (On the origin of species) de Charles Darwin en 1859, de multiples définitions de ce terme ont été proposées. Schluter (2000) définit une radiation adaptative comme « l'évolution de la diversité écologique et phénotypique au sein d'une lignée qui se multiplie rapidement », Losos et Mahler (2010) mentionnent que « le terme radiation adaptative devrait être réservé aux clades montrant une disparité écologique et phénotypique exceptionnelle », enfin, Matsubayashi et Yamaguchi (2022) propose qu'une « radiation adaptative est reconnue comme un type spécifique de radiation pour lequel l'étendue de la différenciation phénotypique se produit au sein d'un groupe phylogénétique en lien avec l'utilisation de différentes ressources écologiques ». Toutes ces définitions ont néanmoins deux éléments principaux en commun – la notion de spéciation rapide d'un clade et la disparité phénotypique associée à une diversité écologique. Ces deux éléments sont en effet des pièces centrales de toute étude portant sur des radiations évolutives (Pinto et al. 2008; Grant et Grant 2020). Schluter (2000) propose la présence de quatre éléments pour tester la radiation adaptative d'un clade : (1) un ancêtre commun récent, (2) une corrélation entre le phénotype et l'environnement, (3) une utilité de trait (*c.-à-d.* un trait physiologique ou morphologique qui permet à un individu d'être bien adapté à son environnement), et (4) une spéciation rapide.

Mais qu'en est-il des radiations qui ne résultent pas d'une divergence écologique ? Bien que les radiations évolutives soient généralement caractérisées par une augmentation rapide

du taux de diversification et par une augmentation de la disparité morphologique et écologique (Simpson 1953), les facteurs à l'origine de ces événements sont multiples et diffèrent selon les clades (McMillan et Palumbi 1995; Harmon et al. 2003; Gavrilets et Losos 2009; Monteiro et Nogueira 2011). Il a notamment été observé de nombreuses fois que la divergence écologique n'est pas toujours le facteur déclenchant principal d'une spéciation et d'une radiation (Schluter 2000; Lieberman 2012; Soulebeau et al. 2015). De plus, le rôle des facteurs abiotiques dans les radiations est de plus en plus remarqué (Schluter 2000; Lieberman 2012; Soulebeau et al. 2015; Simões et al. 2016). Simões et collaborateurs (2016) proposent alors quatre types différents de radiations évolutives définis selon la nature des facteurs qui en sont à l'origine. (1) Les radiations climatiques sont induites par un changement de climat dans une région suivi d'une spéciation allopatrique (Maguire et Stigall 2008), (2) les radiations géographiques suivent une augmentation des opportunités de spéciation allopatrique dans une région (Near et Benard 2004), (3) les radiations exaptatives induites par la co-option d'un trait (*c.-à-d.* un trait existant qui acquiert une nouvelle fonction) (Armbruster 1997) et (4) les radiations adaptatives causées par des facteurs d'origine biotique tels qu'une innovation clé ou un nouveau comportement, et souvent accompagnées d'une divergence éco-morphologique (Mahler et al. 2013; Marques et al. 2018; Meyer et al. 2019). Il est toutefois souvent difficile de déterminer les facteurs à l'origine de la radiation d'un clade. En effet, il est rare qu'un seul et unique type de facteur soit la cause d'une radiation ; c'est le plus souvent une combinaison de plusieurs facteurs (Schluter 2000; Czekanski-Moir et Rundell 2019). Les chercheurs en biologie évolutive ont ainsi proposé de classer les radiations en deux grandes catégories plus générales, les radiations adaptatives et les radiations non-adaptatives (Figure 1) (Matsubayashi et Yamaguchi 2022).

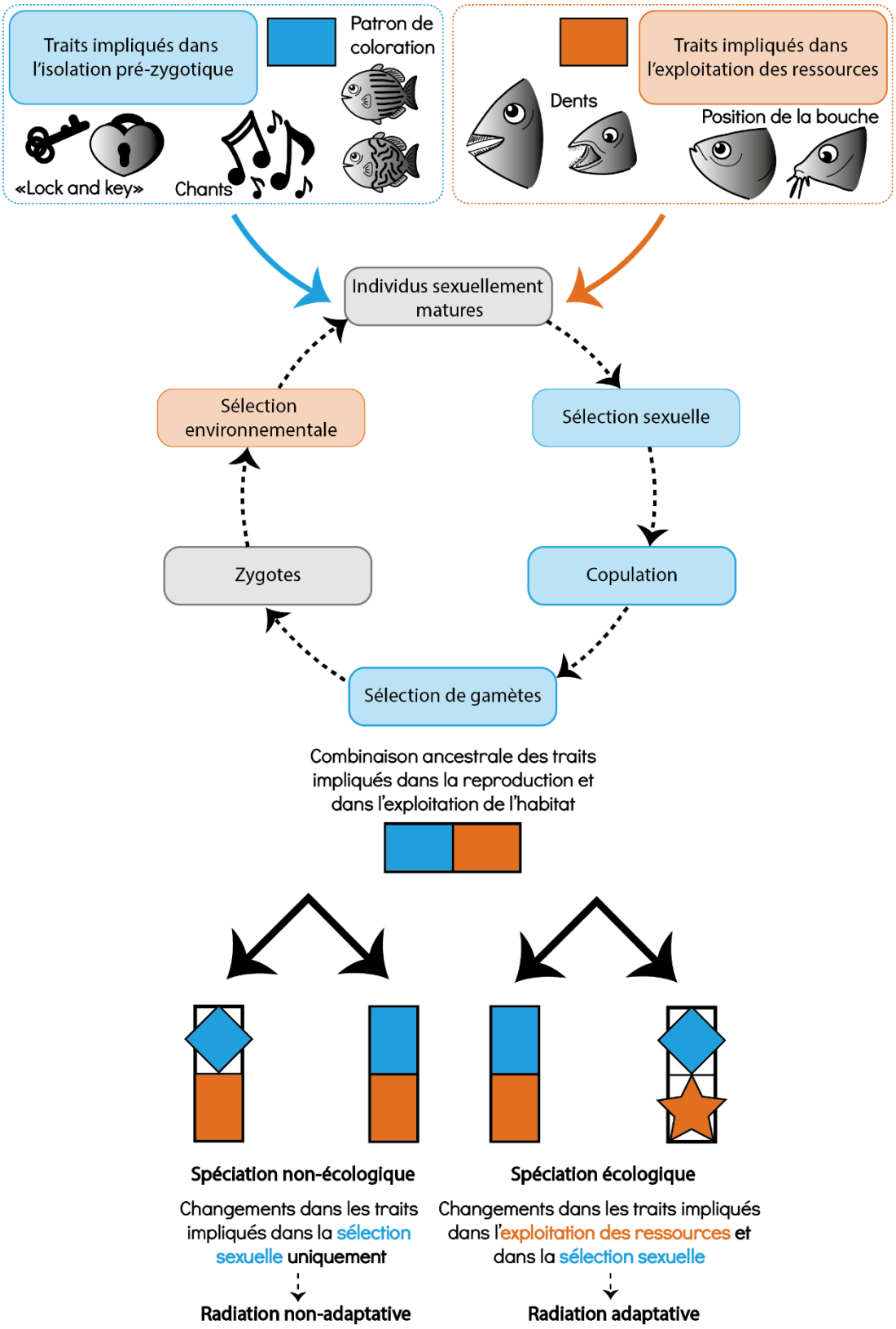

Traits impliqués dans l'isolation pré-zygotique
Patron de coloration
«Lock and key»
Chants
Traits impliqués dans l'exploitation des ressources
Dents
Position de la bouche
Individus sexuellement matures
Sélection environnementale
Sélection sexuelle
Zygotes
Copulation
Sélection de gamètes
Combinaison ancestrale des traits impliqués dans la reproduction et dans l'exploitation de l'habitat
Spéciation non-écologique
Changements dans les traits impliqués dans la sélection sexuelle uniquement
Radiation non-adaptative
Spéciation écologique
Changements dans les traits impliqués dans l'exploitation des ressources et dans la sélection sexuelle
Radiation adaptative

Figure 1. Représentation des deux principaux types de radiation évolutive. La radiation adaptative provient d'une diversification spécifique issue d'une spéciation écologique opérant sur un changement de traits impliqués dans l'exploitation des ressources (orange) et de traits impliqués dans la sélection sexuelle (bleu). La radiation non-adaptative, quant à elle, provient d'une spéciation opérant sur un changement de traits uniquement impliqués dans la sélection sexuelle. Basée sur la figure 1 dans Czekanski-Moir et Rundell (2019).

Tel que mentionné précédemment, une radiation adaptative est caractérisée par la diversification phénotypique d'un clade en lien avec l'utilisation de ressources écologiques variées (Matsubayashi et Yamaguchi 2022). Une telle diversification phénotypique correspond à ce que Losos et Mahler (2010) appellent la « disparité adaptative ». Elle est au centre de la définition d'une radiation adaptative, toutefois elle n'est pas le seul patron observable dans une radiation adaptative. En effet, cette variation de trait en réponse à une opportunité écologique (*c.-à-d.* un relâchement de la sélection agissant sur certains traits d'importance écologique (Yoder et al. 2010)), n'est pas le seul patron représentant la relation entre une radiation et des facteurs écologiques (Yoder et al. 2010). En effet, Gavrilets et Losos (2009) proposent dix patrons de propriétés temporelles, spatiales, génétiques et morphologiques pour les radiations adaptatives. Pour ne nommer que quelques exemples, le « dépassement » (*overshooting* en anglais) représente l'augmentation de la diversité spécifique suivie d'un déclin qui finit par atteindre un plateau. Un tel patron peut résulter d'une diminution du taux de spéciation et/ou d'une augmentation du taux d'extinction. L'« effet de région » (*area effect* en anglais) propose que les régions géographiques plus étendues offrent davantage de facteurs écologiques pouvant entraîner la spéciation. Une étendue plus large représenterait en effet de plus grandes possibilités d'avoir des espaces hétérogènes et ainsi des niches écologiques variées, mais pourrait aussi soutenir des populations plus larges, ce qui induirait davantage de mutations. Ainsi, une plus grande région représenterait de plus grandes opportunités d'avoir des événements de spéciation allopatrique et parapatrique. Enfin, l'« effet du nombre de *loci* » mentionne qu'un nombre plus faible de *loci* induirait un effet de sélection plus fort sur chaque *locus*. Chaque *locus*

contribuerait à plus de traits, ainsi les changements génétiques nécessaires à la divergence seraient plus faibles (Gavrilets et Losos 2009).

Au contraire, une radiation non-adaptative est caractérisée par la diversification d'une lignée avec une divergence écologique minimale ou secondaire (Rundell et Price 2009; Matsubayashi et Yamaguchi 2022). L'isolation reproductive ne résulte pas d'une sélection naturelle divergente (Matsubayashi et Yamaguchi 2022). Des populations isolées reproductivement peuvent exposer différents phénotypes qui ne représentent pas des adaptations à l'utilisation de différentes ressources (Rundell 2011). Cette caractéristique est une des raisons pour lesquelles les radiations non-adaptatives sont souvent associées à de la redondance fonctionnelle dans les écosystèmes, ce qui peut en influencer la résilience (Czekanski-Moir et Rundell 2019). Un facteur potentiel déclenchant ce genre de radiation pourrait être une divergence de sélection sexuelle basée sur des caractères sexuels qui ne sont pas en lien direct avec l'utilisation de ressources (Wellenreuther et Sánchez-Guillén 2016; Matsubayashi et Yamaguchi 2022). Un bon exemple d'isolation reproductive non-associée à une sélection divergente de niches est la spéciation des Demoiselles induite par la divergence de coloration et de comportements qui entraîne un isolement précopulatoire (Wellenreuther et Sánchez-Guillén 2016). Un tel phénomène peut conduire à ce que Czekanski-Moir et Rundell (2019) définissent comme le « conservatisme de niche ». La similarité écologique entre des espèces proches parentes est alors plus élevée que ce qui pourrait être attendu en se basant uniquement sur leurs relations phylogénétiques. Un tel patron n'est pas retrouvé dans le cas d'une radiation adaptative. En résumé, la nature de la spéciation et plus précisément la nature du facteur qui mène à la spéciation détermine le type de radiation qui peut en résulter.

Afin de caractériser une radiation évolutive et de savoir quels facteurs pourraient en être à l'origine, plusieurs paramètres peuvent être utilisés, les plus communs étant la dynamique évolutive de la diversité taxonomique et de la disparité morphologique (Simões et al. 2016). Ces deux paramètres apportent des informations complémentaires sur ce type d'événements évolutifs. Ils peuvent varier conjointement ou au contraire être indépendants l'un de l'autre, c'est pourquoi Foote (1993) propose trois modèles d'évolution d'un clade en

se basant sur cette relation. Tout d'abord, dans le modèle d'évolution *avec des contraintes morphologiques* l'augmentation de la diversité taxonomique n'est pas suivie d'une augmentation de la disparité morphologique. Les morphologies restent alors similaires et les formes extrêmes ne sont pas exprimées. Le modèle d'évolution *sans contrainte morphologique* décrit une augmentation de la diversité taxonomique et de la disparité morphologique. Enfin, dans le modèle d'évolution *favorisant les extrêmes morphologiques,* la disparité morphologique augmente avec un taux de diversification taxonomique plus faible. Ainsi, les variations au cours du temps de la diversité taxonomique et de la disparité morphologique ne sont pas toujours synchronisées et apportent des informations cruciales sur la direction évolutive des clades et des contraintes associées. Déterminer les patrons de variation au cours du temps de la disparité morphologique et les facteurs qui peuvent les influencer deviennent des éléments centraux afin de caractériser les radiations évolutives.

2. LA DISPARITÉ MORPHOLOGIQUE ET LA DIVERSITÉ TAXONOMIQUE : COMMENT DES PATRONS PEUVENT ÊTRE RÉVÉLATEURS DE TRAJECTOIRES ÉVOLUTIVES ?

La disparité morphologique quantifie les variations de forme et de taille entre des individus ou des taxons à une échelle macro-évolutive (Foote 1993, 1997; Gould 1991). Bien qu'elle ne considère pas le rang taxonomique des organismes (Neige 2003), elle constitue un outil très important pour étudier les patrons évolutifs des formes de vie du passé. En effet, la morphologie est la source d'information principale disponible pour l'étude des organismes fossiles.

Cette approche permet de capturer les variations de formes et de tailles entre les spécimens en se basant sur divers paramètres appelés « descripteurs morphologiques » (Figure 2) (Hopkins et Gerber 2017). Il en existe de différentes natures, ayant chacune ses avantages et ses inconvénients. Les descripteurs continus incluent la morphométrie traditionnelle, c'est-à-dire des données mesurées sur la base de ratios (*p. ex.* mesure d'angle, longueur, périmètre), mais également la morphométrie géométrique basée sur le placement

de points de référence homologues (*c.-à-d.* placés au même endroit sur l'ensemble des spécimens) appelés "landmarks", traduits sous la forme de coordonnées géométriques en deux ou trois dimensions (Hopkins et Gerber 2017). Les descripteurs discrets correspondent à des observations catégorisées (Hopkins et Gerber 2017). Les matrices phylogénétiques sont grandement utilisées en tant que descripteurs discrets afin d'étudier la disparité morphologique, surtout lorsqu'il s'agit d'espèces éteintes. En revanche, la grande quantité de données manquantes qu'elles renferment rend souvent les analyses statistiques subséquentes plus difficiles.

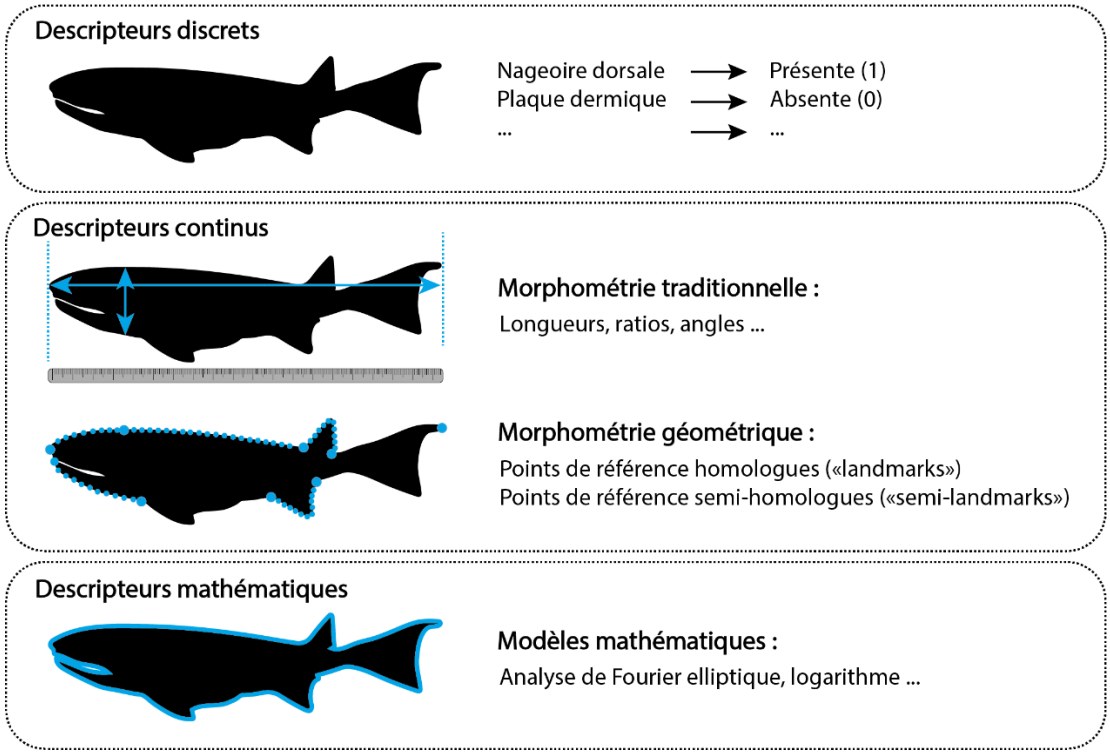


Figure 2. Représentation des différents descripteurs morphologiques utilisés dans l'étude de la disparité morphologique. Silhouette de *Cheirolepis canadensis* (Arratia et Cloutier 1996). Inspirée de Guillerme et al. (2020).

Afin de pallier à cela, de nouvelles méthodes statistiques et de nouveaux supports informatiques émergent depuis quelques années, tels que la « Maximum Observed Rescaled Distance » remplaçant la distance Euclidienne dans le calcul des matrices de distance, rendant les études de disparité morphologique plus tolérantes aux données manquantes (Lehmann et al. 2019; Lloyd 2016). Enfin, les descripteurs basés sur des modèles représentent les formes en se basant sur des modèles géométriques, tout comme Raup l'a démontré en 1966 en utilisant cette méthode pour décrire la forme spiralée de la coquille des invertébrés en utilisant un logarithme décrivant des spirales.

Utiliser différents types de descripteurs permet d'obtenir une information plus complète concernant les formes étudiées. La morphométrie géométrique et les descripteurs discrets sont souvent utilisés de concert pour leur complémentarité dans l'étude de la morphologie, notamment lorsqu'il s'agit d'espèces fossiles. La morphométrie géométrique est basée sur des points de référence homologues correspondant à un ensemble de points anatomiques pouvant être reconnus d'un individu à l'autre et entre les populations étudiées (Bookstein 1991). Ils regroupent l'information morphologique sous la forme de coordonnées géométriques à deux ou trois dimensions (dépendamment s'ils sont placés sur des photographies ou des modèles 3D), ce qui permet de visualiser la forme et d'en suivre les variations (Klingenberg 2010; Webster et Sheets 2010). Toutefois, les données manquantes et la reconnaissance de l'homologie (*c.-à-d.* similitudes anatomiques ou moléculaires héritées d'un ancêtre commun (Müller et Newman 2003)) des structures d'intérêt constituent les principales limites de cette méthode. Cela devient d'autant plus compliqué lorsqu'il s'agit d'espèces éteintes – les spécimens fossiles pouvant être incomplets, déformés par les processus taphonomiques et l'échelle phylogénétique étudiée plutôt étendue (Hetherington et al. 2015). Les descripteurs discrets sont quant à eux présentés sous forme de matrices de caractères regroupant des caractères binaires ou multiples. Ces caractères décrivent l'état des structures morphologiques en les « codant » selon des catégories définies *a priori* pour chaque taxon étudié (Foote 1999). La reconnaissance des homologies est une fois de plus importante dans ce cas-ci, mais contrairement à la morphométrie géométrique, ces matrices discrètes peuvent intégrer une certaine quantité de données manquantes et sont donc moins

limitées lorsque l'échantillon étudié comprend une grande échelle taxonomique (Ciampaglio et al. 2001; Schaeffer et al. 2020). En revanche, l'utilisation de matrices discrètes n'apporte pas de mesure de disparité continue et ne permet pas d'obtenir une description de la forme géométrique (Gerber 2019; Schaeffer et al. 2020). Ainsi, l'utilisation de descripteurs de natures différentes permet d'obtenir une représentation de la disparité morphologique plus complète en compensant les limites de chacun par les avantages des autres.

3. LA MODULARITÉ : UN POTENTIEL MOTEUR BIOLOGIQUE À L'ÉVOLUTION

Certains groupes de vertébrés actuels tels que les actinoptérygiens (c.-à-d. poissons à nageoires rayonnées) présentent une importante disparité morphologique qui reflète souvent une grande diversité écologique (Fricke et al. 2021). L'apparition de cette disparité morphologique au cours de l'évolution d'une lignée peut être facilitée par diverses propriétés organisationnelles des organismes vivants, telles que l'intégration morphologique (Evans et al. 2021; Larouche et al. 2017). L'intégration morphologique correspond à la covariation entre les différentes parties d'un organisme et représente à quel point ces parties vont être liées les unes aux autres (Wagner et al. 2007). Il existe un patron particulier d'intégration morphologique appelé "modularité" selon lequel un organisme peut être subdivisé en sous-unités quasi-indépendantes les unes des autres appelées "modules" (Zelditch et Goswami 2021). Chaque module est composé d'éléments fortement liés les uns aux autres mais peu liés aux éléments appartenant aux autres modules. Ainsi, le niveau d'intégration morphologique à l'intérieur d'un module est plus élevé qu'entre les modules (Figure 3) (Winther 2001; Klingenberg 2014). Cette quasi-indépendance des différentes régions du système pourrait augmenter l'évolvabilité, soit la capacité à évoluer d'un organisme (Kirschner et Gerhart 1998; Brandon 2005).

Les patrons de modularité peuvent être détectés à plusieurs niveaux - entre individus, entre populations, et entre lignées (Cheverud 1982). En ce qui concerne la modularité entre individus, les modules peuvent être liés à des propriétés fonctionnelles et/ou

développementales (Klingenberg 2008; Wagner et al. 2007). L'intégration développementale et fonctionnelle est étroitement liée au génotype et aux corrélations génétiques (*c.-à-d.* relations génétiques entre plusieurs caractères phénotypiques) et peut alors résulter d'une

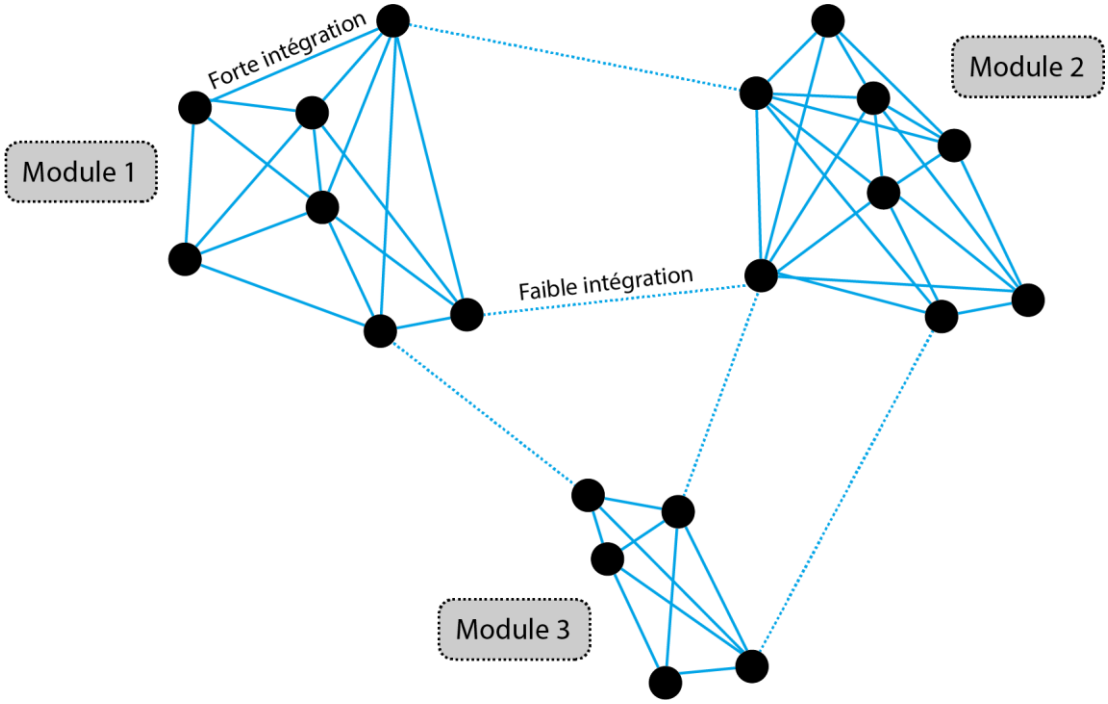


Figure 3. Représentation schématique de la modularité. Trois modules sont ici représentés, composés de plusieurs éléments morpho-anatomiques (points noirs) fortement intégrés les uns aux autres (traits pleins) mais peu intégrés aux éléments des autres modules (traits pointillés).

intégration évolutive suite à des processus de sélection et de co-sélection (Cheverud 1996). Ainsi, les processus d'intégration morphologique et de modularité à l'échelle de l'individu peuvent influencer l'intégration au niveau des populations. Des associations fonctionnelles et développementales de certains traits peuvent induire une plus forte intégration entre ces derniers et mener à une intégration variationnelle, c'est-à-dire, que la variation d'un de ces traits induirait la variation des autres (Zelditch et Goswami 2021).

Ce que l'on appelle alors "modularité variationnelle" s'intéresse à la forme et la taille d'un organisme et définit des modules comme étant des ensembles de traits qui co-varient. Ce patron est détectable à l'échelle des populations et des espèces et peut provenir de corrélations génétiques et d'associations fonctionnelles entre des traits (Wagner et al. 2007; Zelditch et Goswami 2021).

Les analyses de modularité variationnelle reposent sur des mesures morphométriques (*p. ex.* mesures linéaires ou morphométrie géométrique). Comme mentionné précédemment, la morphométrie géométrique utilise des ensembles de points de référence homologues afin de transformer la forme en une matrice de coordonnées géométriques (Zelditch et al. 2012). Les analyses statistiques subséquentes permettant de quantifier les patrons de modularité variationnelle comportent plusieurs étapes. Premièrement, des hypothèses de modularité *a priori* sont définies, basées sur des connaissances fonctionnelles, développementales ou encore évolutives des organismes étudiés. Ensuite, l'ensemble des points de référence homologues est divisé en sous-ensembles afin de représenter les différents modules hypothétiques. Enfin, une analyse statistique permet d'évaluer l'adéquation de chacune des hypothèses. Pour ce faire, la corrélation/covariance à l'intérieur de chacun des sous-ensembles est comparée à celle d'entre les sous-ensembles (Adams et Collyer 2016, 2019; Esteve-Altava 2017; Zelditch et Goswami 2021). Il est ensuite possible de comparer les hypothèses entre elles afin de déterminer la plus vraisemblable à l'aide de tests statistiques supplémentaires tels que le critère d'information de déviance (DIC) ou la modélisation graphique (Adams et Collyer 2019; Spiegelhalter et al. 2002; Zelditch et Goswami 2021).

L'étude des patrons de modularité permet ainsi d'identifier des scénarios évolutifs permettant de mieux comprendre comment la diversification des organismes s'est façonnée au fil du temps. Elle devient alors un outil essentiel pour la caractérisation des grandes transformations qui se sont opérées lors de la diversification des premiers vertébrés à mâchoires.

4. LES GNATHOSTOMES BASAUX : UNE BRÈVE HISTOIRE DE LEUR ÉVOLUTION

Les vertébrés à mâchoire, ou gnathostomes, représentent 99 % des vertébrés actuels. (Brazeau et Friedman 2015). Des micro-restes datant de l'Ordovicien moyen (470,0 – 458,4 Ma) constitués d'écailles de *Skiichthys halsteadi* et *Tantalepis gatehousei* (Darriwilien, 467,3 – 458,4 Ma) semblables à des écailles placoïdes de requin représentent l'un des plus anciens gnathostomes putatifs connus (Andreev et al. 2015; Long et al. 2019; Sansom et al. 2012; Smith et Sansom 1997). Toutefois, les plus anciens spécimens articulés (*c.-à-d.* les spécimens dont les différentes parties et os ont été préservés dans leur position anatomique d'origine) de gnathostomes proviennent du Silurien (443,8 – 419,2 Ma) (Lu et al. 2026; Zhu et al. 2013, 2009). Les vertébrés à mâchoires se sont ensuite rapidement diversifiés durant le Dévonien (419,2 – 358,9 Ma) et le Carbonifère (358,9 – 298,9 Ma) (Coates 2009; Zhu et al. 2009) colonisant une grande diversité d'habitats (Frey et al. 2019; Young 2010; Sallan et Friedman 2012). Au Paléozoïque, quatre grands groupes de gnathostomes sont reconnus – les chondrichthyens (les poissons cartilagineux) et les ostéichthyens (les poissons osseux), tous deux considérés comme des groupes monophylétiques; les « placodermes » (les poissons à armures ou gnathostomes souche) et les « acanthodiens » (les chondrichthyens souche ou « requins à épines »), deux groupes considérés paraphylétiques (Figure 4) (Brazeau et Friedman 2015).

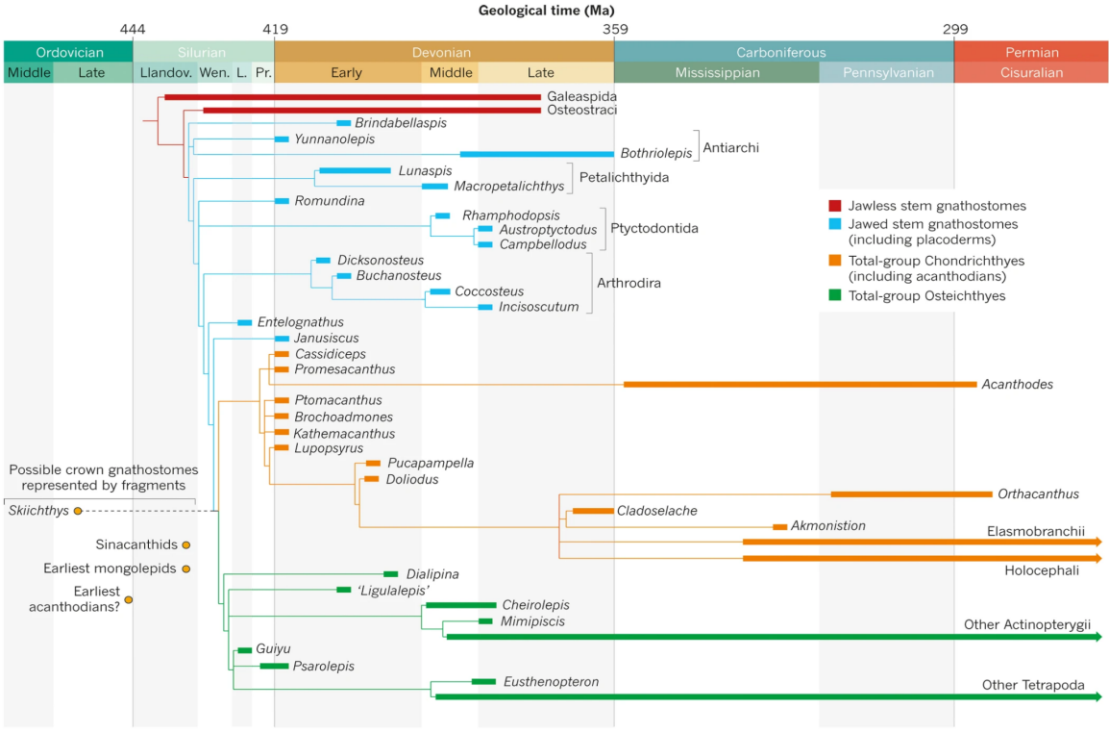


Figure 4. Phylogénie simplifiée des gnathostomes basaux. Issue de la figure 3 de Brazeau et Friedman (2015).

4.1 Les « placodermes » : les poissons cuirassés du passé.

Bien que les « placodermes » soient considérés comme le groupe souche des gnathostomes (Dupret et al. 2014), leur statut monophylétique n'en reste pas pour le moins débattu (King et al. 2017; Qiao et al. 2016). La monophylie des placodermes a été suggérée par plusieurs études (Denison 1978; Goujet et Young 2004; King et al. 2017; King et Rücklin 2020; Young 2008) mais ce statut a été remis en question à de nombreuses reprises (Johanson 2002; Qiao et al. 2016; Zhu et al. 2021). Le statut paraphylétique semble être entraîné par les membres les plus dérivés du groupe, ceux apparus après la première diversification des lignées durant le Silurien, tandis que les « placodermes » du Silurien – Dévonien inférieur semblent rester monophylétiques (Young 2010).

La caractéristique principale des « placodermes » est la présence d'une armure constituée de plaques dermiques osseuses recouvrant la tête et une partie du tronc. Grâce à ces robustes plaques osseuses, les « placodermes » sont très bien préservés et représentés dans le registre fossile (Figure 5).



Figure 5. Boucliers céphalique et thoracique du "placoderme" *Bothriolepis canadensis* Whiteaves (Dévonien supérieur). Crédit photo: Fossiilid.info

Environ 335 genres de « placodermes » sont connus (Young 2010), le plus ancien, h *Shimenolepis granifera*, provenant du Silurien inférieur (443,1 - 432,9 Ma) (Wang 1991). Le spécimen articulé le plus ancien, *Silurolepis platydorsalis*, date quant à lui du Silurien moyen (432,9 - 426,7 Ma) (Zhang et al. 2010). Les épisodes majeurs de diversification de ce groupe se sont produits au cours du Dévonien (419,62 - 358,86 Ma) (Carr 1995). Ils constituaient un groupe de vertébrés dominants dans les eaux du Paléozoïque, incluant à la fois les plus larges [*Dunkleosteus*, Dévonien Supérieur (Carr 2010) et *Titanichthys*, Dévonien supérieur (Boyle et Ryan 2017)] et le plus petit [*Minicrania*, Dévonien inférieur (Zhu et Janvier 1996)] vertébrés du Dévonien (Boyle et Ryan 2017; Carr 2010; M. Zhu et Janvier 1996). Ils occupaient des niches écologiques très diverses, ce qui est supporté par leurs morphologies variées et leurs différents types d'alimentation (*p. ex.*, alimentation par filtration :

Titanichthys; prédateur pélagique : *Dunkleosteus*; alimentation sur le benthos : *Bothriolepis*) (Béchard et al. 2014; Carr 2010; Coatham et al. 2020).

À la suite de l'extinction massive se déroulant à la transition entre le Dévonien et le Carbonifère, les « placodermes » ont complètement disparu du registre fossile (Sallan et Coates 2010).

4.2 Les « acanthodiens » : les poissons armés d'épines

Les « acanthodiens », aussi connus sous le nom de « requins à épines », constituent aujourd'hui un groupe de gnathostomes basaux caractérisé par la présence de plusieurs épines associées à toutes leurs nageoires, à l'exception de la nageoire caudale (Figure 6) (Larouche et al. 2019; Miller et al. 2003; Watson 1937).

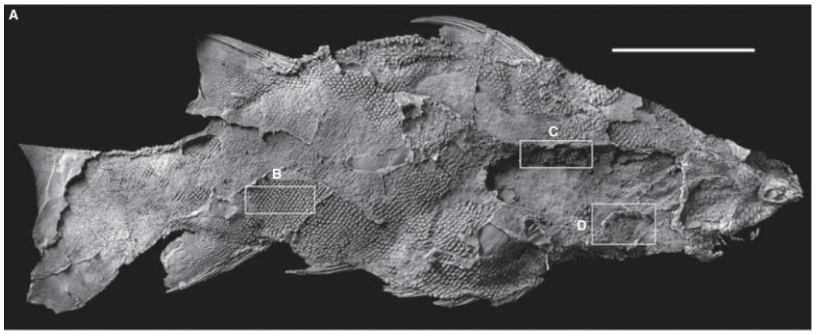


Figure 6. "Acanthodien" *Ptomacanthus anglicus* Miles (Dévonien inférieur). Issue de la figure 2 dans Brazeau 2012.

Le statut phylogénétique des « acanthodiens » reste problématique notamment en ce qui concerne les relations à l'intérieur du groupe qui demeurent peu résolues. Ces organismes partagent des caractéristiques à la fois avec les ostéichthyens et les chondrichthyens, ce qui en fait un groupe clé dans la phylogénie des gnathostomes (Brazeau 2009; Brazeau et de Winter 2015; Chevrinais et al. 2017; Davis et al. 2012; Rücklin et al. 2021). En effet, ils ont

été proposés comme étant le groupe souche des ostéichthyens, notamment le genre *Acanthodes* (Davis et al. 2012), comme le groupe souche des chondrichthyens (Chevrinais et al. 2017; King et al. 2017; King et Rücklin 2020; Qiao et al. 2016), ou encore des deux (Brazeau et Friedman 2014). Toutefois, certains « acanthodiens » tels que *Kathemacanthus*, *Vernicomacanthus*, *Seretolepis*, ou encore *Parexus*, semblent plus proches des chondrichthyens que de tous les autres « acanthodiens », supportant ainsi leur statut de groupe souche des chondrichthyens (Burrow et al. 2013; Chevrinais et al. 2017; Cui et al. 2021; Davis et al. 2012; Dearden et al. 2021). De nos jours, le statut paraphylétique de ce groupe est largement accepté dans la littérature (Brazeau et Friedman 2014; King et al. 2017; Miller et al. 2003).

Les premières heures de l'histoire évolutive des « acanthodiens » sont peu connues, la plupart des espèces étant décrites uniquement à partir d'éléments isolés tels que des épines, des écailles et des spirales de dents (Burrow et Rudkin 2014; Denison 1979). Apparu au Silurien avec des genres tels que Fanjingshania (Andreev et al. 2022 (a)) et *Qianodus* (Andreev et al. 2022 (b)) ce groupe aurait connu sa première diversification majeure durant le Silurien Supérieur et le Dévonien Inférieur (Zhao et Zhu 2007). Les « acanthodiens » étaient essentiellement des vertébrés marins épipélagiques et vivaient proches des côtes, jusque dans les zones supérieures des baies (Lund et al. 2012; Zhao et Zhu 2007). Ils sont des consommateurs pélagiques secondaires et comprennent à la fois des filtreurs microphages et des prédateurs (Chevrinais et al. 2017; Long 1986; Stiefel 2021).

4.3 Les chondrichthyens : les poissons au squelette de cartilage.

Les chondrichthyens sont des poissons cartilagineux dont les représentants actuels sont subdivisés en deux grands groupes, les Elasmobranchii et les Holocephali (Nelson et al. 2016). Les squelettes cartilagineux sont peu conservés durant la fossilisation et beaucoup d'espèces sont uniquement connues par des fragments minéralisés isolés, tels que des écailles, des épines et des dents (Figure 7).



Figure 7. Chondrichthyen *Phoebodus saidselachus* Frey et al. (Dévonien supérieur). Issue de la figure 1 dans Frey et al. 2019.

Doliodus latispinosus est le plus vieux spécimen articulé connu, daté du Dévonien inférieur (Miller et al. 2003) et de multiples écailles de chondrichthyens proviennent du Silurien (Andreev et al. 2020; Märss et Gagnier 2001). Néanmoins, de possibles écailles de requins seraient datées de l'Ordovicien moyen (Sansom et al. 2012, 1996). Après la fin du Dévonien et suite à la période de crise majeure de la biodiversité qui s'y déroule, la diversité des chondrichthyens augmente et pourrait être associée à de nouvelles opportunités écologiques amenées par la perte de certains groupes d' « acanthodiens » et de sarcoptérygiens aquatiques et surtout par l'extinction des « placodermes » (Richards et al. 2017; Sallan et Coates 2010). La majorité des premiers chondrichthyens occuperait la zone médiane de la colonne d'eau, allant des habitats pélagiques aux zones démersales (Frey et al. 2019; Lund et al. 2015). Les premiers chondrichthyens présentaient des morphologies variées, marquées par un profond dimorphisme sexuel et de nombreuses stratégies d'alimentation différentes telles que la succion active benthique, la filtration ou encore la prédation (Griffin et al. 2026; Lund et al. 2015; Schnetz et al. 2024).

4.4 Les ostéichthyens : les poissons tout en os.

Les ostéichthyens constituent le groupe majeur de vertébrés actuels avec plus de 65 800 espèces (Cloutier et Long, 2020 ; Fricke et al. 2021). Appelés également « poissons

osseux », ils sont représentés par deux grands clades, les actinoptérygiens (les poissons à nageoires rayonnées) et les sarcoptérygiens (les poissons à nageoires charnues). Caractérisés par un squelette osseux, ils sont bien préservés dans le registre fossile (Figure 8).

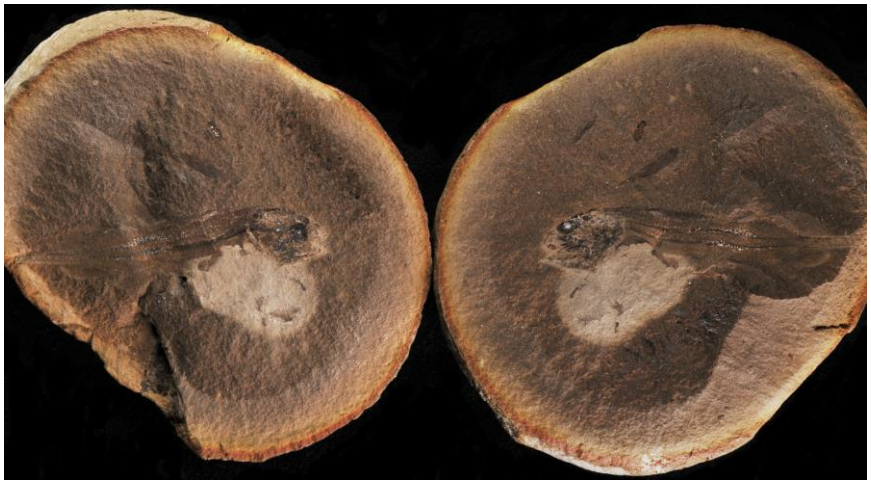


Figure 8. Larve du cœlacanthe (Ostéichthyens, sarcoptérygien) *Rhabdoderma exiguum* Eastman (Carbonifère supérieur). Crédit photo : Marie Boirot et Olivia Vanhaesebroucke

La première apparition des ostéichthyens dans le registre fossile remonte au Ludlow (Silurien moyen, 427,4 – 423,0 Ma) avec *Guiyu oneiros* connu comme le plus ancien spécimen articulé (Zhu et al. 2009). Durant le Dévonien, le clade des sarcoptérygiens représentait la plus grande majorité des ostéichthyens de l'époque, avec seulement une vingtaine d'actinoptérygiens connus à partir de spécimens articulés datés du Dévonien (Choo et al. 2019; Cloutier et Ahlberg 1996; Cloutier et Arratia 2004). Les sarcoptérygiens ont connu une importante première diversification durant le Dévonien, avec les Porolépiformes représentés par une douzaine de genres (Mondéjar-Fernández et al. 2021), les Dipnoi par 89 genres environ (R Cloutier, pers. comm.), les Onychodontida par 6 genres (Lu et Zhu 2009; Mann et al. 2017), les Actinistia (ou cœlacanthes) par 61 genres (R. Cloutier, pers. comm.), et avec 153 espèces de Tétrapodomorphes aquatiques (Cloutier et al. 2020). Durant le Dévonien moyen – supérieur, des poissons aux allures de tétrapodes tels que *Panderichthys*,

Elpistostege, Qikiqtania et *Tiktaalik* émergent des sarcoptérygiens (Boisvert et al. 2008; Cloutier et al. 2020; Shubin et al. 2006; Stewart et al. 2022). À partir du milieu du Dévonien et au cours du Carbonifère, les tétrapodes se sont rapidement diversifiés et ont colonisé la terre (Ahlberg 2018; Ahlberg et Clack 2020). Ce changement dans la diversité et l'écologie des sarcoptérygiens serait chronologiquement corrélé avec le bouleversement de la faune des vertébrés à la transition entre le Dévonien et le Carbonifère durant lequel les actinoptérygiens deviennent dominants (Friedman 2015). En effet, les actinoptérygiens sont connus depuis des dépôts à la fois marins et d'eau douce, et atteignent une disparité morphologique et une diversité écologiques élevées au Carbonifère inférieur, incluant des formes compactes et des espèces anguilliformes (Friedman 2015; Lund et al. 2015; Sallan et Coates 2013; Sallan et Friedman 2011).

5. La transition Silurien – Dévonien – Carbonifère : les montagnes russes écologiques

Les gnathostomes ont évolué au travers de plusieurs épisodes de profonds changements dans l'environnement aquatique. Les environnements aquatiques présents lors du Silurien, du Dévonien et du Carbonifère peuvent être séparés en trois grands types d'habitats aquatiques : les océans, les mers épicontinentales et les milieux d'eau douce (lacs, rivières, fleuves) (Sandberg et al. 1982; Savoy 1992; Rodriguez et al. 1986)

Le Dévonien moyen est marqué par une prolifération des récifs, qui occupent à ce moment-là la plus grande superficie de leur histoire (Bridge et al. 2022 ; Copper et al. 2002). À la même époque, sur les continents, les premières forêts apparaissent (Jurina 2024) transformant peu à peu le paysage et accompagnant la diversification de plusieurs groupes d'invertébrés terrestres (Buatois et al. 2022; Rolfe et Lawson 1997; Morris et al. 2015). La présence de plantes sur la terre ferme étant de plus en plus importante, des changements atmosphériques se produisent (Chen et al. 2021). Les niveaux de CO_2 diminuent et les niveaux de O_2 augmentent, participant ainsi à un refroidissement général à la surface de la

Terre (Chen et al. 2021). La présence grandissante de plantes sur les continents entraîne également une augmentation de l'apport en matière organique depuis les eaux continentales sur les plateaux continentaux (Algeo et al. 2001). La fluctuation des niveaux de la mer induite par la variation de la couverture du glacier de Laurussia due aux variations de la température globale mène à la formation de mers épicontinentales peu profondes (Lakin et al. 2016; Golonka 2020). Ces événements ont notamment été associés au temps de la première diversification d'une nouvelle lignée de sarcoptérygiens, les tétrapodes (Ahlberg 2018; George et Bliek 2011). Cette période du milieu du Dévonien est aussi marquée par une augmentation de l'activité tectonique associée à une activité volcanique plus importante (Golonka 2020) ce qui mène à l'ouverture de l'océan Paleotethys et à la formation de larges plateformes de carbonates aux sites de collision des plaques (Golonka 2020). Ces changements majeurs ont profondément affecté les milieux aquatiques et ont mené à la disparition de plusieurs groupes structuraux benthiques, tels que les coraux rugueux et tabulés (Oliver 1990) et les stromatoporoïdes (Kershaw et Jeon 2024), à la fin du Dévonien moyen, ainsi qu'à plusieurs crises de la biodiversité durant le Dévonien supérieur (Hartenfels 2024).

La première crise remarquable du Dévonien Supérieur est connue sous le nom de « l'événement Kellwasser » à la limite entre le Frasnien et le Famennien (371 Ma). Il est caractérisé par une abondance de shales noires dans le registre sédimentaire, provenant d'un important niveau de matière organique continentale déposée, soulignant des conditions anoxiques à grande échelle (Carmichael et al. 2019). Ces conditions anoxiques auraient pu mener à la décimation des récifs coralliens à la fin du Frasnien avec l'extinction de 80 % des genres de coraux tabulés et 60 % des genres de coraux rugueux (Ma et al. 2025), accompagnée de l'extinction de 80 % des espèces d'ostracodes (Guillam et Forel 2025) et de plus de 75 % des espèces de brachiopodes (Ma et al. 2025) qui jouaient un rôle central dans les réseaux trophiques du Dévoniens (Chevrinais et al. 2017). La seconde crise connue sous le nom de « l'événement Hangenberg » se produit elle à la limite entre le Famennien et le Tournaisien (359 Ma), à la transition du Dévonien et du Carbonifère. Elle est caractérisée par la perte de plusieurs groupes de poissons (Sallan et Coates 2010). Sallan et Coates (2010) ont

notamment décrit une chute de la diversité des « acanthodiens », des « placodermes » et des sarcoptérygiens aquatiques à la fin du Dévonien, constituant un bouleversement majeur dans l'organisation des milieux aquatiques qui voient leurs groupes dominants disparaître, libérant alors de nombreuses niches écologiques (Young 2010; Boyle et Ryan 2017). Une perte de plus de 50 % de la diversité au sein des vertébrés incluant l'extinction des « placodermes » serait associée à cet événement (Carr 1995, Sallan et Coates 2010) (Figure 9).

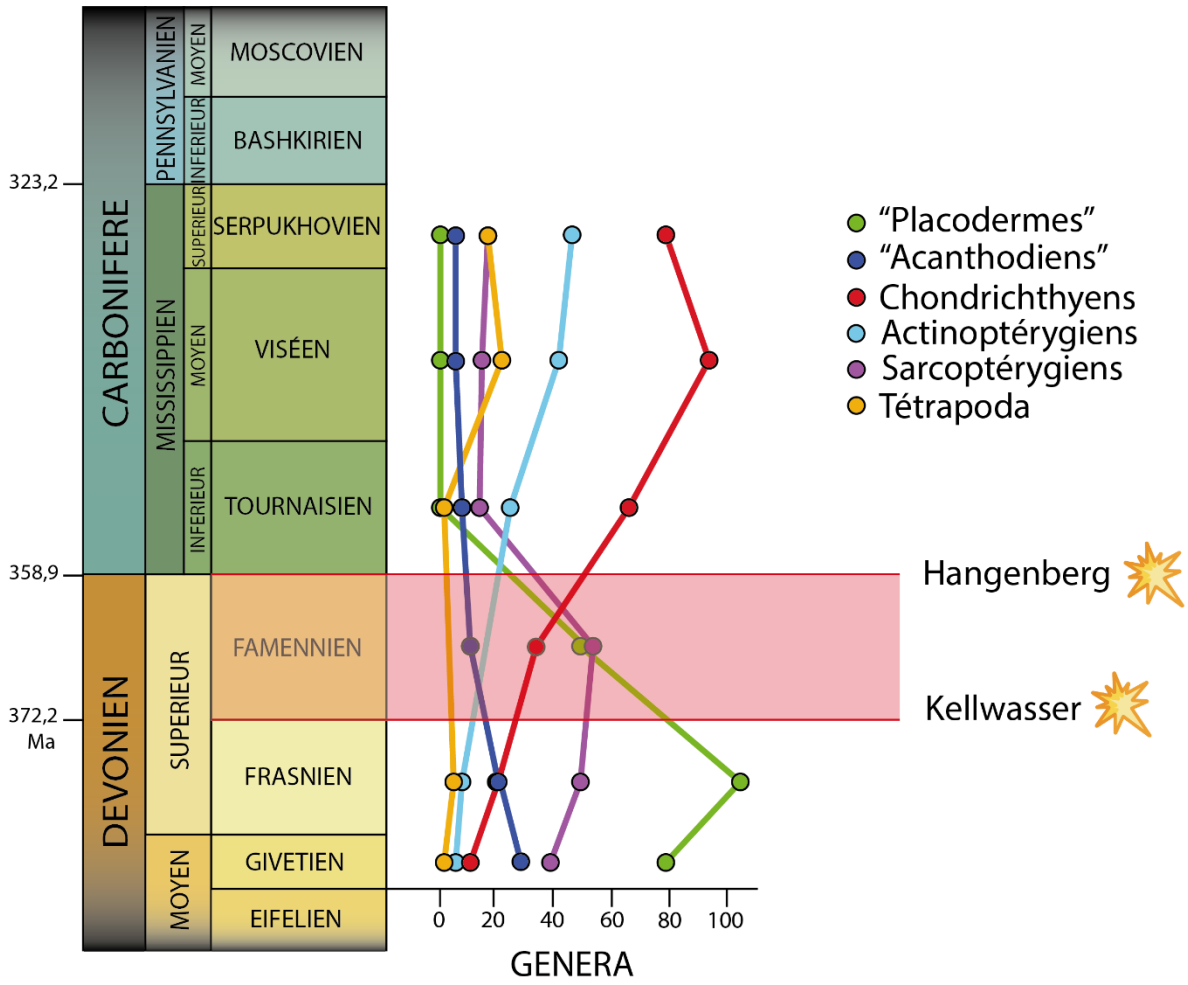


Figure 9. Diversité des grands groupes de gnathostomes à la fin du Dévonien et au début du Carbonifère. L'encadré rouge représente la période d'extinction marquée par les

événements Kellwasser et Hangenberg. Adaptée et traduite à partir de la figure 1 dans Sallan et Coates (2010).

La transition entre le Dévonien supérieur et le Carbonifère inférieur est ainsi profondément marquée par la succession de deux principales crises de la biodiversité, constituant « l'extinction de la fin du Dévonien » et comptant parmi les cinq extinctions massives de l'histoire de la Terre (Bambach et al. 2004; Buggisch 1991; Carmichael et al. 2019; Kaiser et al. 2016). La période du Carbonifère devient une période de récupération importante pour les écosystèmes. C'est une période de transition entre l'effet de serre présent durant le Dévonien et l'âge glaciaire du Paléozoïque tardif (Lakin et al. 2016). Selon Liu et al. (2019), ce refroidissement progressif aurait permis d'augmenter la circulation océanique et les upwellings sur les plateaux continentaux. La productivité des océans se serait intensifiée. Au même moment, durant le Viséen (346 Ma), la réémergence des récifs coralliens et leur rôle structurel central dans les écosystèmes marins constitue un élément clé de la récupération des milieux aquatiques (Figure 10) (Yao et al. 2020). Finalement, durant le Carbonifère supérieur (323,4 Ma), un dernier événement géologique majeur vient bouleverser les milieux aquatiques. Laurussia et Gondwana, deux masses continentales présentes durant le Dévonien, entrent en collision et forment la Pangée (Sampfli et al. 2013). Cet événement supprime une vaste surface de plateaux continentaux et modifie la circulation des océans (Sampfli et al. 2013; Golonka et Ford 2000).

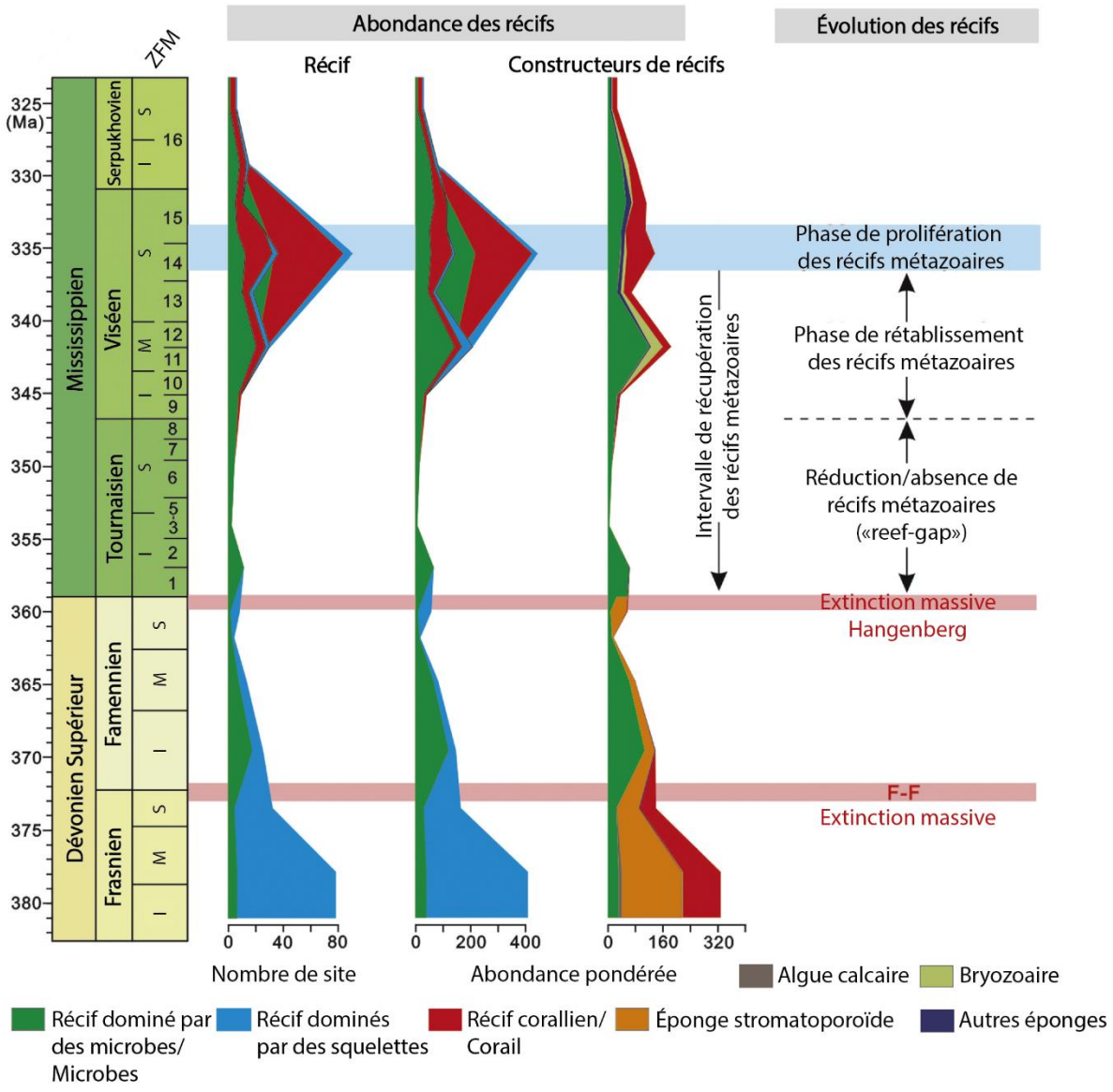


Figure 10. Variation de l'abondance des récifs et de leur composition durant le Dévonien Supérieur et le Mississippien. Abréviations : I, Inférieur ; M, Moyen ; S, Supérieur ; ZFM, Zone de foraminifères du Mississippien. Adaptée et traduite de la figure 7 dans Yao et al. (2020).

6. LE REGISTRE FOSSILE : LA VÉRITABLE MACHINE À REMONTER LE TEMPS

Dans cette étude, nous nous concentrons uniquement sur la disparité morphologique des premiers vertébrés à mâchoire dont les seules informations proviennent du registre fossile. La qualité de préservation des fossiles est donc un enjeu majeur pour la sélection des espèces étudiées notamment pour l'utilisation de l'approche par morphométrie géométrique. La préservation des fossiles dépend de nombreux facteurs biologiques et physico-chimiques (Schopf 1975; Wilson 1988) affectant la préservation des organismes entre le moment de la mort et son recouvrement par les sédiments (*p. ex.* la granulométrie des sédiments, le taux de sédimentation, le transport, la fragmentation), ou une fois l'organisme enfoui (*p. ex.* la minéralisation, la compression). Certaines conditions peuvent affecter négativement la préservation des fossiles, telles qu'un fort taux de fragmentation ou de charognage (Wilson 1988). La probabilité de préservation n'est pas la même pour l'ensemble des organismes. Un bon exemple de cela est la faible représentativité des organismes ne possédant pas de squelette minéralisé tels que les chondrichthyens ou encore les larves et juvéniles de poissons (Cloutier 2010; Kidwell et Holland 2002). Les parties molles d'un organisme telles que les muscles ou les nerfs sont en effet les plus à même d'être dégradées et perdues lors de la fossilisation (Purnell et al. 2018). Toutefois, certaines conditions particulières telles que l'absence de charognards, de décomposition ou de destruction diagénétique, peuvent mener à des conditions de préservation exceptionnelles, caractérisées par une concentration ou une qualité de préservation des fossiles bien supérieures à ce qui est normalement attendu (Seilacher et al. 1985). De tels dépôts fossilifères sont appelés des Konzentrat- ou Konservat-Lagerstätten respectivement (Nudds et Selden 2008). Pour cette étude, nous nous concentrons sur des vertébrés provenant de trois périodes géologiques principales, le Silurien (443,8 – 419,2 Ma), le Dévonien (419,2 – 358,9 Ma) et le Carbonifère (358,9 – 298,9 Ma), représentant les périodes d'apparitions et de diversification des premiers groupes de vertébrés à mâchoires (Coates 2009; Zhu et al. 2009). De tels dépôts exceptionnels sont reconnus pour chacune de ces périodes à travers le monde, nous offrant alors des représentations des plus fidèles de la diversité des vertébrés au travers de chacune d'elles. La Formation de Gogo

(Dévonien supérieur, Gogo Station, Australie de l'Ouest) représente un récif corallien de la fin du Dévonien et a offert des fossiles préservés en trois dimensions de grande qualité ainsi que la préservation de tissus mous sur nombreux spécimens (Long et al. 2009). La Formation d'Escuminac (Dévonien supérieur, Miguasha, Québec, Canada) représente un ancien estuaire tropical connu pour sa concentration en fossiles et une qualité de préservation exceptionnelle (Cloutier et al. 2011). La Formation d'Heath (Carbonifère moyen, Bear Gulch, Montana, États-Unis) conserve quant à elle la communauté d'une ancienne baie tropicale (Grogan et Lund 2002).

Bien qu'il existe peu de Lagerstätten pour les vertébrés du Silurien, celui de Qujing en Chine a tout de même révélé le plus ancien spécimen articulé d'ostéichthyen et plusieurs « placodermes » (Zhang et al. 2010; Zhu et al. 2009, 2016). Pour les gnathostomes, de tels dépôts fossilifères ont déjà amené des informations cruciales sur de nouvelles structures anatomiques conduisant à une compréhension avancée de l'anatomie, de l'écologie et des relations interspécifiques au sein de ce groupe (Chevrinais et al. 2016, 2017; Long et al. 2009; Newman et al. 2021; Zhu et al. 2013, 2009).

Les fossiles constituent la plus importante fenêtre sur l'histoire de la vie passée que nous avons. La qualité du registre fossile, et plus particulièrement les Lagerstätten, sont des éléments clés pour la caractérisation de la morphologie, de l'écologie et de notre compréhension des relations intra- et interspécifiques des espèces éteintes (Chevrinais et al. 2016; Kidwell et Holland 2002; Long et al. 2009).

7. OBJECTIFS SPÉCIFIQUES ET ORGANISATION DE LA THÈSE

Ce projet de recherche présente de nouvelles informations concernant l'évolution des premiers vertébrés à mâchoires. Son but principal est d'apporter un support supplémentaire à la caractérisation des radiations évolutives ayant mené à la diversification de ce groupe au travers d'une période marquée par des transformations environnementales majeures, et plus

généralement d'apporter une meilleure compréhension des mécanismes évolutifs à l'origine de la biodiversité.

Dans un premier temps (objectif 1), nous nous sommes concentrés sur une étude approfondie de la disparité morphologique au sein des deux lignées d'ostéichthyens basaux – les actinoptérygiens et les sarcoptérygiens – qui constituent un modèle d'étude particulièrement pertinent pour notre démarche. En effet, ce groupe est remarquablement bien représenté dans le registre fossile, nous offrant alors un matériel quantitatif représentatif de leur diversité, et les trajectoires évolutives de ses deux lignées sont complètement différentes autour de la transition Dévonien-Carbonifère. Les sarcoptérygiens sont un groupe dominant des eaux dévoniennes et connaissent d'importantes pertes de diversité lors de cette transition, alors que les actinoptérygiens, très peu diversifiés durant le Dévonien, connaissent un véritable essor au début du Carbonifère. Nous avons utilisé une approche en morphométrie géométrique afin de quantifier cette disparité et d'en estimer les variations au cours du temps. Les variations morphologiques ont été visualisées à l'aide d'« espaces morphologiques », un espace statistique multidimensionnel permettant de représenter la proximité des espèces d'un point de vue morphologique. Cette étude nous a permis d'apporter une compréhension supplémentaire de l'effet des changements environnementaux profonds du milieu du Paléozoïque sur la diversification des ostéichthyens basaux. Elle nous a permis de générer des hypothèses écologiques quant aux changements de diversité observés dans les lignées de part et d'autre de l'extinction massive de la fin du Dévonien et d'identifier de potentiels processus évolutifs associés. Les hypothèses pour cet objectif sont :

Hypothèse 1 : La disparité morphologique des actinoptérygiens devrait augmenter avec la diversité taxonomique, suggérant une radiation adaptative pour le groupe des actinoptérygiens serait associée à l'exploitation de nouvelles niches écologiques à la suite du Dévonien. De nouvelles régions de l'espace morphologique seront ainsi occupées.

Hypothèse 2a : La disparité morphologique des sarcoptérygiens diminuera au travers de la crise du Dévonien, reflétant une perte de diversité fonctionnelle liée à une perte de diversité taxonomique.

Hypothèse 2b : Lors du Dévonien, une nouvelle lignée entame une transition vers les milieux terrestres (les tétrapodes) (Alhberg et al. 2018). Les espèces proches de cette transition présenteront une morphologie innovante au sein des sarcoptérygiens, se traduisant par l'occupation d'une nouvelle région de l'espace morphologique.

Dans un second temps, nous avons recherché la présence de propriétés organisationnelles facilitant l'apparition de nouvelles formes au cours de l'évolution. La recherche de patrons de modularité variationnelle au sein des actinoptérygiens (objectif 2) a permis de mettre en lumière la présence de modules crâniens ayant pu faciliter les radiations adaptatives et la diversification du groupe en lien avec une diversification écologique et trophique. Bien que la disparité morphologique des sarcoptérygiens et des actinoptérygiens ait été quantifiée dans le premier objectif, l'étude de la modularité crânienne se focalise ici sur les actinoptérygiens. Ce choix a été motivé par la disponibilité des spécimens comparables – les sarcoptérygiens ont un crâne beaucoup plus variable entre les différentes classes, rendant alors la collecte de données moins précise – ainsi que par la pertinence de la modularité pour comprendre les mécanismes associés à la radiation de ce groupe, soutenue par des études réalisées sur les lignées d'actinoptérygiens récents (Gartner et al. 2023). Pour cet objectif, une approche en morphométrie géométrique a permis de capturer la forme du crâne. Les patrons de modularité ont ensuite été testés par deux méthodes complémentaires – le ratio de covariances (CR) et l'approche par matrice de distances – afin d'obtenir une interprétation la plus représentative possible. Les hypothèses pour cet objectif sont :

Hypothèse 1 : De par ses propriétés fonctionnelles, la mâchoire constituerait un module variationnel.

Hypothèse 2 : De par son rôle dans l'exploitation de l'habitat et par ses contraintes développementales, la région pré-orbitale constituerait un module variationnel.

Hypothèse 3 : De par son rôle dans la respiration et l'alimentation du poisson, la joue constituerait un module variationnel.

Enfin, l'étude de la relation entre la disparité morphologique et la diversité écologique des premiers vertébrés à mâchoires (objectif 3) a permis de confirmer le rôle important que la divergence d'habitats a joué dans les épisodes de diversification de ces groupes. Pour cet objectif, nous avons utilisé une matrice de caractères morpho-écologiques discrets et continus. Nous avons ainsi pu intégrer l'ensemble des groupes de vertébrés à mâchoires du Dévonien et du Carbonifère. Nous avons exploré statistiquement la structure de l'espace des traits fonctionnels de ce clade afin de suivre les changements qui ont pu s'opérer au niveau de la structure des communautés de vertébrés aquatiques entre le Dévonien et le Carbonifère. Afin de visualiser cette diversité écologique, des espaces éco-morphologiques ont été construits. Les hypothèses pour cet objectif sont :

Hypothèse 1 : Des modifications morphologiques, notamment le raccourcissement du bouclier thoracique chez plusieurs groupes d'arthrodires, pourraient avoir joué un rôle dans le changement de mode de locomotion des « placodermes » en augmentant leur flexibilité (Carr, 1995). La répartition écologique des « placodermes » devrait refléter cette transition du fond marin vers la colonne d'eau. Nous attendons alors que les groupes les plus basaux de « placodermes » occupent des zones benthiques et démersales, et que les groupes plus dérivés soient présents dans les zones pélagiques.

Hypothèse 2 : Les formes basales d'actinoptérygiens devraient être regroupées dans l'espace éco-morphologique, représentant une faible diversité écologique, et les actinoptérygiens du Dévonien supérieur et du Carbonifère inférieur devraient être répartis dans la majorité des habitats.

Hypothèse 3 : De par le comportement opportuniste, les chondrichthyens occuperaient les niches laissées par les groupes éteints à la fin du Dévonien.

CHAPITRE 1

LA DISPARITÉ MORPHOLOGIQUE ET LA RADIATION ÉVOLUTIVE DES ACTINOPTÉRYGIENS BASAUX AU TRAVERS DE LA CRISE DU DÉVONIEN-CARBONIFÈRE

1.1 RÉSUMÉ EN FRANÇAIS DU PREMIER ARTICLE

Les écosystèmes aquatiques du Dévonien étaient dominés par les « placodermes » et les sarcoptérygiens aquatiques. Après la crise de la biodiversité à la fin du Dévonien, les actinoptérygiens ont connu leur premier grand événement de diversification et sont rapidement devenus des acteurs majeurs de la diversité des vertébrés.

Dans cette étude, nous avons analysé la diversification morphologique des actinoptérygiens du Dévonien et du Carbonifère en quantifiant leur disparité par une approche en morphométrie géométrique en deux dimensions. Cette approche permet d'estimer la disparité à partir de données continues en intégrant l'information géométrique liée aux variations de forme de plusieurs structures morphologiques. Treize points de référence homologues (« landmarks ») et 203 points de référence semi-homologues (« semi-landmarks ») ont été digitalisés sur les reconstructions paléontologiques de la forme du corps de 84 espèces, tandis que 18 landmarks et 50 semi-landmarks ont été digitalisés sur les reconstructions de la vue latérale du crâne de 86 espèces.

Lorsque nous comparons la variation de la forme du corps et celle de la diversité taxonomique au cours du temps, les patrons sont congruents et atteignent un maximum au Viséen. En revanche, le patron de variation de la forme du crâne n'est pas entièrement congruent, présentant une première augmentation au Dévonien Supérieur. Les changements de la forme du corps seraient associés à des propriétés locomotrices, tandis que les changements de la forme du crâne seraient associés à des propriétés fonctionnelles de

l'appareil alimentaire. Ainsi, ce patron suggère fortement que la diversification des actinoptérygiens a été induite par une divergence des stratégies trophiques. Cette radiation évolutive semble résulter d'une réponse adaptative à de nouvelles opportunités écologiques, apportées par de profonds changements environnementaux dans les océans du Paléozoïque moyen.

Cet article, intitulé « *Morphological disparity and evolutionary radiation of early actinopterygians through the Devonian-Carboniferous crisis* », a été publié en Janvier 2026 dans la revue *Diversity* dans une collection spéciale sur l'évolution des poissons (*Evolutionary History of Fishes*, C. Ciampaglio et R.C. Shell, éditeurs) . En tant que première auteure, j'ai contribué à l'essentiel de la conceptualisation du projet, à l'établissement du cadre méthodologique, à l'acquisition des données, aux analyses et à la rédaction du manuscrit. Le professeur Richard Cloutier, co-auteur, a contribué à l'établissement de la question de recherche et à la révision du premier manuscrit. Une version abrégée de l'article a également été présentée lors de la 16ème édition de l'*International Symposium on Early and Lower Vertebrates* à Valence (Espagne) en Juin 2022.

Ce projet a été financé par une bourse des Fonds de recherche du Québec – Nature et Technologies (FRQNT) [https://doi.org/10.69777/325538] que j'ai reçue pour mon doctorat et par les subventions (06133 et 05887) du Conseil de Recherches en Sciences Naturelles et en Génie du Canada (CRSNG) du professeur Richard Cloutier.

1.2 MORPHOLOGICAL DISPARITY AND EVOLUTIONARY RADIATION OF EARLY ACTINOPTERYGIANS THROUGH THE DEVONIAN-CARBONIFEROUS CRISIS

Olivia Vanhaesebroucke[1] and Richard Cloutier[1,2]

[1] Département de Biologie, Chimie et Géographie, Université du Québec à Rimouski, Rimouski, QC, Canada.

[2] Center of Excellence on the Evolution of Life, Basin Studies and Applied Paleontology, Paleontological Research and Education Center, Mahasarakham University, Maha Sarakham 44150, Thailand.

ABSTRACT

"Placoderm" and sarcopterygian fishes dominated Devonian waters. Following the end-Devonian crisis, actinopterygians rapidly became major contributors to vertebrate diversity. This transition constitutes the first major diversification event of actinopterygians. Here, we investigate the morphological diversification of Devonian and Carboniferous actinopterygians by quantifying disparity using two-dimensional (2D) geometric morphometrics, which estimates disparity from continuous data and brings geometric information related to the shape changes in several morphological features. In total, 13 landmarks and 203 semi-landmarks were digitized on the body shape reconstructions of 84 species, and 18 landmarks and 50 semi-landmarks were digitized on the reconstructions of the lateral view of the skulls of 86 species. When compared to variations in taxonomic diversity over time, the pattern of body shape variations is congruent, reaching a maximum during the Viséan, but the pattern of skull disparity is not entirely congruent, presenting a first increase during the Late Devonian. Changes in body shape are associated with locomotory properties, while changes in skull shape are associated with functional properties of the feeding apparatus. This pattern strongly suggests the diversification of actinopterygians to be driven by divergence in trophic strategies. This evolutionary radiation seems to be the result of an adaptive response to new ecological opportunities, triggered by big environmental changes in mid-Paleozoic oceans.

Key-words: end-Devonian crisis; geometric-morphometric; ecomorphology; Paleozoic; osteichthyans; palaeogeography; adaptive radiation

1. INTRODUCTION

Actinopterygians, ray-finned fishes, are a group of osteichthyans that today represents the most diversified group of extant vertebrates, with more than 30,000 species [1]. They colonized almost all aquatic environments, and this ecological diversity is reflected in their impressive morphological disparity. However, the early history of actinopterygians is still poorly known. The oldest articulated specimen of osteichthyan is known from the Ludlow stage (Middle Silurian, 427.4 million years ago (Mya)) with the sarcopterygian *Guiyu oneiros* [2]. Nevertheless, the first articulated specimens of actinopterygians date back to the Lower Devonian (419.6 Mya) with *Meemannia eos* [3] and later genera like *Austelliscus* [4], *Dialipina* [5] and *Cheirolepis* [6,7]. At that time, the vertebrate community was dominated by "placoderms" (armoured fishes) and aquatic sarcopterygians [8], with only about twenty species of actinopterygians known from articulated specimens from the Devonian [9,10].

Osteichthyans evolved through various episodes of major changes in the aquatic environment [11]. The Late Devonian–Early Carboniferous transition is characterized by two successive biodiversity crises known as the Kellwasser [12] (Frasnian–Famennian boundary, 371 Mya) and the Hangenberg [13] (Devonian–Carboniferous boundary, 359 Mya) events that greatly modified aquatic biodiversity. Together, they constitute the end-Devonian mass extinction, one of the "Big Five" mass extinctions [12–14]. More than 50% of all vertebrate diversity was lost, including the extinction of dominant groups such as "placoderms" [8,15]. Simultaneously, the high tectonic activity levels lead to the formation of inland seas [16] and a large carbonate platform on the continental shelf [17] during the Early Carboniferous, which produced more diverse shallow aquatic habitats [18]. In addition, the re-emergence of coral reefs during the Early Carboniferous [19] brought new marine habitats with complex structures. These environmental changes associated with the loss of the majority of the dominant Devonian vertebrate groups may have contributed to the rapid diversification of

chondrichthyans and actinopterygians that became major contributors to the aquatic vertebrate community during the Early Carboniferous [8,16,17,20].

Indeed, during the Early Carboniferous, actinopterygians experienced their first major and rapid diversification [8,21], which could be identified as an evolutionary radiation [22,23]. Evolutionary radiations are one of the most interesting evolutionary processes. Such events are characterized by a rapid increase in the diversification rate (*i.e.*, difference between the speciation and the extinction rates) and an increase in the morphological disparity and the ecological diversity [24]. Several factors can trigger such events within clades [25–28]. The variation in the taxonomic diversity and the morphological disparity through time are two of the most fundamental parameters characterizing evolutionary radiations [29]; they bring complementary information about such events [30]. Therefore, exploring the patterns of morphological disparity through time and associated factors is crucial for characterizing evolutionary radiations.

The present study aims to investigate the event of rapid diversification of early actinopterygians and their putative evolutionary radiation by exploring body and cranial shape variation among Devonian and Carboniferous actinopterygians. As the taxonomic diversity of actinopterygians rapidly increased after the end-Devonian crisis, following major changes in the aquatic environment [8,22,31], we expect to detect increases in morphological disparity that matched the increase in taxonomic diversity, which could support a diversification of morphology triggered by the colonization of new habitats [32–34]. To support this hypothesis, we also hope to detect simultaneous increases in morphological disparity and in the expansion of the species' geographic repartition. Finally, we expect to observe differences in the variation in body shape and cranial shape disparity through geological time. Indeed, the body shape of fish is mostly related to locomotory properties [33–35], while cranial shape is tightly connected to feeding strategies [36,37]. Even though body shape and trophic specializations are functionally related, body shape can also be related to habitat use and hydrodynamic performance, which may evolve independently from specialized feeding structures [31–33]. Therefore, we could assume that we would first detect an increase in body shape disparity early in actinopterygian history [38], followed by

successive increases in the cranial shape, which could indicate the acquisition of various feeding strategies in lineages that already occupy distinct niches, differentiated by locomotor properties [37,39,40].

2. Materials and Methods

2.1. Taxonomic Diversity

To obtain an estimate of Devonian and Carboniferous actinopterygian taxonomic diversity, we gathered a list of 197 actinopterygian species from the primary literature and published databases [41]. For each species, the first and last occurrence dates were noted (Figure 1, Annexe II Table S1). Our time scale sampling goes from the early Eifelian (Middle Devonian, 393.47 Mya) to the Late Gzhelian (Pennsylvanian, 298.9 Mya), which represents a 94.57 MY time span, and is divided into 11 stages (Eifelian, Givetian, Frasnian, Famennian, Tournaisian, Viséan, Serpukhovian, Bashkirian, Moscovian, Kasimovian and Gzhelian). The preservation state of actinopterygians from the Early Devonian did not allow for complete morphological analyses with geometric morphometrics. We analyzed actinopterygian diversity with the R package 'divDyn' (v.0.8.3) [42].

2.2. Morphological and Palaeogeographical Dataset

As the shape of fossil species is rarely conserved in three dimensions, we used two-dimensional (2D) datasets rather than three-dimensional data. We assembled two separate 2D datasets, including a total of 106 species, using palaeontological reconstructions of (1) the entire body shape (n = 84) and (2) the lateral view of the skull (n = 86) of Devonian and Carboniferous actinopterygian species (Annexe II Table S2). Using Adobe Photoshop (v22.0.0), we modified the reconstruction of the skull, when needed, to put the mouth in a closed position, controlling the morphological variation that could be induced by the opening of the mouth.

Only the species for which adult specimens were identified were compiled. We excluded from the analysis all species known solely from juvenile specimens. GPS coordinates of

today's fossil locality were noted for each species, and their palaeocoordinates based on their respective ages were reconstructed with the R packages 'rgplates' (v.0.6.1) [43,44] and 'sf' (v.1.0-25) [45]. We used the maps from the PALEOMAP PaleoAtlas [46] for Gplates, available on Earthbyte.org, to plot the palaeodistribution of each species (Annexe II Figure S1a–c).

2.3. Landmarking Scheme

We used 2D geometric morphometrics to quantify actinopterygian morphological disparity by digitizing landmarks and semi-landmarks on palaeontological reconstructions. Even if reconstructions may have limitations due to the preservation of fossils and/or the subjective interpretation of structures, this approach allowed us to estimate disparity from continuous data and to obtain geometric information related to the shape changes in several morphological features of early actinopterygians. We digitized 13 landmarks and 203 semi-landmarks for body shape, describing the lateral outline of the body and the positioning and shape of the fins (Figure 2a, Annexe II Table S3). We chose to exclude information about the pelvic fins in this analysis because some species lack these fins. For the cranial shape disparity, we digitized 18 landmarks and 50 semi-landmarks on lateral reconstruction to describe the cranial outline, more precisely the orbital, cheek and lower jaw regions (Figure 2b, Annexe II Table S3). All landmarks and semi-landmarks were digitized using tpsDig2 (v2.32).

Each set of landmarks coordinates was rotated, translated and scaled with a Procrustes superimposition using the *gpagen* function in the R package 'geomorph' (v.4.0.10) [47]. Semi-landmarks were slid using the Procrustes distance minimization criterion [48]. The multidimensional shape data were summarized using principal component analysis (PCA). The first three axes of each PCA were used to build morphospaces.

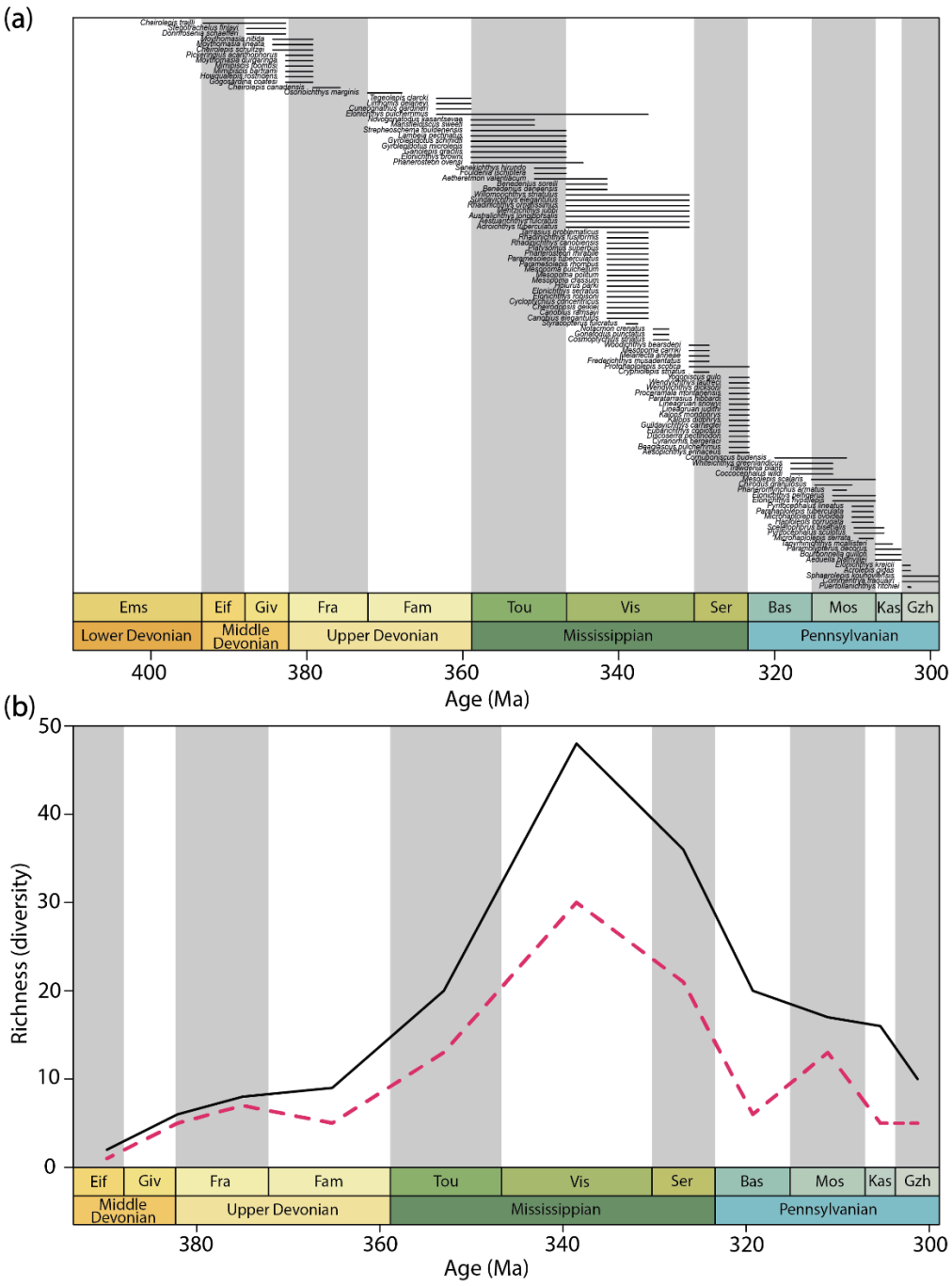


Figure 1. Occurrence and diversity of early actinopterygian species through time. (**a**) Occurrence of each of the 106 species of early actinopterygians analyzed; (**b**) diversity of early actinopterygians through time based on the richness calculated for each stage for the 106 species analyzed (dashed red line) and for the 197 species of early actinopterygians (black line). Bas: Bashkirian; Eif: Eifelian; Fam: Famennian; Fra: Frasnian; Giv: Givetian;

Gzh: Gzhelian; Kas: Kasimovian; Mos: Moscovian; Ser: Serpukhovian; Tou: Tournaisian; and Vis: Viséan.

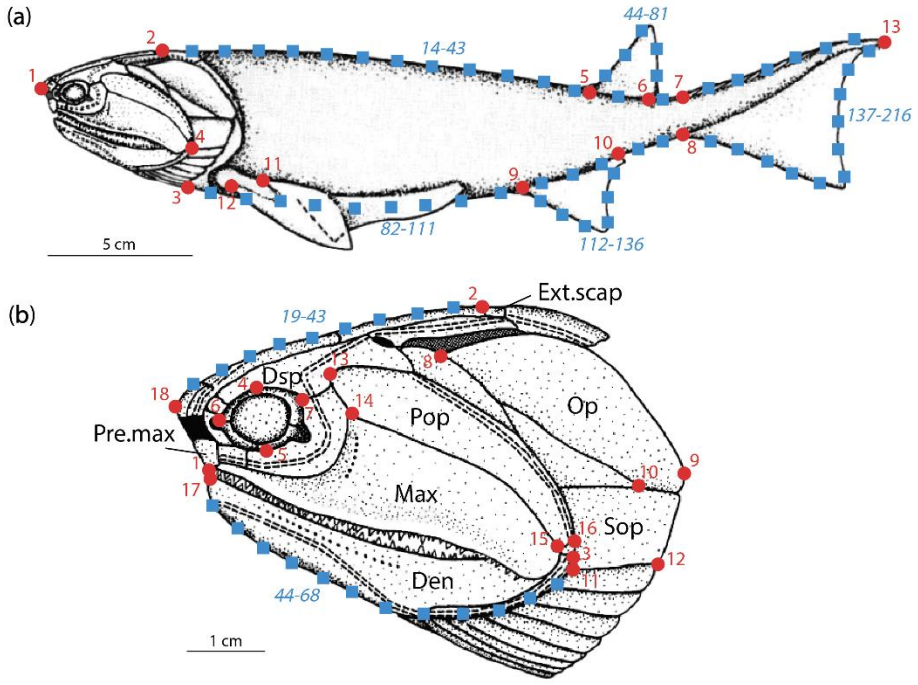


Figure 2. Landmarks (red circles) and semi-landmarks (blue squares) positioning scheme for geometric morphometrics analyses of (**a**) the body shape and (**b**) the lateral view of the skull; *Cheirolepis canadensis* (Arratia and Cloutier, 1996 [7], Figures 3A and 5A). See Annexe II Table S3 for a full description of the landmarks and semi-landmarks. Den: dentary; Dsp: dermosphenotic; Ext.scap: extrascapular; Max: maxillary; Op: Operculum; Pop: preopercular; Pre.max: premaxillary; Sop: subopercular.

2.4. Morphological Disparity Analyses

We estimated morphological disparity using two different metrics, each reflecting different aspects of the distribution of multidimensional data in morphospaces: (1) the Procrustes variance, which measures the dispersion of taxa within the morphospace by estimating the difference among taxa based on the variance in the shape data, and (2) the weighted area of convex hulls, which measures the amount of global morphospace occupation for each group [49]. The latter one is more sensitive to extreme values and cannot

be calculated for groups with two or fewer species. Nevertheless, it provides an intuitive metric for comparing the amount of morphospace occupied by each group.

Procrustes variance was calculated for each geological epoch and stage using the function *morphol.disparity* in the R package 'geomorph' (v.4.0.10) [47] that quantifies groupwise morphological disparity and assesses statistical significance for each pairwise comparison. Using the same set of grouping variables, the area of convex hulls in the multidimensional morphospace was estimated using a modified version of the *chull* function from the 'grDevices' [50] R package (v.4.3.2). We determined the number of PCs to retain for this calculation by using a scree plot that graphically represents the eigenvalues plotted against the corresponding PC number [51,52]. We chose to retain the first five axes for body shape, accounting for 75.52% of the variation, and the first four axes for cranial shape, which account for 78.64% of the variation (Annexe II Figure S2). We calculated the surface area for each pair of PCs and weighed each by the combined proportion of variance explained by the two axes (Annexe II Table S4).

As mentioned above, our time scale is divided into 11 stages. To be free from the time scale and to control potential biases in this subdivision (as stages are usually defined after major biodiversity or environmental changes), we also subdivided the total time interval into 11 equal time bins of 8.6 million years [53]. Then, we quantified the Procrustes variance for each time bin with the *dispRity* function in the R package 'dispRity' (v.1.9) [54]. The resulting two patterns of morphological disparity were highly congruent. To refine the presentation of our results, we present the morphological disparity along the stages from the international chronostratigraphic chart [53] in the main text. Species that overlapped two or more different stages were classified according to their stage of appearance. All disparity analyses were performed in R v.4.3.2 using the packages 'geomorph' [47], 'grDevices' [50] and 'dispRity' [54].

3. RESULTS

3.1. Body Shape Disparity

The first axis of PCA (PC1) explains 40.08% of the variation in body shape among 84 species, separating elongated and fusiform bodies, such as *Cheirolepis trailli*, from deep and short bodies, such as *Platysomus superbus* (Figure 3a).

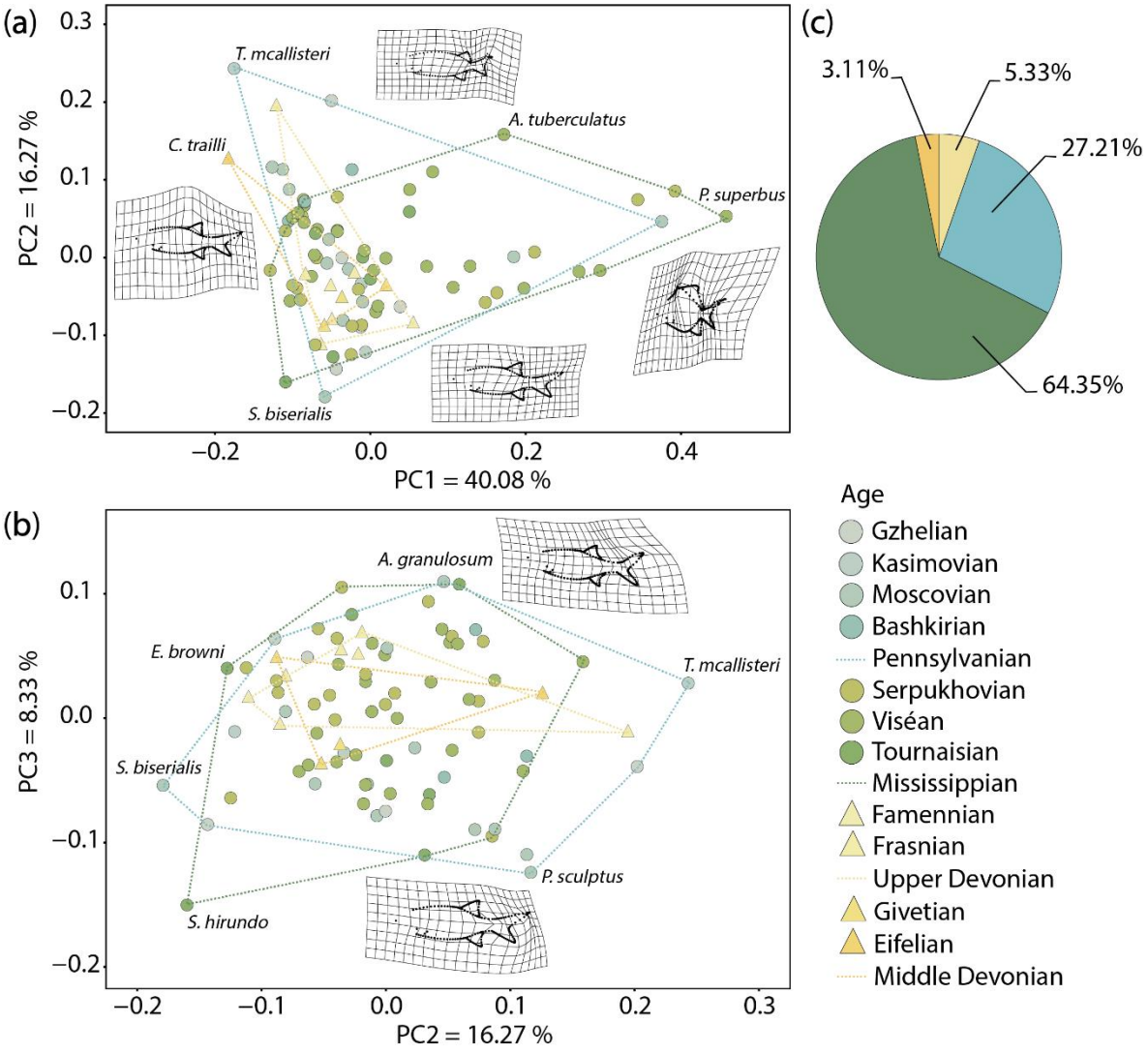


Figure 3. Body shape morphological disparity of 84 early actinopterygians per age. (a) Morphospace of principal components 1 and 2; (b) morphospace of principal components 2 and 3. Deformation grids show the differences between the extreme forms along each axis and the mean shape. See Supplementary Figure S3 for the deformation grids of each species; (c) The pie charts illustrate the proportion of total disparity each epoch represents based on its respective Procrustes variance.

PC1 also clearly discriminates between Devonian and Carboniferous species. Devonian species are all located in the left portion of the morphospace, characterized by an elongated and fusiform shape. On the contrary, Carboniferous species display various body shapes, spreading across all of the morphospace.

During the Devonian, body shape disparity increases slightly during the Frasnian, followed by a decrease during the Famennian. Subsequently, two successive increases in body shape occurred during the Carboniferous; first, during the Mississippian and then during the Middle-Late Pennsylvanian, with a decrease during the Bashkirian (Figure 4). Overall, Mississippian species represent 56.83% of the total disparity, with the Viséan and Serpukhovian actinopterygians being the most disparate (Supplementary Tables S4 and S5), followed closely by the Moscovian species.

PC2 represents a difference in the caudal fin shape, explaining 16.27% of the variation (Figure 3a). The tail is elongated in species such as *Sceletophorus biserialis* and rather short in species such as *Tanyrhinichthys mcallisteri*. Finally, PC3 (8.33% of the variation) also seems to represent variation in the caudal region (Figure 3b). This third axis separates species with an elongated caudal peduncle, such as *Senekichthys hirundo*, from shortened caudal peduncle, such as *Amphicentrum granulosum*. The difference between Devonian and Carboniferous species is less defined in PC2 and PC3; Carboniferous species occupy a larger morphospace but lack a clear shift from Devonian species (Figure 3b).

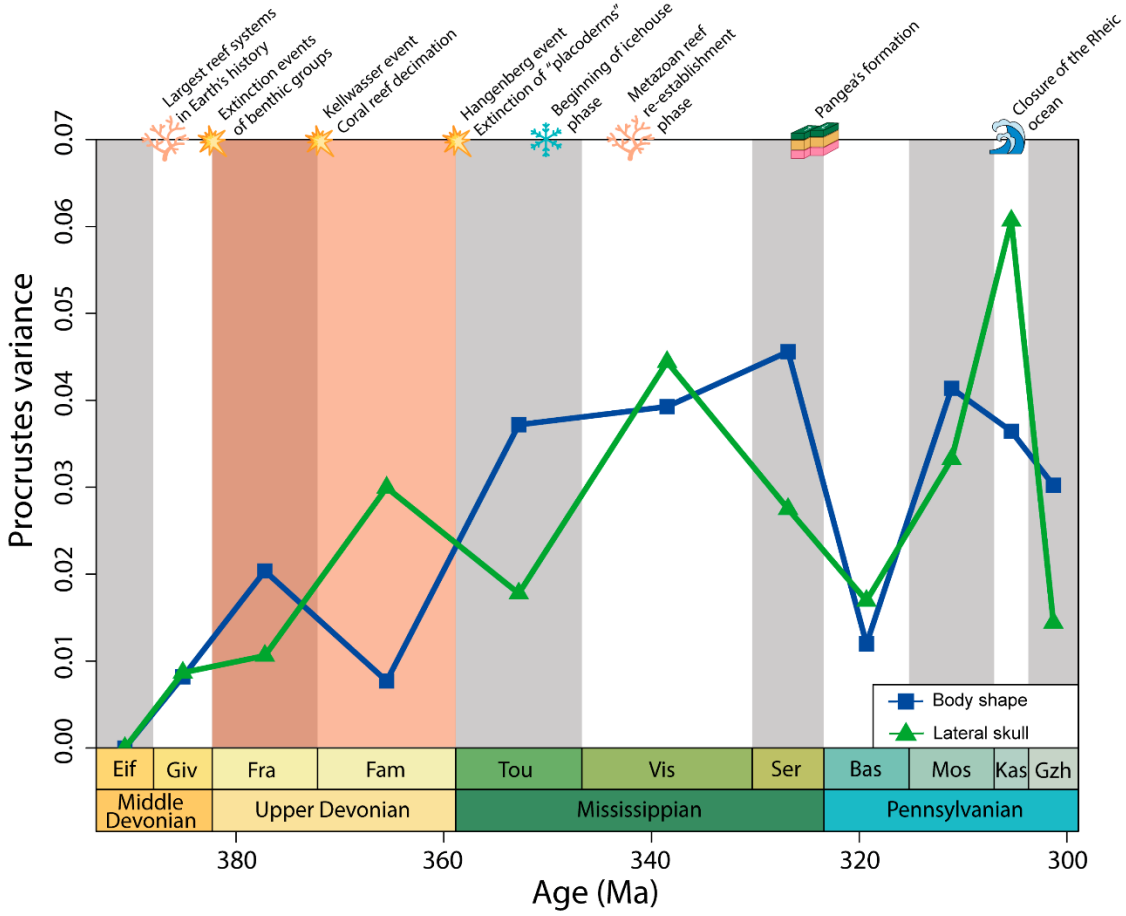


Figure 4. Procrustes variance for body shape (blue squares) and lateral skull shape (green triangles) disparity through time. Major Devonian and Carboniferous geological and biological events are represented: the largest reef systems in Earth's history [55], the extinction events of benthic groups [56,57], the Kellwasser event and coral reef decimation [12], the Hangenberg event and the extinction of "placoderms" [13,15], the beginning of the icehouse phase [58], the metazoan reef re-establishment phase [19], the Pangea's formation [59], and the closure of the Rheic ocean [59]. The coloured box, including the Frasnian and Famennian stages, corresponds to the end-Devonian mass extinction event.

3.2. Cranial Shape Disparity

PC1, explaining 48.15% of the cranial shape variation, represents the difference between short and deep skulls, such as in *Platysomus superbus*, and elongated, narrower skulls, such as in *Tanyrhinichthys mcallisteri* (Figure 5a). Most of this variation seems to be explained by the epoch. Similarly to body shape, the skulls of Devonian species, all located

in the left portion of the morphospace, are mainly characterized by an elongated shape, while Carboniferous species seem to explore diverse shapes, being spread across the entire morphospace.

PC2 (13.90% of the cranial variation) represents the variation in shape and orientation of the opercular series (Figure 5b). In species such as *Cycloptychius concentricus*, the opercular bones are narrow and more rectangular in shape, whereas in *Gyrolepidotus schmidti*, they are more square. There is no remarkable shift in shape between Devonian and Carboniferous species across this axis.

Finally, PC3 (10.23% of the cranial variation) mainly represents a difference in the shape of the snout (Figure 5b). In *Tanyrhinichthys mcallisteri*, the snout is elongated and extends in front of the mouth (ventrally oriented mouth), whereas in *Cheirolepis canadensis*, the snout is short and terminal (terminal or dorsally oriented mouth). However, this axis seems driven by two species (*Tanyrhinichthys mcallisteri* and *Tegeolepis clarcki*) that differ greatly from all the others packed together. Thus, it seems to represent the variation in skull shape induced by extreme morphologies present in a few unusual species.

The disparity of the lateral shape of the skull shows three consecutive periods of increase and decrease through the Devonian and Carboniferous (Figure 4). A first increase in morphological disparity begins during the Eifelian and lasts until it decreases after the Famennian. The second increase starts right after the end of the Devonian and lasts until it decreases again after the Viséan. And finally, the morphological disparity of the skull increases during the Pennsylvanian and lasts until reaching its maximum during the Kasimovian.

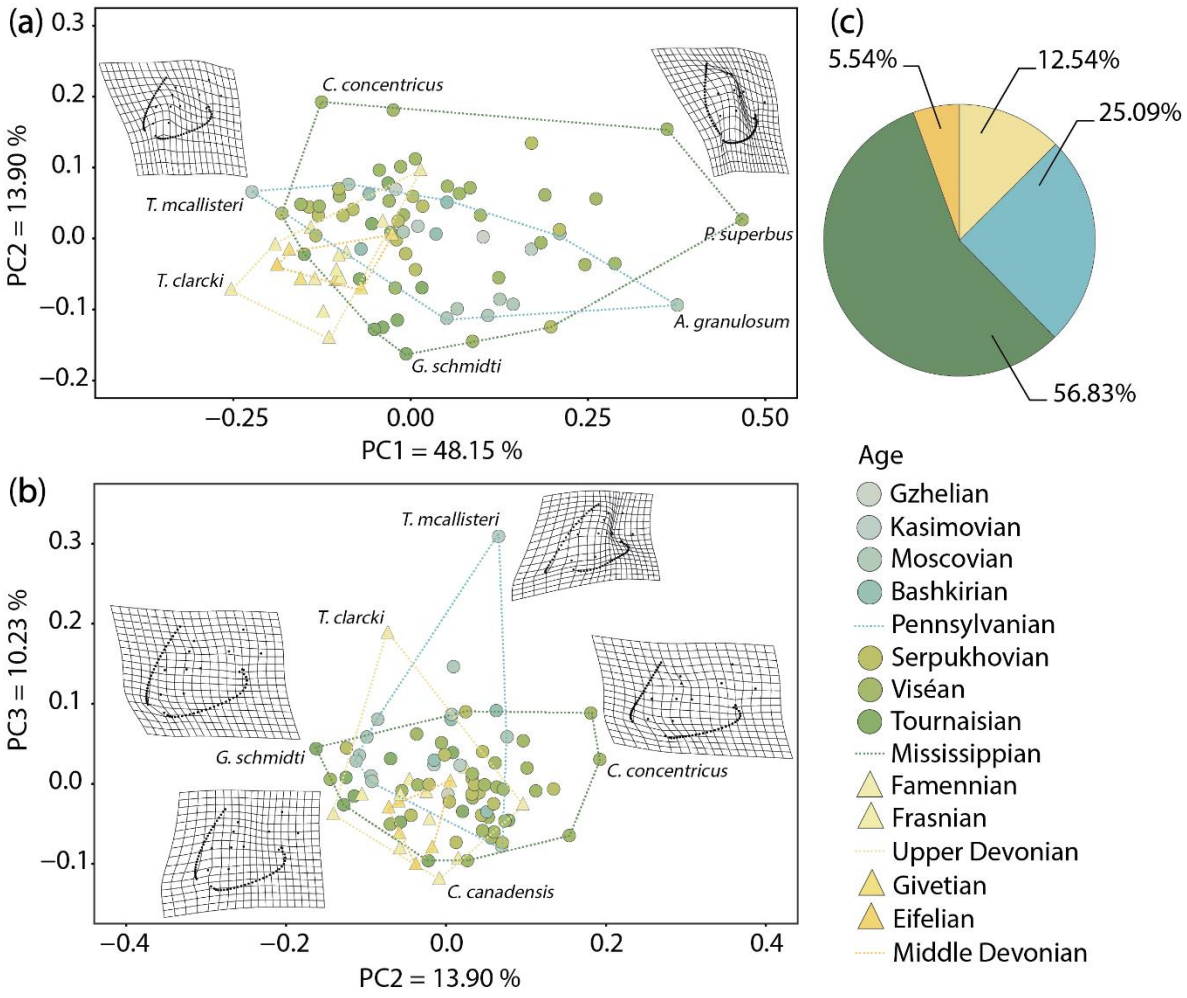


Figure 5. Lateral skull shape morphological disparity of 86 early actinopterygians per age. (**a**) Morphospace of principal components 1 and 2; (**b**) morphospace of principal components 2 and 3. Deformation grids show the differences between the extreme forms along each axis and the mean shape. See Supplementary Figure S4 for the deformation grids of each species; (**c**) The pie charts illustrate the proportion of total disparity each epoch represents based on its respective Procrustes variance.

3.3. Early Actinopterygian Taxonomic Diversity and Morphological Disparity Variation Through Time

The taxonomic diversity of actinopterygians presents one major increase during the Early Carboniferous, reaching maximum richness during the Viséan before decreasing during the Late Carboniferous (Figure 1b). This variation through time is congruent with

what we observed for the morphological disparity of body shape, reaching a maximum during the Viséan (Figure 4). However, it is not entirely congruent with the pattern of variation through time of the morphological disparity of the lateral shape of the skull (Figure 4). The maximum skull disparity is reached during the Kasimovian, when the taxonomic diversity of actinopterygians decreases. We thus have a mismatch between the time of maximum taxonomic diversity and the time of maximum skull morphological disparity. Looking at the major geologic Devonian and Carboniferous events (Figure 4), we can see that the morphological disparity of the body shape dropped with the coral decimation induced by the Kellwasser event at the Frasnian–Famennian boundary and with the tectonic activity at the Mississippian–Pennsylvanian boundary, leading to the formation of Pangea. However, the main body shape disparity increases following the Hangenberg crisis and the loss of dominant groups of aquatic vertebrates (e.g., "placoderms"). Concerning the skull disparity, the Devonian pattern of variation is inverted compared to the body shape disparity. We detected an increase in disparity after the Kellwasser event during the Famennian and a decrease after the Hangenberg crisis. During the Carboniferous, the pattern of morphological disparity of the skull is similar to that of the body shape. A first increase occurred at the same time as the re-emergence of coral reefs, and a second one corresponded to the closure of the Rheic Ocean at the end of the Carboniferous.

3.4. Palaeogeographic Distribution of Early Actinopterygians

Even if the repartition of actinopterygians during the Devonian and Carboniferous varies in latitudes and longitudes, most species occupied waters near the equator or just south of the equator (Figure 6). Most of the variation observed in the species repartition is due to colonization of austral waters during the Late Devonian and Early Carboniferous, which was then limited by the southern ice cover during the Late Carboniferous, after which the species are again concentrated in the equatorial region of Pangea (Annexe II Figure S1).

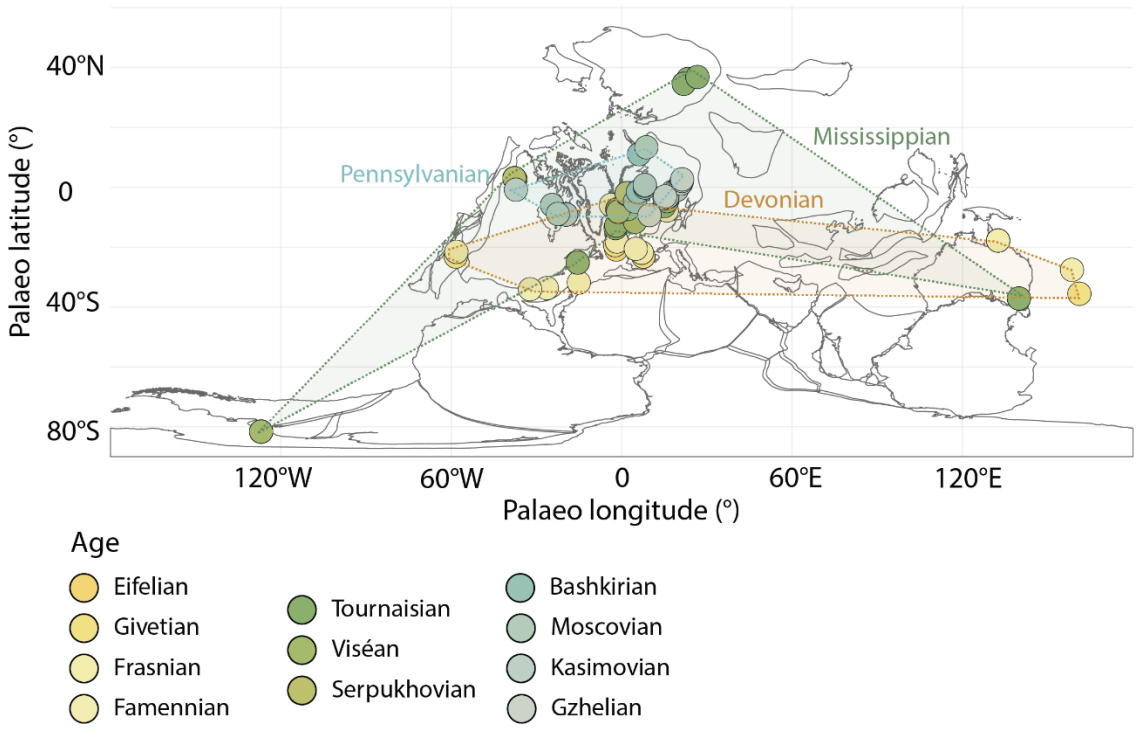


Figure 6. Palaeogeographic distribution of the 106 species of early actinopterygians analyzed based on the reconstruction of their palaeocoordinates. Each dot represents a species included in the analyses. The palaeogeographic reconstruction of the background represents continents 359 million years ago (Devonian–Carboniferous transition) and has been produced with the R package 'sf' [45] and 'rgplates' [43,44].

4. Discussion

The main goal of this study was to explore the putative evolutionary radiation of early actinopterygians by examining the patterns of morphological disparity of body and skull shapes during their first episode of diversification in the Devonian and Carboniferous periods. The variation in taxonomic diversity over time is congruent with the observed morphological disparity of body shape, which reached a maximum during the Viséan (Early Carboniferous), but is not entirely congruent with the pattern of skull disparity. Furthermore, we found patterns of morphological disparity in body and skull shapes to be inverted during the Devonian and similarly during the Carboniferous.

The variation in body shape was best explained by the difference between the elongated and fusiform shapes of Devonian species and the deep and short shapes of Carboniferous species. Most of the variation in skull shape corresponded to a difference between elongated and narrowed skulls, mostly found in Devonian species, and shortened and deep skulls, predominant in Carboniferous species. However, we also detected variation in skull shape not associated with the age of the fish but with differences in the orientation of the opercular series and the mouth.

4.1. Body Shape Disparity Explained by Locomotory Properties and Ecological Opportunities

The most remarkable shape shift in early actinopterygians concerns the emergence of new shapes during the Early Carboniferous. Short and deep bodies arose, such as in the Viséan *Platysomus superbus* [60], in addition to the Devonian elongated and fusiform shapes conserved in Early Carboniferous species, such as in the Serpukhovian *Fubarichthys copiosus* [61]. This change in the general body shape of fish is most likely related to a change in the locomotory mode. Indeed, while locomotion and feeding strategies are often related, the general body shape is primarily constrained by swimming performance [31,33,62], while trophic specializations are more reflected in cranial morphology [37,41].

Fishes move through a dense medium, which involves hydrodynamic constraints [63]. The fish must generate a force to move forward that limits drag [62]. There are two main methods used to generate thrust in extant fish that influence the type of swimming [33,62] that have been recognized among fossil fish [64]. The first one consists of using the undulation of the body and produces steady, straight-line swimming [33,62]. This type of locomotion is often associated with pelagic fishes living in open spaces and travelling long distances [65]. It requires an elongated body to generate sufficient undulations and a fusiform shape to limit drag by being more hydrodynamic [66,67]. The second method relies on median and paired fins to produce the force necessary to move in water [62]. Instead of maximizing the speed, this provides greater maneuverability [68]. This type of locomotion is usually associated with short and deep bodies that are laterally compressed, which help

weave in and out between obstacles, and is mostly found in more complex habitats, such as reefs or kelp forests [33,35]. Although some deep-bodied fishes may have already been present during the Mid-Late Tournaisian [69] and associated with complex structure in wetlands [70], in this study, we found short and deep bodies to arise simultaneously with the re-emergence of the coral reef during the Early Carboniferous [19]. These new complex shallow marine aquatic habitats constituted new ecological opportunities for post-Devonian actinopterygians, which involved new constraints regarding locomotion and differed from what was needed in open waters. This is also supported by the difference in tail shape we observed, with variation in the caudal peduncle proportions. The variation in shape found in the caudal region was the second main source of variation in body shape in our analyses. The caudal fin shape has already been studied for its influence on fossil fish swimming [64,71] and habitat use [35]. Reef fishes tend to have shorter and deeper caudal peduncles, which help rapid starts by using the tail to promote thrust, whereas non-reef fishes tend to have shallower caudal peduncles, which facilitate steady swimming [35]. Finally, this hypothesis is also supported by the size reduction in actinopterygians, observed by Sallan and Galimberti [72], after the end-Devonian crisis. This size reduction could be driven by ecological constraints, especially the emergence of more complex habitats. Indeed, in actual reef systems, small-sized fishes are usually associated with more complexity in the habitat [32].

Thus, the emergence of new habitats during the Early Carboniferous may have contributed to the rapid increase in taxonomic diversity and body shape disparity we detected during the Mississippian by triggering various types of locomotion [73].

4.2. Skull Shape Disparity Explained by Feeding Strategies and Ecological Opportunities

Similarly to body shape, the main source of variation in skull shape corresponds to a difference between elongated and narrow skulls, such as in the Devonian *Tegeolepis clarcki*, compared to shortened and deep skulls, such as in the Carboniferous *Platysomus superbus*. However, even if this axis of variation seemed again to be explained by the age of the species, a great amount of variation was not. The second and third axes of variation represented

differences in the orientation of the opercular series and the mouth, which were not discriminated by age; Devonian and Carboniferous species overlapped. In species such as the Viséan *Cycloptychius concentricus*, the opercular bones are narrow and more rectangular in shape, whereas in the Tournaisian *Gyrolepidotus schmidti*, they are more square. The opercular bones of fish are functionally involved with the jaws and the gill rakers, and differences in their shape could be explained by different feeding strategies [37]. Kimmel et al. [74] found a dynamic evolution in the opercular shape of teleosts, which could reflect adaptations to diverse ecologies.

Regarding the general shape of the snout, the variation was driven by extreme morphologies carried by a few unusual species. In the Kasimovian *Tanyrhinichthys mcallisteri* and the Famennian *Tegeolepis clarcki*, the snout is elongated and extends in front of the mouth (ventrally oriented mouth), whereas in the Frasnian *Cheirolepis canadensis*, the snout is short and terminal. Again, the emergence of new shapes in the Carboniferous morphospace could be related to the different aquatic habitats after the Devonian, which was accompanied by a diversification in feeding strategies [36,39].

Thus, the rapid increase in the skull shape disparity of early actinopterygians is most likely to be an adaptive response to the emergence of new habitats and the loss of competitors during the Early Carboniferous.

4.3. Is There an Early Adaptive Radiation of Actinopterygians?

The main findings of this study regarding the variation in shape of early actinopterygians strongly support the adaptive radiation of the group after the Hangenberg crisis, associated with new habitats and new feeding strategies. We detected major morphological modifications that are most likely adaptations to new ecologies. This radiation may also have been triggered by climatic and geographic factors, which modified the aquatic environment through the Devonian and Carboniferous periods. The post-Hangenberg crisis was marked by the loss of dominant groups of vertebrates [8] and accompanied by profound environmental changes [13]. The beginning of the Late Palaeozoic Ice Age [58] and the formation of Pangea during the Carboniferous [59] deeply impacted the oceanic dynamics

intensified ocean productivity. In recent marine systems, upwellings are known to play a key role in fish assemblages by increasing primary productivity near the coasts [77,78]. In our analyses, actinopterygian diversity and morphological disparity increased during the Early Carboniferous. This rise broadly coincides with Early Mississippian cooling and geochemical evidence for intensified ocean circulation and episodic nutrient upwelling, processes that can enhance nutrient delivery to continental shelves and stimulate marine primary productivity [76,79,80], thereby expanding the ecological opportunity for actinopterygian diversification.

Entering the Late Carboniferous, the collision of Laurussia and Gondwana formed Pangea [59]. This major geological event impacted aquatic diversity by eliminating vast continental shelf environments and modifying ocean circulation [59,81]. In addition, the southern ice cap covered most of the southern region of Pangea, which may have limited the geographic distribution of species and led them to be located around the equator. This may explain the drop in both species diversity and morphological disparity observed in our analyses at the beginning of the Pennsylvanian. The majority of the species included in this study come from formations on the Euramerica continent, which could introduce sampling biases into the species' palaeodistribution interpretation [73,82]. The observed pattern remains meaningful, but must be interpreted cautiously given the uneven sampling among latitudes. Indeed, actinopterygians may have spread to high latitudes early during the Middle Devonian [4], and their absence in the fossil record seems to be mostly due to the lack of systematic collecting efforts [4]. High latitude sites such as the Minusinsk Basin, which have been systematically studied, include several species of actinopterygians [83,84]. Thus, increasing the sampling effort in such regions would contribute to refining palaeodistribution models of early actinopterygians and clarify key evolutionary transitions in the group by revealing a preserved cryptic diversity [82], which could test the stability of the trends observed here.

Finally, the time of the first increase in skull disparity does not correspond to the time of the first increase in body shape disparity. Indeed, skull shape appeared to diversify before body shape, during the Late Devonian. This discrepancy between the two systems is

congruent with what Sallan and Friedman observed [22] and with Igielman et al. (2025) [85], who found a substantial jaw disparity among early actinopterygians from the Devonian and exposed great mandible and dentition variations. Furthermore, the early history of the clade remains uncertain due to the limited number of fossils from actinopterygian species from the Late Devonian. Giles et al. (2023) [86] demonstrated that recent new species described from the Late Devonian may suggest a diversification of the group before the Mass extinction event, which may have acted as a bottleneck event for the surviving lineages, which rapidly diversified during the Early Carboniferous. Still, our findings challenge the "radiation-in-stages" proposed by Streelman and Danley [38] as a general model for vertebrate evolution in which the first stage of radiation is triggered by divergence in habitats, usually associated with the apparition of new ecomorphs, and then followed by a divergence in the trophic strategies associated with modifications of morphological elements of the feeding system. Our results support a trophic divergence, witnessed by early skull and jaw diversification in the group, as the first factor for the diversification of actinopterygians at the Devonian–Carboniferous transition.

5. Conclusions

The mid-Paleozoic period was a time of remarkable changes in actinopterygian evolutionary history. The transition between the Devonian and the Carboniferous constitutes the time of the first actinopterygian diversification, which most likely corresponds to their first evolutionary radiation. By exploring their morphological disparity, we found strong support for an adaptive radiation triggered by new ecological opportunities. Major geographic and climatic events marked this transition, with the beginning of the Late Paleozoic Ice Age and the formation of Pangea, which directly impacted ocean circulation and aquatic habitats. Actinopterygians may have then thrived in the new habitats, developing adaptations to new life modes. We found that trophic divergence is most likely the main diversification factor, with morphological variation associated with the feeding apparatus and locomotion mode. Further investigation of aquatic habitats and interspecific interactions

could help strengthen our understanding of this event, which marks the first diversification of the most diverse group of extant vertebrates.

Author Contributions: O.V. and R.C. conceptualized the study and established the research goals. O.V. designed the study and the methodology frameworks, acquired the data, performed the analyses and created the visualizations. O.V. wrote and revised the original draft. R.C. supervised and reviewed. All authors have read and agreed to the published version of the manuscript.

Funding: O.V. was funded by Fonds de recherche du Québec—Nature et Technologies (FRQNT), [https://doi.org/10.69777/325538] and R.C. was funded by Natural Sciences and Engineering Research Council of Canada (NSERC) Discovery grants 06133 and 05887. Institutional Review Board Statement: Not applicable. Data

Availability Statement: Data and code are available on GitHub: https://github.com/oliviavanhaesebroucke/Early-actinopterygians-disparity (accessed on 26 January 2026).

Acknowledgments: We thank L. Houle (UQAR) for his statistical advice and support. We thank O. Larouche (Western University) for his advice about methodology. We thank Mahasarakham University for its support during the RC visit.

Conflicts of Interest: The authors declare no conflicts of interest. The funders had no role in the design of the study; in the collection, analyses or interpretation of data; in the writing of the manuscript; or in the decision to publish the results.

6. References

1. Fricke, R. Eschmeyer's Catalog of Fishes: Genera/Species by Family/Subfamily; Electronic Version Accessed; California Academy of Sciences: San Francisco, CA, USA, 2021.

2. Zhu, M.; Zhao, W.; Jia, L.; Lu, J.; Qiao, T.; Qu, Q. The oldest articulated osteichthyan reveals mosaic gnathostome characters. *Nature* **2009**, 458, 469–474.

3. Zhu, M.; Wang, W.; Yu, X. *Meemannia eos*, a basal sarcopterygian fish from the Lower Devonian of China – expanded description and significance. In *Morphology, Phylogeny and Paleobiogeography of Fossil Fishes*; Elliott, D.K., Maisey, J.G., Yu, X., Miao, D., Eds.; Verlag Dr. Friedrich Pfeil: München, Germany, **2010**; pp. 199–214.

4. Figueroa, R.T.; Weinschütz, L.C.; Friedman, M. The oldest Devonian circumpolar ray-finned fish? *Biol. Lett.* **2021**, 17, 20200766.

5. Schultze, H.-P.; Cumbaa, S.L. *Dialipina* and the characters of basal actinopterygians. In *Major Events in Early Vertebrate Evolution*; Ahlberg, E., Ed.; CRC Press: London, UK, **2001**; p. 448.

6. Pearson, D.M.; Westoll, T.S. The Devonian actinopterygian *Cheirolepis agassiz*. *Earth Environ. Sci. Trans. Roy. Soc. Edinb.* **1979**, 70, 337–399.

7. Arratia, G.; Cloutier, R. Reassessment of the morphology of *Cheirolepis canadensis* (Cheirolepididae: Actinopterygii). In *Devonian Fishes and Plants of Miguasha, Québec, Canada*; Schultze, H.P., Cloutier, R., Eds.; Verlag Dr. Friedrich Pfeil: München, Germany, **1996**; pp. 165–197.

8. Sallan, L.C.; Coates, M.I. End-Devonian extinction and a bottleneck in the early evolution of modern jawed vertebrates. *Proc. Natl. Acad. Sci. USA* **2010**, 107, 10131–10135.

9. Cloutier, R.; Arratia, G. Early diversification of actinopterygians. *In Recent Advances in the Origin and Early Radiation of Vertebrate*; Arratia, G., Wilson, M.V.H., Cloutier, R., Eds.; Verlag Dr. Friedrich Pfeil: München, Germany, **2004**; pp. 217–270.

10. Choo, B.; Long, J.A.; Trinajstic, K.A. New genus and species of basal actinopterygian fish from the Upper Devonian Gogo Formation of Western Australia. *Acta Zool.* **2009**, 90, 194–210.

11. Vanhaesebroucke, O.; Larouche, O.; Cloutier, R. Early sarcopterygian morphological disparity through the Devonian-Carboniferous crisis. *Sci. Rep.* **2025**, 16, 1623.

12. Carmichael, S.K.; Waters, J.A.; Königshof, P.; Suttner, T.J.; Kido, E. Paleogeography and paleoenvironments of the Late Devonian Kellwasser Event: A review of its sedimentological and geochemical expression. *Glob. Planet. Change* **2019**, 183, 102984.

13. Kaiser, S.I.; Aretz, M.; Becker, R.T. The global Hangenberg crisis (Devonian–Carboniferous transition): Review of a first-order mass extinction. In *Devonian Climate, Sea Level and Evolutionary Events*; Becker, R.T., Königshof, P., Brett, C.E., Eds.; Geological Society of London: London, UK, **2016**; Volume 423, pp. 1–10.

14. Bambach, R.K.; Knoll, A.H.; Wang, S.C. Origination, extinction, and mass depletions of marine diversity. *Paleobiology* **2004**, 30, 522–542.

15. Young, G.C. Placoderms (Armored Fish): Dominant vertebrates of the Devonian Period. *Annu. Rev. Earth Planet. Sci.* **2010**, 38, 523–550.

16. Aretz, M.; Corradini, C.; Denayer, J. The Devonian-Carboniferous boundary around the globe: A complement. *Palaeobio. Palaeoenv.* **2021**, 101, 633–662.

17. Derycke, C.; Olive, S.; Groessens, E.; Goujet, D. Paleogeographical and paleoecological constraints on Paleozoic vertebrates (Chondrichthyans and Placoderms) in the Ardenne Massif: Shark radiations in the Famennian on both sides of the Palaeotethys. *Palaeogeogr. Palaeoclim. Palaeoecol.* 2014, 414, 61–67.

18. Grogan, E.; Lund, R. The geological and biological environment of the Bear Gulch Limestone (Mississippian of Montana, USA) and a model for its deposition. *Geodiversitas* 2002, 24, 295–315.

19. Yao, L.; Aretz, M.; Wignall, P.B.; Chen, J.; Vachard, D.; Qi, Y.; Shen, S.; Wang, X. The longest delay: Re-emergence of coral reef ecosystems after the Late Devonian extinctions. *Earth Sci. Rev.* 2020, 203, 103060.

20. Lund, R.; Greenfest-Allen, E.; Grogan, E.D. Ecomorphology of the Mississippian fishes of the Bear Gulch Limestone (Heath Formation, Montana, USA). *Environ. Biol. Fishes* 2015, 98, 739–754.

21. Henderson, S.; Dunne, E.M.; Fasey, S.A.; Giles, S. The early diversification of ray-finned fishes (Actinopterygii): Hypotheses, challenges and future prospects. *Biol. Rev.* 2023, 98, 284–315.

22. Sallan, L.C.; Friedman, M. Heads or tails: Staged diversification in vertebrate evolutionary radiations. *Proc. R. Soc. B* 2011, 279, 2025–2032.

23. Giles, S.; Xu, G.-H.; Near, T.J.; Friedman, M. Early members of 'living fossil' lineage imply later origin of modern ray-finned fishes. *Nature* 2017, 549, 265–268.

24. Simpson, G.G. The Major Features of Evolution; Columbia University Press: New York, NY, USA; Chichester, UK, 1953; p. 434.

25. Harmon, L.J.; Schulte, J.A.; Larson, A.; Losos, J.B. Tempo and mode of evolutionary radiation in iguanian lizards. *Science* **2003**, 301, 961–964.

26. Monteiro, L.R.; Nogueira, M.R. Evolutionary patterns and processes in the radiation of Phyllostomid bats. *BMC Evol. Biol.* **2011**, 11, 137.

27. Gavrilets, S.; Losos, J.B. Adaptive radiation: Contrasting theory with data. *Science* **2009**, 323, 732–737.

28. McMillan, W.O.; Palumbi, S.R. Concordant evolutionary patterns among Indo-West pacific butterflyfishes. *Proc. R. Soc. B* **1997**, 260, 229–236.

29. Simões, M.; Breitkreuz, L.; Alvarado, M.; Baca, S.; Cooper, J.C.; Heins, L.; Herzog, K.; Lieberman, B.S. The evolving theory of evolutionary radiations. *Trends Ecol. Evol.* **2016**, 31, 27–34.

30. Foote, M. Discordance and concordance between morphological and taxonomic diversity. *Paleobiology* **1993**, 19, 185–204.

31. Langerhans, R.B.; Layman, C.A.; Langerhans, A.K.; Dewitt, T.J. Habitat-associated morphological divergence in two neotropical fish species. *Biol. J. Linn. Soc.* **2003**, 80, 689–698.

32. Alvarez-Filip, L.; Gill, J.A.; Dulvy, N.K. Complex reef architecture supports more small-bodied fishes and longer food chains on Caribbean reefs. *Ecosphere* **2011**, 2, 1–17.

33. Friedman, S.T.; Price, S.A.; Wainwright, P.C. The effect of locomotion mode on body shape evolution in teleost fishes. *IOB* **2021**, 3, obab016.

34. Price, S.A.; Friedman, S.T.; Corn, K.A.; Martinez, C.M.; Larouche, O.; Wainwright, P.C. Building a body shape morphospace of teleostean fishes. *Integr. Comp. Biol.* **2019**, 59, 716–730.

35. Larouche, O.; Benton, B.; Corn, K.; Friedman, S.; Gross, D.; Iwan, M.; Kessler, B.; Martinez, C.; Rodriguez, S.; Whelpley, H.; et al. Reef-associated fishes have more maneuverable body shapes at a macroevolutionary scale. *Coral Reefs* **2020**, 39, 1427–1439.

36. Westneat, M.W. Skull biomechanics and suction feeding in fishes. In *Fish Physiology*; Shadwick, R.E., Lauder, G.V., Eds.; Academic Press: Cambridge, MA, USA, **2005**; Volume 23, pp. 29–75.

37. Gidmark, N.J.; Pos, K.; Matheson, B.; Ponce, E.; Westneat, M.W. Functional morphology and biomechanics of feeding in fishes. In *Feeding in Vertebrates: Evolution, Morphology, Behavior, Biomechanics*; Bels, V., Whishaw, I.Q., Eds.; Springer International Publishing: Cham, Switzerland, **2019**; pp. 297–332.

38. Streelman, J.T.; Danley, P.D. The stages of vertebrate evolutionary radiation. *Trends Ecol. Evol*. **2003**, 18, 126–131.

39. Friedman, M.; Pierce, S.E.; Coates, M.; Giles, S. Feeding structures in the ray-finned fish *Eurynotus crenatus* (Actinopterygii: Eurynotiformes): Implications for trophic diversification among Carboniferous actinopterygians. *Earth Environ. Sci. Trans. Roy. Soc. Edinb.* **2018**, 109, 33–47.

40. Lombardo, C.; Tintori, A. Feeding specializations in Late Triassic fishes. *Sez. Museol. Sci. E Nat.* **2005**, 2005, 25–32.

41. Schultze, H.-P.; Mickle, K.E.; Poplin, C.; Hilton, E.J.; Grande, L. Handbook of Paleoichthyology: Actinopterygii I; Verlag Dr. Friedrich Pfeil.: München, Germany, **2021**; Volume 8A, p. 299.

42. Kocsis, Á.T.; Reddin, C.J.; Alroy, J.; Kiessling, W. The R package divDyn for quantifying diversity dynamics using fossil sampling data. *Methods Ecol. Evol.* **2019**, 10, 735–743.

43. Müller, R.D.; Cannon, J.; Qin, X.; Watson, R.J.; Gurnis, M.; Williams, S.; Pfaffelmoser, T.; Seton, M.; Russell, S.H.J.; Zahirovic, S. GPlates: Building a virtual earth through deep time. *Geochem. Geophys. Geosyst.* **2018**, 19, 2243–2261.

44. Kocsis, A.T.; Raja, N.B.; Williams, S.; Dowding, E.M. Rgplates: R Interface for the GPlates Web Service and Desktop Application. Zenodo **2025**.

45. Pebesma, E.; Bivand, R. (Eds.) Spatial Data Science: With Applications in R; Chapman and Hall/CRC: New York, NY, USA, **2023**; p. 314.

46. Scotese, C.R. PALEOMAP PaleoAtlas for GPlates–EarthByte. Available online: https://www.earthbyte.org/paleomap-paleoatlasfor-gplates/ (accessed on 20 November 2025).

47. Adams, D.C.; Otárola-Castillo, E. Geomorph: An R package for the collection and analysis of geometric morphometric shape data. *Methods Ecol. Evol.* **2013**, 4, 393–399.

48. Gunz, P.; Mitteroecker, P. Semilandmarks: A method for quantifying curves and surfaces. *Hystrix* **2013**, 24, 103–109.

49. Guillerme, T.; Cooper, N.; Brusatte, S.L.; Davis, K.E.; Jackson, A.L.; Gerber, S.; Goswami, A.; Healy, K.; Hopkins, M.J.; Jones, M.E.H.; et al. Disparities in the analysis of morphological disparity. *Biol. Lett.* **2020**, 16, 20200199.

50. R Core Team. R: A Language and Environment for Statistical Computing. **2023**. Available online: https://www.R-project.org/.

51. Ledesma, R.D.; Valero-Mora, P.; Macbeth, G. The scree test and the number of factors: A dynamic graphics approach. *Span. J. Psychol.* **2015**, 18, E11.

52. Joliffe, I.; Morgan, B. Principal component analysis and exploratory factor analysis. *Stat. Methods Med. Res.* **1992**, 1, 69–95.

53. Cohen, K.; Harper, D.; Gibbard, P.; Car, N. The ICS International Chronostratigraphic Chart this Decade. Episodes **2025**, 48, 105–115.

54. Guillerme, T. dispRity: A modular R package for measuring disparity. *Methods Ecol. Evol.* **2018**, 9, 1755–1763.

55. Bridge, T.C.L.; Baird, A.H.; Pandolfi, J.M.; McWilliam, M.J.; Zapalski, M.K. Functional consequences of Palaeozoic reef collapse. *Sci. Rep.* **2022**, 12, 1386.

56. Oliver, W.A. Extinctions and migrations of Devonian rugose corals in the Eastern Americas Realm. *Lethaia* **1990**, 23, 167–178.

57. Kershaw, S.; Jeon, J. Stromatoporoids and extinctions: A review. *Earth-Sci. Rev.* **2024**, 252, 104721.

58. Fielding, C.R.; Frank, T.D.; Isbell, J.L. The Late Paleozoic Ice Age—A review of current understanding and synthesis of global climate patterns. In *Resolving the Late Paleozoic Ice Age in Time and Space*; Fielding, C.R., Frank, T.D., Isbell, J.L., Eds.; Geological Society of America: Boulder, CO, USA, **2008**; p. 354.

59. Stampfli, G.M.; Hochard, C.; Vérard, C.; Wilhem, C.; von Raumer, J. The formation of Pangea. *Tectonophysics* **2013**, 593, 1–19.

60. Traquair, R.H.X. On the structure and affinities of the Platysomidæ. *Earth Environ. Sci. Trans. Roy. Soc. Edinb.* **1880**, 29, 343–391.

61. Lowney, K.A. Certain Bear Gulch (Namurian A, Montana) Actinopterygii (Osteichthyes) and a reevaluation of the evolution of the Paleozoic actinopterygians. Ph.D. Thesis, New York University, New York, NY, USA, **1980**. Available online:

https://www.proquest.com/docview/303023402/abstract/2968AFFF3D2546BDPQ/1 (accessed on 20 November 2025).

62. Sfakiotakis, M.; Lane, D.M.; Davies, J.B.C. Review of fish swimming modes for aquatic locomotion. *IEEE J. Ocean. Eng.* **1999**, 24, 237–252.

63. Lindsey, C.C. Form, function, and locomotory habits in fish. In *Fish Physiology*; Academic Press: Cambridge, MA, USA, **1978**; Volume 7, pp. 1–100.

64. Fletcher, T.; Altringham, J.; Peakall, J.; Wignall, P.; Dorrell, R. Hydrodynamics of fossil fishes. *Proc. R. Soc. B: Biol. Sci.* **2014**, 281, 20140703.

65. Di Santo, V.; Goerig, E.; Wainwright, D.K.; Akanyeti, O.; Liao, J.C.; Castro-Santos, T.; Lauder, G.V. Convergence of undulatory swimming kinematics across a diversity of fishes. *Proc. Natl. Acad. Sci. USA* **2021**, 118, e2113206118.

66. Liu, Y.; Jiang, H.; Liu, Y.; Jiang, H. Optimum curvature characteristics of body/caudal fin locomotion. *J. Mar. Sci. Eng.* **2021**, 9, 537.

67. Chen, J.; Friesen, W.O.; Iwasaki, T. Mechanisms underlying rhythmic locomotion: Body–fluid interaction in undulatory swimming. *J. Exp. Biol.* **2011**, 214, 561–574.

68. Schakmann, M.; Korsmeyer, K.E. Fish swimming mode and body morphology affect the energetics of swimming in a wave-surge water flow. *J. Exp. Biol.* **2023**, 226, jeb244739.

69. Wilson, C.D.; Pardo, J.D.; Anderson, J.S. A primitive actinopterygian braincase from the Tournaisian of Nova Scotia. *R. Soc. Open Sci.* **2018**, 5, 171727.

70. Rygel, M.C.; Calder, J.H.; Gibling, M.R.; Gingras, M.K.; Melrose, C.S.A. Tournaisian forested wetlands in the Horton Group of Atlantic Canada. In *Wetlands Through Time*; Greb, S.F., DiMichele, W.A., Eds.; Geological Society of America: Boulder, CO, USA, **2006**; 332p.

71. Zhong, Y.; Wu, J.; Wang, C.; Li, Y.; Song, J. Hydrodynamic effects of the caudal fin shape of fish in carangiform undulatory swimming. *Proc. Inst. Mech. Eng. C* **2022**, 236, 6385–6394.

72. Sallan, L.; Galimberti, A.K. Body-size reduction in vertebrates following the End-Devonian mass extinction. *Science* **2015**, 350, 812–815.

73. Flannery-Sutherland, J.T.; Henderson, S.; Fasey, S.A.; Giles, S. Diversification dynamics of the Palaeozoic actinopterygian radiation. *bioRxiv* **2025**, bioRxiv:2025.04.14.648759.

74. Kimmel, C.B.; Small, C.M.; Knope, M.L. A Rich diversity of opercle bone shape among teleost fishes. *PLoS ONE* **2017**, 12, e0188888.

75. Lakin, J.A.; Marshall, J.E.A.; Troth, I.; Harding, I.C. Greenhouse to Icehouse: A biostratigraphic review of latest Devonian– Mississippian glaciations and their global effects. In *Devonian Climate, Sea Level and Evolutionary Events*; Becker, R.T., Königshof, P., Brett, C.E., Eds.; Geological Society of London: London, UK, **2016**; Volume 423, p. 481.

76. Liu, J.; Algeo, T.J.; Qie, W.; Saltzman, M.R. Intensified oceanic circulation during Early Carboniferous cooling events: Evidence from Carbon and Nitrogen isotopes. *Palaeogeogr. Palaeoclim. Palaeoecol*. **2019**, 531, 108962.

77. Eisele, M.H.; Madrigal-Mora, S.; Espinoza, M. Drivers of reef fish assemblages in an upwelling region from the eastern tropical Pacific ocean. *J. Fish Biol.* **2021**, 98, 1074–1090.

78. Lopez-Lopez, L.; Preciado, I.; Muñoz, I.; Decima, M.; Molinero, J.C.; Tel, E. Does upwelling intensity influence feeding habits and trophic position of planktivorous fish? *Deep. Sea Res. Part I Oceanogr. Res. Pap.* **2017**, 122, 29–40.

79. Cheng, K.; Elrick, M.; Romaniello, S.J. Early Mississippian ocean anoxia triggered organic Carbon burial and Late Paleozoic cooling: Evidence from Uranium isotopes recorded in marine limestone. *Geology* **2020**, 48, 363–367.

80. Perkins, R.B.; Piper, D.Z.; Mason, C.E. Trace-element budgets in the Ohio/Sunbury Shales of Kentucky: Constraints on ocean circulation and primary productivity in the Devonian–Mississippian Appalachian Basin. *Palaeogeogr. Palaeoclim. Palaeoecol.* **2008**, 265, 14–29.

81. Golonka, J.; Ford, D. Pangean (Late Carboniferous–Middle Jurassic) paleoenvironment and lithofacies. *Palaeogeogr. Palaeoclim. Palaeoecol.* **2000**, 161, 1–34.

82. Henderson, S.; Dunne, E.M.; Giles, S. Sampling biases obscure the early diversification of the largest living vertebrate group. *Proc. R. Soc. B Biol. Sci.* **2022**, 289, 20220916.

83. Kazantseva, A.A. Palaeoniscids of Bystraia Formation of the Minusinsk Troughs. In *Ocherki po filogenii I Sistematike Iskopaemykh Ryb I Bezcheliustnykh*; Nauka: Moscow, Russia, **1968**; pp. 87–112.

84. Matveeva, A.A. Palaeoniscids from the Izyk-Chul' Horizon of the Minusinsk Depression. *Vopr. Ikhtiol.* **1958**, 11, 154–161.

85. Igielman, B.; Figueroa, R.T.; Higgins, R.R.; Pierce, S.E.; Coates, M.I.; Troyer, E.M.; Fernandez, V.; Dollman, K.; Lu, J.; Zhu, M.; et al. The lower jaw of Devonian ray-finned fishes (Actinopterygii): Anatomy, relationships, and functional morphology. *Anat. Record.* **2025**.

86. Giles, S.; Feilich, K.; Warnock, R.C.M.; Pierce, S.E.; Friedman, M. A Late Devonian actinopterygian suggests high lineage survivorship across the End-Devonian Mass Extinction. *Nat. Ecol. Evol*. **2023**, 7, 10–19.

CHAPITRE 2

LA DISPARITÉ MORPHOLOGIQUE DES SARCOPTÉRYGIENS BASAUX AU TRAVERS DE LA CRISE DU DÉVONIEN-CARBONIFÈRE

2.1 RÉSUMÉ EN FRANÇAIS DU DEUXIÈME ARTICLE

Des adaptations morphologiques majeures ont caractérisé le début de l'histoire évolutive des sarcoptérygiens durant la période du Dévonien (419 – 359 Ma) et du Carbonifère (359 – 299 Ma), ponctuée de changements environnementaux et de crises de la biodiversité. Nous présentons ici une analyse en morphométrie géométrique de la morphologie des premiers sarcoptérygiens afin d'explorer l'impact des contraintes environnementales et phylogénétiques sur leur morphologie. Ces trois analyses reposent sur la digitalisation de points de référence homologues (« landmarks ») et de points de référence semi-homologues (« semi-landmarks ») en deux dimensions sur des reconstructions paléontologiques du corps complet, de la joue et du toit crânien. Des changements majeurs de la forme semblent associés à des changements géologiques et biologiques entre le Dévonien supérieur et le Carbonifère inférieur (Mississippien). Une augmentation de la diversité de formes se produit durant le Dévonien moyen, période marquée par l'apparition des premières forêts, qui ont fortement influencé les milieux d'eau douce et transitionnels, ainsi que par le pic de diversification des écosystèmes récifaux. La disparité du toit crânien et de la joue diminue lors de l'extinction massive de la fin du Dévonien, avant de se rétablir au cours du Mississippien moyen et supérieur, avec la réémergence des récifs métazoaires et la diversification des groupes survivants tels que les actinistiens. La disparité du toit crânien est principalement associée à l'héritage phylogénétique et semble majoritairement influencée par l'absence du joint intracrânien chez les dipneustes et les tétrapodes. Les changements environnementaux survenus entre le Dévonien et le Carbonifère constituent un tournant majeur dans l'histoire évolutive des premiers sarcoptérygiens, en ayant profondément impacté leur disparité morphologique.

Cet article, intitulé « *Early sarcopterygian morphological disparity through the Devonian-Carboniferous crisis* », a été publié dans *Scientific Reports* en Décembre 2025 dans une collection spéciale sur la biodiversité et l'évolution des poissons (*Fish biodiversity and evolution*, J.S. Albert, P. Chakrabarty and R. Betancur-R, éditeurs). En tant que première auteure, j'ai contribué à l'élaboration du projet et de sa méthodologie. J'ai réalisé la collecte de données, les analyses statistiques, les visuels et écrit la première version du manuscrit. Le docteur Olivier Larouche, second auteur, a supervisé les analyses, a participé à la revue de littérature et à la révision de l'article. Le professeur Richard Cloutier, troisième auteur, a participé à l'élaboration du projet ainsi qu'à la révision de l'article. Une version abrégée de l'article a aussi été présentée au *4th Palaeontological Virtual Congress* en ligne en Mai 2023.

Ce projet a été financé par une bourse des Fonds de recherche du Québec – Nature et Technologies (FRQNT) [https://doi.org/10.69777/325538] que j'ai reçue pour mon doctorat et par les subventions (06133 et 05887) du Conseil de Recherches en Sciences Naturelles et en Génie du Canada (CRSNG) du professeur Richard Cloutier.

2.2 EARLY SARCOPTERYGIAN MORPHOLOGICAL DISPARITY THROUGH THE DEVONIAN-CARBONIFEROUS CRISIS

Olivia Vanhaesebroucke[1], Olivier Larouche[2] and Richard Cloutier[1,3]

[1] Département de Biologie, Chimie et Géographie, Université du Québec à Rimouski, Rimouski, QC, Canada.

[2] Western Carolina University, Biology Department, Cullowhee, North Carolina, United States of America

[3] Center of Excellence on the Evolution of Life, Basin Studies and Applied Paleontology, Paleontological Research and Education Center, Mahasarakham University, Maha Sarakham 44150, Thailand.

Major morphological adaptations characterized the early evolutionary history of sarcopterygians during the Devonian (419–359 Ma) and the Carboniferous (359–299 Ma), punctuated by environmental changes and biodiversity crises. Here we present geometric morphometrics analyses of early sarcopterygian morphology to explore the impact of environmental and phylogenetic constraints on their morphology. Three analyses were performed by digitizing 2D landmarks and semi-landmarks on palaeontological reconstructions of the body shape, cheek, and skull roof. Major changes in shape seem associated with geological and biological changes from the Late Devonian and Early Carboniferous (Mississippian). An increase in shape diversity occurred during the Middle Devonian, when the first forests appeared, influencing freshwater and transitional environments, and when reef ecosystems were the most diversified. Skull roof and cheek disparity decrease during the end-Devonian mass extinction and recover during the Mid-Late Mississippian, with the reemergence of metazoan reefs and the rise of surviving groups such as actinistians. The skull roof disparity is associated primarily with shared ancestry and appears to be largely driven by the lack of an intracranial joint in dipnoans and tetrapods. The Devonian to Carboniferous environmental changes constitute a major turning point in early sarcopterygian history by having deeply impacted their morphological disparity.

Key-words: End-Devonian crisis, Palaeoenvironments, Palaeozoic, Geometric morphometrics, Reefs emergence, Tetrapod-like fishes

Sarcopterygians are a group of diverse jawed vertebrates, with its current piscine representatives being the "lobed-finned fishes," the actinistians (or coelacanths, two species) and lungfishes (six species), but which also includes all tetrapods, representing approximately 35,500 species[1]. The first occurrence of sarcopterygians in the fossil record dates back to the middle Silurian (Ludlow stage; 427.4–423.0 Ma), with Guiyu oneiros as the earliest known articulated specimen[2]. Sarcopterygians diversified during the late Silurian (427.4–419.2 Ma) and Lower Devonian (419.2–393.3 Ma), dominating this era's vertebrate diversity along with "placoderms" (armoured fishes)[3]. During the Middle–Late Devonian (393.3–358.9 Ma), terrestrial habitats increased in complexity with the emergence of the first forests and the diversification of terrestrial arthropods, including insects[4,5]. Around that time, a new lineage of tetrapod-like fishes arose within sarcopterygians, the "elpistostegalians," including Panderichthys[6], Qikiqtania[7] and Tiktaalik[8]. From the end of the Devonian through the Carboniferous, tetrapods greatly diversified as they colonized a spectrum of terrestrial habitats[9,10], while piscine sarcopterygian diversity decreased[3]. This shift in sarcopterygian diversity and ecology chronologically correlates with geographic changes associated with the Devonian–Carboniferous transition, especially the Kellwasser (Frasnian–Famennian boundary, 371 Ma) and Hangenberg (Devonian–Carboniferous boundary, 359 Ma) events that constitute the end-Devonian mass extinction[11–13]. Indeed, modifications to the atmospheric composition[14], the amplitude of the tides[15] and sea level variations[16], the formation of inland seas resulting from tectonic activity[11], and the formation of large carbonate platforms[17] all impacted the diversity of shallow aquatic habitats and may have played an important role in the diversification of early jawed vertebrates, including sarcopterygians, and their morphology[18,19]. The following Carboniferous period was a time of deep recovery, especially for the marine habitat, with the reemergence of metazoan coral reefs[20] that created new ecological niches for the surviving sarcopterygian lineages.

The present study aims to explore the major eco-morphological modifications in the postcranial and cranial anatomy of early sarcopterygians from the Devonian and Carboniferous, and the relationships of these modifications to palaeoenvironmental data and phylogenetic relationships. As tetrapod-like sarcopterygians initiated a water-to-land

transition, we expect to detect a major change in the morphospace occupation for these taxa related to their drastic change of environment[21]. Although among sarcopterygians, only tetrapods conquered the land, their aquatic close relatives are likely to exhibit a set of shared adaptations that would eventually facilitate this transition. This period is also marked by major biodiversity crises ranging from the late Middle Devonian to the Early Carboniferous. We then expect to find the general pattern of morphological disparity variation to coincide with these crisis events. Finally, early sarcopterygians inhabited various aquatic habitats, with some taxa associated with freshwater environments while others were predominantly found in marine systems[22–24]. Transitions between marine and freshwater habitats have happened several times during the evolutionary history of fishes[25,26]. Considering the chemo-physical and structural differences between these two environments[25,26], we also expect to detect differences in morphological disparity related to the types of aquatic habitats occupied by early sarcopterygians.

Methods

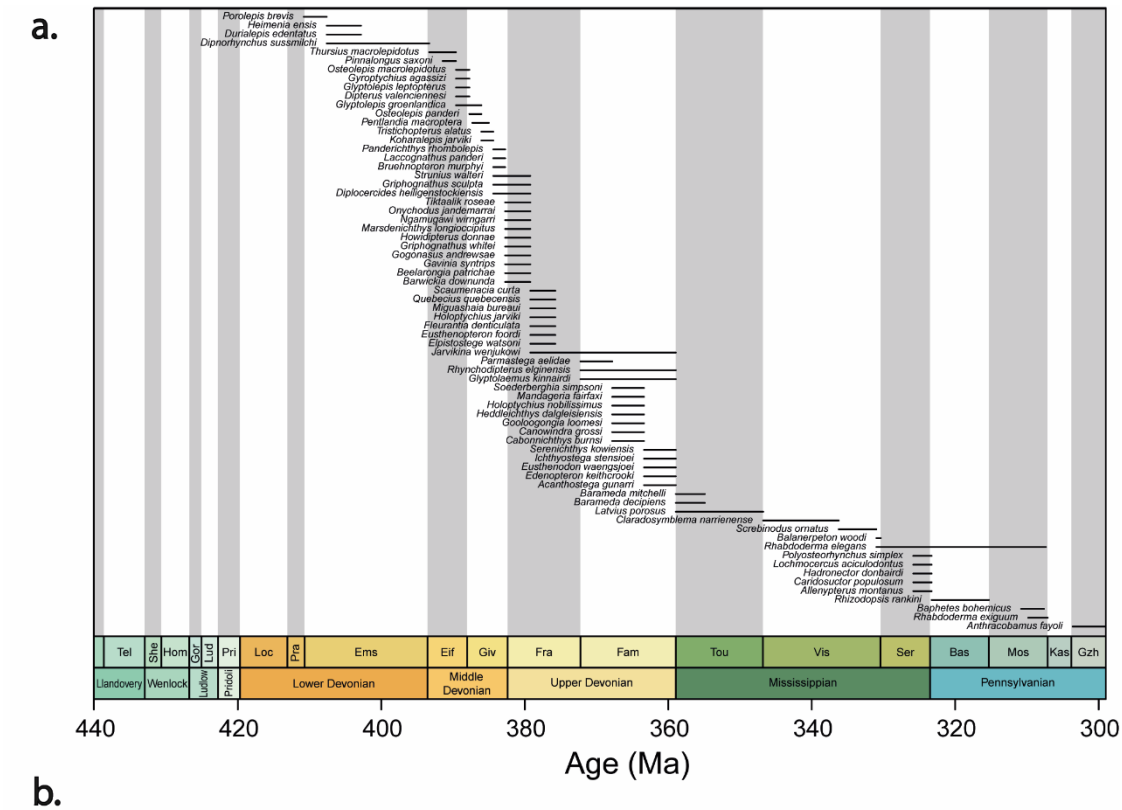
Taxonomic diversity

In order to get an estimate of the taxonomic diversity of early sarcopterygians during the Devonian and the Carboniferous periods, we gathered a list of 279 early sarcopterygian species from previously published databases[3,27] and additional sources from the primary literature. For each species, the first and last occurrence dates were noted (Fig. 1, see Annexe III Table S1). Our time scale sampling goes from the Ludfordian (late Ludlow, 425.6 Ma) to the late Gzhelian (Pennsylvanian, 298.9 Ma), which represents a 126.7 MY time span, and is divided into 7 epochs (Ludlow, Pridoli, Lower Devonian, Middle Devonian, Upper Devonian, Mississippian, and Pennsylvanian). We analysed sarcopterygian diversity with the R package 'divDyn'[28].

Morphological dataset

Two-dimensional datasets are used rather than 3D information because the shape of fossil species is rarely conserved in three dimensions. We therefore assembled three separate

two-dimensional datasets, including a total of 70 species, using palaeontological reconstructions of (1) the entire body shape (n=36), (2) the cheek region (n=39), and (3) the skull roof (n=47) of Devonian and Carboniferous sarcopterygian species (see Annexe III Table S2). Only the species for which adult specimens were identified were compiled. We excluded from the analyses all species known solely from juvenile specimens (with the exception of *Serenichthys kowiensis*). Our full dataset comprises nine different groups of early sarcopterygians: Onychodontida (n=2), Actinistia (coelacanths) (n=12), Porolepiformes (n=9), Dipnoi (n=12), Rhizodontida (n=4), "Osteolepiformes" (n=22), "Elpistostegalia" (n=2), and Tetrapoda (n=7). Palaeoenvironmental data for each studied species were gathered from the literature (see Supplementary material Table S2 online) and included two variables. The first one broadly characterizes the type of aquatic habitats inhabited by early sarcopterygians and comprises three different levels along the salinity gradient: marine (n=16), estuarine (n=9), and freshwater species (n=45). The second variable was meant to capture more precise aspects of the palaeoenvironment of each species whenever sufficient information was available. It includes 10 precise palaeoenvironments: reef (n=5), coastal marine (n=1), bay (n=5), estuary (n=10), lagoon (n=8), fluvial delta (n=1), alluvial plain (n=7), oxbow lake and meandering river (n=7), calm freshwater lake (n=12), and dynamic freshwater lake (n=5). Species for which no precise details on the palaeoenvironment were available were removed from this second analysis.


a.
Porolepis brevis
Heimenia ensis
Durialepis edentatus
Diplorhynchus sussmilchi
Thursius macrolepidotus
Pinnalongus saxorii
Osteolepis macrolepidotus
Gyroptychius agassizi
Glyptolepis leptopterus
Dipterus valenciennesi
Glyptolepis groenlandica
Osteolepis panderi
Pentlandia macroptera
Tristichopterus alatus
Koharalepis jarviki
Panderichthys rhombolepis
Laccognathus panderi
Bruehnopteron murphyi
Strunius walteri
Griphognathus sculpta
Diplocercides heiligenstockiensis
Tiktaalik roseae
Onychodus jandemarrai
Ngamugawi wirngarri
Marsdenichthys longioccipitus
Howidipterus donnae
Griphognathus whitei
Gogonasus andrewsae
Gavinia syntrips
Beelarongia patrichae
Barwickia downunda
Scaumenacia curta
Quebecicus quebecensis
Miguashaia bureaui
Holoptychius jarviki
Fleurantia denticulata
Eusthenopteron foordi
Elpistostege watsoni
Jarvikina werjukowi
Parmastega aelidae
Rhynchodipterus elginensis
Glyptolaemus kinnairdi
Soederberghia simpsoni
Mandageria fairfaxi
Holoptychius nobilissimus
Heddleichthys dalgleishensis
Gooloogongia loomesi
Cariowindra grossi
Cabonnichthys burnsi
Serenichthys kowiensis
Ichthyostega stensioei
Eusthenodon waengsjoei
Edenopteron keithcrookii
Acanthostega gunnari
Barameda mitchelli
Barameda decipiens
Latvius porosus
Claradosymblema narrienense
Screbinodus ornatus
Balanerpeton woodi
Rhabdoderma elegans
Polyosteorhynchus simplex
Lochmocercus aciculodontus
Hadronector donbairdi
Caridosuctor populosum
Allenypterus montanus
Rhizodopsis rankini
Baphetes bohemicus
Rhabdoderma exiguum
Anthracobamus fayoli
Tel
Sil
Hom
Gor
Lud
Pri
Loc
Pra
Ems
Eif
Giv
Fra
Fam
Tou
Vis
Ser
Bas
Mos
Kas
Gzh
Llandovery
Wenlock
Ludlow
Pridoli
Lower Devonian
Middle Devonian
Upper Devonian
Mississippian
Pennsylvanian
440
420
400
380
360
340
320
300
Age (Ma)

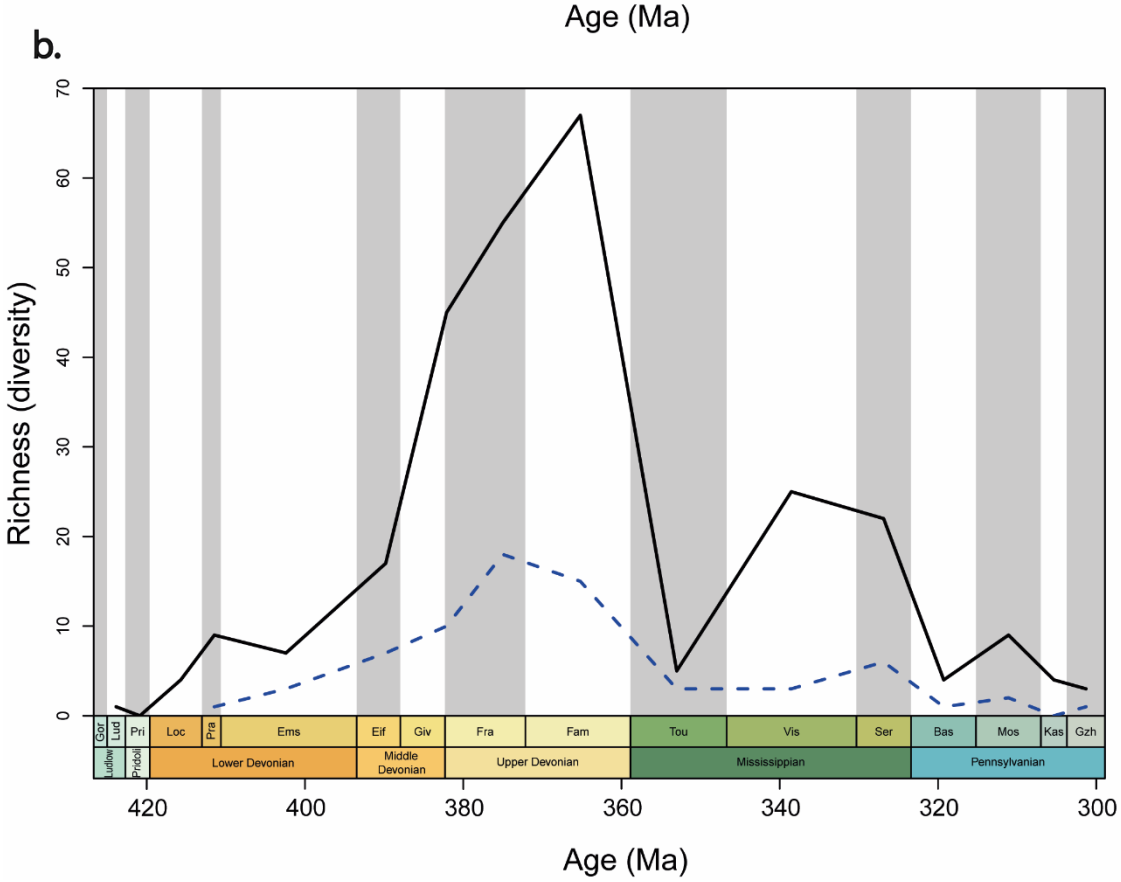

b.
Richness (diversity)
0
10
20
30
40
50
60
70
Gor
Lud
Pri
Loc
Pra
Ems
Eif
Giv
Fra
Fam
Tou
Vis
Ser
Bas
Mos
Kas
Gzh
Ludlow
Pridoli
Lower Devonian
Middle Devonian
Upper Devonian
Mississippian
Pennsylvanian
420
400
380
360
340
320
300
Age (Ma)

Fig. 1. Occurrence and diversity through time of early sarcopterygian species. (a) Occurrence of each of the 70 species of early piscine sarcopterygians analysed; (b) Diversity through time of early sarcopterygians based on the richness calculated for each stage for the 70 species analyzed (dashed blue line), and 279 species of early sarcopterygian (black line). Bas: Bashkirian; Eif: Eifelian; Ems: Emsian; Fam: Famennian; Fra: Frasnian; Giv: Givetian; Gor: Gorstian; Gzh: Gzhelian; Hom: Homerian; Kas: Kasimovian; Loc: Lochkovian; Lud: Ludfordian; Mos: Moscovian; Pra: Pragian; Pri: Pridoli; Ser: Serpukhovian; She: Sheinwoodian; Tel: Telychian; Tou: Tournaisian; Vis: Viséan.

Landmarking schemes

We used 2D geometric morphometrics to quantify sarcopterygian morphological disparity, digitizing landmarks and semi-landmarks on palaeontological reconstructions. This approach allowed us to estimate disparity from continuous data and to obtain geometric information related to shape changes of several morphological features of early sarcopterygians. First, for the full body shape, we digitized 11 landmarks and 196 semi-landmarks describing the lateral body outline and the positioning and shapes of fins (Fig. 2a, see Annexe III Table S3). Second, for the cranial shape disparity, we digitized 16 landmarks on lateral reconstructions to describe the orbital and cheek regions (Fig. 2b, see Annexe III Table S3). And third, we used 23 landmarks to analyse shape variation on the skull roof (Fig. 2c, see Annexe III Table S3 online). By capturing morphological variation in the skull from two different perspectives (dorsal and lateral), this allows us to interpret some of the major changes that occurred within this structure from a three-dimensional perspective. All landmarks and semi-landmarks were digitized using *tpsDig2* (v2.32)[29].

Each set of landmark coordinates was rotated, translated, and scaled with a Procrustes superimposition using the *gpagen* function in 'geomorph' (v.4.0.1)[30]. Semi-landmarks were slid using the Procrustes distance minimisation criterion[31]. The multidimensional shape data were summarized using principal component analyses, and the first two axes of each PCA were used to build morphospaces.

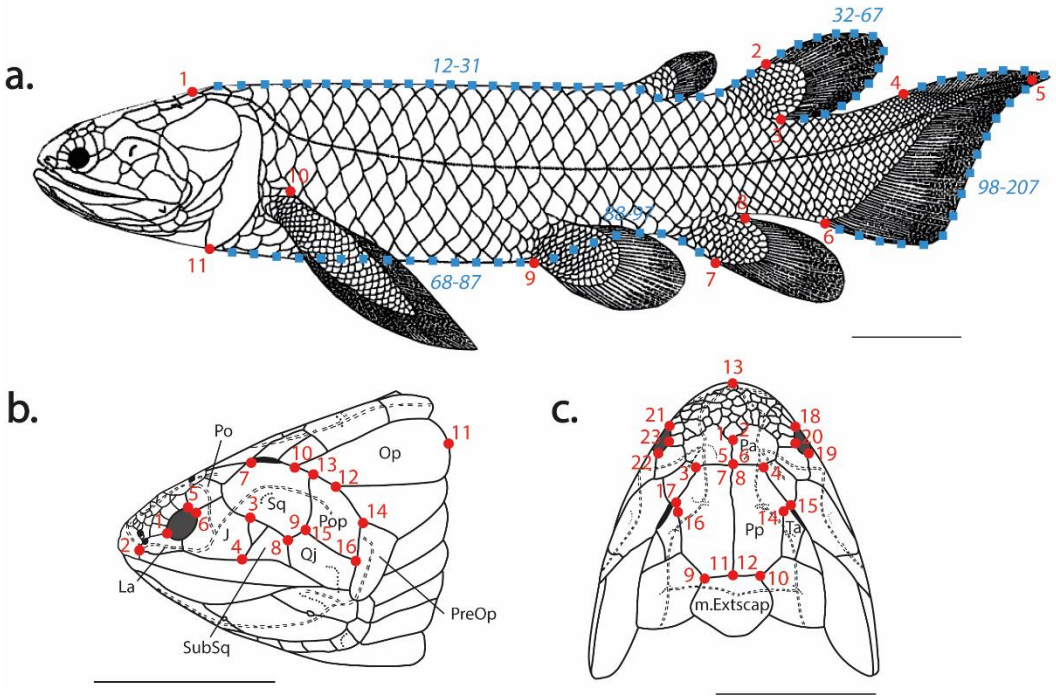


Fig. 2. Landmarks (red circles) and semi-landmarks (blue squares) positioning scheme for geometric morphometrics analyses of (a) the body shape, (b) the cheek, and (c) the skull roof. *Holoptychius jarviki* (Cloutier and Schultze, 1996). See Annexe III Table S3 for a full description of the landmarks and semi-landmarks. Scale bars, 5 cm. J: jugal; La: lacrimal; m.Extscap: median extrascapular; Op: Operculum; Pa: parietal; Po: postorbital; Pop: preopercular; Pp: postparietal; PreOp: preoperculo-submandibular; Qj: quadratojugal; Sq: squamosal; SubSq: Subsquamosal; Ta: Tabular.

Morphological disparity analyses

We estimated morphological disparity using two different metrics suitable for multidimensional data, each reflecting different aspects of the distribution of the points in morphospaces: (1) the Procrustes variance that measures the dispersal of taxa within morphospace by providing an estimate of the difference among taxa based on the variance in the shape data, and (2) the area of convex hulls that measures the amount of global morphospace occupation for each group[32]. The latter is more sensitive to extreme values and cannot be estimated for groups with two species or less. However, it provides an intuitive

metric to compare the extent of morphospace occupied by each group. Procrustes variance was calculated for each epoch, each group of sarcopterygians, and each palaeoenvironment using the function *morphol.disparity* in the package 'geomorph'[30], which quantifies groupwise morphological disparity, and assesses statistical significance for each pairwise comparison[33]. Using the same set of grouping variables, the area of convex hulls in the multidimensional morphospace was estimated using a modified version of the *chull* function from the 'grDevices' package[34] based on the first two axes of the PCA. We also estimated a weighted surface area based on the first five principal components of the PCA. This was done by calculating the surface area for each pair of PCs and weighting each by the combined proportion of variance explained by the two axes (see Annexe III Fig. S1, Tables S5 and S6 online). Given that the results were qualitatively similar, we focus on the findings based on the first two PCs in the main text, as these contain most of the biologically interpretable shape changes. As mentioned above, our time scale is divided into 7 epochs. To be independent of the time scale and to control for potential biases in this subdivision (stages are usually defined after major changes in biodiversity or environment), we also subdivided the total time interval into 7 equal time bins of 18.1 million years each. We then quantified the sum of variances for each equal time bin with the *dispRity* function in the package 'dispRity'[35]. The resulting two patterns of morphological disparity were highly congruent. To streamline the presentation of our results, we present the morphological disparity along the epochs from the international chronostratigraphic chart in the main text. Species that overlapped two or more different epochs were classified according to their epoch of appearance. All disparity analyses were performed in R v.4.3.2 using the packages 'geomorph'[30], 'grDevices'[34], and 'dispRity'[35].

Lagerstätte effect

Lagerstätten are deposits exhibiting exceptional preservation conditions, characterized by a concentration or a preservation quality of fossils much superior to what is normally the case[36]. Several Lagerstätten are well known for the period of interest of our data sampling, such as the Gogo Formation[37] (Late Devonian, Gogo Station, Western Australia), Escuminac Formation[22] (Late Devonian, Miguasha, Quebec, Canada), and the Heath

Formation[38] (Mid-Carboniferous, Bear Gulch, Montana, USA). The impact of Lagerstätten on diversity and disparity estimates is referred as the "Lagerstätte effect"[39]. As most of the Mississippian species that we sampled come from the Heath Formation of Bear Gulch (Montana, USA), we investigated the potential impact of the Lagerstätte effect in our estimates by analyzing the data both with and without the Bear Gulch species.

Results

Body shape disparity

The first axis of the PCA (PC1) explains 49.20% of the variation among 36 species, and contrasts species with shortened bodies and a tri-lobed caudal fin, such as the actinistian *Allenypterus montanus*, to species with more fusiform body shapes with a heterocercal or diphycercal caudal fin, such as in the rhizodont *Gooloogongia loomesi* (Fig. 3a). PC1 also separates the Actinistia from the remaining sarcopterygians (Fig. 3a). Actinistians occupy a relatively larger area in the morphospace than the other groups, having the largest convex hull surface area (see Annexe III Table S4 online), and representing 43.89% of the total disparity.

PC1 also clearly discriminates Devonian from Carboniferous species (Fig. 4a). Frasnian sarcopterygians represent 17.55% of the total disparity, the Famennian species 20.44%, while the Serpukhovian piscine sarcopterygians represent 35.53%. The Upper Devonian and Mississippian constitute the epochs with most of the body shape disparity among early sarcopterygians (see Annexe III Table S7 online). Body shape disparity increased during the beginning of the Middle Devonian (Eifelian) reaching a maximum during the Middle Devonian (Givetian) and the Upper Devonian (Famennian). Body shape disparity then decreases towards the end of the Carboniferous (Fig. 6).

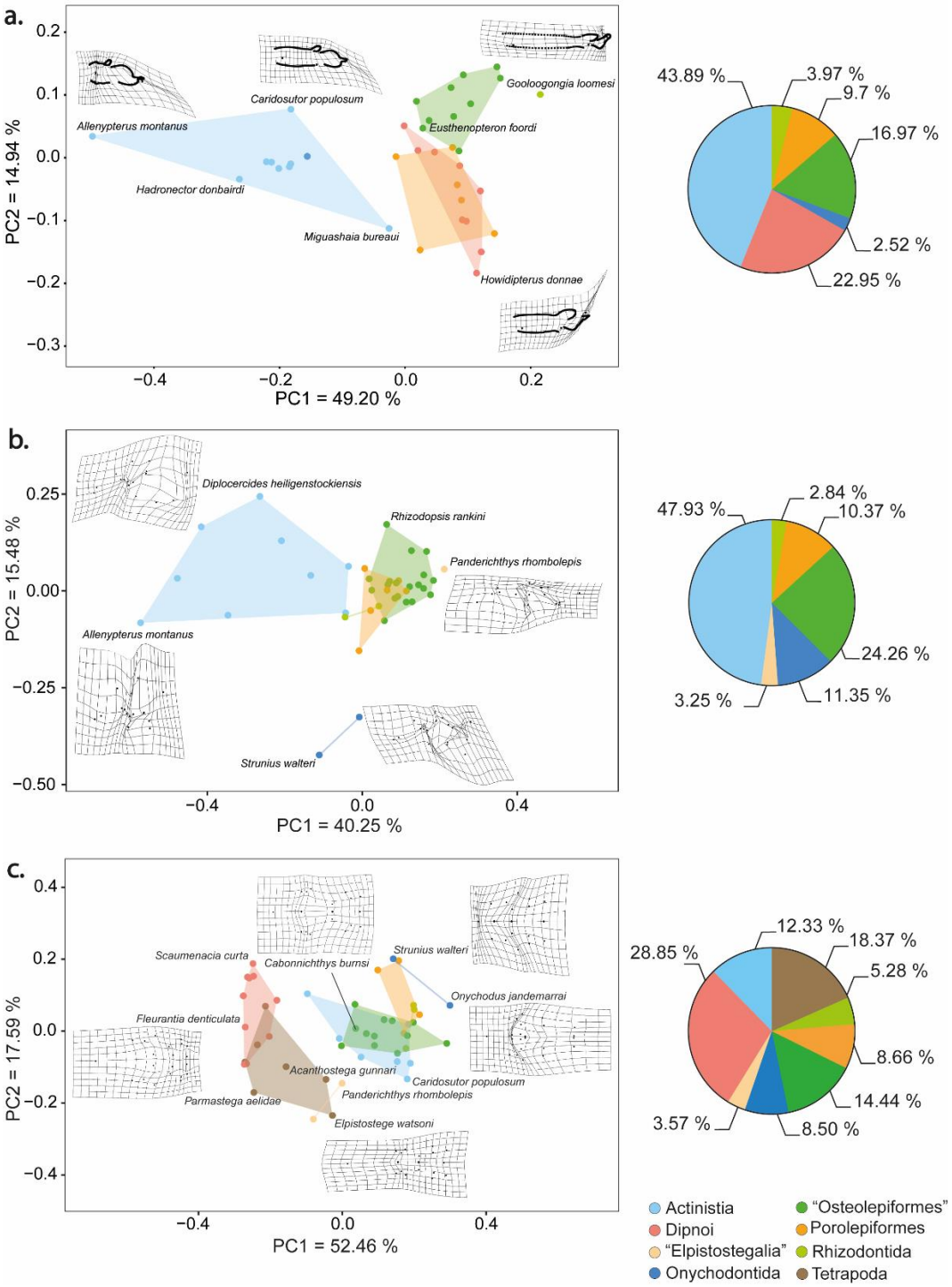


Fig. 3. Morphological disparity of basal sarcopterygians per taxonomic group. Morphospace of principal components 1 and 2. (a) Body shape (n=36 species); (b) Cheek (n=39 species); and (c) Skull roof (n=47 species). Deformation grids show the differences between the

extreme forms along each axis and the mean shape. The pie charts illustrate the proportion of disparity each group represents based on their respective Procrustes variance. If categories include only one species, it will be represented by a single dot.

Finally, PC1 presents a gradient from the marine species mostly concentrated on the left half of the morphospace to the freshwater species that mostly occupy the right half, with estuarine species overlapping both spaces (Fig. 5a). Freshwater species represent nearly half of the total disparity (49.04%) (see Annexe III Table S7 online). Looking at the palaeoenvironment of early sarcopterygians on a finer scale, PC1 seems to separate the bay environment representing 33.54% of the total disparity from all other palaeoenvironments (Fig. 5b, see Annexe III Table S7 online).

PC2 explains 14.94% of the variation and represents mostly a difference in the shape of the tail. The tail may be heterocercal, such as in the dipnoan *Howidipterus donnae*, whereas *Cabonnichthys burnsi* and other "Osteolepiformes" are characterized by a diphycercal tail (Fig. 3a).

Cheek disparity

PC1 explains 40.25% of the morphological variation of the cheek region among sarcopterygians. This represents a shift from a deeper and shorter skull, such as in the actinistian *Allenypterus montanus*, to a more flattened and elongated skull as in the "elpistostegalian" *Panderichthys rhombolepis* (Fig. 3b). PC2 explains 15.48% of the skull variation, representing differences in the position and size of the opercular series. At one extremity of the axis, the opercular series is narrow and dorsally positioned as in the onychodont *Strunius walteri*, whereas at the other extremity the opercular series is wider as in the actinistian *Diplocercides heiligenstockiensis*. The distinction between the skulls of Devonian and Carboniferous species is less pronounced than for full body shape, especially along PC1 (Fig. 4b). Devonian species are spread across the entire morphospace exhibiting substantial cheek disparity. Carboniferous species are mostly differentiated among themselves by the level of elongation of their skulls.

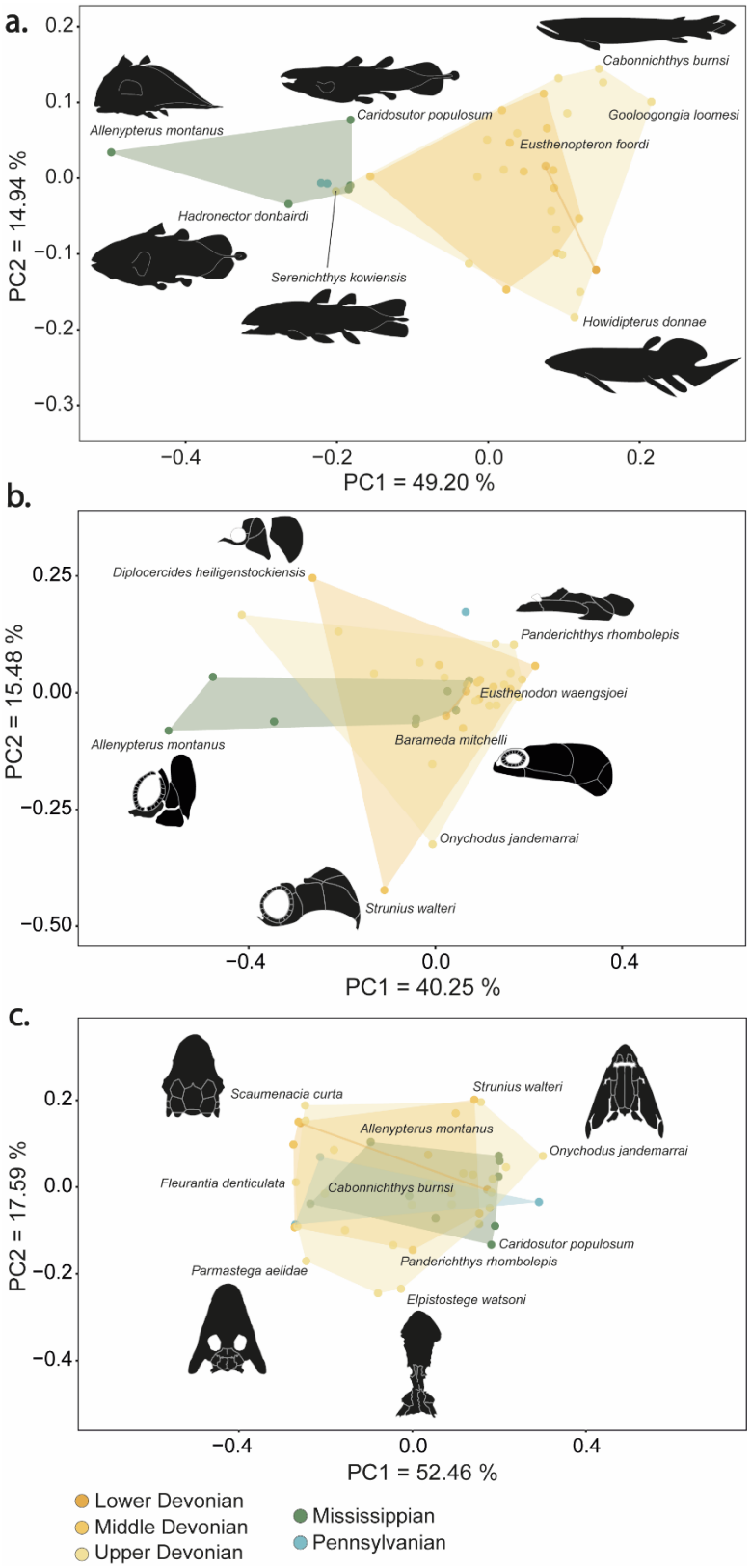

a.
Cabonnichthys burnsi
Caridosutor populosum
Gooloogongia loomesi
Allenypterus montanus
Eusthenopteron foordi
Hadronector donbairdi
Serenichthys kowiensis
Howidipterus donnae
PC2 = 14.94 %
PC1 = 49.20 %
b.
Diplocercides heiligenstockiensis
Panderichthys rhombolepis
Eusthenodon waengsjoei
Allenypterus montanus
Barameda mitchelli
Onychodus jandemarrai
Strunius walteri
PC2 = 15.48 %
PC1 = 40.25 %
c.
Scaumenacia curta
Strunius walteri
Allenypterus montanus
Onychodus jandemarrai
Fleurantia denticulata
Cabonnichthys burnsi
Caridosutor populosum
Panderichthys rhombolepis
Parmastega aelidae
Elpistostege watsoni
PC2 = 17.59 %
PC1 = 52.46 %
Lower Devonian
Middle Devonian
Upper Devonian
Mississippian
Pennsylvanian

Fig. 4. Morphological disparity of basal sarcopterygians per geological epoch. Principal component analysis showing PC1 versus PC2 disparity based on 2D geometric morphometrics. (a) Body shape (n=36 species); (b) Cheek (n=39 species); and (c) Skull roof (n=47 species). If categories include only one species, it will be represented by a single dot.

However, the change in the shape of sarcopterygian skulls seems to be better explained by shared ancestry; the different groups of sarcopterygians being separated in the morphospace (Fig. 3b). Again, actinistians stand out from the rest of sarcopterygians, being characterized by shorter and deeper heads. They exhibit higher levels of cheek disparity with a Procrustes variance significantly higher than all the other groups (0.0961, $p<0.05$), and by occupying a larger area of the morphospace (see Annexe III Tables S4 and S7 online). They account for 47.93% of the total cheek disparity across sarcopterygians. This pattern is similar to that of the full body shape disparity. The Onychodontida are also clearly separated from the rest with narrower and more dorsally positioned opercular series, a characteristic that most likely reflects the plesiomorphic condition of the cheek region in basal actinopterygians. Finally, the Dipnomorpha and Tetrapodomorpha are closely packed and are characterized by more elongated and flattened heads. Looking at the aquatic palaeoenvironments and habitats (Fig. 5c–d, see Annexe III Tables S4 and S7 online), marine species occupied a larger area in the morphospace. Marine species accounted for more than half of the total cheek disparity (52.73%) and had a significantly higher Procrustes variance (0.1297, $p<0.001$) than the freshwater species (0.0397, $p<0.001$). Freshwater species are densely clustered, exhibiting a more flattened and elongated cheek region. Lagoonal, estuarine, and bay species seem more spread out across the morphospace (Fig. 5d, see Annexe III Tables S4 and S7 online).

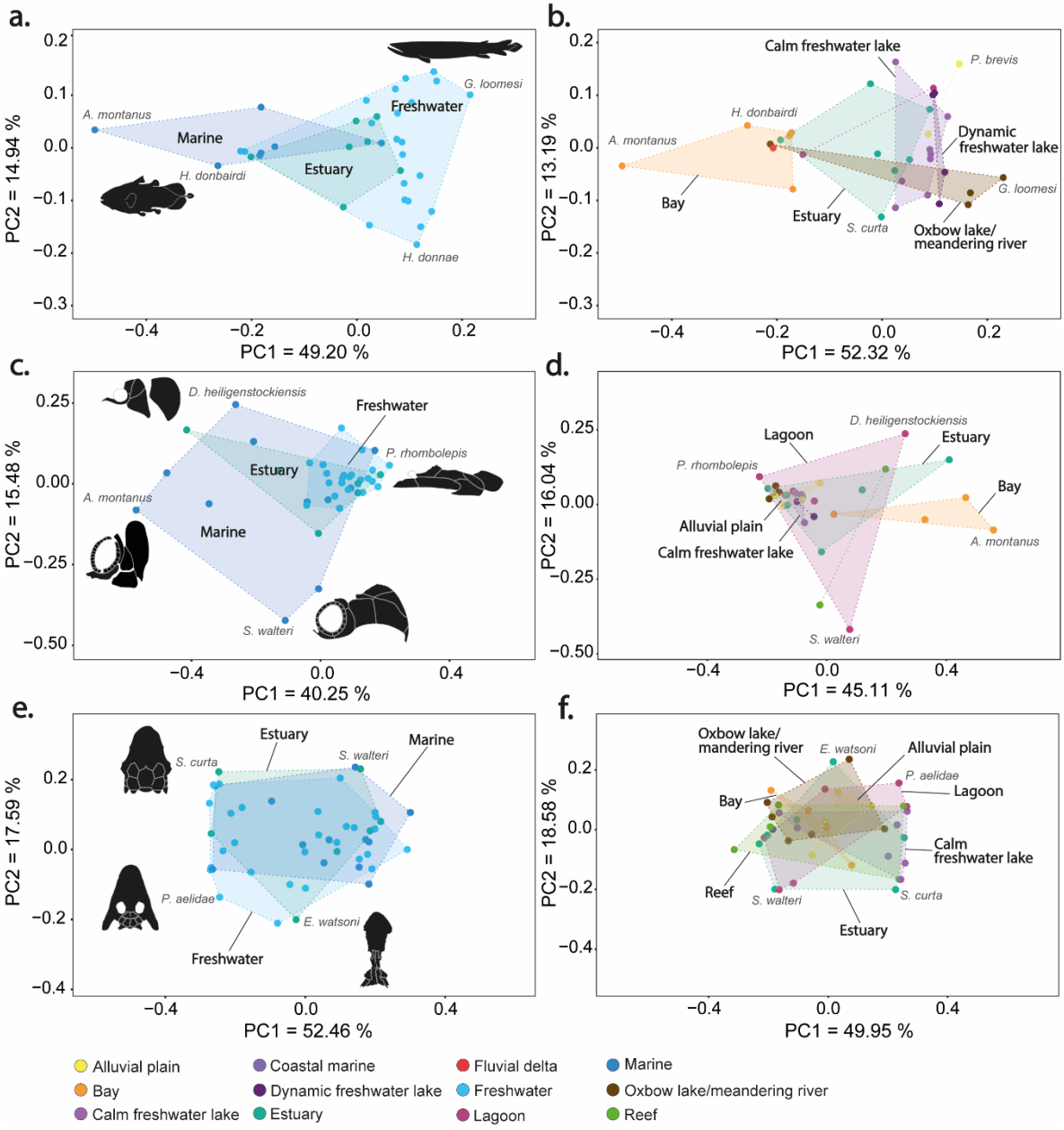


Fig. 5. Morphological disparity of basal sarcopterygians per aquatic habitats. Morphospace of principal components 1 and 2. (a–b). Body shape; (c–d). Cheek; (e–f). Skull roof. b, d, and f represent more precise palaeoenvironments and exclude species with no detailed information about it. If categories include only one species, it will be represented by a single dot.

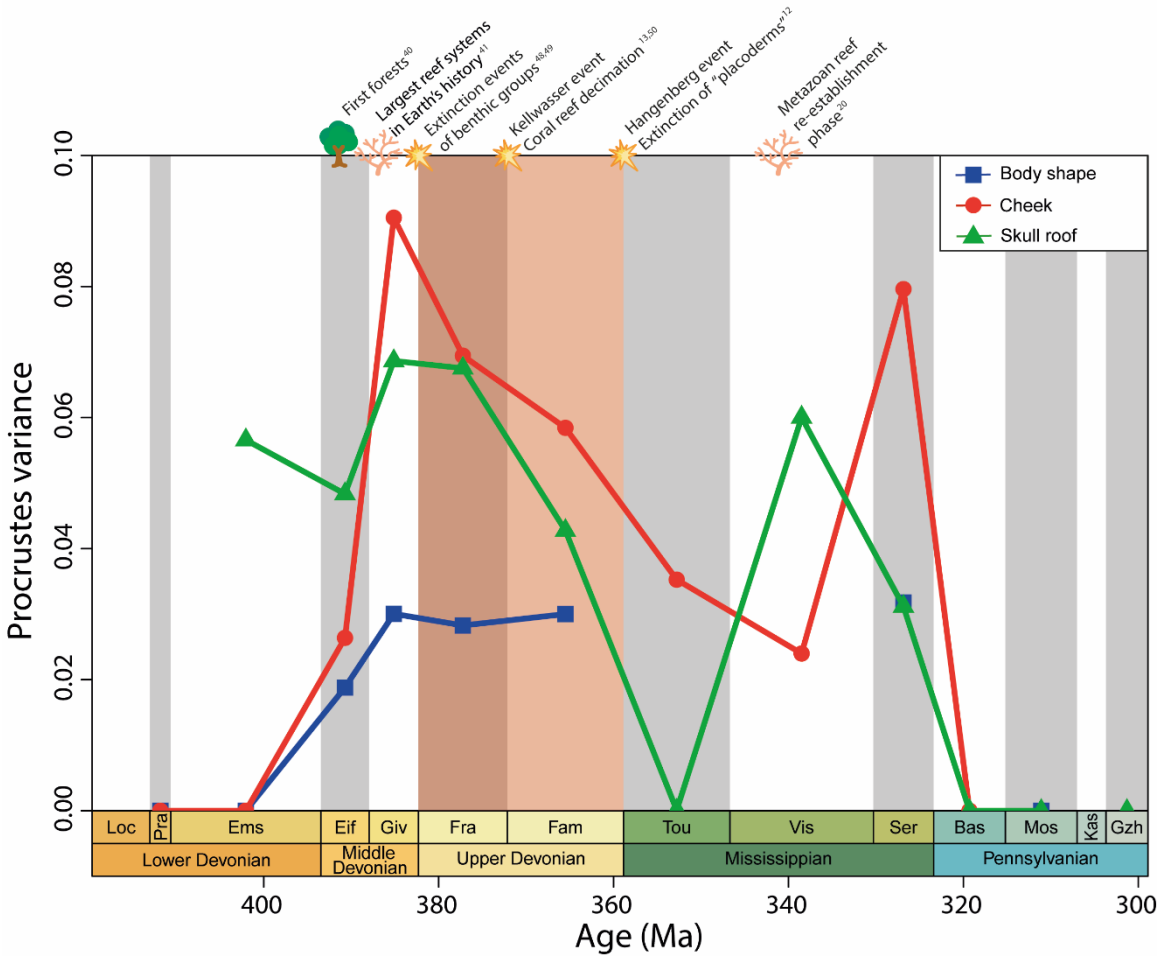


Fig. 6. Procrustes variance for body shape (blue squares), cheek (red dots), and skull roof (green triangles) disparity through time. Major Devonian and Carboniferous geological and biological events are represented.

Skull roof disparity

Among the three morphological systems studied, the skull roof displays the greatest disparity. Indeed, PC1 explains 52.46% of the variation in skull roof shape among early sarcopterygians (Fig. 3c), representing primarily differences in the shape and position of parietals and postparietals. They vary from elongated and anteriorly positioned as in the onychodont *Onychodus jandermarrai*, to shortened and posteriorly positioned as in the dipnoan *Fleurantia denticulata*. PC2 explains 17.59% of the variation. It represents a change in the width of the skull roof accompanying the migration of the eyes from a lateral position

as in the onychodont *Strunius walteri*, to a more dorsal and median position in the tetrapod *Elpistostege watsoni*.

Even if Late Devonian species seem to present a higher morphological disparity (Fig. 4c, see Annexe III Table S7 online), there is no obvious change between the skull roof shapes of Devonian and Carboniferous species (Fig. 4c). Similarly, no major change in shape is detected among the palaeoenvironments (Fig. 5e–f). However, when focusing on the disparity among sarcopterygian groups, obvious differences can be observed among three of them (Fig. 3c). The first group consists of the Actinistia, Onychodontida, Porolepiformes, Rhizodontida, and "Osteolepiformes" that form a tight cluster towards the right portion of the morphospace. Here as well, the Actinistia appears to be a highly disparate group, exhibiting the broadest distribution in shape space (Fig. 3c, see Annexe III Table S4 online). The second group is the "Elpistostegalia" characterized by a shift of the orbits towards the top of the skull; they occupy the lower portion of the morphospace and overlap with the Tetrapoda. Finally, the third grouping is the Dipnoi and Tetrapoda clustered in the left portion of the morphospace, which are characterized by a shortening of the posterior (otico-occipital) region of the skull roof.

Early sarcopterygian diversity and morphological disparity variation through time

The diversity of sarcopterygians presents two successive peaks of maximum richness, the first during the Famennian and the second during the Mid-Late Mississippian (Viséan) (Fig. 1b). A decrease in sarcopterygian richness is observed between the Devonian and the Carboniferous. In all three analyses, morphological disparity for each age was estimated as the sum of Procrustes variances (Fig. 6). Body shape disparity increases during the Middle Devonian before it stabilises during the Upper Devonian. Skull roof and cheek disparity seem to follow a similar pattern. A first maximum is reached during late Middle Devonian and early Upper Devonian, which corresponds to the time of appearance of the first forests on land, and the peak of coral reef ecosystems[40,41]. A second maximum is reached during the Middle and Upper Mississippian, which appears to correspond to the time of recovery of metazoan reefs[20] (Fig. 6). Both skull roof and cheek disparities decrease simultaneously with the Upper Devonian biodiversity crises. A small discrepancy is observed between the first

morphological disparity maximum during the Givetian and the maximum species diversity during the Famennian (Figs. 1b and 6).

Lagerstätte effect

The morphological disparity results excluding the Bear Gulch species are presented in the supplementary information (see Annexe III Fig. S2 online). The major trends of disparity remain the same, although patterns of cheek disparity seem to be impacted by the absence of these Mississippian species, which include three actinistians from our database. Indeed, when excluding the species from Bear Gulch, the cheek disparity peak of the Serpukhovian is no longer present, and may therefore represent a consequence of a Lagerstätte effect, which suggests that the disparity peak observed during the Serpukhovian in our all-species analyses could be influenced by the presence of the Bear Gulch Lagerstätte species and could be the result of a Lagerstätte effect.

Discussion

The main goal of this study was to explore the patterns of morphological disparity (body shape, cheek region, and skull roof) among Devonian and Carboniferous sarcopterygians, and to explore changes in overall disparity through time. The main source of body shape disparity opposed elongated and fusiform morphologies to shorter and deeper body shapes. The cheek region showed a shift from deeper and shorter skulls to flattened and elongated ones, as well as some variation in the position of the opercular series. Finally, the major sources of disparity for the skull roof were variation in width, as well as in the position of the eyes, parietal, and postparietal bones. These observed patterns were found to be explained in part by shared ancestry within the major groups of sarcopterygians, the geological epochs, and habitat types.

Devonian environmental changes influenced the early diversification of sarcopterygians

The Devonian and Carboniferous periods are punctuated by major climatic, geological and biological events that could have impacted sarcopterygian history. The first maximum of both sarcopterygian morphological disparity and species richness dates to the Middle–Upper Devonian. During the Middle Devonian, reefs proliferated and occupied the largest marine surface area in Earth's history[41,42]. Concurrently on land, the first forests appeared[40] and progressively transformed the terrestrial landscape, which was accompanied by the diversification of several groups of terrestrial invertebrates[4,5,43]. The increased presence of plants on land also led to a change in the atmospheric composition, decreasing CO_2 levels and increasing O_2 levels[14], both of which are associated with global cooling[14]. Simultaneously, these changes facilitated an increase in the organic matter input from continental waters, especially along the continental shelves[44]. Moreover, the fluctuation in the Laurussia ice cap covering induced by the variation of global temperature generated changes in the sea level and the formation of epicontinental shallow seas[16,45]. These events have been associated with the timing of early diversification of new sarcopterygian lineages such as the first tetrapod-like fishes, likely during the early-middle Devonian[9,46]. During the Devonian, sarcopterygians dominated the jawed vertebrate diversity along with "placoderms"[3] and the use of different niches by new sarcopterygian lineages could explain the increase in morphological disparity that we observed.

This period is also characterized by an increase of tectonic activity associated with volcanic activity[45], which led to the opening of the Paleotethys ocean and the formation of large carbonate platforms at collision sites[45]. These major changes deeply impacted the aquatic living forms and led to several biodiversity crises during the Upper Devonian that contributed to the Late Devonian mass extinction[47]. From a biological point of view, structural benthic groups such as rugose and tabulate corals[48] and stromatoporoids[49] were lost during the first crisis at the end of the Givetian (Middle Devonian). The second remarkable crisis, known as the Kellwasser event (Frasnian–Famennian boundary, 371 Ma), is characterized by an abundance of black shales originating from a high level of organic

matter deposition (originating from the continental environment), underlying large scale anoxic conditions[13]. This consequential anoxia event in aquatic habitats could have led to the coral reef decimation by the end of the Frasnian (Upper Devonian), with 80% of tabulate corals[50] and 60% of rugose coral genera[50] going extinct along with 80% of ostracod species[51] and more than 75% of brachiopod species[50], all of which played a key role in Devonian trophic networks[52]. Finally, the Hangenberg event marking the Devonian– Carboniferous boundary[12] (359 Ma), is characterized by the loss of several fish groups[3]. Particularly, Sallan and Coates[3] described a crash in the diversity of piscine sarcopterygians and "placoderms" at the Devonian– Carboniferous boundary[3], constituting a major turn-over in the aquatic organisation because of their dominant place among vertebrates during the Devonian, when they occupied a wide range of ecological niches[53,54]. The loss of several piscine sarcopterygian groups during these successive crises[3] accompanying the loss of several ecological niches could help explain the observed decrease of both skull roof and cheek disparity during the Upper Devonian.

The aquatic habitats influenced cheek disparity

The sarcopterygian cheek region showed a shift from deeper and shorter skulls to flattened and elongated ones, as well as some variation in the position of the opercular series. In fishes, the cheek region corresponds to the region extending laterally from the orbit to the posterior extremity of the skull, including the opercular series. The cheek region plays structural and functional roles in the jaw suspension and is an important muscle attachment site for several jaw muscles, but is also involved in the structural support and flexibility of the head[55] and associated kinematics of breathing and feeding. This region is therefore deeply involved in the diversity of jaw movements and ecological adaptation of fishes[55]. This could explain the strong response of the cheek disparity facing the fall of several aquatic systems with the end-Devonian crisis.

Focusing on the influence of the type of aquatic habitats, we observed low cheek morphological disparity in freshwater species despite their taxonomic richness. Indeed, when considering cheek shape, marine species appeared significantly more disparate than freshwater sarcopterygians. The aquatic environment constitutes a highly complex system of

various habitats and environmental constraints[56]. Differences in physical characteristics between freshwater and marine aquatic habitats constitute a potential driver for morphological diversification within fishes[25,57,58]. The differences in the patterns of morphological disparity of the cheek region between marine and freshwater fish species have never been studied before. However, more general patterns associated with other aspects of fish diversification could provide additional insights to this investigation. First of all, marine and freshwater systems share common structural and functional characteristics, which have led to similar ecologies of their respective communities despite their independent evolutionary histories[59,60]. The feeding apparatus tends to have similar adaptations in freshwater and marine systems that are dependent on organismal dietary preferences[61]. Given that the cheek bones are functionally involved with the jaws and gill rakers, differences in feeding strategies likely explain some of the morphological variation in this region among marine fishes. Moreover, in our analyses, most of the marine species were actinistians and dipnoans, groups for which the increase in the cheek region variation corresponds to the period directly following the Devonian[62]. These two groups were predominantly found in marine waters and in coastal systems (e.g. estuaries, deltas, bays) which went through important changes during the early Carboniferous. The re-emergence of the coral reefs during the Viséan (Middle Mississippian) complexified the marine system, whereas the early Carboniferous coasts were dominated by delta and estuary systems due to the end-Devonian—Early Carboniferous marine transgressions[63,64]. This could have offered new ecological opportunities to these two groups, triggering their ecomorphological diversification during their recovery period following the end-Devonian mass extinction.

As for the lack of variation of the cheek region for the freshwater species, this could be indicative of a decoupling between the early diversification of the freshwater sarcopterygians and their subsequent ecological diversification in terms of trophic habits. It has also been shown that, contrary to the actinopterygian lineage, early sarcopterygians tend to lose skull bones mainly through fusion of elements[65]. This tendency could have led to a more stable and less modular skull in the derived sarcopterygian lineages close to the transition from freshwater systems to land[65,66]. The specific paleoenvironmental categories

used in this study involve relatively few taxa, which may introduce sampling biases into the comparisons. The observed patterns remain meaningful, but these limitations should be considered when interpreting the results. A more robust analysis could be performed in future work, by using a broader sampling to test the stability of these trends.

Shared ancestry influenced skull roof disparity

Unlike the cheek region, skull roof disparity did not seem to be profoundly influenced by the type of aquatic system, which could suggest little or no ecological constraints associated with these habitats. Moreover, no clear change was detected for skull roof shape between the Devonian and the Carboniferous. The main sources of disparity for the skull roof were variation in width, as well as in the position of the eyes, parietal, and postparietal bones, and was best explain by shared ancestry. An elongation and a decreasing depth of the skull was observed within the "Osteolepiformes" and Porolepiformes. However, this is without generating a substantial increase in disparity within these groups, despite their high species richness. Looking at jaws, Troyer et al.[67] also detected low morphological disparity and low evolutionary rates among tetrapodomorphs, which could indicate few morphological changes during the initial stages of terrestrialisation. In taxa such as extant crocodilians, it has been suggested that such modifications of the skull roof shape could be advantageous for lateral snapping, particularly in aquatic habitats or transitional zones[21]. This could explain the observed changes of the skull roof in early tetrapods and their close relatives that were most likely primarily aquatic, despite displaying some adaptations facilitating the progressive use of terrestrial habitats[66]. Another striking example of this is the dorsal migration of the eyes accompanying the flattening and elongation of the preorbital region, and the shortening of the parietal and postparietal shields. In these semi-aquatic animals, dorsally oriented eyes could have allowed them to spot prey on land during a time of major diversification of terrestrial plants and invertebrate groups[4,68,69]. The last remarkable result concerning the skull roof disparity was the segregation of dipnoans and tetrapods from the other groups along the first axis of the PCA, opposing a skull with an elongated preorbital region (such as in tetrapods and dipnoans) with a skull more elongated in the post-orbital region. In all early sarcopterygians, an intracranial joint is located on the top of the skull, separating the

ethmosphenoid and the otoccipital regions[70]. The intracranial joint is thought to increase the biting force and could have facilitated the processing of large-sized prey[70]. This structure is absent in dipnoans and tetrapods, which have a fused neurocranium[71]. This could explain why these two groups form a tight cluster, separated from the other lineages, in our skull roof analyses.

Post-crisis ecological opportunities influenced body shape disparity

Contrary to what has been observed for cheek and skull roof disparity, body shape disparity seems to remain stable across the end-Devonian crises. Fish overall body shape is most closely linked to locomotory patterns[72]. The changes associated with the end-Devonian crises may have had minimal impacts on potential ecological opportunities that would trigger new types of locomotion, which could explain this stability in sarcopterygian postcranial shape through the crises. However, Sallan and Galimberti[73] reported an overall reduction in body sizes for most of the fish lineages following the Devonian crisis. Thus, the selective pressures during this period, especially the change in the atmosphere, may have been more consequential for organismal size, and less so for body shapes. This may also suggest a more resilient response from body shape facing these crises compared to the skull, which could be more strongly impacted by ecological constraints associated with feeding and breathing[74].

The following Carboniferous period was a time of deep recovery[75] especially with the re-emergence of coral reef ecosystems during the Viséan that created new ecological niches in marine habitats[20]. Reefs are particularly important for the structure of marine ecosystems, providing more structurally complex habitats, and have already been shown to be tightly linked to the diversification of fishes[76–78]. Despite the apparent stability of body shape morphological disparity, a major shift in body shape of early sarcopterygians is observed between the Devonian and Early Carboniferous forms. The main source of body shape disparity among early sarcopterygians opposed more elongated and fusiform morphologies to shorter and deeper body shapes. This pattern is similar to those observed among actinopterygians[79] and could suggest a conserved first axis of body morphological diversification among osteichthyans.

In our analyses, we found this shift to also correlate to the rise of actinistians during the Early Carboniferous, which generated new shapes among piscine sarcopterygians. Indeed, Clement et al.[27] demonstrated a rapid increase in rates of morphological evolution in actinistians during the Carboniferous (around the Viséan) and in all our analyses, actinistians appear to be the most disparate group of early sarcopterygians, accounting for nearly half of the total morphological disparity for the complete body shape. Moreover, actinistians exhibit distinct body shapes from the other sarcopterygians. Although actinistians are often referred to as "living fossils" and are proposed as a model of bradytelic evolution[80,81], the early history of actinistians is marked by a dramatic change in their morphology[27,67,82–84]. In their recent preprint, Rivero-Vega et al.[84] detected successive peaks of morphological diversification in the early history of actinistians before their decline during the Mesozoic. Basal actinistians retained a shape closer to that of the other sarcopterygians (lungfishes and porolepiforms), characterised by a heterocercal caudal fin and a more elongated postorbital region[82], while Carboniferous and Palaeozoic actinistians expanded into entirely new regions of the morphospaces. This could explain the position in morphospace of the Devonian Miguashaia[27,82] near the other sarcopterygian groups in the analyses compared to the other actinistians. Miguashaia appears closer to a generalised sarcopterygian shape rather than a later-branching actinistian shape, characterised by a tri-lobed tail such as in the extant *Latimeria*[27,83]. Before their body shape stabilised during the Mesozoic, some early actinistians exhibited unusual shapes such as in the Carboniferous *Allenypterus montanus*[27,82,83]. The high morphological disparity of actinistians during the Palaeozoic is even more remarkable when compared to other groups such as the "Osteolepiformes" which represented the largest group in all our analyses and did not present comparable levels of morphological disparity. Troyer et al.[67] also found actinistians to exhibit high disparity and elevated rates of jaw morphological change compared to other groups of sarcopterygians. The periods during which the diversity of actinistians increased have been correlated to abiotic factors such as tectonic activity and changes in ocean levels[27] and also seem to correspond to the re-emergence of corals systems during the Viséan[20,41]. Thus, the biogeography and ecological opportunities following the end-Devonian crises could have

contributed to the morphological diversification of actinistians, found in habitats ranging from lagoons to reefs, during the Carboniferous.

Conclusion

The mid-Palaeozoic era was a crucial time for sarcopterygian evolutionary history, marked by tremendous ecological changes triggered by the tectonic activity and atmospheric modifications associated with the Late Devonian. We found variation patterns of sarcopterygian morphological disparity to be cohesive with the main ecological events happening throughout this era, notably the extinction and re-emergence of coral reefs, which play an important structural role in marine ecosystems and fish diversification. Actinistians appeared to be the most disparate group of early sarcopterygians, which provides additional support for the early radiation of actinistians to have been accompanied by high ecomorphological disparity. We found a similar pattern of morphological disparity variation for the skull roof and the cheek region, with a decrease during the end-Devonian mass extinction, followed by a recovery period during the Mid-Late Mississippian. We found evidence that the increase in cheek morphological disparity during the Mississippian might have been associated with a Lagerstätte effect from the Bear Gulch species, but as our dataset includes several Lagerstätten from different ages, the effect of one of them in particular might be minimal. Furthermore, we found cohesive triggering ecological factors during the Mississippian that could support this disparity. While this study provides valuable insights on the morphological diversification of early branching sarcopterygian lineages, a deeper study of the morphological disparity among early tetrapodomorphs could bring additional information regarding the morphological innovations attributed to the water-to-land transition.

Data availability: Data and code are available on GitHub: https://github.com/oliviavanhaesebroucke/Early-sarcopterygian-disparity.git.

References

1. IUCN. IUCN Red List of Threatened Species (2025).

2. Zhu, M. et al. The oldest articulated osteichthyan reveals mosaic gnathostome characters. *Nature* 458, 469–474 (2009).

3. Sallan, L. C. & Coates, M. I. End-Devonian extinction and a bottleneck in the early evolution of modern jawed vertebrates. *Proc. Natl. Acad. Sci.* 107, 10131–10135 (2010).

4. Rolfe, W. D. I. & Lawson, J. D. Early terrestrial arthropods: A fragmentary record. *Philos. Trans. R Soc. Lond. B Biol. Sci.* 309, 207–218 (1997).

5. Morris, J. L. et al. Investigating Devonian trees as geo-engineers of past climates: Linking palaeosols to palaeobotany and experimental geobiology. *Palaeontology* 58, 787–801 (2015).

6. Boisvert, C. A., Mark-Kurik, E. & Ahlberg, P. E. The pectoral fin of *Panderichthys* and the origin of digits. *Nature* 456, 636–638 (2008).

7. Stewart, T. A., Lemberg, J. B., Daly, A., Daeschler, E. B. & Shubin, N. H. A new elpistostegalian from the Late Devonian of the Canadian Arctic. *Nature* 608, 563–568 (2022).

8. Shubin, N. H., Daeschler, E. B. & Jenkins, F. A. The pectoral fin of *Tiktaalik roseae* and the origin of the tetrapod limb. *Nature* 440, 764–771 (2006).

9. Ahlberg, P. E. Follow the footprints and Mind the gaps: A new look at the origin of tetrapods. *Earth Environ. Sci. Trans. R Soc. Edinb*. 109, 115–137 (2018).

10. Ahlberg, P. E. & Clack, J. A. The smallest known Devonian tetrapod shows unexpectedly derived features. *R. Soc. Open. Sci.* 7, e192117 (2020).

11. Aretz, M., Corradini, C. & Denayer, J. The Devonian-Carboniferous boundary around the globe: A complement. *Palaeobiodiversity Palaeoenvironments*. 101, 633–662 (2021).

12. Kaiser, S. I., Aretz, M. & Becker, R. T. The global Hangenberg Crisis (Devonian–Carboniferous transition): review of a first-order mass extinction, in *Devonian Climate, Sea Level and Evolutionary Events* (eds. Becker, R. T., Königshof, P. & Brett, C. E.), Vol. 423 0 (Geological Society of London, 2016).

13. Carmichael, S. K., Waters, J. A., Königshof, P., Suttner, T. J. & Kido, E. Paleogeography and paleoenvironments of the Late Devonian Kellwasser event: A review of its sedimentological and geochemical expression. *Glob. Planet. Change* 183, e102984 (2019).

14. Chen, B. et al. Devonian paleoclimate and its drivers: A reassessment based on a new conodont $\delta^{18}O$ record from South China. *Earth-Sci. Rev.* 222, e103814 (2021).

15. Byrne, H. M., Green, J. M., Balbus, S. A. & Ahlberg, P. E. Tides: A key environmental driver of osteichthyan evolution and the fish-tetrapod transition? *Proc. R. Soc. Math. Phys. Eng. Sci.* 476, e20200355 (2020).

16. Lakin, J. A., Marshall, J. E. A., Troth, I. & Harding, I. C. Greenhouse to icehouse: A biostratigraphic review of latest Devonian– Mississippian glaciations and their global effects, in *Devonian Climate, Sea Level and Evolutionary Events* (eds. Becker, R. T., Königshof, P. & Brett, C. E.), Vol. 423 0 (Geological Society of London, 2016).

17. Derycke, C., Olive, S., Groessens, E. & Goujet, D. Paleogeographical and paleoecological constraints on Paleozoic vertebrates (chondrichthyans and placoderms) in the Ardenne massif: shark radiations in the Famennian on both sides of the Palaeotethys. *Palaeogeogr. Palaeoclimatol. Palaeoecol*. 414, 61–67 (2014).

18. Grogan, E. & Lund, R. The geological and biological environment of the Bear Gulch Limestone (Mississippian of Montana, USA) and a model for its deposition. *Geodiversitas* 24, 295–315 (2002).

19. Lund, R., Greenfest-Allen, E. & Grogan, E. D. Ecomorphology of the Mississippian fishes of the Bear Gulch Limestone (Heath Formation, Montana, USA). *Environ. Biol. Fishes.* 98, 739–754 (2015).

20. Yao, L. et al. The longest delay: Re-emergence of coral reef ecosystems after the Late Devonian extinctions. *Earth-Sci. Rev.* 203, e103060 (2020).

21. Hohn-Schulte, B., Preuschoft, H., Witzel, U. & Distler-Hoffmann, C. Biomechanics and functional preconditions for terrestrial lifestyle in basal tetrapods, with special consideration of *Tiktaalik roseae*. *Hist. Biol*. 25, 167–181 (2013).

22. Cloutier, R., Proust, J. N. & Tessier, B. The Miguasha Fossil-Fish-Lagerstätte: A consequence of the Devonian land–sea interactions. *Palaeobiodiversity Palaeoenvironments*. 91, 293–323 (2011).

23. Trinajstic, K., Briggs, D. E. G. & Long, J. A. The Gogo Formation Lagerstätte: A view of Australia's first great barrier reef. *J. Geol. Soc.* 179, jgs2021–jgs2105 (2021).

24. Opluštil, S., Martínek, K. & Tasáryová, Z. Facies and architectural analysis of fluvial deposits of the Nýřany member and the Týnec Formation (Westphalian D – Barruelian) in the Kladno-Rakovník and pilsen basins. *Bull. Geosci*. 80, 45–66 (2005).

25. de Brito, V. et al. Patterns of phenotypic evolution associated with marine/freshwater transitions in fishes. *Integr. Comp. Biol*. 62, 406–423 (2022).

26. Lovejoy, N. R., Albert, J. S. & Crampton, W. G. R. Miocene marine incursions and marine/freshwater transitions: Evidence from Neotropical fishes. *J. South. Am. Earth Sci*. 21, 5–13 (2006).

27. Clement, A. M. et al. A Late Devonian coelacanth reconfigures actinistian phylogeny, disparity, and evolutionary dynamics. *Nat. Commun*. 15, e7529 (2024).

28. Kocsis, Á. T., Reddin, C. J., Alroy, J. & Kiessling, W. The R package DivDyn for quantifying diversity dynamics using fossil sampling data. *Methods Ecol. Evol*. 10, 735–743 (2019).

29. Rohlf, F. The Tps series of software. Hystrix Ital. J. Mammal. 26, 1–4 (2015). 30. Adams, D. C. & Otárola-Castillo, E. Geomorph: An R package for the collection and analysis of geometric morphometric shape data. *Methods Ecol. Evol*. 4, 393–399 (2013).

31. Gunz, P. & Mitteroecker, P. Semilandmarks: A method for quantifying curves and surfaces. *Hystrix Ital. J. Mammal* 24 (2013).

32. Guillerme, T. et al. Disparities in the analysis of morphological disparity. *Biol. Lett*. 16, e20200199 (2020).

33. Zelditch, M., Swiderski, D. & Sheets, H. D. Geometric Morphometrics for Biologists: A Primer (Academic, 2012).

34. R Core Team. R: A Language and Environment for Statistical Computing (2023).

35. Guillerme, T. dispRity: A modular R package for measuring disparity. *Methods Ecol. Evol.* 9, 1755–1763 (2018).

36. Seilacher, A. et al. Sedimentological, ecological and temporal patterns of fossil Lagerstätten. *Philos. Trans. R Soc. Lond. B Biol. Sci*. 311, 5–24 (1997).

37. Long, J. A. & Trinajstic, K. The Late Devonian Gogo Formation Lägerstatte of Western Australia: Exceptional early vertebrate preservation and diversity. *Annu. Rev. Earth Planet. Sci.* 38, 255–279 (2010).

38. Lund, R., Greenfest-Allen, E. & Grogan, E. D. Habitat and diversity of the Bear Gulch fish: Life in a 318 million year old marine Mississippian Bay. *Palaeogeogr Palaeoclimatol Palaeoecol.* 342–343, 1–16 (2012).

39. Flannery Sutherland, J. T., Moon, B. C., Stubbs, T. L. & Benton, M. J. Does exceptional preservation distort our view of disparity in the fossil record? *Proc. R. Soc. B Biol. Sci.* 286, e20190091 (2019).

40. Jurina, A. L. First Devonian forests on earth: Appearance, composition of plants, types of forest ecosystems, and their distribution. *Mosc. Univ. Geol. Bull*. 79, 233–242 (2024).

41. Bridge, T. C. L., Baird, A. H., Pandolfi, J. M., McWilliam, M. J. & Zapalski, M. K. Functional consequences of Palaeozoic reef collapse. *Sci. Rep*. 12, 1386 (2022).

42. Copper, P. Ancient reef ecosystem expansion and collapse. Coral Reefs. 13, 3–11 (1994).

43. Buatois, L. A. et al. The invasion of the land in deep time: Integrating Paleozoic records of paleobiology, ichnology, sedimentology, and geomorphology. *Integr. Comp. Biol*. 62, 297–331 (2022).

44. Algeo, T. J., Scheckler, S. E. & Maynard, J. B. 12. Effects of the Middle to Late Devonian spread of vascular land plants on weathering regimes, marine biotas, and global climate, in *Plants Invade the Land: Evolutionary and Environmental Perspectives* (eds Gensel, P. G. & Edwards, D.) 213–236 (Columbia University, 2001).

45. Golonka, J. Late Devonian paleogeography in the framework of global plate tectonics. *Glob. Planet. Change*. 186, 103129 (2020).

46. George, D. & Blieck, A. Rise of the earliest tetrapods: An Early Devonian origin from marine environment. *PLoS One*. 6, e22136 (2011).

47. Hartenfels, S. Upper Devonian to Mississippian global environmental change and impact on conodonts. *Palaeobiodiversity Palaeoenvironments*. 104, 629–682 (2024).

48. Oliver, W. A. Extinctions and migrations of Devonian rugose corals in the Eastern Americas realm. *Lethaia* 23, 167–178 (1990).

49. Kershaw, S. & Jeon, J. Stromatoporoids and extinctions: A review. *Earth-Sci. Rev*. 252, 104721 (2024).

50. Ma, K. et al. Astronomically forced dynamics of Late Devonian (Famennian) sea level and biotic recovery in Western Junggar, Northwest China. *Glob. Planet. Change*. 245, 104677 (2025).

51. Guillam, E. & Forel, M. B. Marine ostracod faunas through the Late Devonian extinction events. Part II: The Hangenberg event. *Earth-Sci. Rev*. 268, 105172 (2025).

52. Chevrinais, M., Jacquet, C. & Cloutier, R. Early establishment of vertebrate trophic interactions: Food web structure in Middle to Late Devonian fish assemblages with exceptional fossilization. *Bull. Geosci*. 92, 491–510 (2017).

53. Young, G. C. Placoderms (armored fish): Dominant vertebrates of the Devonian period. *Annu. Rev. Earth Planet. Sci*. 38, 523–550 (2010).

54. Boyle, J. & Ryan, M. J. New information on *Titanichthys* (Placodermi, Arthrodira) from the Cleveland Shale (Upper Devonian) of Ohio, USA. *J. Paleontol*. 91, 318–336 (2017).

55. DeLaurier, A. Evolution and development of the fish jaw skeleton. *WIREs Dev. Biol. 8, e337 (2019).*

56. Merritt, R. & Wallace, J. B. W. Aquatic habitats, in Encyclopedia of Insects (eds Resh, V. H. & Cardé, R. T.) 45–59 (Academic, 2003).

57. Price, S. A., Holzman, R., Near, T. J. & Wainwright, P. C. Coral reefs promote the evolution of morphological diversity and ecological novelty in labrid fishes. *Ecol. Lett.* 14, 462–469 (2011).

58. Friedman, S. T., Collyer, M. L., Price, S. A. & Wainwright, P. C. Divergent processes drive parallel evolution in marine and freshwater fishes. *Syst. Biol*. 71, 1319–1330 (2022).

59. Sazima, I. Similarities in feeding behaviour between some marine and freshwater fishes in two tropical communities. *J. Fish. Biol*. 29, 53–65 (1986).

60. Sabino, J. et al. Following fish feeding associations in marine and freshwater habitats. *Mar. Freshw. Res*. 68, 381–387 (2017).

61. Alsafy, M. A. M. et al. Anatomy, histology, and morphology of fish gills in relation to feeding habits: A comparative review of marine and freshwater species. *BMC Zool.* 10, 3 (2025).

62. Schaeffer, B. Rates of evolution in the coelacanth and dipnoan fishes. *Evolution* 6, 101–111 (1952).

63. Archer, A. W., Feldman, H. R., Kvale, E. P. & Lanier, W. P. Comparison of drier- to wetter-interval estuarine roof facies in the Eastern and Western interior coal basins, USA. *Palaeogeogr. Palaeoclimatol. Palaeoecol*. 106, 171–185 (1994).

64. Edmunds, W. E., Berg, T. M. & Sevon, W. D. The Mississippian and Pennsylvanian (Carboniferous) Systems in the United-States - Pennsylvania and New-York (United States Government Printing Office, 1979).

65. Rawson, J. R. G., Esteve-Altava, B., Porro, L. B., Dutel, H. & Rayfield, E. J. Early tetrapod cranial evolution is characterized by increased complexity, constraint, and an offset from fin-limb evolution. *Sci. Adv*. 8, eadc8875 (2022).

66. Neenan, J. M., Ruta, M., Clack, J. A. & Rayfield, E. J. Feeding biomechanics in *Acanthostega* and across the fish–tetrapod transition. *Proc. R. Soc. B Biol. Sci.* 281, 20132689 (2014).

67. Troyer, E. M. et al. Macroevolutionary role reversals in the earliest radiation of bony fishes. *Curr. Biol*. 35, 4631–4641e3 (2025).

68. Fröbisch, N. B. & Witzmann, F. Early tetrapods had an eye on the land. *Nature* 574, 494–495 (2019).

69. MacIver, M. A. & Finlay, B. L. The neuroecology of the water-to-land transition and the evolution of the vertebrate brain. *Philos. Trans. R Soc. B Biol. Sci*. 377, 20200523 (2021).

70. Dutel, H., Herbin, M., Clément, G. & Herrel, A. Bite force in the extant coelacanth *Latimeria*: The role of the intracranial joint and the basicranial muscle. *Curr. Biol*. 25, 1228–1233 (2015).

71. Ahlberg, P. E., Clack, J. A. & Lukševičs, E. Rapid braincase evolution between *Panderichthys* and the earliest tetrapods. Nature 381, 61–64 (1996).

72. Friedman, S. T., Price, S. A. & Wainwright, P. C. The effect of locomotion mode on body shape evolution in teleost fishes. *Integr. Org. Biol*. 3, obab016 (2021).

73. Sallan, L. & Galimberti, A. K. Body-size reduction in vertebrates following the end-Devonian mass extinction. *Science* 350, 812– 815 (2015).

74. Wainwright, P. C., Westneat, M. W. & Bellwood, D. R. Linking feeding behaviour and jaw mechanics in fishes, in *Biomechanics in Animal Behaviour* (eds Domenici, P. & Blake, R. W.) (Garland Science, 2000).

75. Fagerstrom, J. A. The history of Devonian-Carboniferous reef communities: Extinctions, effects, recovery. *Facies* 30, 177–191 (1994).

76. Siqueira, A. C., Morais, R. A., Bellwood, D. R. & Cowman, P. F. Trophic innovations fuel reef fish diversification. *Nat. Commun*. 11, 2669 (2020).

77. Lingo, M. E. & Szedlmayer, S. T. The influence of habitat complexity on reef fish communities in the Northeastern Gulf of Mexico. *Environ. Biol. Fishes*. 76, 71–80 (2006).

78. Bellwood, D. R., Goatley, C. H. R. & Bellwood, O. The evolution of fishes and corals on reefs: Form, function and interdependence. *Biol. Rev*. 92, 878–901 (2017).

79. Claverie, T. & Wainwright, P. C. A morphospace for reef fishes: Elongation is the dominant axis of body shape evolution. *PLoS One*. 9, e112732 (2014).

80. Cloutier, R. & Forey, P. L. Diversity of extinct and living actinistian fishes (Sarcopterygii), in *The Biology* of Latimeria chalumnae *and Evolution of Coelacanths* (eds Musick, J. A. & Bruton, M. N. & Balon, E. K.) Vol. 12, 59–74 (Springer Netherlands, Dordrecht, 1991).

81. Amemiya, C. T. et al. Complete *HOX* cluster characterization of the coelacanth provides further evidence for slow evolution of its genome. *Proc. Natl. Acad. Sci*. 107, 3622–3627 (2010).

82. Zhu, M. et al. Earliest known coelacanth skull extends the range of anatomically modern coelacanths to the Early Devonian. *Nat. Commun*. 3, 772 (2012).

83. Friedman, M. & Coates, M. I. A newly recognized fossil coelacanth highlights the early morphological diversification of the clade. *Proc. R. Soc. B Biol. Sci*. 273, 245–250 (2005).

84. Rivero-Vega, R. A., Berv, J. S., Clarke, J. T. & Friedman, M. Variable patterns of phenotypic evolution among canonical 'living fossil' lineages. (Preprint) (2024).

Acknowledgements: We thank L. Houle (UQAR) for his statistical advice and support. We thank Camila Cupello and an anonymous reviewer for their insightful comments on the original manuscript. We thank Mahasarakham University for support during R.C. visit.

Author contributions: O.V.: conceptualization, data curation, formal analysis, funding acquisition, methodology, visualization, writing original draft; O.L.: supervision, writing and reviewing; R.C.: conceptualization, supervision, writing and reviewing. All authors gave final approval for publication and agreed to be held accountable for the work performed therein.

Funding: O.V. was funded by a scholarship from Fonds de recherche du Québec – Nature et Technologies (FRQNT) [https://doi.org/10.69777/325538]. R.C was funded by Natural Sciences and Engineering Research Council of Canada (NSERC) Discovery grants 06133 and 05887.

Competing interests: The authors declare no competing interests.

CHAPITRE 3

MODULARITÉ VARIATIONNELLE DES ACTINOPTÉRYGIENS BASAUX : LES UNITÉS STRUCTURALES DU CRÂNE DES POISSONS DU PALÉOZOÏQUE

3.1 RÉSUMÉ EN FRANÇAIS DU TROISIÈME ARTICLE

Les actinoptérygiens (poissons à nageoires rayonnées) représentent le groupe de vertébrés actuels le plus diversifié. Leur succès écologique se reflète d'ailleurs dans leur remarquable disparité morphologique. Les actinoptérygiens sont apparus durant le Silurien supérieur – Dévonien inférieur, et ont connu leur première grande diversification durant le Carbonifère inférieur (Mississippien), à la suite de profonds changements environnementaux associés à la crise d'extinction de la fin du Dévonien (les événements de Kellwasser et de Hangenberg). La perte de groupes de vertébrés dominants, tels que les sarcoptérygiens et les « placodermes », aurait ouvert des niches écologiques ayant favorisé la radiation évolutive des actinoptérygiens.

La modularité est un patron particulier d'intégration morphologique présentant les organismes comme composés de sous-ensembles quasi-indépendants appelés modules. Elle augmenterait l'évolvabilité et favorisait la diversification morphologique. Nous avons ici exploré les patrons de modularité variationnelle des crânes des actinoptérygiens basaux à la recherche de modules morpho-fonctionnels qui auraient pu faciliter l'apparition de disparité morphologique au niveau de cette région. Nous avons utilisé une approche en morphométrie géométrique en deux dimensions (2D), pour capturer la forme latérale du crâne de 56 espèces du Dévonien et du Carbonifère à partir de reconstructions paléontologiques. Nous avons digitalisé 23 points de référence homologues (« landmarks ») et 150 points de référence semi-homologues (« semi-landmarks »). Le placement des points ciblait principalement trois région du crâne : la mâchoire, la région orbitale et la série operculaire (ou joue).

Quatre hypothèses de modularité *a priori* basées sur des propriétés morpho-fonctionnelles et développementales ont été testées à partir du coefficient CR (« Covariance

Ratio ») et de l'approche par matrice de distances. Un module formé par la mâchoire est fortement soutenu et suggérerait une certaine indépendance fonctionnelle liée aux stratégies alimentaires. Ce module de la mâchoire semblerait présent chez l'ensemble des premiers gnathostomes, indiquant une organisation modulaire bien conservée au travers des différentes lignées. Il pourrait avoir contribué à leur succès évolutif permettant des adaptations à différentes stratégies alimentaires. Ces résultats concordent avec la radiation adaptative trophique proposée pour les actinoptérygiens basaux durant le Carbonifère Inférieur.

Cet article, intitulé « Variational modularity of early actinopterygians: the building blocks of the Palaeozoic fish head », a été présenté dans une version abrégée à la 18ème édition de l'*International Symposium on Early and Lower Vertebrates* à Berrechid (Maroc) en Février 2026. En tant que première auteure, j'ai contribué à l'élaboration du projet et de sa méthodologie. J'ai réalisé la collecte de données, les analyses statistiques, les visuels et écrit la première version du manuscrit. Le docteur Olivier Larouche, second auteur, a supervisé les analyses. Le professeur Richard Cloutier, troisième auteur, a participé à l'élaboration du projet ainsi qu'à la révision de l'article.

Ce projet a été financé par une bourse des Fonds de recherche du Québec – Nature et Technologies (FRQNT) [https://doi.org/10.69777/325538] que j'ai reçue pour mon doctorat et par les subventions (06133 et 05887) du Conseil de Recherches en Sciences Naturelles et en Génie du Canada (CRSNG) du professeur Richard Cloutier.

3.2 VARIATIONAL MODULARITY OF EARLY ACTINOPTERYGIANS: THE BUILDING BLOCKS OF THE PALAEOZOIC FISH HEAD

Olivia Vanhaesebroucke[1], Olivier Larouche[2], and Richard Cloutier[1,3]

[1] Département de Biologie, Chimie et Géographie, Université du Québec à Rimouski, Rimouski, QC, Canada.

[2] Western Carolina University, Biology Department, Cullowhee, North Carolina, United States of America

[3] Center of Excellence on the Evolution of Life, Basin Studies and Applied Paleontology, Paleontological Research and Education Center, Mahasarakham University, Maha Sarakham 44150, Thailand.

ABSTRACT

Actinopterygians (ray-finned fishes) are the most diverse and the most speciose group of living vertebrates. Their ecological success is reflected in a remarkable morphological disparity. Originating during the Upper Silurian – Lower Devonian, actinopterygians underwent their first major diversification during the Carboniferous (Mississippian), following profound environmental changes associated with the Late Devonian extinction events (Kellwasser and Hangenberg crises). The decline of dominant vertebrate groups, such as sarcopterygians and "placoderms," likely opened ecological niches that facilitated the evolutionary radiation of actinopterygians. Modularity, a pattern of morphological integration presenting organisms as being composed of quasi-independent subsets called modules, is thought to increase evolvability (*i.e.*, the capacity to produce selectively useful variation) and promote morphological diversification. Our study explores the variational modularity of early actinopterygian skulls. Using two-dimensional (2D) geometric morphometrics, we analysed lateral skull reconstructions of 56 Devonian and Carboniferous species, based on 23 landmarks and 150 semi-landmarks. The landmarking scheme targeted three morpho-functional regions: the jaw, the orbit region, and the opercular series. Modularity was assessed using the covariance ratio (CR) coefficient and the distance matrix approach across four morpho-functional hypotheses. A strong jaw module suggests functional independence related to feeding strategies. This jaw module then seems conserved across all early gnathostomes, suggesting a well-established modularity pattern in early

gnathostomes, which could have participated to their evolutionary success. These findings align with the Mississippian diversification of actinopterygians as being associated with both ecological opportunity and intrinsic factors, with skull modularity potentially enhancing evolvability and facilitating the exploitation of new niches.

Key-words: Functional modules, Morphological disparity, Geometric morphometrics, Trophic divergence

Introduction

Biological organisms are intricate and diverse assemblages of parts connected through developmental or functional associations, yet they must remain globally integrated to operate as a whole (Olson and Miller 1999). Morphological integration describes the degree to which different parts of an organism covary, constraining or allowing their independent variation (Wagner et al. 2007; Klingenberg 2008), thereby shaping the overall morphological variation. Modularity refers to a particular pattern of integration in which organisms are organised into quasi-independent subsets, called "modules" (Zelditch and Goswami 2021). Each module comprises traits that are strongly integrated internally but only weakly connected to traits in other modules (Winther 2001; Klingenberg 2014).

Patterns of modularity can be identified at different hierarchical levels – within individuals, populations, or lineages (Cheverud 1996), and are closely linked to both functional and developmental organisation (Klingenberg 2008; Wagner et al. 2007). These associations may result from genetic correlations shaped by evolutionary integration through selection and co-selection (Cheverud 1996). Functional and developmental coupling among traits may produce higher covariation, leading to a variational integration, wherein variation in one trait induces variation in others. Thus, variational modularity investigates the structure of this covariation, defining modules as sets of traits that co-vary and can be detected at both population and species levels (Wagner et al. 2007; Zelditch and Goswami 2021). At population levels, such quasi-independence among modules may enhance evolvability (*i.e.,* the capacity to produce heritable variation that can be selected) (Kirschner and Gerhart 1998;

Brandon 2005), and is thought to have facilitated the diversification of highly disparate vertebrate clades such as actinopterygians (Evans et al. 2023; Larouche et al. 2018). Although evolvability cannot be observed directly in fossil organisms, its effect can be inferred from patterns of morphological variation through time in the fossil record. Thus, modularity is considered a key factor in major evolutionary radiations (Brandon 2005; Dellinger et al. 2019; Zelditch and Goswami 2021; Kirschner and Gerhart 1998).

Actinopterygians are a highly diversified group of vertebrates that includes more than 30,000 species today (Fricke 2021). The oldest articulated fossils of actinopterygians date back to the Lower Devonian (419.6 Ma) with *Meemannia eos* (M. Zhu et al. 2010), while some fragments of the presumptive early actinopterygian *Andreolepis hedei* come from the Late Silurian (424 Ma) (Chen et al. 2016). Actinopterygians survived through various episodes of major changes in the environment, such as the end-Devonian Mass Extinction (Devonian-Carboniferous boundary, 359 Ma) (Carmichael et al. 2019; Kaiser et al. 2016), which affected both their diversity and ecomorphological disparity, especially their skull shape (Sallan and Coates 2010; Vanhaesebroucke and Cloutier 2026; Flannery-Sutherland et al. 2025). The skull provides a key system for studying ecological adaptations in this group by this central role in several adaptations related to breathing, feeding, and the sensory system (Gartner et al. 2023; Cooper et al. 2010; Ascarrunz et al. 2019). Indeed, exploring patterns of morphological integration and modularity in the skulls may offer insights into the developmental and functional basis of early actinopterygian disparity and success.

Although if cranial modularity is well documented in extant taxa (Gartner et al. 2023; Cooper et al. 2013; Hugi et al. 2025), the modular organisation of the skull in early actinopterygians remains poorly characterised. The lack of quantitative analyses on early representatives of this group limits our understanding of how an early modular organisation might have contributed to the morphological diversification and evolution of actinopterygians throughout mid-Palaeozoic environmental perturbations.

In this study, we investigate the patterns of cranial variational modularity in early actinopterygians from the Devonian and Carboniferous using two-dimensional (2D)

geometric morphometrics approaches. We tested how modular structures may have arisen from functional shifts across major mid-Palaeozoic transitions and contributed to the adaptive trophic radiation of early actinopterygians. Jaws constituted a major innovation in vertebrate history (Khaner 2007; Mallat 1996; Miyashita 2016). Extant fishes show high disparity in jaw morphology, which tends to correlate with their feeding mechanics (Albertson et al. 2003; Konow et al. 2008; Wainwright et al. 2004; Wainwright and Richard 1995). We then expect the jaw region (lower jaw and maxillary arcade) to constitute a first variational and functional module. Furthermore, vision, including eye diameter and positioning, are closely related to habitats and feeding behaviors in fishes (Goatley and Bellwood 2009; Ingram and Shurin 2009; Warrant and Locket 2004). In extant species, Cooper et al. (2010) proposed the preorbital region as a module related to trophic biomechanics that has a strong association with the radiation of the African Rift-Lake cichlids. At least for teleosts, the modularity of this region is also supported by genetic studies showing a craniofacial variation in zebrafish mutants with changes in the length of the preorbital region (Albertson and Yelick 2007; Cooper et al. 2013; LeClair et al. 2009). We expect to detect an evolutionarily conserved orbital module in early actinopterygians. Finally, the opercular series and cheekbones, plays a key role in the breathing and the feeding behaviour of fishes and exhibits great diversity within both extant and extinct fishes (Ascarrunz et al. 2019; Lauder 1982; Wainwright et al. 2004). Despite the disparity of this region, the functional property of these regions could benefit from the morphological integration of its structures, which could support these regions as a hypothesised variational module.

Material and methods

1. Taxonomic diversity

To obtain an estimate of the taxonomic diversity of early actinopterygians during the Devonian and Carboniferous periods, we gathered a list of 197 early actinopterygian species from primary literature and previously published databases (Sallan and Coates 2010; Schultze et al. 2021). For each species, the first (FAD) and last (LAD) appearance dates were

noted (Figure 1, Annexe IV Table S1); FAD and LAD are determined as the oldest and youngest age limits of the geological time identified for a given species. Our time scale sampling goes from the Early Eifelian (Middle Devonian, 393.47 Ma) to the Late Gzhelian (Pennsylvanian, 298.9 Ma), which represents a 94.57 Ma time span, and is divided into 11 stages (Eifelian, Givetian, Frasnian, Famennian, Tournaisian, Viséan, Serpukhovian, Bashkirian, Moscovian, Kasimovian, and Gzhelian). The preservation state of actinopterygians from the Early Devonian did not allow for complete morphological analyses with geometric morphometrics. We analyzed actinopterygian diversity with the R package 'divDyn' (v.0.8.3) (Kocsis et al. 2019).

2. Morphological dataset

Two-dimensional (2D) datasets were used rather than 3D information because the shape of fossil species is rarely conserved in three dimensions. We assembled a 2D dataset, including a total of 56 species, using palaeontological reconstructions of the lateral view of the skull of Devonian and Carboniferous actinopterygian species (Annexe IV Table S1). Even if reconstructions may have limitations due to the preservation of fossils and the subjective interpretation of structures, this approach allowed us to estimate disparity from continuous data and to obtain geometric information related to the shape changes in several morphological features of early actinopterygians. Using *Adobe Photoshop* (v22.0.0), we modified the reconstructions of the skull to put the mouth in a closed position, controlling the morphological variation that could be induced by the opening of the mouth. Only the species for which adult specimens were described were compiled, excluding species known solely from juvenile specimens.

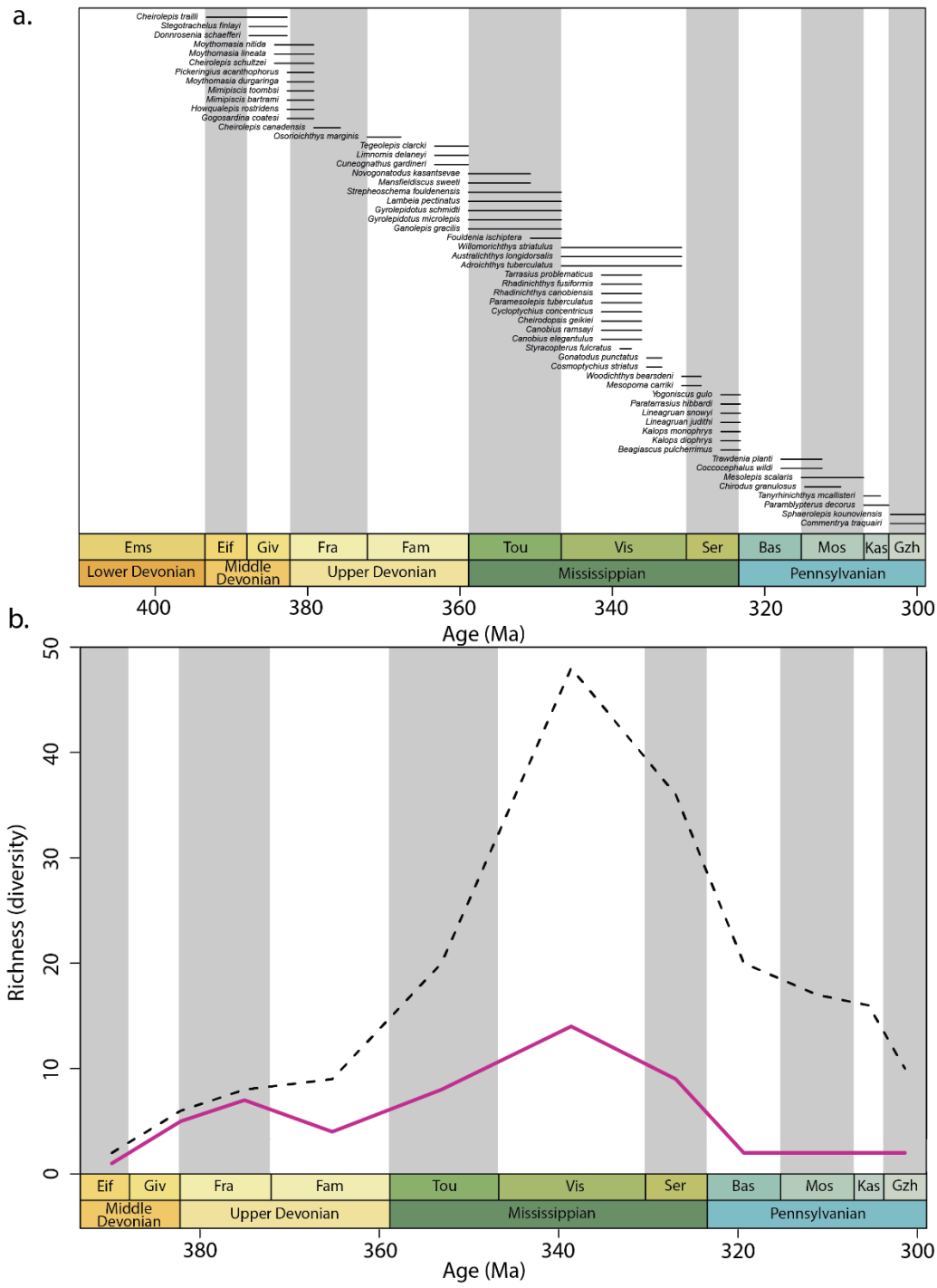


Figure 1. Temporal occurrence and diversity of early actinopterygian species through the Devonian and Carboniferous. (a) Temporal occurrence for the 56 species of early actinopterygians analysed; (b) diversity of early actinopterygians through time based on the

richness calculated for each stage for the 56 species analysed (dark pink line) and for the 197 species of early actinopterygians (dashed black line). Bas: Bashkirian; Eif: Eifelian; Fam: Famennian; Fra: Frasnian; Giv: Givetian; Gzh: Gzhelian; Kas: Kasimovian; Mos: Moscovian; Ser: Serpukhovian; Tou: Tournaisian; and Vis: Viséan.

3. Landmarking scheme

Skull shape variations were quantified using 2D-landmark-based geometric morphometrics. We digitised 23 landmarks and 150 semi-landmarks describing the outline of the cheek, the operculum, the orbit, and the jaw regions of actinopterygian skull (Figure 2a, Annexe IV Table S2). All landmarks and semi-landmarks were digitized using *tpsDig2* (v2.32) (Rohlf 2015).

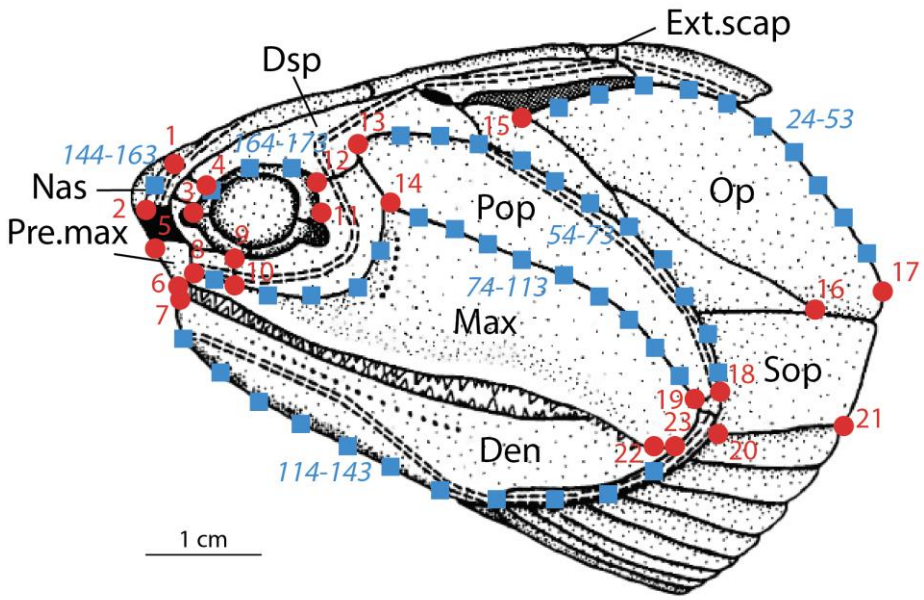


Figure 2. Landmarks (red circles) and semi-landmarks (blue squares) positioning scheme for geometric morphometrics analyses of the lateral view of the skull; *Cheirolepis canadensis* (Arratia and Cloutier, 1996, Figures 6A). See Annexe IV Table S2 for a full description of the landmarks and semi-landmarks. Den: dentary; Dsp: dermosphenotic; Ext.scap: extrascapular; Max: maxillary; Nas: nasal; Op: operculum; Pop: preopercular; Pre.max: premaxillary; Sop: subopercular

Each set of landmark coordinates was rotated, translated, and scaled with a Procrustes superimposition using the *gpagen* function in 'geomorph' (v.4.0.1) (Adams and Otárola-Castillo 2013). Semi-landmarks were slid using the Procrustes distance minimisation criterion (Gunz and Mitteroecker 2013). A multivariate regression of shape variation on centroid sizes was used to test for allometry (Klingenberg 2016). The shape-size relationship explained 8% of the variation for actinopterygians and was found to be statistically significant ($F_{1,54} = 4.68$, $p = 0.002$, $R^2 = 0.080$). We therefore decided to remove the effect of allometry, and size-corrected coordinates were used for the following analyses.

4. Modular a priori hypotheses

Four a priori hypotheses of modularity were formulated based on three putative modules (Figure 3, see Annexe IV for a full description of the putative modules). Partitioning of landmarks into putative modules was based on either shared developmental patterns (*e.g.,* gene expression involved in the development of several structures), functional associations of traits (*e.g.,* integration due to coordination of elements during breathing or feeding), or topological relationships (*e.g.,* connection of the different regions through articulations or bone sutures).

5. Morphological integration and modularity tests

Morphological integration patterns were estimated based on the partial least squares (PLS) analysis, which quantified integration between putative modules for each hypothesis (Adams and Collyer 2016). We used two different approaches to test modularity hypotheses: (1) the covariance ratio (CR) and (2) the distance matrix approach. The CR ratio calculates the ratio of covariation between modules relative to covariation within modules (Adams 2016). This metric was preferred over Escoufier's RV coefficient, known to be more sensitive to the sample size and the number of variables (Adams 2016).

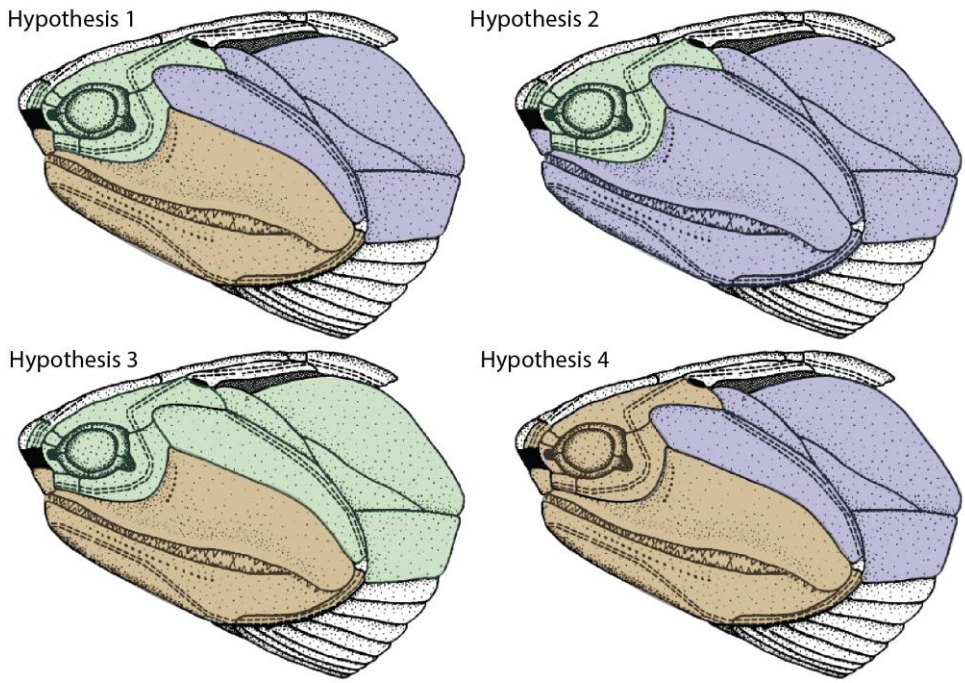


Figure 3. Graphical representation of the four a priori hypotheses of modularity. Elements of the same colour belong to the same hypothetical variational module. *Cheirolepis canadensis* (Arratia and Cloutier, 1996, Figures 6A). See Annexe IV Table S3 for a complete description of the hypotheses.

Optimal modular hypotheses were identified using the Z_{CR}, which consists of pairwise comparisons of CR effect sizes (Adams and Collyer 2019). For the distance matrix approach (Monteiro et al. 2005; Klingenberg and Monteiro 2005), the landmark configuration was divided into three separate partitions of shape. For each partition, pairwise Procrustes distances were computed among specimens (each specimen representing a species), and the resulting distance matrices were used to generate a correlation matrix. This correlation matrix was then analysed using graphical modelling, which assesses the quasi-independence of modules (each module representing one or a combination of partitions) and evaluates the fit of modularity models to the observed correlations (Zelditch et al. 2009; Magwene 2001, 2009). Model comparisons were based on the deviance information criterion (DIC), with

differences of at least four considered to indicate support for one modularity hypothesis over another (Spiegelhalter et al. 2002).

To control for potential phylogenetic constraints, we performed a preliminary phylogenetic analysis on 33 species of early actinopterygians. For each modularity hypothesis, we quantified the CR ratio and morphological integration both with and without incorporating phylogenetic information, in order to assess the influence of shared ancestry on the resulting patterns. We used the topology of an unpublished phylogenetic tree from Mickle (2012), which was selected due to its broad taxonomic inclusion of most species in our dataset, and pruned it to retain only the 33 species they have in common from the 77 included (see Annexe IV Figure S1). As the resulting patterns were the same with and without the phylogenetic information, we decided to present the analyses including all 56 species without phylogeny in the main document (see Annexe IV Table S3 for the preliminary phylogenetic analyses).

All statistical analyses were performed in R (v.4.3.2) using the package 'geomorph' (Adams and Otárola-Castillo 2013), 'Morpho' (Schlager 2017), and 'ggm' (Sadeghi and Marchetti 2012).

Results

All hypotheses show significant modular structure, as indicated by the CR coefficient values lower than 1 (*p-value* = 0.001) (Table 1). Hypothesis 1 (orbital, opercular/cheek and jaw modules) scores the lowest CR value (CR = 0.795, *p-value* = 0.001), closely followed by Hypothesis 2 (orbital and opercular/cheek + jaw modules) (CR = 0.806, *p-value* = 0.001). Standardized effect sizes (Z_{CR}) are strongly negative for all hypotheses, however, Hypotheses 1 and 3 (jaw and orbital + opercular/cheek modules) display the most pronounced deviations from null expectations, displaying the strongest modular signal. In both hypotheses, the jaw is identified as a separate module. Hypothesis 4 (orbital + jaw and opercular/cheek modules) was the only one found to have a significantly lower modular signal compared to Hypothesis 1.

The distance matrix approach supports different hypotheses depending on the fitting procedure. The "simultaneous-fit approach" uses data from a Procrustes superimposition applied to the entire configuration of landmarks, therefore preserving the information about the relative sizes and spatial relationships among shape partitions (Klingenberg 2009). With this approach, Hypothesis 3 is recognised as the best fit, while Hypothesis 1 is strongly rejected. The "separate-subsets approach" performs a second Procrustes superimposition for each individual partition of shape (Klingenberg 2009). This approach eliminates the variation in relative size and positioning of partitions. Thus, when only the shape of individual partitions is considered, no remarkable differences among hypotheses are noted. Hypothesis 1 exhibit the lowest DIC, but the other hypotheses remain close, indicating comparable level of modularity support.

Table 1. Results of modularity testing using the CR metric and the distance matrix approach, and morphological integration using PLS analyses.

Hypothesis	CR coefficient			Distance matrix approach (simultaneous-fit approach)		Distance matrix approach (separate subsets approach		Morphological integration	
	CR	*p-value*	Z_{CR}	DIC	ΔDIC	DIC	ΔDIC	PLS	p-value
1	0.795	0.001	-13.47	58.09	27.25	-3.94	0	0.882	0.001
2	0.806	0.001	-10.99	32.89	2.05	-3.81	0.13	0.874	0.001
3	0.850	0.001	-12.42	30.84	0	-1.56	2.38	0.929	0.001
4	0.860	0.001	-10.91*	33.69	3.05	-2.48	1.46	0.939	0.001

*Z_{CR} pairwise comparison significantly different with Hypothesis 1 (*p-value* = 0.03)

PLS analyses were performed for all hypotheses to quantify the strength of correlations among modules, giving an estimate of morphological integration among them. All PLS scores are close to 1, indicating a strong signal for morphological integration across all hypotheses (Table 1). Hypothesis 2 (PLS = 0.874, *p-value* = 0.001) followed by Hypothesis 1 (PLS = 0.882, *p-value* = 0.001) show the lowest level of integration, which is congruent with the modular signal described above.

Overall, all hypotheses are supported by a significant level of modularity among their putative modules. Support varies depending on the methods, with Hypothesis 3 as best fitting with the simultaneous-fit approach, while the CR coefficient best supports Hypotheses 1 and 3.

Discussion

The main goal of this study was to explore modularity patterns of the skull in Devonian and Carboniferous actinopterygians. Our results provide strong evidence of a modular organisation. Considering the different approaches, Hypotheses 1 and 3 were best supported. Hypothesis 1 is composed of three distinct modules (the jaw, the orbit region and the opercular region) and was best supported by the CR coefficient, but the least supported hypothesis by the simultaneous fit approach. Hypothesis 3 is composed of two distinct modules (the jaw and the orbit + opercular regions) and was best fitting with the simultaneous fit approach and the Z_{CR} analysis. In both cases, the jaw represented a distinct module, which strongly supports this region as being more independent from the rest of the skull. However, Hypothesis 2 was also among the most supported by all analyses regrouping the cheek region with the jaw. This could mean that even if the jaw emerged as a modular part of the skull, it remains tightly integrated with the cheek region but loosely connected to the orbit region.

1. The actinopterygian skull: a modular organisation as driver for morphological disparity

The fish skull is composed of numerous articulated bones and cartilages, which increase the cranial kinesis properties, whereas functional and biomechanical constraints limit its variation to preserve unity and stability to function as a whole (Mork and Crump 2015; Parsons et al. 2018). However, the shape of the osteological structures and connections among them constitute a tremendous source of disparity among fishes usually associated to the ecology (Westneat 2005; Montuelle and Kane 2019; Evans et al. 2017; Lauder 1982). Skull morphological integration has been studied on extant actinopterygian taxa, and linked to developmental (Lehoux and Cloutier 2015; Schmidt and Starck 2010), genetic (Cooper et al. 2013), and morphological properties (Larouche et al. 2023; Cooper et al. 2010). A putative

preorbital module in extant African Rift-Lake cichlids has been identified (Cooper et al. 2010) and supported by craniofacial variation in zebrafish mutants (Cooper et al. 2013). This aligns with our findings in which, within two of the most supported analyses, the orbital region constituted a separate module. This module may be related to ecological functional properties. Indeed, the eye positioning is closely related to habitat use and trophic position in fishes (Warrant and Locket 2004; Ingram and Shurin 2009; Goatley and Bellwood 2009).

Regarding the ecological properties of the skull, extinct fishes show high disparity in jaw morphology, which tends to correlate with their feeding mechanics (Troyer et al. 2025). Jaws also showed recurrent modifications in their anatomy, such as the complexification of dermal bones associated with progressive ossification of the lower jaws of "placoderms" (Zhu et al. 2019; Young 2010), the variation of jaw musculature in actinopterygians (Wainwright et al. 2015; Friel and Wainwright 1999; Datovo and Rizzato 2018; Westneat 2005), and the variation of jaw kinematics in aquatic vertebrates (Hulsey et al. 2005; Bellwood et al. 2015; Wainwright et al. 2015). Early history of jawed vertebrates is marked by the rapid reach of a maximum functional diversity in jaw morphology during the Devonian, mostly within "placoderms" and sarcopterygians (Troyer et al. 2025; Anderson et al. 2011a), and recent findings suggest the modularity of the "placoderms" jaw, especially considering the unusual jaw shape of the Late Devonian *Alienacanthus malkowskii* (Jobbins et al. 2024). In our analyses, the jaw was also strongly supported by all the different approaches. Identifying an early jaw module also within the actinopterygian lineage indicates a strongly conserved jaw module across all gnathostomes, which could have played a key role in the evolutionary success of the group, allowing for rapid morphological adaptations and for various trophic specialisations among this clade (Anderson et al. 2011; Miyashita 2016).

Despite the clear modular signal for the jaw, it also appeared integrated with the cheek. The cheek plays a key functional and structural role in jaw suspension in fishes (DeLaurier 2019). It is an important muscle attachment site for the jaw muscles and is involved in breathing and feeding movements (DeLaurier 2019). The tight integration between the jaw

and the cheek region in our analyses could attest for their functional connection related to feeding, even in early actinopterygians.

Finally, these modularity patterns align with early actinopterygian morphological disparity. Indeed, a rapid increase in skull disparity associated with the Devonian-Carboniferous transition and the early stage of the diversification of the group during the Late Devonian and early Mississippian, driven by a variation in the cheek region and the length of the preorbital region, was detected (Vanhaesebroucke and Cloutier 2026). The relative independence of the modular skull regions may have contributed shaping the skull of early actinopterygians during their major diversification event during the mid-Palaeozoic. This event is usually associated with an evolutionary radiation triggered by a trophic divergence and the exploitation of new niches during the Carboniferous recovery phase (Sallan and Friedman 2011). Modularity could then constitute an important biological property that may support and allow rapid morphological diversification associated with rapid speciation events (Neves et al. 2025).

2. Disparity in modularity analyses and future investigations

The disparity observed among modularity analyses highlights the importance of methodological complementary approaches when investigating modular organisation. Even if modularity is a key concept in evolutionary biology, its evaluation remains challenging (Zelditch and Goswami 2021). Using different approaches provides different perspectives on morphological integration. Indeed, the main differences in this study results regard the two different methods used in the distance matrix approach. Indeed, the simultaneous-fit approach presented the most unexpected result, identifying Hypothesis 1 as the least supported, being in disagreement with all the other analyses. This approach uses data from Procrustes superimposition applied to the entire configuration of landmarks, preserving the information related to the respective sizes and spatial relationships among partitions of shape (Klingenberg 2009). Therefore, when these information are conserved, the most subdivided hypothesis is the least supported. This could suggest partially integrated modules (Klingenberg 2014) and support the previous statement suggesting the skull to be modular

but functionally integrated to work as a whole. The subdivision of the skull may then be more complex, involving hierarchical modules (Klingenberg 2014). Including approaches that do not solely rely on covariation patterns, such as the organisational modularity framework based on network analyses (Esteve-Altava 2017, 2020), could provide a complementary perspective to capture structural relationships among skull elements. This method has already been applied to extinct taxa (Esteve-Altava et al. 2014), and allows the integration of a three-dimensional aspect of the skull organisation, which is usually limited in landmark-based approaches due to the preservation of fossils. Testing the modularity patterns with this network method could therefore help corroborate the results obtained here. Finally, further investigations into modularity across actinopterygian evolution, especially through the inclusion of more recent taxa, would help determine whether these patterns are conserved through time.

Conclusion

This variational modularity analysis of the early actinopterygian skull describes a strong modular signal of its organisation. Even if the different approaches gave slightly different results, the jaw was a strongly supported module. This is congruent with what was observed in other groups of early gnathostomes (Jobbins et al. 2024), suggesting a well-established modularity pattern in early taxa. This module is supported by both ecological and developmental properties. Thus, the early establishment of developmental and functional partitioning of the actinopterygian body plan may have contributed to the successful morphological diversification that accompanied their major diversification and trophic radiation at the end of the Devonian. Even if further investigation will confirm and refine these patterns, this study lays the groundwork for a deeper investigation into the evolution of the body plan organisation of the most successful clade of vertebrates.

Acknowledgments: We thank L. Houle (UQAR) for his statistical advice and support. We thank C. Vanhaesebroucke and C. Vanhaesebroucke for helping compile the matrix.

Data availability: Data and code are available on GitHub:

https://github.com/oliviavanhaesebroucke/Early-actinopterygian-modularity

Fundings: O.V. was funded by Fonds de recherche du Québec – Nature et Technologies (FRQNT), [https://doi.org/10.69777/325538] and R.C. was funded by Natural Sciences and Engineering Research Council of Canada (NSERC) Discovery grants 06133 and 05887.

Authors contribution: O.V. and R.C. conceptualized the study and established the research goals. O.V. designed the study, acquired the data, performed the analyses, and created the visualisations. OV. and O.L. design the methodology frameworks. O.L. provided part of the R script. O.V. wrote and revised the original draft. O.L. and R.C. supervised and reviewed.

Conflict of interest: Conflicts of Interest: The authors declare no conflicts of interest. The funders had no role in the design of the study; in the collection, analyses, or interpretation of data; in the writing of the manuscript; or in the decision to publish the results.

References

Adams, Dean C. 2016. 'Evaluating modularity in morphometric data: challenges with the RV coefficient and a new test measure'. Methods in Ecology and Evolution 7 (5): 565–72.

Adams, D. C., and M. L. Collyer. 2016. 'On the comparison of the strength of morphological integration across morphometric datasets'. Evolution 70 (11): 2623–31.

Adams, D. C., and M. L. Collyer. 2019. 'Comparing the strength of modular signal, and evaluating alternative modular hypotheses, using covariance ratio effect sizes with morphometric data'. Evolution 73 (12): 2352–67.

Adams, D. C., and E. Otárola-Castillo. 2013. 'Geomorph: An R package for the collection and analysis of geometric morphometric shape data'. Methods in Ecology and Evolution 4 (4): 393–99.

Albertson, R. C., J. T. Streelman, and T. D. Kocher. 2003. 'Directional selection has shaped the oral jaws of lake malawi cichlid fishes'. Proceedings of the National Academy of Sciences 100 (9): 5252–57.

Albertson, R. C., and P. C. Yelick. 2007. '*Fgf8* haploinsufficiency results in distinct craniofacial defects in adult zebrafish'. Developmental Biology 306 (2): 505–15.

Anderson, P. S. L., M. Friedman, M. D. Brazeau, and E. J. Rayfield. 2011. 'Initial radiation of jaws demonstrated stability despite faunal and environmental change'. Nature 476 (7359): 206–9.

Ascarrunz, E., M. R. Sánchez-Villagra, R. Betancur-R, and M. Laurin. 2019. 'On trends and patterns in macroevolution: Williston's law and the branchiostegal series of extant and extinct osteichthyans'. BMC Evolutionary Biology 19 (1): 117.

Bellwood, D. R., C. H. R. Goatley, O. Bellwood, D. J. Delbarre, and M. Friedman. 2015. 'The rise of jaw protrusion in spiny-rayed fishes closes the gap on elusive prey'. Current Biology 25 (20): 2696–700.

Brandon, R. N. 2005. 'Evolutionary modules: conceptual analyses and empirical hypotheses'. *In* Modularity: understanding the development and evolution of natural complex systems, W. Callebaut and D. Rasskin-Gutman (eds). MA: MIT Press. Cambridge. 472p.

Carmichael, S. K., J. A. Waters, P. Königshof, T. J. Suttner, and E. Kido. 2019. 'Paleogeography and paleoenvironments of the Late Devonian Kellwasser event: a review of its sedimentological and geochemical expression'. Global and Planetary Change 183: 102984.

Chen, D., H. Blom, S. Sanchez, P. Tafforeau, and P. E. Ahlberg. 2016. 'The stem osteichthyan *Andreolepis* and the origin of tooth replacement'. Nature 539 (7628): 237–41.

Cheverud, J. M. 1996. 'Developmental integration and the evolution of pleiotropy'. Integrative and Comparative Biology 36 (1): 44–50.

Cooper, W. J., K. Parsons, A. McIntyre, B. Kern, A. McGee-Moore, and R. C. Albertson. 2010. 'Bentho-pelagic divergence of cichlid feeding architecture was prodigious and consistent during multiple adaptive radiations within African Rift-Lakes'. PLOS One 5 (3): e9551.

Cooper, W. J., R. M. Wirgau, E. M. Sweet, and R. C. Albertson. 2013. 'Deficiency of zebrafish *fgf20a* results in aberrant skull remodeling that mimics both human cranial disease and evolutionarily important fish skull morphologies'. Evolution & Development 15 (6): 426–41.

Datovo, A., and P. P. Rizzato. 2018. 'Evolution of the facial musculature in basal ray-finned fishes'. Frontiers in Zoology 15 (1): 40.

DeLaurier, A. 2019. 'Evolution and development of the fish jaw skeleton'. WIREs Developmental Biology 8 (2): e337.

Dellinger, A. S., S. Artuso, S. Pamperl, et al. 2019. 'Modularity increases rate of floral evolution and adaptive success for functionally specialized pollination systems'. Communications Biology 2 (1): 453.

Esteve-Altava, B.. 2017. ‘Challenges in identifying and interpreting organizational modules in morphology’. Journal of Morphology 278 (7): 960–74.

Esteve-Altava, B.. 2020. ‘A node-based informed modularity strategy to identify organizational modules in anatomical networks’. Biology Open 9 (10): bio056176.

Esteve-Altava, B., J. Marugán-Lobón, H. Botella, and D. Rasskin-Gutman. 2014. ‘Random loss and selective fusion of bones originate morphological complexity trends in tetrapod skull networks’. Evolutionary Biology 41 (1): 52–61.

Evans, K. M., T. J. Buser, O. Larouche, and M. A. Kolmann. 2023. ‘Untangling the relationship between developmental and evolutionary integration’. Seminars in Cell & Developmental Biology 145: 22–27.

Evans, K. M., B. T. Waltz, V. A. Tagliacollo, B. L. Sidlauskas, and J. S. Albert. 2017. ‘Fluctuations in evolutionary integration allow for big brains and disparate faces’. Scientific Reports 7 (1): 40431.

Flannery-Sutherland, J. T., S. Henderson, S. A. Fasey, and S. Giles. 2025. ‘Diversification dynamics of the palaeozoic actinopterygian radiation’. Preprint, bioRxiv.

Fricke, R.. 2021. ‘Eschmeyer’s Catalog of Fishes: Genera/Species by Family/Subfamily’. Electronic Version Accessed.

Friel, J. P., and P. C. Wainwright. 1999. ‘Evolution of complexity in motor patterns and jaw musculature of tetraodontiform fishes’. Journal of Experimental Biology 202 (7): 867–80.

Gartner, S. M., O. Larouche, K. M. Evans, and M. W. Westneat. 2023. ‘Evolutionary patterns of modularity in the linkage systems of the skull in wrasses and parrotfishes’. Integrative Organismal Biology 5 (1): obad035.

Goatley, C. H. R., and D. R. Bellwood. 2009. ‘Morphological structure in a reef fish assemblage’. Coral Reefs 28 (2): 449–57.

Gunz, P., and P. Mitteroecker. 2013. ‘Semilandmarks: a method for quantifying curves and surfaces’. Hystrix, the Italian Journal of Mammalogy 24 (1).

Hugi, A. L., H. Chan, A. Rummel, et al. 2025. ‘Developmental and functional interactions structure patterns of variational modularity in the lunar wrasse skull’. Integrative and Comparative Biology 65 (3): 560–71.

Hulsey, C. D., G. J. Fraser, and J. T. Streelman. 2005. ‘Evolution and development of complex biomechanical systems: 300 million years of fish jaws’. Zebrafish 2 (4): 243–57.

Ingram, T., and J. B. Shurin. 2009. ‘Trait-based assembly and phylogenetic structure in northeast pacific rockfish assemblages’. Ecology 90 (9): 2444–53.

Jobbins, M., M. Rücklin, M. R. Sánchez Villagra, et al. 2024. ‘Extreme lower jaw elongation in a placoderm reflects high disparity and modularity in early vertebrate evolution’. Royal Society Open Science 11 (1): 231747.

Kaiser, S. I., M. Aretz, and R. Thomas Becker. 2016. ‘The global Hangenberg Crisis (Devonian–Carboniferous transition): review of a first-order mass extinction’. *In* Devonian Climate, Sea Level and Evolutionary Events, R. T. Becker, P. Königshof, and C. E. Brett (eds). Geological Society of London. 423p.

Khaner, O.. 2007. ‘Evolutionary innovations of the vertebrates’. Integrative Zoology 2 (2): 60–67.

Kirschner, M., and J. Gerhart. 1998. ‘Evolvability’. Proceedings of the National Academy of Sciences 95 (15): 8420–27.

Klingenberg, C. Peter. 2008. ‘Morphological integration and developmental modularity’. Annual Review of Ecology, Evolution, and Systematics 39: 115–32.

Klingenberg, C. Peter. 2009. ‘Morphometric integration and modularity in configurations of landmarks: tools for evaluating a priori hypotheses’. Evolution & Development 11 (4): 405–21.

Klingenberg, C. Peter. 2014. ‘Studying morphological integration and modularity at multiple levels: concepts and analysis’. Philosophical Transactions of the Royal Society B: Biological Sciences 369 (1649): 20130249.

Klingenberg, C. Peter. 2016. ‘Size, shape, and form: concepts of allometry in geometric morphometrics’. Development Genes and Evolution 226 (3): 113–37.

Klingenberg, C. P., and L. R. Monteiro. 2005. Distances and directions in multidimensional shape spaces: implications for morphometric applications. Systematic Biology 54 (4): 678–88.

Kocsis, A. T., C. J. Reddin, J. Alroy, and W. Kiessling. 2019. ‘The R package divDyn for quantifying diversity dynamics using fossil sampling data’. Methods in Ecology and Evolution 10 (5): 735–43.

Konow, N., D. R. Bellwood, P. C. Wainwright, and A. M. Kerr. 2008. ‘Evolution of novel jaw joints promote trophic diversity in coral reef fishes’. Biological Journal of the Linnean Society 93 (3): 545–55.

Larouche, O., S. M. Gartner, M. W. Westneat, and K. M. Evans. 2023. ‘Mosaic evolution of the skull in labrid fishes involves differences in both tempo and mode of morphological change’. Systematic Biology 72 (2): 419–32.

Larouche, O., M. L. Zelditch, and R. Cloutier. 2018. ‘Modularity promotes morphological divergence in ray-finned Fishes’. Scientific Reports 8 (1): 7278.

Lauder, G. V. 1982. ‘Patterns of evolution in the feeding mechanism of actinopterygian fishes’. American Zoologist 22 (2): 275–85.

LeClair, E. E., Stephanie R. M., A. Huang, J. M. Topczewska, and J. Topczewski. 2009. ‘Craniofacial skeletal defects of adult zebrafish glypican 4 (knypek) mutants’. Developmental Dynamics 238 (10): 2550–63.

Lehoux, C., and R. Cloutier. 2015. ‘Building blocks of a fish head: developmental and variational modularity in a complex system’. Journal of Experimental Zoology Part B: Molecular and Developmental Evolution 324 (7): 614–28.

Magwene, P. M. 2001. ‘New tools for studying integration and modularity’. Evolution 55 (9): 1734–45.

Magwene, P. M. 2009. ‘Statistical methods for studying modularity: a reply to Mitteroecker and Bookstein’. Systematic Biology 58 (1): 146–49.

Mallat, J. 1996. ‘Ventilation and the origin of jawed vertebrates: a new mouth’. Zoological Journal of the Linnean Society 117 (4): 329–404.

Mickle, K. E. 2012. ‘Unraveling the systematics of palaeoniscoid fishes--lower actinopterygians in need of a complete phylogenetic revision’. University of Kansas. Thesis.

Miyashita, T. 2016. ‘Fishing for jaws in early vertebrate evolution: a new hypothesis of mandibular confinement’. Biological Reviews 91 (3): 611–57.

Monteiro, L. R., V. Bonato, and S. F. Dos Reis. 2005. ‘Evolutionary integration and morphological diversification in complex morphological structures: mandible shape divergence in spiny rats (Rodentia, Echimyidae)’. Evolution & Development 7 (5): 429–39.

Montuelle, S. J., and E. A. Kane. 2019. ‘Food capture in vertebrates: a complex integrative performance of the cranial and postcranial systems’. *In* Feeding in vertebrates: evolution, morphology, behavior, biomechanics, V. Bels and I. Q. Whishaw (eds). Springer International Publishing. 865p.

Mork, L., and G. Crump. 2015. ‘Zebrafish craniofacial development: a window into early patterning’. Current Topics in Developmental Biology 115: 235-269.

Neves, M. P., H. W. Chan, E. C. M. Santos, and K. M. Evans. 2025. ‘Cranial modularity drives phenotypic diversification and adaptive radiation of Antarctic icefishes’. Proceedings of the National Academy of Sciences 122 (40): e2503283122.

Olson, E. C., and R. L. Miller. 1999. Morphological Integration. University of Chicago Press. 355p.

Parsons, K. J., Y. H. Son, A. Crespel, et al. 2018. ‘Conserved but flexible modularity in the zebrafish skull: implications for craniofacial evolvability’. Proceedings of the Royal Society B: Biological Sciences 285 (1877): 20172671.

Rohlf, F. 2015. ‘The Tps series of software’. Hystrix 26 (1): 9-12.

Sadeghi, K., and G. Marchetti. 2012. ‘Graphical Markov models with mixed graphs in R’. The R Journal. 4: 2073-4859.

Sallan, L. C., and M. I. Coates. 2010. ‘End-Devonian extinction and a bottleneck in the early evolution of modern jawed vertebrates’. Proceedings of the National Academy of Sciences 107 (22): 10131–35.

Sallan, L. C., and M. Friedman. 2011. ‘Heads or tails: staged diversification in vertebrate evolutionary radiations’. Proceedings of the Royal Society B: Biological Sciences 279 (1735): 2025–32.

Schlager, S.. 2017. ‘Morpho and Rvcg – shape analysis in R: R-packages for geometric morphometrics, shape analysis and surface manipulations’. *In* Statistical shape and deformation analysis, G. Zheng, S. Li, and G. Székely (eds). Academic Press. 508p.

Schmidt, K., and J. M. Starck. 2010. ‘Developmental plasticity, modularity, and heterochrony during the phylotypic stage of the zebra fish, *Danio rerio*’. Journal of Experimental Zoology Part B: Molecular and Developmental Evolution 314 (2): 166–78.

Schultze, H.-P., K. E. Mickle, C. Poplin, E. J. Hilton, and L. Grande. 2021. Handbook of paleoichthyology: Actinopterygii I. München: Verlag Dr. Friedrich Pfeil. 299p.

Spiegelhalter, D. J., N. G. Best, B. P. Carlin, and A. Van Der Linde. 2002. ‘Bayesian measures of model complexity and fit’. Journal of the Royal Statistical Society: Series B (Statistical Methodology) 64 (4): 583–639.

Troyer, E. M., R. A. Rivero-Vega, X. Cui, et al. 2025. ‘Macroevolutionary role reversals in the earliest radiation of bony fishes’. Current Biology 35 (19): 4631-4641.e3.

Vanhaesebroucke, O., and R. Cloutier. 2026. ‘Morphological disparity and evolutionary radiation of early actinopterygians through the Devonian–Carboniferous crisis’. Diversity 18 (2): 83.

Wagner, G. P., M. Pavlicev, and J. M. Cheverud. 2007. ‘The road to modularity’. Nature Reviews Genetics 8 (12): 921–31.

Wainwright, P. C., D. R. Bellwood, M. W. Westneat, J. R. Grubich, and A. S. Hoey. 2004. ‘A functional morphospace for the skull of labrid fishes: patterns of diversity in a complex biomechanical system’. Biological Journal of the Linnean Society 82 (1): 1–25.

Wainwright, P. C., M. D. McGee, S. J. Longo, and L. P. Hernandez. 2015. 'Origins, innovations, and diversification of suction feeding in vertebrates'. Integrative and Comparative Biology 55 (1): 134–45.

Wainwright, P. C., and B. A. Richard. 1995. 'Predicting patterns of prey use from morphology of fishes'. Environmental Biology of Fishes 44 (1): 97–113.

Warrant, E. J., and N. A. Locket. 2004. 'Vision in the deep sea'. Biological Reviews 79 (3): 671–712.

Westneat, M.. W. 2005. 'Skull biomechanics and suction feeding in fishes'. Fish Physiology 23: 29-75.

Winther, R. G. 2001. 'Varieties of modules: kinds, levels, origins, and behaviors'. Journal of Experimental Zoology 291 (2): 116–29.

Young, G. C. 2010. 'Placoderms (armored fish): dominant vertebrates of the Devonian period'. Annual Review of Earth and Planetary Sciences 38: 523–50.

Zelditch, M. L., and A. Goswami. 2021. 'What does modularity mean?' Evolution & Development 23 (5): 377–403.

Zelditch, M. Leah, A. R. Wood, and D. L. Swiderski. 2009. 'Building developmental integration into functional systems: function-induced integration of mandibular shape'. Evolutionary Biology 36 (1): 71–87.

Zhu, M., W. Wang, and X. Yu. 2010. '*Meemannia eos*, a basal sarcopterygian fish from the Lower Devonian of China –expanded description and significance'. *In* Morphology, phylogeny and paleobiogeography of fossil fishes, D.K. Elliott, J.G. Maisey, X. Yu, and D. Miao (eds). München: Verlag Dr. Friedrich Pfeil. 472p.

Zhu, Y.-A., P. A. Ahlberg, and M. Zhu. 2019. 'The evolution of vertebrate dermal jaw bones in the light of maxillate placoderms'. Evolution and Development of Fishes 1: 71-86.

CHAPITRE 4

L'ÉCOMORPHOLOGIE DES GNATHOSTOMES DU SILURIEN AU CARBONIFÈRE ET LA DYNAMIQUE D'ÉCOMORPHOESPACES PARTAGÉS ET INNOVANTS

4.1 RÉSUMÉ EN FRANÇAIS DU QUATRIÈME ARTICLE

La transition entre le Dévonien et le Carbonifère représente une période charnière dans l'histoire des gnathostomes. Les groupes de gnathostomes présents à cette époque ont du s'adapter à de nouvelles niches écologiques ainsi que faire face à plusieurs contraintes environnementales. Afin d'étudier ces transitions écomorphologiques et d'explorer la diversité fonctionnelle de ces groupes, nous avons codé une matrice écomorphologique comprenant 27 caractères discrets et 5 caractères continus pour 358 espèces du Silurien, du Dévonien et du Carbonifère. Dû à la faible disponibilité d'espèces suffisamment complètes pour le Silurien, nous avons par la suite concentré nos analyses sur les deux autres périodes uniquement. Un cadrage non-métrique multidimensionnel nous a permis de construire des écomorphoespaces basés sur la distance de Gower afin d'observer la répartition des espèces dans l'espace fonctionnel selon leur classe et leur âge. Afin de pallier à la présence de données manquantes dans notre matrice, nous avons réalisé une imputation par forêts aléatoires. La diversité fonctionnelle de nos assemblages a été estimée par divers paramètres incluant la richesse fonctionnelle, la dispersion et la redondance. Nous avons détecté le passage d'une période d'exploration écologique durant le Dévonien à une période de stabilisation et de redondance fonctionnelle durant le Carbonifère. Les assemblages dévoniens ont montré une plus grande richesse et divergence fonctionnelles, avec notamment les « placodermes » et les sarcoptérygiens qui occupaient une grande diversité de rôles écologiques dans l'écomorphoespace. L'extinction de la majorité de ces espèces durant la crise de la fin du Dévonien a mené à la libération de niches écologiques pour les espèces survivantes. Au sein des sarcoptérygiens, l'évolution de morphologies spécialisées chez les tétrapodomorphes et les cœlacanthes en lien avec l'utilisation de niches écologiques extrêmes, aurait permis aux sarcoptérygiens de survivre à la crise. Durant le Carbonifère, les

chondrichthyens et les actinoptérygiens se sont étalés dans les espaces libérés ainsi que dans de nouveaux habitats, tels que les récifs. Les chondrichthyens se sont tout d'abord diversifiés dans une stratégie généraliste avant de se spécialiser. Malgré leur importante diversification taxonomique, les actinoptérygiens montraient une forte redondance fonctionnelle, mais à l'intérieur de niches différentes. Ces patrons sont cohérents avec ceux d'une radiation adaptative induite par une opportunité écologique, un comportement opportuniste et une divergence trophique à la suite du Dévonien.

Cet article, intitulé « Ecomorphology of jawed vertebrates during the Silurian-Carboniferous and the dynamics of shared and innovative ecomorphospaces », a été présenté dans une version abrégée à la 17ème édition de l'*International Symposium on Early and Lower Vertebrates* (ISELV) à Rimouski (Canada) en Juin 2024. En tant que première auteure, j'ai contribué à l'élaboration du projet et de sa méthodologie. J'ai réalisé la collecte de données, les analyses statistiques, les visuels et écrit la première version du manuscrit. Le docteur John Llewelyn, second auteur, a supervisé les analyses et participé à la révision de l'article. Le professeur Richard Cloutier, troisième auteur, a participé à l'élaboration du projet ainsi qu'à la révision de l'article.

Ce projet a été financé par une bourse des Fonds de recherche du Québec – Nature et Technologies (FRQNT) [https://doi.org/10.69777/325538] que j'ai reçue pour mon doctorat et par les subventions (06133 et 05887) du Conseil de Recherches en Sciences Naturelles et en Génie du Canada (CRSNG) du professeur Richard Cloutier.

4.2 ECOMORPHOLOGY OF JAWED VERTEBRATES DURING THE SILURIAN-CARBONIFEROUS AND THE DYNAMICS OF SHARED AND INNOVATIVE ECOMORPHOSPACES

Olivia Vanhaesebroucke[1], John Llewelyn[2], and Richard Cloutier[1,3]

1 Département de Biologie, Chimie et Géographie, Université du Québec à Rimouski, Rimouski, QC, Canada.

2 Global Ecology Lab, Flinders University, SA, Australia.

3 Center of Excellence on the Evolution of Life, Basin Studies and Applied Paleontology, Paleontological Research and Education Center, Mahasarakham University, Maha Sarakham 44150, Thailand.

ABSTRACT

The Devonian-Carboniferous transition constitutes a critical time in the history of early jawed vertebrates. At least four major groups of gnathostomes ("placoderms", "acanthodians", chondrichthyans, and osteichthyans) have been adapting to new ecological and environmental constraints. Examining patterns of ecomorphological disparity provides a framework for assessing how these groups diversified functionally and partitioned in ecological niches during this major evolutionary transition. To study these ecomorphological transitions and the functional diversity of the gnathostome ecosystem, we compiled a matrix of 27 discrete and 5 continuous ecomorphological characters for 358 species of Devonian and Carboniferous early gnathostomes. A non-metric multidimensional scaling (NMDS) analysis was performed, and ecomorphospaces were built based on the first two axes. Owing to the morphological incompleteness of the fossil record, we used a missForest model imputation protocol to encompass missing data. Functional diversity metrics were then quantified to explore functional richness, dispersion and redundancy across jawed vertebrate classes and geological time. We detected a shift from ecological experimentations and niche exploration during the Devonian toward a stabilization and functional redundancy during the Carboniferous. Devonian assemblages showed high functional richness and divergence, with "placoderms" and sarcopterygians occupying a wide range of ecological roles within the ecomorphospace. The extinction of most of these taxa during the end-Devonian crises led to

the opening of ecological opportunities for surviving clades. Within sarcopterygians, the evolution of specialized morphologies of tetrapodomorph and coelacanth fishes related to complex and transitional habitats may have facilitated the sarcopterygian survival. During the Carboniferous, chondrichthyans and actinopterygians expanded into vacated and new emerging habitats, including reef ecosystems. Chondrichthyans initially thrived through more generalist strategies before increasing specializations. Actinopterygians diversified through high functional redundancy across diverse ecological niches. These patterns are consistent with adaptive radiation driven by ecological opportunity, opportunistic behaviour, and trophic divergence following the Devonian crisis.

Keywords: Non-metric multidimensional scaling; Palaeozoic fish; Adaptive radiation; Mass extinction; Functional disparity

Introduction

The oldest articulated specimen of jawed vertebrate, or gnathostome, is dated back from the middle Silurian (Ludlow; 427.4 – 423.0 million years ago (Ma)), with *Guiyu oneiros* (Zhu et al. 2009). The following Devonian and Carboniferous periods (419.2 – 298.9 Ma) represent a critical phase in the ecological and functional diversification of gnathostomes (Sallan and Coates 2010), marked by the progressive restructuring of aquatic ecosystems under the influence of tectonic, climatic and biogeochemical perturbations (Königshof et al. 2021; Racki 2005; Carmichael et al. 2019). During the Devonian (419.2 – 358.9 Ma), the expansion of epicontinental seas (Johnson et al. 1985; Blakey 2008) and the proliferation of complex reefal systems (Copper 2002; Bridge et al. 2022) promoted a wide spectrum of ecological adaptations among gnathostomes. Conversely, these changes created environmental instability driven, among other events, by the rise of terrestrial vegetation (Otoo 2025; Buatois et al. 2022; Algeo and Scheckler 1998) which enhanced nutrient fluxes to oceanic systems and contributed to recurrent episodes of widespread anoxia (Algeo and Scheckler 1998; Carmichael et al. 2019). These environmental changes contributed to the decimation of reefal systems (ca. 80% of tabulate and 60% of rugose corals (Ma et al. 2025)

following the “Kellwasser event” of the late Frasnian (371 Ma) (Carmichael et al. 2019). A second major crisis, the “Hangenberg event”, took place at the Devonian-Carboniferous transition (359 Ma) (Königshof et al. 2021; Kaiser et al. 2016) and was characterized by the loss of dominant groups of gnathostomes such as the “placoderms” (armoured fishes), “acanthodians” (stem-chondrichthyans or spiny sharks), and several piscine sarcopterygians (lobe-finned fishes), while chondrichthyans (cartilaginous fishes) and actinopterygians (ray-finned fishes) rapidly diversified (Sallan and Coates 2010; Vanhaesebroucke and Cloutier 2026).

The Carboniferous period (358.9 – 298.9 Ma) constituted an important time for taxonomic recovery. The progressive decrease in temperature during this transitional period between the Devonian greenhouse effect and the Late Palaeozoic Ice Age (Lakin et al. 2016) led to an increase in oceanic circulation and upwellings on continental shelves (Liu et al. 2019). This may have intensified marine primary productivity. At the same time, during the Viséan (346 Ma), the reemergence of coral reefs constituted a major event in the recovery of aquatic systems (Yao et al. 2020). These habitat transformations and reorganizations likely reshaped the locomotion and feeding strategies among jawed vertebrates, leading to increased ecomorphological variation (Frey et al. 2019; Young 2010; Sallan and Friedman 2011).

Despite extensive works on taxonomic diversity (Brazeau and Friedman 2015; Sallan and Coates 2010), changes in ecomorphological disparity of gnathostomes remain poorly understood. Here, we explored changes in ecomorphological disparity of early gnathostomes across the Devonian crises and Carboniferous recoveries, to see how these events may have influenced the occupation of ecological and functional morphospaces. As the actinopterygian taxonomic diversity rapidly rising after the end-Devonian crisis is often associated with trophic divergence and adaptive radiation (Sallan and Friedman 2012; Vanhaesebroucke and Cloutier 2026), we expect to detect an increase in their ecomorphological disparity with new shapes occupying new spaces in the ecomorphospace. During the Devonian, a new lineage of tetrapod-like fishes (“elpistostegalians”) arises within the sarcopterygians (Boisvert et al.

2008; Cloutier et al. 2020; Stewart et al. 2022). Although among vertebrates, only tetrapods colonized the land, their aquatic close relatives are likely to exhibit a set of shared adaptations that would eventually facilitate this transition (Ahlberg 2018). Considering the chemico-physical and structural difference between these two environments (Hohn-Schulte et al. 2013), we expect to detect a shift in the ecomorphological occupation of the group. Two major groups of early gnathostomes never really recovered following the end-Devonian crises – the "placoderms" went extinct and the "acanthodians" decreased until the Permian (Sallan and Coates 2010; Young 2010). This loss accompanied by the formation of new habitats during the Early Carboniferous (Yao et al. 2020) may have triggered the ecological diversification of the surviving lineages, including the chondrichthyans which thrived after the Devonian (Schnetz et al. 2024). We then expect a major shift in ecomorphological space occupation between the Devonian and the Carboniferous, with surviving lineages replacing the extinct ones in their respective niches. Using morphological traits to assign ecological niches has been previously used for both extinct (Llewelyn et al. 2025; Chevrinais et al. 2017; Lund et al. 2015) and extant species (Friedman et al. 2020; Larouche et al. 2020); these methods demonstrate the reliability of the relationship between morphology and ecology to explore the ecological distribution of species. We then proposed a quantification of the occupation of ecological and functional spaces based on discrete and continuous ecologically relevant morphological traits, allowing us to link changes in ecomorphospaces occupation to documented paleoenvironmental and biotic shifts.

Material and methods

1. *Taxonomic diversity*

To study the ecomorphological transition between the Siluro-Devonian and the Carboniferous, we gathered a list of 358 gnathostome species from the Silurian (n=3), Devonian (n=190), and Carboniferous (n=165) from the primary literature and published databases (Sallan and Coates 2010; Schultze et al. 2021; Denison 1979, 1978; Zangerl 2004). Only the species for which adult articulated specimens were identified were compiled; we

excluded all species known solely from isolated remains or juvenile specimens. The matrix includes 73 “placoderms”, 43 “acanthodians”, 58 chondrichthyans, 110 actinopterygians, and 74 sarcopterygians. For each species, the first and last occurrence dates were noted (Figure 1, Annexe V Table S1). Gnathostome diversity (richness) was plotted using the R package ‘divDyn’ (v.0.8.3) (Kocsis et al. 2019). To ensure the representativity of our sample, we also plotted diversity for an extended sample including 471 species (see Annexe V, Figure S1).

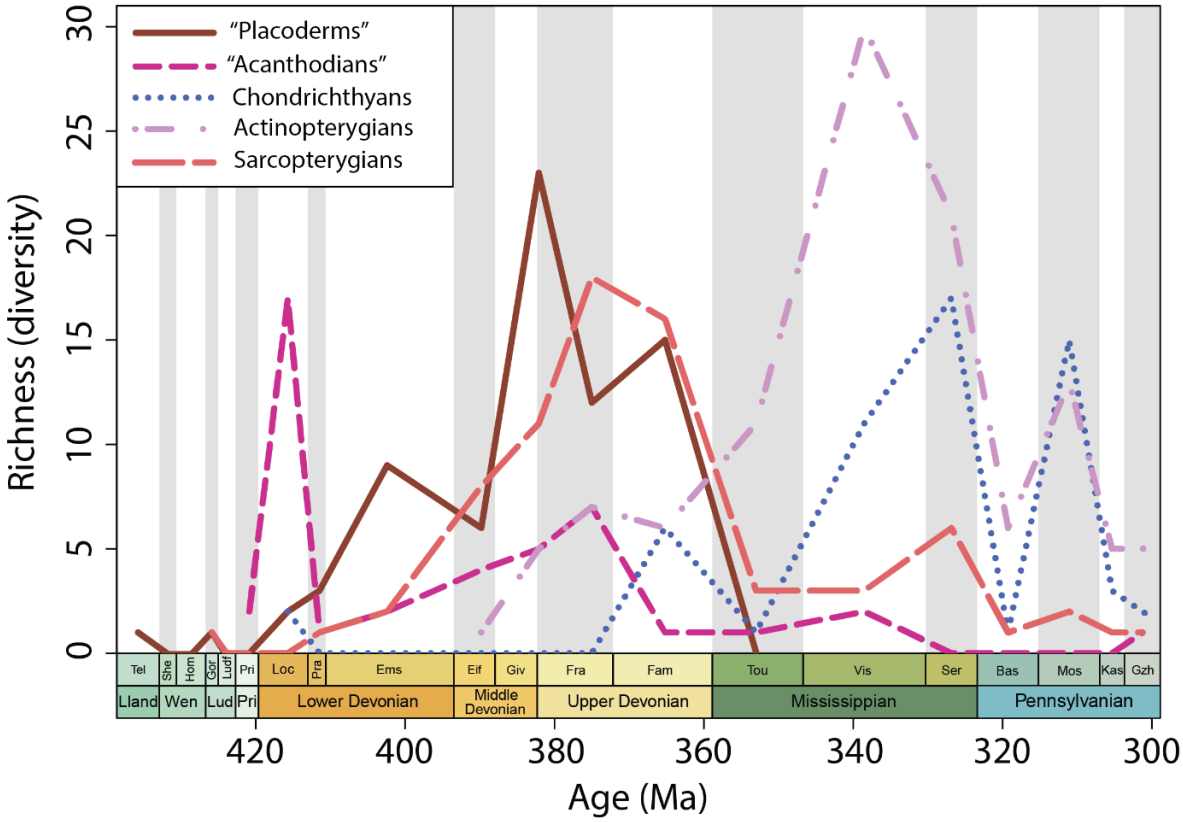


Figure 1. Taxonomic diversity (richness) through time including the 358 early gnathostome species. “Placoderms” (n=73; brown line), “acanthodians” (n=43; dark pink, short-dashed line), chondrichthyan (n=58; blue dotted line), actinopterygians (n=110; light violet dash dotted line), and sarcopterygians (n=74; red dashed line). Bas: Bashkirian; Eif: Eifelian; Ems: Emsian; Fam: Famennian; Fra: Frasnian; Giv: Givetian; Gor: Gorstian; Gzh: Gzhelian; Hom: Homerian; Kas: Kasimovian; Lland: Llandovery; Loc: Lochkovian; Lud: Ludlow; Ludf: Ludfordian; Mos: Moscovian; Pra: Pragian; Pri: Pridoli; Ser: Serpukhovian; She: Sheinwoodian; Tel: Telychian; Tou: Tournaisian; and Vis: Viséan; Wen: Wenlock.

2. *Morphological dataset*

Following the classification of Palaeozoic habitats proposed by Lund et al. (2015), we defined four main ecological categories for aquatic habitats: benthic, demersal, pelagic, and structurally complex habitats, such as reefal systems, and added an aquatic-terrestrial transitional habitat (see description in Annexe V, Table S2). We compiled a matrix of 32 ecomorphological characters (27 discrete and 5 continuous, Annexe V, Table S2) selected for their ecological relevance and codability in fossil taxa. For example, lateral body shape and the position and shape of fins link to a species ecology because they are associated with maneuverability and locomotion (Larouche et al. 2020; Schakmann and Korsmeyer 2023), whereas mouth position, type of dentition, and eye size were used as indicators of diet and vertical position in the water column (Goatley and Bellwood 2009; Ingram and Shurin 2009; Warrant and Locket 2004). We incorporated 16 extant species representing morphotypes characteristic of each habitat type to anchor ecological interpretations by polarizing the datasets. *Albula vulpes* and *Trachurus trachurus* represent a pelagic body shape; *Balistapus undulatus, Carcharhinus melanopterus, Cottus gobio, Ctenochaetus striatus, Gnathodentex aureolineatus, Labrus bergylta,* and *Zebrasoma velifer* display reef-associated morphologies; *Callorhinchus melanopterus, Poroderma africanum, Protopterus annectens, Spectrunculus grandis,* and *Squalus acanthias* illustrate demersal body shapes, while *Raja montagui* represents a benthic morphology and *Cryptobranchus alleganiensis* an aquatic-terrestrial transitional habitat. Character coding was based on descriptions from primary literature and direct observations of available specimens. For continuous variables, linear measurements were derived from the largest known specimen of each taxon.

3. *Data transformations*

Before imputing missing traits and analysis, we assessed the proportion of missing data per taxon and per trait to identify which entries were most incomplete. Missing data have been known to reduce imputation accuracy and resolution, particularly when taxa are characterized by few observed characters (Wiens 1998; Prevosti and Chemisquy 2010). To

optimise taxon sampling and imputation reliability, taxa with more than 60% missing data were excluded, resulting in the removal of 33 species (56 “placoderms”, 43 “acanthodians”, 59 chondrichthyans, 117 actinopterygians, and 66 sarcopterygians were kept in the imputation). Continuous characters were then log-transformed to stabilize variance and control skewed distribution of data (Legendre and Legendre 2012) (see Annexe V Figure S2). To remove the effect of overall size on shape-related variation, we applied the Mosimann approach (Mosimann 1970; Klingenberg 2016) expressing each measurement by the geometric mean of all variables. Therefore, the geometric mean variable does not provide independent information once the ratios are computed, and including it in the multivariate analyses may result in redundancy and collinearity among variables (Mosimann 1970; Klingenberg 2016). In accordance with the degrees of freedom for this method ($p - 1$) and to limit this redundancy, we removed the geometric mean from subsequent analyses.

4. *Non-multidimensional scaling*

First, we explored the ecomorphological disparity by using an ordination performed on both discrete and continuous characters. Group-specific traits (*e.g.,* dermal plates, fin spines) were excluded to retain traits that were applicable across all taxonomic classes, reducing the dataset to 21 discrete and 4 continuous characters. In addition, for anatomically incomplete species, random forest machine learning was used to impute missing data using the R package ‘missForest’ (v.1.6.1) (Stekhoven and Bühlmann 2012). The optimized imputation model reached a Percentage of Falsely Classified entries (PFC) for discrete characters of 12.7% and a Normalized Root Mean Squared Error (NRMSE) for continuous characters of 29.7%, indicating moderate imputation accuracy overall, suitable for broad-scale analysis of trait variation across taxa (Stekhoven and Bühlmann 2012).

The Non-metric Multidimensional Scaling (NMDS) based on Gower distances (Lehmann et al. 2019) allowed us to associate taxa based on their ecomorphological similarities. Gower’s distances were calculated with the *daisy* function of the ‘cluster’ R package (v.2.1.8.1) (Maechler et al. 2026), and the NMDS were generated by the *metaMDS* function from the

'vegan' package (v.2.7.2) (Oksanen et al. 2016). Based on the stress values, we retained the first six axes (< 0.1 for k = 6), although, to ease graphical representations, only the first two were used to plot ecomorphospaces. Ordination fit (R^2 = 0.99) indicated a reliable representation of pairwise distances.

Variations in patterns of ecomorphological occupation were explored across taxonomic classes of early gnathostomes and across geological periods (Figure 2). An Unweighted Pair Group Method with Arithmetic mean based on Gower distances (UPGMA) was computed with the 'stats' R function *hclust* (v.4.5.1) (R Core Team 2023) and used as a hierarchical cluster algorithm to identify groups of taxa sharing ecomorphological similarities (Legendre and Legendre 2012) (see Annexe V, Figure S3). Bootstrapped cophenetic correlations were high (mean = 0.86), suggesting a relatively strong structure in the dataset, while the observed cophenetic correlation for the UPGMA was lower (0.56). This may suggest that the clustering analysis captures only part of the dataset structure, which might include shape gradients. Therefore, the ecomorphological patterns will be interpreted based on the ordination approach.

To test the stability of the eco-morphological trends when the dataset includes mixed characters, the same analyses were conducted using only discrete characters (see Annexe V Figure S4) with a best miss forest model (mtry = 8, ntree = 300) reaching a PFC of 14.6%.

5. *Trait-spaces*

Distances between species in trait space were calculated for our mixed characters matrix using Gower distances and the R 'gawdis' package (v.0.1.5) (de Bello et al. 2021). A Principal Coordinates Analysis (PCoA) was applied to these Gower distances to ordinate species in lower dimensional space. The first eight axes, which accounted for 74% of the variation, were retained to estimate functional diversity metrics with the R package 'mFD' (v.1.0.7) (Magneville et al. 2022). To be able to compute functional richness (FRic: the volume of functional space occupied by an assemblage) and functional divergence (Fdiv: the way the species are distributed within each assemblage, whether close or far from the center

of its functional space) (Magneville et al. 2022), we removed the 2 Silurian species from the analyses because we had fewer species than the number of axes used. We also computed the functional evenness (Feve: a measure of the homogeneity of the distribution in functional space) and functional specialization (Fspe: the weighted mean distance of species from the center of the global functional space). All these metrics were computed for each taxonomic class of early gnathostomes (Figure 3) and each geological period (Figure 4). However, species diversity varied among the different periods and classes, and as mentioned by Mammola et al. (2021) and Llewelyn et al. (2025), functional diversity metrics can be correlated with species diversity. We therefore also computed Standardized Effect Sizes (SES) to control the impact of species richness on these functional diversity metrics (Hurtado-Materon and Murillo-García 2023). We first generated 1000 randomly shuffled species groups (periods and classes), conserving the number of species for each taxonomic group. Then, for each functional diversity metric, we calculated the mean and standard deviation based on these null models. The resulting null mean values were subtracted from the observed values for each functional metric, removing the effect of group size. Finally, we divided the result by the standard deviation to allow for comparisons across scales. We plotted raw and SES metrics to visualize their variation among groups.

Results

1. Early jawed vertebrate taxonomic diversity

During the Devonian, “placoderms” and sarcopterygians were the two most diverse groups of early jawed vertebrates (Figure 1). They decreased greatly during the middle-late Famennian, which corresponds to the Hangenberg event (Kaiser et al. 2016), leading to the extinction of “placoderms” at the end of the Famennian. At the same time, actinopterygians and chondrichthyans rapidly diversified, with a maximum of species diversity detected during the Mid-Late Mississippian (Figure 1). “Acanthodians” reached a maximum during the Early Devonian, then decreased slowly throughout the Devonian and Carboniferous (Figure 1) until their extinction during the Permian. These diversity patterns are stable when

using an extended sample (see Annexe V, Figure S1), and appear highly congruent with the patterns of species diversity from other diversity studies (Schnetz et al. 2024; Henderson et al. 2023).

2. *Ecomorphospaces: patterns of habitat occupation*

Ecomorphospaces were constructed from the first two axes of the NMDS (Figure 2). Using extant analogs as ecomorphological references, we identified four main habitats: (1) structurally complex habitats including species such as *C. striatus* and *B. undulatus*, characterized by laterally compressed, short-bodied morphologies; (2) aquatic-terrestrial transitional habitats, represented by the elongated and limbed *C. alleganiensis*; (3) pelagic habitats with the fusiform *A. vulpes*, and (4) benthic habitats represented by the dorso-ventrally flattened *R. montagui.* We also recognized a fifth habitat, the demersal zone represented by *S. acanthias*. This group forms a more diffuse cluster, likely reflecting the intermediate morphology of species inhabiting this environment, which often share traits with both pelagic and benthic forms. Thus, the position of the demersal habitat between these two in the ecomorphospace may indicate a transitional ecological condition.

Regarding the ecomorphological distribution of species according to their taxonomic class (Figure 2a), the tetrapod-like fishes such as *Tiktaalik rosae* and the early tetrapod *Acanthostega gunarri* clustered within the aquatic-terrestrial transitional habitat. The structurally complex habitat cluster included several actinopterygian and coelacanth (sarcopterygian) species, while the pelagic cluster was dominated by actinopterygians and "acanthodians". The remaining sarcopterygians (onychodonts, porolepiforms, dipnoans, basal tetrapodomorphs) were located close to the center of the functional space, which could suggest more generalist morphologies, while actinopterygians showed tighter clustering but occupied more ecologically extreme habitats. The demersal zone was mostly occupied by "placoderms" and chondrichthyans, which exhibited more transitional morphologies. Although these two groups were spread across the center of the functional space, they were forming distinct clusters within their respective assemblages.

In terms of the age of species (Figure 2b), Devonian taxa were spread throughout the entire ecomorphospace, although only a few exhibited trait combinations characteristic of structurally complex habitats. In contrast, Carboniferous species tend to cluster within the structurally complex and pelagic zones, with several species occupying the middle of the functional space. No Carboniferous species were associated with aquatic-terrestrial transitional habitats, because, Carboniferous tetrapods were excluded from the analyses in order to focus on early jawed vertebrates.

Although the UPGMA analysis showed low support (cophenetic correlation of 0.56), indicating that it captured only part of the dataset structure, it still revealed the same four groups identified by the NMDS (see Annexe V, Figure S3). This low support may reflect the presence of intermediate trait combinations associated with transitional morphologies, which can impact clear group delimitations. This seems congruent with what we observed in the ecomorphospaces where several species plot in the transitional regions among the main clusters, supporting the existence of transitional forms between them.

3. Functional diversity of early jawed vertebrates

Four functional metrics were estimated for each taxonomic class (Figure 3) and each geological period (Figure 4). Overall, the patterns of variation were consistent between raw values and standardized effect sizes (SES). Functional richness, however, appeared to be influenced by species richness within groups.

Actinopterygians were the most diversified group in the analyses (n=117). They exhibited the highest functional richness based on raw values, suggesting a substantial functional disparity. In contrast, SES corrected values for actinopterygians marked the lowest functional richness of all groups. This discrepancy indicates a high degree of functional redundancy among actinopterygians, which is congruent with the clustering observed in the NMDS.

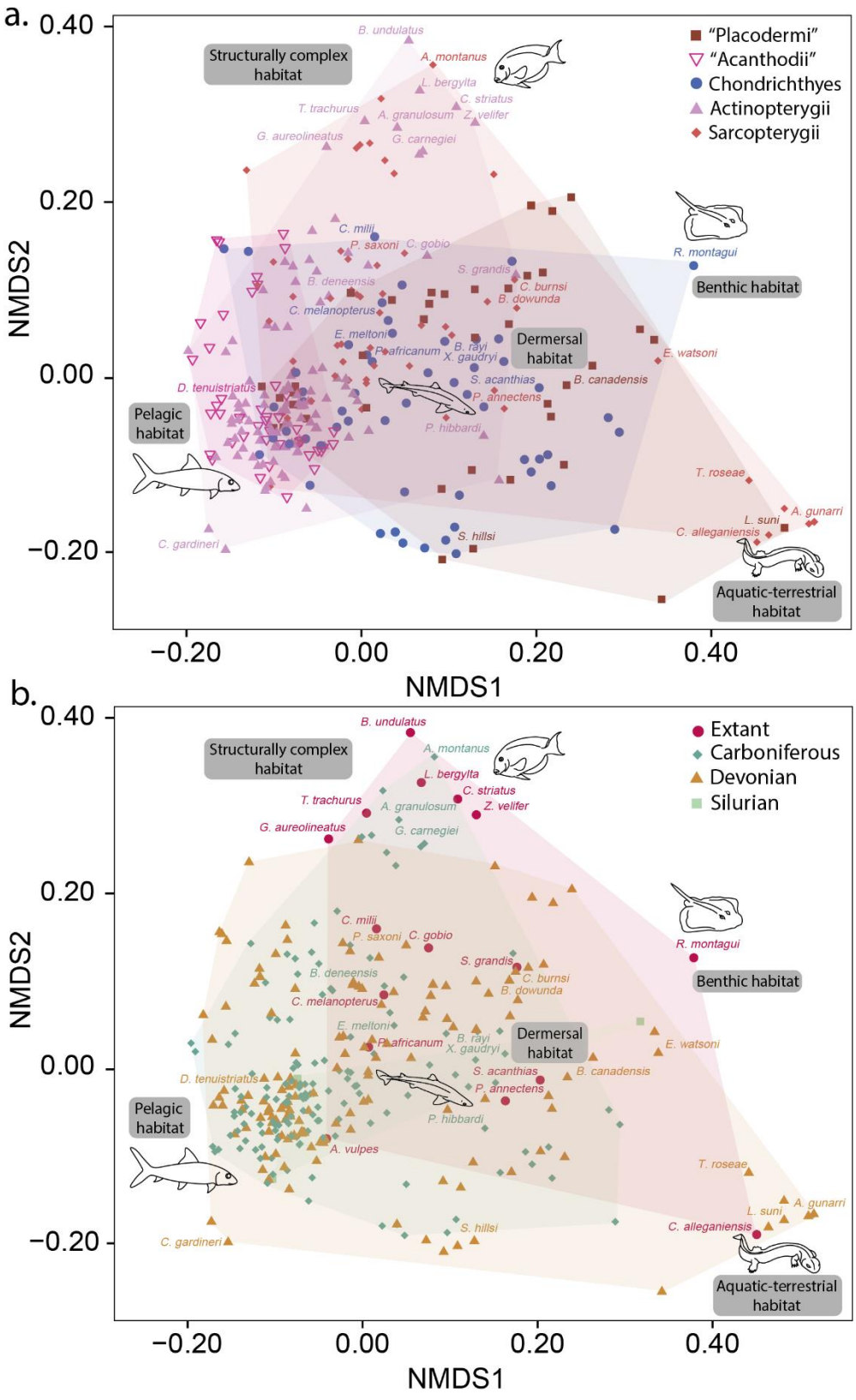

a.
b.
NMDS1
NMDS2
0.40
0.20
0.00
−0.20
−0.20
0.00
0.20
0.40
Structurally complex habitat
Benthic habitat
Dermersal habitat
Pelagic habitat
Aquatic-terrestrial habitat
"Placodermi"
"Acanthodii"
Chondrichthyes
Actinopterygii
Sarcopterygii
Extant
Carboniferous
Devonian
Silurian
B. undulatus
A. montanus
L. bergylta
C. striatus
T. trachurus
A. granulosum
Z. velifer
G. aureolineatus
G. carnegiei
C. milii
P. saxoni
C. gobio
R. montagui
S. grandis
C. burnsi
B. deneensis
B. dowunda
C. melanopterus
E. meltoni
P. africanum
B. rayi
X. gaudryi
E. watsoni
S. acanthias
B. canadensis
D. tenuistriatus
P. annectens
P. hibbardi
T. roseae
A. gunarri
L. suni
C. alleganiensis
S. hillsi
C. gardineri
A. vulpes

Figure 2. Ecomorphospaces (**a.**) per taxonomic class and (**b.**) per geological period of 325 early gnathostomes and 16 extant species based on the first two axes of the NMDS based on Gower distances (k=2, stress = 0.21). 21 discrete characters and 4 continuous variables were included. Silhouettes represent the shape of extant species used to polarize the ecomorphological matrix, and the different aquatic habitats are indicated in grey boxes.

This result is further supported by their low functional evenness and divergence scores, which also suggest clustering and redundancy.

Actinopterygians were the most diversified group in the analyses (n=117). They exhibited the highest functional richness based on raw values, suggesting a substantial functional disparity. In contrast, SES corrected values for actinopterygians marked the lowest functional richness of all groups. This discrepancy indicates a high degree of functional redundancy among actinopterygians, which is congruent with the clustering observed in the NMDS. This result is further supported by their low functional evenness and divergence scores, which also suggest clustering and redundancy.

Sarcopterygians showed a similar pattern characterized by relatively low functional specialization, richness and divergence, indicating a more generalist combination of traits. Again, this agrees with the NMDS results, where most sarcopterygians are located near the center of the functional space, with the exception of elpistostegalians and tetrapods.

In contrast, chondrichthyans exhibited the highest scores across all metrics, except for functional specialization, which nevertheless remained comparatively high. These patterns were independent of the size of the group, suggesting a strong biological signal. They indicate a relatively homogeneous distribution of species within the total functional space, without definite clustering. However, their relatively high functional divergence suggests some degree of specialization within the chondrichthyan assemblage, two patterns consistent with the NMDS results.

Across all metrics, Devonian functional richness was consistently higher than that for the Carboniferous, especially based on SES values, indicating greater Devonian functional disparity. This pattern is also clearly visible in raw data, suggesting a strong underlying

biological signal, rather than just a signal from the size of the sample. Functional divergence during the Devonian appeared unaffected by species richness within assemblages, whereas Carboniferous divergence was notably lower in the SES results, implying greater redundancy among Carboniferous taxa. Functional evenness scores indicated relatively homogeneous species distribution in both periods, although the Carboniferous assemblage exhibited slightly less evenness with SES values. Finally, functional specialization scores suggest that Devonian species occupied more specialized positions within the overall functional space, whereas Carboniferous SES values indicate more generalist forms.

Discussion

The ecomorphological distribution of early jawed vertebrates revealed a dynamic occupation of functional spaces, reflecting both ecological diversification and morphological constraints across the Devonian-Carboniferous transition. The NMDS identified distinct ecomorphological clusters corresponding to five major aquatic habitat types - structurally complex, pelagic, benthic, demersal, and aquatic-terrestrial; yet, several taxa occupied transitional positions within the ecomorphospace, such as “placoderms”, sarcopterygians and chondrichthyans, suggesting the presence of transitional ecological strategies.

These intermediate morphologies may represent key stages in habitat specialization during the early history of gnathostomes. Overall, Devonian assemblages exhibited higher functional richness and divergence, which can be interpreted as a phase of ecological exploration (Legras et al. 2018; Magneville et al. 2022). In contrast, Carboniferous assemblages were characterized by increased functional redundancy and reduced disparity, suggesting a shift toward ecological stabilization (Magneville et al. 2022). These patterns then support a two-phased evolution of early jawed vertebrates, characterized by a first phase of ecological innovation and exploration, followed by functional stabilization.

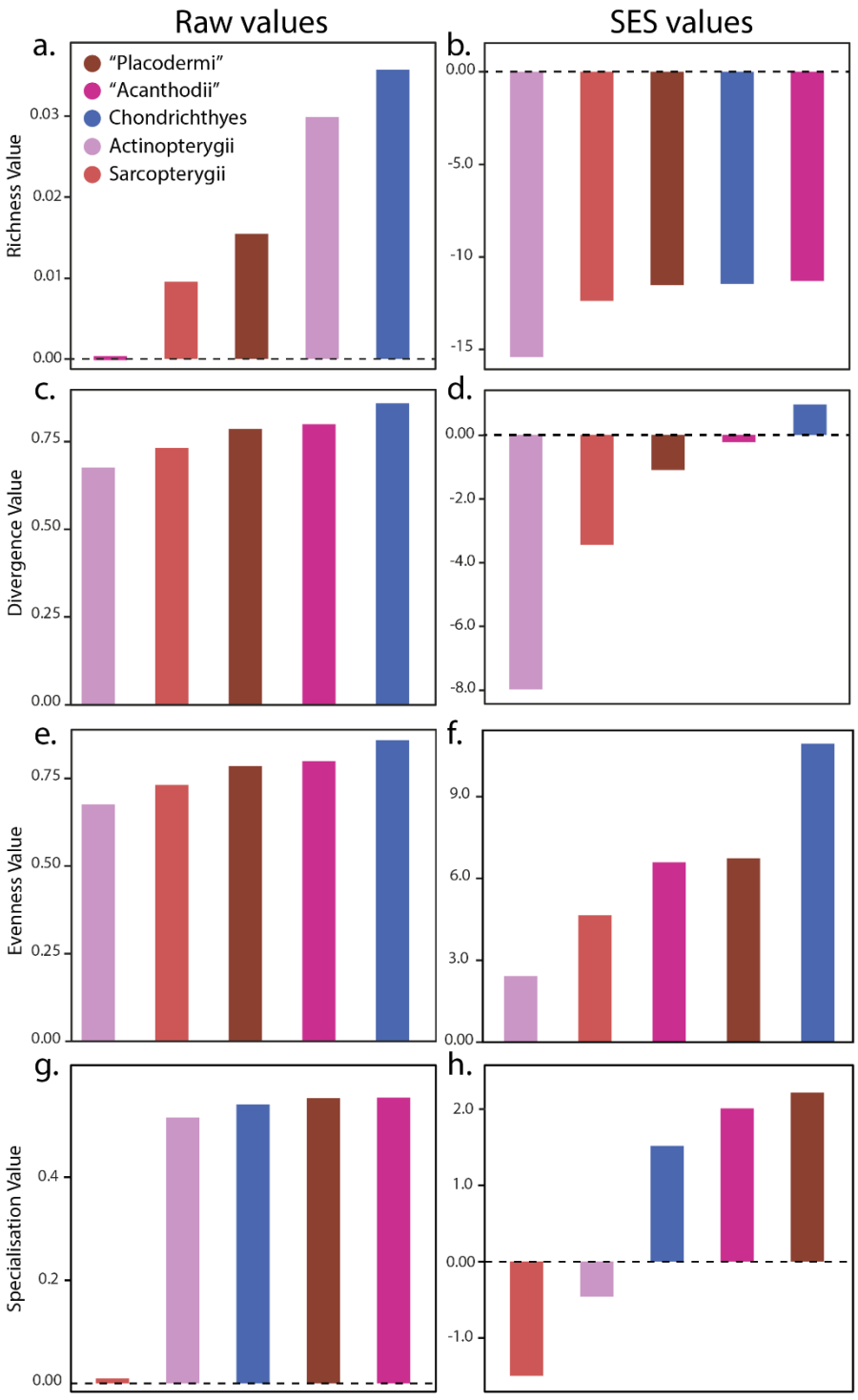


Figure 3. Functional diversity metrics per taxonomic class. Richness (a.) and (b.), divergence (c.) and (d.), evenness (e.) and (f.), and specialization (g.) and (h.). Panels on the

left present the metrics with no control for species diversity (raw values), whereas the panels on the right present the metrics with the standardized effect sizes, controlling for species diversity (SES values).

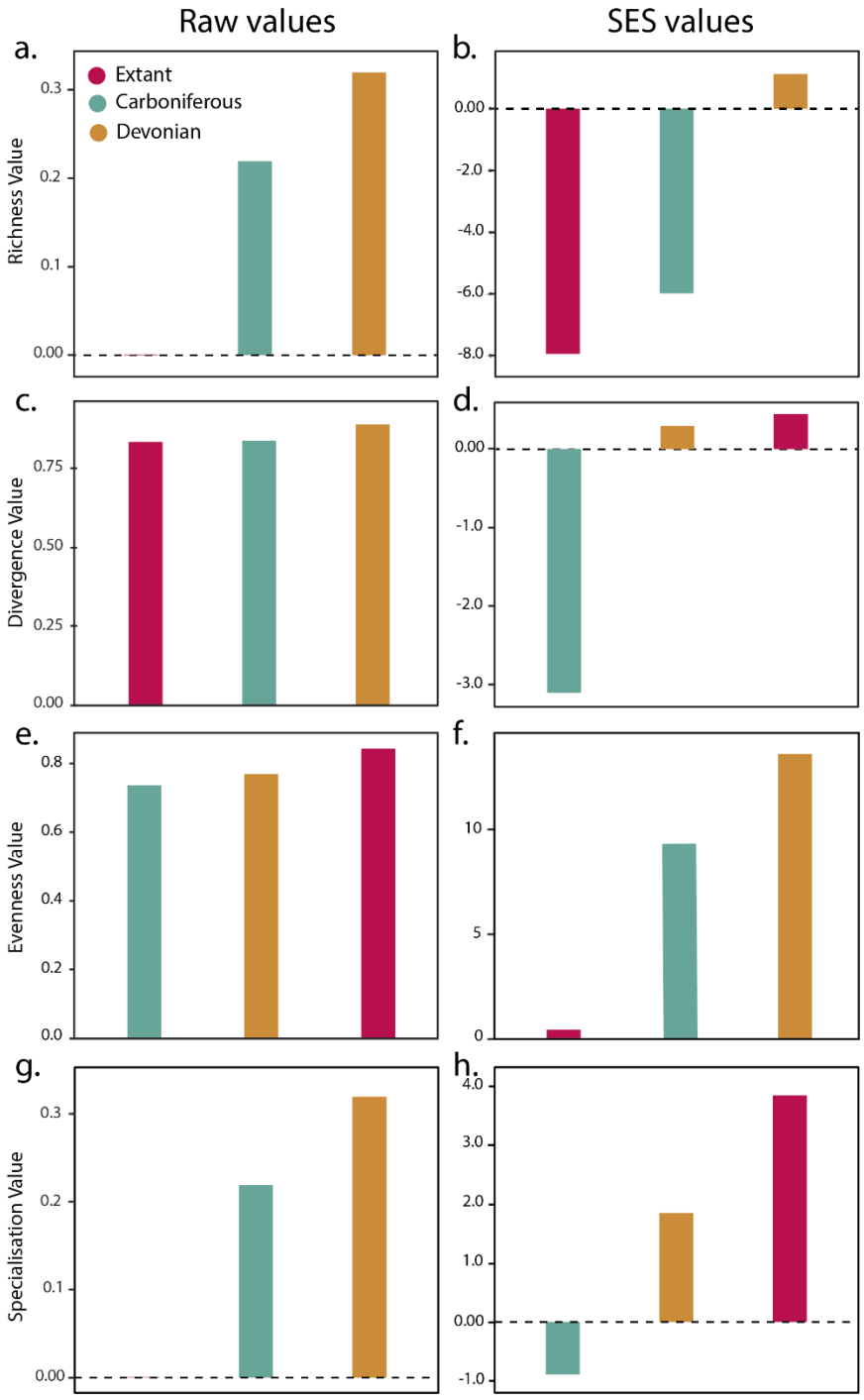


Figure 4. Functional diversity metrics per geological period. Richness (a.) and (b.), divergence (c.) and (d.), evenness (e.) and (f.), and specialization (g.) and (h.). The panels on the left present the metrics with no control for species diversity (raw values), whereas the panels on the right present the metrics with the standardized effect sizes, controlling for species diversity (SES values).

1. "Placoderms" and the loss of Devonian functional richness

Among Devonian jawed vertebrates, "placoderms" were the most abundant group (Young 2010; Sallan and Coates 2010). They included both the largest Devonian vertebrate such as *Dunkleosteus* (Carr and Hlavin 2010) and *Titanichthys* (Boyle and Ryan 2017) from the Late Devonian, and the smallest with *Minicrania* from the Early Devonian (Zhu and Janvier 1996). Their morphological diversity reflects a wide spectrum of ecological adaptations and feeding strategies, including suspension feeders (e.g., *Titanichthys*), pelagic predators (e.g., *Dunkleosteus*), and benthic foragers (e.g., *Bothriolepis*) (Coatham et al. 2020; Béchard et al. 2014; Carr and Hlavin 2010). This diversity is reflected in their wide dispersion across the eco-morphospace, with no clear clustering witnessing ecological experimentations. Their extinction following the end-Devonian Mass Extinction, likely removed a major contributor to functional diversity. This loss may have opened ecological opportunities that facilitated the diversification of surviving clades, especially chondrichthyans and actinopterygians during the Carboniferous (Henderson et al. 2023; Schnetz et al. 2024).

2. Chondrichthyans: from generalists to specialists

Chondrichthyans exhibited the most generalized set of functional traits, most of them located in transitional regions between pelagic and demersal habitats. Such generalized morphologies may have supported opportunistic behaviour in the post-crisis period, enabling rapid diversification into vacated ecological niches during the recovery phase of the Mississippian (Grogan et al. 2012). Despite this overall generalist distribution, their high functional divergence suggests an ongoing ecological specialization within the clade. This scenario is consistent with the second diversification event proposed by Schnetz et al. (2024)

which could have been triggered by the rise of holocephalans at that time. Devonian benthic "placoderms" would have then been ecologically replaced by the Mississippian durophagous holocephalan chondrichthyans (Richards et al. 2017). According to Griffin et al. (2026), chondrichthyan evolution in general shows a trend from generalists towards more ecological specialists. However, this pattern should be carefully interpreted, as the ecological diversity of early chondrichthyans is likely underestimated due to preservation biases (Schnetz et al. 2024). A more detailed investigation incorporating additional dental characters could provide further insights and help confirm these patterns.

3. Actinopterygians: taxonomic diversification with functional redundancy

In contrast, actinopterygians represented the most species-rich group but exhibited the highest functional redundancy. While taxa clustered in distinct regions of the eco-morphospace, indicating the occupation of multiple habitats, many shared overlapping functional traits. This pattern suggests that actinopterygians diversified through local ecological specialization within a limited set of functional strategies, resulting in high taxonomic diversity without proportional expansion of functional space. This pattern aligns with disparity studies showing a Late Devonian-Early Carboniferous increase in actinopterygian morphological disparity, driven by the emergence of new extreme morphotypes (Vanhaesebroucke and Cloutier 2026). Indeed, short and deep-bodied taxa, such as in the Platysomidea, appeared during the Early Mississippian (Mickle and Bader 2009; Wilson et al. 2021) alongside the persistence of elongated and fusiform Devonian shapes in Mississippian species, such as *Lambeia pectinatus* (Mickle 2017). Their association with structurally complex habitats supports the idea that the reestablishment of reef ecosystems in the Early Carboniferous created new ecological opportunities (Yao et al. 2020; Sallan and Galimberti 2015; Vanhaesebroucke and Cloutier 2026). However, the detected functional redundancy may also be related to sampling biases, as most of the actinopterygian species in this study come from Euramerican localities. Increasing the sampling effort in other regions may reveal a preserved cryptic functional diversity (Henderson et al. 2022).

4. *Sarcopterygians: between generalists and extreme specialists*

Most sarcopterygian species occupied the center of the functional space, reflecting a conservative combination of traits. However, two distinct taxonomic groups extended toward the extremes of the eco-morphospace, indicating the exploration of specialized ecological niches.

The first group, composed of tetrapod-like fishes (or "elpistostegalians") such as *Tiktaalik rosae*, was associated with aquatic-terrestrial habitats. This distribution suggests that tetrapod-like features linked to terrestrial adaptations had already evolved in close relatives of early tetrapods (Cloutier et al. 2020; Shubin et al. 2006; Lemberg et al. 2021). This close relation can be supported by the study of Anderson et al. (2013) who found no strong functional shifts between derived piscine tetrapodomorphs and early tetrapods regarding the jaw biomechanics. Although sarcopterygians were dominant jawed vertebrates during the Devonian, they experienced substantial losses following the end-Devonian crisis (Sallan and Coates 2010). The ecological differentiation and specialization of certain lineages, such as tetrapods and close relatives, may have contributed to the survival of the clade (Otoo 2025).

The second group, the coelacanths, were mainly associated with structurally complex habitats. This pattern supports the hypothesis that their diversification was influenced by abiotic factors (Clement et al. 2024) and may align with the re-emergence of coral reef systems during the Viséan (Bridge et al. 2022; Yao et al. 2020; Vanhaesebroucke et al. 2025). Elevated rates of jaw evolution in this group may have further facilitated their ecological specialization (Troyer et al. 2025).

5. The Devonian-Carboniferous functional turnover

The Devonian-Carboniferous transition represents a crucial time in vertebrate evolutionary history, marked by major climatic (Huang et al. 2018), tectonic (Ma et al. 2025), and biological changes (Algeo and Scheckler 1998; Zhang et al. 2020) that reshaped both

terrestrial and aquatic ecosystems. Devonian assemblages consistently exhibited higher functional richness and divergence, indicating a larger exploration of ecological space.

The subsequent decline in functional richness during the Carboniferous coincides with the Kellwasser and Hangenberg events (Carmichael et al. 2019; Kaiser et al. 2016), which disrupted aquatic ecological niches and eliminated key functional groups, such as "placoderms" (Sallan and Coates 2010; Ma et al. 2025; Guillam and Forel 2025). Carboniferous assemblages exhibit lower functional divergence (especially with SES values), suggesting an increased redundancy among surviving lineages.

Functional specialisation also declines, with most Carboniferous taxa occupying central regions of the eco-morphospace. This shift toward generalist strategies may reflect ecological filtering during the extinction events. However, this pattern may be slightly influenced by the exclusion of Mississippian tetrapods from the studied sample, which could have contributed to additional functional extremes.

6. Ecological reorganisation and faunal replacement

The transition between Devonian and Carboniferous assemblages is marked by a clear shift in clade dominance and ecological roles. Devonian ecosystems were largely structured by "placoderms", "acanthodians", and piscine sarcopterygians, which together occupied a wide range of functional space. Following the end-Devonian extinction, these groups declined drastically and were replaced by chondrichthyans and actinopterygians (Sallan and Coates 2010; Young 2010). These surviving clades largely overlapped the functional space previously occupied by extinct groups, indicating ecological replacement rather than only expansion into entirely novel niches. This pattern supports the hypothesis that post-extinction radiation of chondrichthyans and actinopterygians may have been supported by the reoccupation of vacated ecological roles, combined with some innovations into new available habitats (Sallan and Coates 2010).

7. Limitations and future investigations

Despite these results, several limitations should be considered when interpreting the observed patterns. First, even if the reliability of morphology has been demonstrated previously in both extinct (Chevrinais et al. 2017; Llewelyn et al. 2025; Lund et al. 2015) and extant species (Larouche et al. 2020; Friedman et al. 2021) to explore ecological distribution, the relationship between morphology and ecology is not always a one-to-one relationship. Indeed, many aquatic fishes use more than just one habitat (*e.g.,* vertical migration, reproductive migration (Bennett et al. 2002)), requiring different adaptations, but also because some morphological traits can be suitable for different habitats that require similar adaptations. For example, in pelagic environments, similar hydrodynamic constraints can lead to convergent morphologies (Rincon-Sandoval et al. 2020) across taxa occupying different ecological roles. As a result, some regions of the functional space may gather taxa with distinct ecological behaviours, making the ecological interpretation more difficult. To encompass this limitation, we may include paleogeographic coordinates of the different species, helping to clarify their repartitions. The incompleteness of certain taxonomic groups, especially those known from fragmentary material, required the use of trait imputations. While this approach allows a broader taxonomic inclusion, it may introduce uncertainty (Prevosti and Chemisquy 2010; Wiens 1998) and reduce the resolution of functional patterns. Instead of using imputations directly, we may try to complete the matrix with the collaboration and insights of other colleagues, which may increase the reliability of the imputation model. Finally, even if the fossil record may preserve a representative functional diversity in some habitats (Tyler and Kowalewski, 2020), the fossil record itself is uneven, with certain environments, such as deep marine habitats, being less preserved (Vilhena and Smith 2013; Holland 2016). This preservation bias may influence the distribution of taxa in ecomorphospaces. These limitations highlight the importance of integrating additional paleodata and increasing collaborative work in future studies.

Conclusion

Early jawed vertebrates went through major ecological restructuration across the Devonian-Carboniferous transition. They have been shifted from a phase of ecological

experimentation and niche exploration towards a stabilization and an increase of functional redundancy. Devonian assemblages were characterized by a high functional richness and divergence, with “placoderms” and sarcopterygians dominating various habitats and occupying specialized positions in the ecomorphospace. The end-Devonian crises greatly impacted these groups, leading to the complete extinction of “placoderms” and several piscine sarcopterygians (onychodontiforms, porolepiforms, and some tetrapodomorph lineages), which have opened ecological spaces for survivors. However, the diversification of tetrapod-like fishes (“elpistostegalians”) and coelacanths, associated with aquatic-terrestrial and structurally complex habitats, witnessed how sarcopterygian lineages evolved specialized morphologies that helped the clade to survive the crisis. During the Carboniferous, chondrichthyans and actinopterygians colonized the vacated but also new emerging habitats, such as reefs. Chondrichthyans succeeded thanks to their generalist morphologies that later tended towards diverse specializations, while actinopterygians opted for functional redundancy within a wide ecological spectrum, rapidly diversifying within each specialised habitat. These findings support the adaptive radiation suggested for these two groups following the Devonian crises, driven by opportunistic behaviour and trophic divergence. Thus, the Devonian-Carboniferous transition constitutes a key time in the jawed vertebrate evolution.

Acknowledgments: We thank L. Houle (UQAR) for his statistical advice and support. We thank T. Gardrat (Université de Sherbrooke) for helping to compile the matrix.

Data availability: Data and code are available on GitHub: https://github.com/oliviavanhaesebroucke/Ecomorphological-disparity-of-early-jawed-vertebrates

Fundings: O.V. was funded by Fonds de recherche du Québec – Nature et Technologies (FRQNT), [https://doi.org/10.69777/325538] and R.C. was funded by Natural Sciences and Engineering Research Council of Canada (NSERC) Discovery grants 06133 and 05887.

Authors contribution: O.V. and R.C. conceptualized the study and established the research goals. O.V. designed the study, acquired the data, performed the analyses, and created the

visualisations. OV. and J.L. design the methodology frameworks. J.L. wrote the original script for imputation model and functional diversity metrics. O.V. wrote and revised the original draft. J.L. and R.C. supervised and reviewed.

Conflict of interest: Conflicts of Interest: The authors declare no conflicts of interest. The funders had no role in the design of the study; in the collection, analyses, or interpretation of data; in the writing of the manuscript; or in the decision to publish the results.

References

Ahlberg, P. E. 2018. 'Follow the footprints and mind the gaps: a new look at the origin of tetrapods'. Earth and Environmental Science Transactions of the Royal Society of Edinburgh 109 (1–2): 115–37.

Algeo, T. J., and S. E. Scheckler. 1998. 'Terrestrial-marine teleconnections in the Devonian: links between the evolution of land plants, weathering processes, and marine anoxic events'. Philosophical Transactions of the Royal Society B: Biological Sciences 353 (1365): 113–30.

Anderson, P. S. L., M. Friedman, and M. Ruta. 2013. 'Late to the table: diversification of tetrapod mandibular biomechanics lagged behind the evolution of terrestriality'. Integrative and Comparative Biology 53: 197-208.

Béchard, I., F. Arsenault, R. Cloutier, and J. Kerr. 2014. 'The Devonian placoderm fish *Bothriolepis canadensis* revisited with three-dimensional digital imagery'. Palaeontologia Electronica 17 (1): 1–9.

Bello, F. de, Z. Botta-Dukát, J. Lepš, and P. Fibich. 2021. 'Towards a more balanced combination of multiple traits when computing functional differences between species'. Methods in Ecology and Evolution 12 (3): 443–48.

Bennett, W. A., W. J. Kimmerer, and J. R. Burau. 2002. 'Plasticity in vertical migration by native and exotic estuarine fishes in a dynamic low-salinity zone'. Limnology and Oceanography 47 (5): 1496–507.

Blakey, R. C. 2008. 'Gondwana Paleogeography from assembly to breakup—A 500 m.y. odyssey'. *In* Resolving the Late Paleozoic Ice Age in Time and Space, C. R. Fielding, T. D. Frank, and J. L. Isbell (eds). Geological Society of America. 441: 1–28.

Boisvert, C. A., E. Mark-Kurik, and P. E. Ahlberg. 2008. 'The pectoral fin of *Panderichthys* and the origin of digits'. Nature 456 (7222): 636–38.

Boyle, J., and M. J. Ryan. 2017. ‘New information on *Titanichthys* (Placodermi, Arthrodira) from the Cleveland Shale (Upper Devonian) of Ohio, USA’. Journal of Paleontology 91 (2): 318–36.

Brazeau, M. D., and M. Friedman. 2015. ‘The Origin and early phylogenetic history of jawed vertebrates’. Nature 520 (7548): 490–97.

Bridge, T. C. L., A. H. Baird, J. M. Pandolfi, M. J. McWilliam, and M. K. Zapalski. 2022. ‘Functional consequences of Palaeozoic reef collapse’. Scientific Reports 12 (1): e1386.

Buatois, L. A., N. S. Davies, M. R. Gibling, et al. 2022. ‘The invasion of the land in deep time: integrating Paleozoic records of paleobiology, ichnology, sedimentology, and geomorphology’. Integrative and Comparative Biology 62 (2): 297–331.

Carmichael, S. K., J. A. Waters, P. Königshof, T. J. Suttner, and E. Kido. 2019. ‘Paleogeography and paleoenvironments of the Late Devonian Kellwasser Event: a review of its sedimentological and geochemical expression’. Global and Planetary Change 183: e102984.

Carr, R. K., and W. J. Hlavin. 2010. ‘Two new species of *Dunkleosteus* Lehman, 1956, from the Ohio Shale Formation (USA, Famennian) and the Kettle Point Formation (Canada, Upper Devonian), and a cladistic analysis of the Eubrachythoraci (Placodermi, Arthrodira)’. Zoological Journal of the Linnean Society 159 (1): 195–222.

Chevrinais, M., C. Jacquet, and R. Cloutier. 2017. ‘Early establishment of vertebrate trophic interactions: food web structure in Middle to Late Devonian fish assemblages with exceptional fossilization’. Bulletin of Geosciences 31: 491–510.

Clement, A. M., R. Cloutier, M. S. Y. Lee, et al. 2024. ‘A Late Devonian coelacanth reconfigures actinistian phylogeny, disparity, and evolutionary dynamics’. Nature Communications 15 (1): e7529.

Cloutier, R., A. M. Clement, M. S. Y. Lee, et al. 2020. ‘*Elpistostege* and the origin of the vertebrate hand’. Nature 579 (7800): 549–54.

Coatham, S. J., J. Vinther, E. J. Rayfield, et C. Klug. 2020. ‘Was the Devonian placoderm *Titanichthys* a suspension feeder?’ Royal Society Open Science 7 (5): e200272.

Copper, P. 2002. ‘Reef development at the Frasnian/Famennian mass extinction boundary’. Palaeogeography, Palaeoclimatology, Palaeoecology 181 (1): 27–65.

Denison, R. 1978. Handbook of Paleoichthyology 2 – Placodermi. H.-P. Schultze (eds). Stuttgart, New York: Gustav Fischer Verlag. 94p.

Denison, R. 1979. Handbook of Paleoichthyology 5 – Acanthodii. H.-P. Schultze (eds). München: Gustav Fischer Verlag. 117p.

Frey, L., M. Coates, M. Ginter, et al. 2019. 'The early elasmobranch *Phoebodus*: phylogenetic relationships, ecomorphology and a new time-scale for shark evolution'. Proceedings of the Royal Society B: Biological Sciences 286 (1912): e20191336.

Friedman, S. T., S. A. Price, and P. C. Wainwright. 2021. 'The effect of locomotion mode on body shape evolution in teleost fishes'. Integrative Organismal Biology 3 (1): obab016.

Goatley, C. H. R., and D. R. Bellwood. 2009. 'Morphological structure in a reef fish assemblage'. Coral Reefs 28 (2): 449–57.

Griffin, B. W., J. N. Keating, P. S. Milla Carmona, et al. 2026. 'Evolution of chondrichthyan jaw morphology, from ecological generalists to specialists'. Paleobiology 52 (1): 131–44.

Grogan, E. D., R. Lund, and E. Greenfest-Allen. 2012. 'The origin and relationships of early chondrichthyans'. *In* Biology of Sharks and Their Relatives, J. C. Carrier, C. A. Simpfendorfer, M. R. Heithaus, and K. E. Yoapk (eds). CRC Press: 3-31.

Guillam, E., and M.-B. Forel. 2025. 'Marine ostracod faunas through the Late Devonian extinction events. Part II: the Hangenberg Event'. Earth-Science Reviews 268: e105172.

Henderson, S., E. M. Dunne, S. A. Fasey, and S. Giles. 2023. 'The early diversification of ray-finned fishes (Actinopterygii): Hypotheses, Challenges and Future Prospects'. Biological Reviews 98 (1): 284–315.

Henderson, S., E. M. Dunne, and S. Giles. 2022. 'Sampling biases obscure the early diversification of the largest living vertebrate group'. Proceedings of the Royal Society B: Biological Sciences 289 (1985): e20220916.

Holland, S. M. 2016. 'The non-uniformity of fossil preservation'. Philosophical Transactions of the Royal Society B: Biological Sciences 371 (1699): e20150130.

Huang, C., M. M. Joachimski, and Y. Gong. 2018. 'Did climate changes trigger the Late Devonian Kellwasser crisis? Evidence from a High-Resolution Conodont. Record from South China'. Earth and Planetary Science Letters 495: 174–84.

Hurtado-Materon, M. A., and O. E. Murillo-García. 2023. 'An integrative approach to understanding diversity patterns and assemblage rules in neotropical bats'. Scientific Reports 13 (1): e8891.

Ingram, T., and J. B. Shurin. 2009. ‘Trait-based assembly and phylogenetic structure in northeast pacific rockfish assemblages’. Ecology 90 (9): 2444–53.

Johnson, J. G., G. Klapper, and C. A. Sandberg. 1985. ‘Devonian eustatic fluctuations in Euramerica’. Geological Society of America Bulletin 96 (5): 567–87.

Kaiser, S. I., M. Aretz, and R. T. Becker. 2016. ‘The global Hangenberg crisis (Devonian–Carboniferous transition): review of a first-order mass extinction’. *In* Devonian Climate, sea level and evolutionary events, R. T. Becker, P. Königshof, and C. E. Brett (eds). Geological Society of London: 387-437.

Klingenberg, Christian Peter. 2016. ‘Size, shape, and form: concepts of allometry in geometric morphometrics’. Development Genes and Evolution 226 (3): 113–37.

Königshof, P., and W. Buggisch. 2005. ‘The Late Devonian Kellwasser crisis: evidence from conodonts and stable isotopes’. Facies 51 (1): 1–15.

Lakin, J. A., J. E. A. Marshall, I. Troth, and I. C. Harding. 2016. ‘Greenhouse to icehouse: a biostratigraphic review of latest Devonian–Mississippian glaciations and their global effects’. *In* Devonian climate, sea level and evolutionary events, R. T. Becker, P. Königshof, and C. E. Brett (eds). Geological Society of London: 439–64.

Larouche, O., K. M. Evans, and M. Friedman. 2020. ‘Integration and modularity in fishes: implications for morphological evolution’. Proceedings of the Royal Society B: Biological Sciences 287 (1927): e20201685.

Legendre, P., and Louis Legendre. 2012. Numerical Ecology. Elsevier.

Legras, G., N. Loiseau, and J.-C. Gaertner. 2018. ‘Functional richness: Overview of indices and underlying concepts’. Acta Oecologica 87: 34–44.

Lehmann, O. E. R., M. D. Ezcurra, R. J. Butler, and G. T. Lloyd. 2019. ‘Biases with the generalized Euclidean distance measure in disparity analyses with high levels of missing data’. Palaeontology 62 (5): 837–49.

Lemberg, J. B., E. B. Daeschler, and N. H. Shubin. 2021. ‘The feeding system of *Tiktaalik roseae*: an intermediate between suction feeding and biting’. Proceedings of the National Academy of Sciences 118 (7): e2016421118.

Liu, J., T. J. Algeo, W. Qie, and M. R. Saltzman. 2019. ‘Intensified oceanic circulation during Early Carboniferous cooling events: evidence from carbon and nitrogen isotopes’. Palaeogeography, Palaeoclimatology, Palaeoecology 531: e108962.

Llewelyn, J., J. A. Long, R. Cloutier, et al. 2025. ‘Trait-space disparity in fish communities spanning 380 million years from the Late Devonian to present’. Palaeogeography, Palaeoclimatology, Palaeoecology 679: e113294.

Lund, R., E. Greenfest-Allen, and E. D. Grogan. 2015. ‘Ecomorphology of the Mississippian fishes of the Bear Gulch Limestone (Heath Formation, Montana, USA)’. Environmental Biology of Fishes 98 (2): 739–54.

Ma, K., L. Hinnov, Z. Wang, et al. 2025. ‘Astronomically forced dynamics of Late Devonian (Famennian) sea level and biotic recovery in western Junggar, northwest China’. Global and Planetary Change 245: e104677.

Maechler, M., P. Rousseeuw, A. Struyf, M. Hubert, and K. Hornik. 2026. ‘Cluster: Cluster Analysis Basics and Extensions’. In R Package Version 2.0.7–1.

Magneville, C., N. Loiseau, C. Albouy, et al. 2022. ‘mFD: An R package to compute and illustrate the multiple facets of functional diversity’. Ecography 2022 (1): e05904.

Mammola, S., C. P. Carmona, T. Guillerme, and P. Cardoso. 2021. ‘Concepts and applications in functional diversity’. Functional Ecology 35 (9): 1869–85.

Mickle, K. E. 2017. ‘The lower actinopterygian fauna from the Lower Carboniferous Albert shale formation of New Brunswick, Canada – a review of previously described taxa and a description of a new genus and species’. Fossil Record 20: 47–67.

Mickle, K. E., and K. Bader. 2009. ‘A new Platysomid from the Upper Carboniferous of Kansas (USA) and remarks on the systematics of deep-bodied lower actinopterygians’. Acta Zoologica 90 (s1): 211–19.

Mosimann, J. E. 1970. ‘Size allometry: size and shape variables with characterizations of the lognormal and generalized gamma distributions’. Journal of the American Statistical Association 65 (330): 930–45.

Oksanen, J., F. G. Blanchet, M. Friendly, et al. 2016. Vegan: community ecology package. ordination methods, diversity analysis and other functions for community and vegetation ecologists. Version 2.3-5.

Otoo, B. K. A. 2025. ‘Prospects for studying continentalization and the origin of terrestrial ecosystems during the Late Paleozoic’. Frontiers in Ecology and Evolution 13: e1606225.

Prevosti, F. J., and M. A. Chemisquy. 2010. ‘The impact of missing data on real morphological phylogenies: influence of the number and distribution of missing entries’. Cladistics 26 (3): 326–39.

R Core Team. 2023. R: A language and environment for statistical computing. R Foundation for Statistical Computing. Vienna, Austria.

Racki, G. 2005. ‘Chapter 2 toward understanding late Devonian global events: few answers, many questions’. *In* Developments in palaeontology and stratigraphy, vol. 20, D. J. Over, J. R. Morrow, P. B. Wignal (eds). Elsevier: 5-36.

Richards, K. R., J. E. Sherwin, T. R. Smithson, et al. 2017. ‘Diverse and durophagous: Early Carboniferous chondrichthyans from the Scottish borders’. Earth and Environmental Science Transactions of The Royal Society of Edinburgh 108 (1): 67–87.

Rincon-Sandoval, M., E. Duarte-Ribeiro, A. M. Davis, et al. 2020. ‘Evolutionary determinism and convergence associated with water-column transitions in marine fishes’. Proceedings of the National Academy of Sciences 117 (52): 33396–403.

Sallan, L. Cole, and M. I. Coates. 2010. ‘End-Devonian extinction and a bottleneck in the early evolution of modern jawed vertebrates’. Proceedings of the National Academy of Sciences 107 (22): 10131–35.

Sallan, L., and M. Friedman. 2011. ‘Heads or Tails: Staged Diversification in Vertebrate Evolutionary Radiations’. Proceedings of the Royal Society B: Biological Sciences 279 (1735): 2025–32.

Sallan, L., and A. K. Galimberti. 2015. ‘Body-size reduction in vertebrates following the End-Devonian Mass Extinction’. Science 350 (6262): 812–15.

Schakmann, M., and K. E. Korsmeyer. 2023. ‘Fish swimming mode and body morphology affect the energetics of swimming in a wave-surge water flow’. Journal of Experimental Biology 226 (6): jeb244739.

Schnetz, L., R. J. Butler, M. I. Coates, and I. J. Sansom. 2024. ‘The skeletal completeness of the Palaeozoic chondrichthyan fossil record’. Royal Society Open Science 11 (1): e231451.

Schnetz, L., E. M. Dunne, I. Feichtinger, R. J. Butler, M. I. Coates, and I. J. Sansom. 2024. ‘Rise and diversification of chondrichthyans in the Paleozoic’. Paleobiology 50 (2): 271–84.

Schultze, H.-P., K. E. Mickle, C. Poplin, E. J. Hilton, and L. Grande. 2021. Handbook of Paleoichthyology: Actinopterygii I. Vol. 8A. München: Verlag Dr. Friedrich Pfeil. 299p.

Shubin, N. H., E. B. Daeschler, and F. A. Jenkins Jr. 2006. ‘The pectoral fin of *Tiktaalik roseae* and the origin of the tetrapod limb’. Nature 440 (7085): 764–71.

Stekhoven, D. J., and P. Bühlmann. 2012. ‘MissForest—Non-parametric missing value imputation for mixed-type data’. Bioinformatics 28 (1): 112–18.

Stewart, T. A., J. B. Lemberg, A. Daly, E. B. Daeschler, and N. H. Shubin. 2022. ‘A new elpistostegalian from the Late Devonian of the Canadian Arctic’. Nature 608 (7923): 563–68.

Troyer, E. M., R. A. Rivero-Vega, X. Cui, et al. 2025. ‘Macroevolutionary role reversals in the earliest radiation of bony fishes’. Current Biology 35 (19): 4631-4641.e3.

Tyler, C. L., and M. Kowalewski. n.d. ‘Fossil samples archive functional diversity in marine ecosystems: an empirical test from a present-day coastal environment’. Proceedings of the National Academy of Sciences of the United States of America 122 (31): e2405727122.

Vanhaesebroucke, O., and R. Cloutier. 2026. ‘Morphological disparity and evolutionary radiation of early actinopterygians through the Devonian–Carboniferous Crisis’. Diversity 18 (2): 83.

Vanhaesebroucke, O., O. Larouche, and R. Cloutier. 2025. ‘Early Sarcopterygian Morphological Disparity through the Devonian-Carboniferous Crisis’. Scientific Reports 16: e1623.

Vilhena, D. A., and A. B. Smith. 2013. ‘Spatial bias in the marine fossil record’. PLoS ONE 8 (10): e74470.

Warrant, E. J., and N. A. Locket. 2004. ‘Vision in the deep sea’. Biological Reviews 79 (3): 671–712.

Wiens, J. J. 1998. ‘Does adding characters with missing data increase or decrease phylogenetic accuracy?’ Systematic Biology 47 (4): 625–40.

Wilson, C. D., C. F. Mansky, and J. S. Anderson. 2021. ‘A platysomid occurrence from the Tournaisian of Nova Scotia’. Scientific Reports 11 (1): e8375.

Yao, L., M. Aretz, P. B. Wignall, J. Chen, D. Vachard, Y. Qi, S. Shen, X. Wang. 2020. ‘The longest delay: re-emergence of coral reef ecosystems after the Late Devonian extinctions’. Earth-Science Review 203: e103060.

Young, G. C. 2010. ‘Placoderms (armored fish): dominant vertebrates of the Devonian period’. Annual Review of Earth and Planetary Sciences 38: 523–50.

Zangerl, R. 2004. Handbook of Paleoichthyology 3A - Chondrichthyes I. Handbook of Paleoichthyology. München: Verlag Dr. Friedrich Pfeil. 115p.

Zhang, F., T. W. Dahl, T. M. Lenton, et al. 2020. ‘Extensive marine anoxia associated with the Late Devonian Hangenberg crisis’. Earth and Planetary Science Letters 533: e115976.

Zhu, M., and P. Janvier. 1996. ‘A small antiarch, *Minicrania lirouyii* gen. et sp. nov., from the Early Devonian of Qujing, Yunnan (China), with remarks on antiarch phylogeny’. Journal of Vertebrate Paleontology 16 (1): 1–15.

Zhu, M., W. Zhao, L. Jia, J. Lu, T. Qiao, and Q. Qu. 2009. ‘The oldest articulated osteichthyan reveals mosaic gnathostome characters’. Nature 458 (7237): e469

CONCLUSION GÉNÉRALE

La disparité morphologique et la radiation évolutive des gnathostomes basaux

Ce projet de doctorat avait pour objectif principal de caractériser les patrons de diversification morphologique des premiers vertébrés à mâchoire au cours de leur première radiation évolutive putative lors du Dévonien et du Carbonifère. Notre approche s'est révélée fortement intégrative. Elle a en effet permis de lier des dynamiques macroévolutives, telles que la disparité morphologique et la diversification écologique des taxons, tout en explorant des mécanismes sous-jacents susceptibles d'avoir façonné ces patrons, notamment la modularité.

Trois objectifs principaux ont alors guidé notre démarche. En partant du postulat qu'une radiation adaptative serait à l'origine des différents groupes de gnathostomes du Dévonien, nous avons tout d'abord cherché à caractériser les variations de disparité morphologique au sein de ces groupes. Nous nous sommes particulièrement intéressés au groupe des ostéichthyens, les poissons osseux, qui nous offraient un modèle d'étude idéal pour cela. En effet, ce groupe dont le registre fossile est très documenté comporte deux classes distinctes, les actinoptérygiens et les sarcoptérygiens, qui ont connu des trajectoires évolutives très différentes au cours de la période du Dévo-Carbonifère (Flannery Sutherland et al. 2025; Sallan et Coates 2010). Les sarcoptérygiens étaient des groupes dominants dans les milieux aquatiques du Dévonien mais ont connu d'importantes pertes de diversité suite à la grande crise de la biodiversité marquant la transition avec le Carbonifère (Carmichael et al. 2019; Kaiser et al. 2016). Toutefois, certaines lignées ont survécu et se sont rapidement diversifiées par la suite, notamment les cœlacanthes et les tétrapodes. Les actinoptérygiens, quant à eux, étaient très peu diversifiés lors du Dévonien mais ont connu une période de rapide diversification suivant la crise de la fin du Dévonien (Flannery Sutherland et al. 2025; Sallan et Coates 2010). Notre étude approfondie de leur disparité morphologique, tant au

niveau crânien qu'au niveau de leur forme globale, a révélé des étapes charnières dans leur évolution et a permis de faire des liens avec de potentiels facteurs biotiques et abiotiques. Des changements morphologiques majeurs coïncident alors avec des épisodes de transformations géologiques et biologiques importantes au cours du Dévonien et du début du Carbonifère.

Lors du Dévonien, les écosystèmes aquatiques sont dominés par les sarcoptérygiens et les « placodermes », dont la disparité morphologique varie de concert avec de grands changements environnementaux. En effet, une première phase d'augmentation de la disparité chez les sarcoptérygiens coïncide avec des transformations majeures des milieux du Dévonien moyen, notamment l'expansion des forêts terrestres et des systèmes récifaux, favorisant l'apparition de morphologies extrêmes et l'émergence des premiers tétrapodes (Ahlberg et al. 2018; Buatois et al. 2022; Bridge et al. 2022). La crise de la fin du Dévonien entraîne une chute marquée de leur disparité, accompagnée de pertes taxonomiques importantes. Cette même période est marquée par une augmentation progressive de la disparité crânienne chez les actinoptérygiens qui, même au travers de la crise, se maintient.

La période de rétablissement durant le début du Carbonifère est marquée par une restructuration des écosystèmes, notamment avec la réémergence des récifs coralliens qui ont été décimés lors de la crise (Yao et al. 2020), ouvrant alors de nouvelles opportunités écologiques pour les lignées survivantes. Cette période se traduit alors par une reprise de la disparité morphologique chez les sarcoptérygiens, majoritairement allouée à la lignée des cœlacanthes retrouvés principalement dans les milieux marins et qui auraient ainsi pu profiter du rétablissement des récifs. Simultanément, les actinoptérygiens connaissent leur première grande diversification taxonomique et deviennent des acteurs majeurs de la diversité des vertébrés. Cette diversification taxonomique est associée à une augmentation de la disparité morphologique, notamment par l'apparition de nouveaux morphotypes extrêmes (des corps trapus et compressés latéralement) et une diversité crânienne principalement liée à des stratégies d'alimentation différentes. Un comportement opportuniste aurait également pu participer à cette diversification, les actinoptérygiens pouvant alors occuper des niches

écologiques laissées par les espèces dévoniennes perdues. Les résultats de cette étude nous permettent alors d'appuyer l'hypothèse d'une radiation adaptative à l'origine de la diversification des actinoptérygiens suite à la crise de la fin du Dévonien. L'augmentation de leur disparité crânienne lors de la fin du Dévonien, et précédant alors leur disparité postcrânienne, nous suggère une radiation trophique, liée à une diversification des modes d'alimentation. Pour ce qui est des sarcoptérygiens, nos résultats corroborent les constats de précédentes études (Troyer et al. 2025; Clement et al. 2024) et soutiennent une radiation des cœlacanthes étroitement liés à des facteurs abiotiques notamment des changements géologiques.

Par la suite, nous nous sommes intéressés à un processus évolutif qui aurait pu fortement participer à l'apparition de cette disparité morphologique au sein des gnathostomes, et contribuer à leur succès évolutif. Nous nous sommes ainsi concentrés sur les patrons d'intégration morphologique et de modularité, reconnus chez plusieurs clades comme ayant participé à d'importants événements de diversification (Albertson et al. 2003; Dellinger et al. 2019; Gartner et al. 2023; Konow et al. 2008; Larouche et al. 2018). Pour cela, nous nous sommes concentrés sur le crâne des actinoptérygiens basaux, représentant le modèle d'étude idéal. En effet, en plus d'avoir un registre fossile riche et une signification écologique importante, l'anatomie du crâne des actinoptérygiens basaux est relativement conservée au sein des différentes lignées (à la différence des sarcoptérygiens (Cloutier 1997)), permettant alors la reconnaissance de plusieurs structures homologues essentielles pour notre étude, et ce même à une échelle taxonomique large. En effet, notre approche se base sur le placement de points de référence homologues (landmarks) afin d'évaluer statistiquement les changements de formes des différentes régions du crâne. Nous avons utilisé deux méthodes principales afin de tester quatre hypothèses concernant les patrons d'intégration morphologique et de modularité au niveau du crâne des actinoptérygiens basaux. La formulation de ces hypothèses s'est basée sur des critères morpho-fonctionnels, développementaux et génétiques liés à trois régions principales du crâne, soit la mâchoire, la région orbitale et la joue. Bien que nos deux approches aient mené à des résultats légèrement différents, un module a été fortement suggéré : la mâchoire. En effet, de nos quatre

hypothèses de départ, les deux plus soutenues par nos analyses présentaient la mâchoire comme une région distincte des autres. Tandis que les analyses d'intégration morphologique suggèrent une forte cohésion entre les différentes régions du crâne, qui pourrait être en lien avec des contraintes morpho-fonctionnelles associées à la respiration et à l'alimentation, la quasi-indépendance de la région de la mâchoire pourrait expliquer sa grande disparité morphologique observée au sein du groupe. Cette disparité de la mâchoire est souvent liée à différentes stratégies alimentaires chez les poissons (Anderson et al. 2011; Wainwright et al. 2000). Le module de la mâchoire a été suggéré par des analyses réalisées sur des taxons actuels (Wainwright et Richard 1995; Westneat 2004) mais également éteints (Jobbins et al. 2024). Identifier alors le même module chez différents groupes de gnathostomes basaux pourrait indiquer un module fortement conservé, qui aurait pu jouer un rôle clé dans le succès évolutif du clade. Ces résultats permettent également de proposer des mécanismes sous-jacents à la radiation trophique proposée pour les actinoptérygiens lors de notre étude sur leur disparité morphologique. En effet, l'augmentation rapide de disparité morphologique crânienne que nous avions associée à la divergence trophique des espèces lors de leur première phase de diversification pourrait alors avoir été facilitée par la modularité de leur crâne, notamment de leur mâchoire. Ce module aurait ainsi pu permettre de générer une variation morphologique importante tout en maintenant la fonctionnalité générale du crâne, ce qui aurait facilité l'exploration de nouvelles niches écologiques lors de leur diversification.

Finalement, nous avons souhaité remettre dans un contexte plus large les variations morphologiques observées lors de nos études approfondies des ostéichthyens. Nous nous sommes alors intéressés à l'évolution de la répartition écologique des espèces de gnathostomes basaux durant le Dévonien et le Carbonifère. Afin de pouvoir incorporer l'ensemble des groupes de gnathostomes basaux malgré l'hétérogénéité du registre fossile et les différences anatomiques entre eux, nous avons opté pour le codage d'une matrice de caractères morphologiques discrets et continus ayant une signification écologique, c'est-à-dire des éléments morphologiques dont les différentes formes vont refléter des adaptations à des modes de vie différents. Ces caractères ont été définis afin de discriminer cinq types d'habitats aquatiques différents présents lors du Dévonien et du Carbonifère : les milieux

pélagiques, démersaux, benthiques, transitionnels entre l'eau et la terre et les milieux structurellement complexes (tels que les récifs). Afin de polariser la matrice et de pouvoir associer une combinaison de caractères à un milieu en particulier, nous avons incorporé 16 espèces actuelles dont l'écologie est bien documentée et la morphologie représentative des contraintes liées à chaque habitat. Nous avons tout d'abord pu identifier une certaine hétérogénéité quant à la distribution dans l'espace fonctionnel de nos différents groupes. Les actinoptérygiens étaient principalement regroupés au niveau des milieux pélagiques et des habitats à structure complexe, suggérant une forte redondance fonctionnelle à l'intérieur du groupe malgré une diversité taxonomique élevée. Certains sarcoptérygiens, notamment des cœlacanthes, se retrouvaient également associés aux milieux complexes, tandis que la lignée constituée des représentants aquatiques les plus proches des tétrapodes (les tétrapodomorphes) se retrouvait dans les milieux de transition eau-terre. Le reste du groupe occupait plutôt une zone transitoire au centre de l'espace fonctionnel, suggérant une morphologie plutôt généraliste. Les « acanthodiens » étaient majoritairement concentrés dans les milieux pélagiques, tandis que les chondrichthyens et les « placodermes » se répartissaient dans l'ensemble de l'espace fonctionnel à l'exception des milieux structurellement complexes. Finalement, nous avons détecté un important chevauchement des assemblages du Dévonien et du Carbonifère. Tous ces résultats corroborent à nouveau ce que nous avions pu observer précédemment ainsi que les hypothèses apportées par des études antérieures.

Pour ce qui est des actinoptérygiens, nous avions proposé que l'apparition des récifs lors du Carbonifère inférieur aurait pu promouvoir l'importante diversification taxonomique de ce groupe à cette époque. En effet, nous avons pu voir ici que lors du Carbonifère, de nouvelles espèces d'actinoptérygiens exposent une combinaison de caractères morphologiques innovante, notamment un corps raccourci et compressé latéralement, attribuée à l'exploitation de milieux structurellement complexes. Toutefois, mis à part ces formes extrêmes, le reste des actinoptérygiens se concentrent dans la zone pélagique. Ainsi, la forte disparité morphologique que nous avions détectée pourrait être liée à l'apparition de formes extrêmes et à la colonisation de certains habitats particuliers, plutôt qu'à un comportement opportuniste et à l'occupation d'une grande diversité d'habitats. La disparité

crânienne que nous avions attribuée à une divergence trophique pourrait alors être liée à la différenciation de stratégies alimentaires à l'intérieur de ces habitats. Ainsi une analyse plus détaillée de ce groupe pourrait aider à étoffer ces patrons.

Concernant les sarcoptérygiens, tels que nos résultats de disparité morphologique l'avaient suggéré, la diversification des cœlacanthes durant le Carbonifère semble associée à la réémergence des récifs. La spécialisation de la lignée des cœlacanthes et des tétrapodomorphes dans des régions extrêmes de notre espace fonctionnel aurait permis au groupe des sarcoptérygiens de survivre à la crise du Dévonien, lors de laquelle les espèces plus généralistes ont été perdues.

Enfin, nous avons pu observer un chevauchement important des espèces dévoniennes de « placodermes » avec les chondrichtyens du Carbonifère. Cela pourrait suggérer un remplacement écologique des « placodermes » suite à leur extinction à la fin du Dévonien par les chondrichthyens, ce qui aurait permis à ce groupe de se diversifier rapidement durant le début du Carbonifère (Sallan et Coates 2010; Schnetz et al. 2024). Ce comportement opportuniste des chondrichtyens pourrait alors suggérer une radiation adaptative liée à une divergence écologique des espèces. Toutefois, la mauvaise préservation de spécimens articulés de chondrichthyens dans le registre fossile limite notre compréhension de leur diversité écologique totale. Une étude incorporant davantage de caractères liés à la dentition permettrait une compréhension approfondie de l'écologie des premiers représentants de ce groupe important de gnathostomes (Cooper et al. 2022). Toutefois, il a été montré que la morphologie des dents de requins pourrait ne pas être le meilleur proxy de l'écologie de l'animal, avec plusieurs formes ayant des performances fonctionnelles équivalentes (Whitenack et Motta 2010). Il pourrait donc être intéressant de coupler ces informations avec des analyses chimiques permettant de calculer des ratios d'isotopes de calcium, de zinc et la présence de métaux dans les dents, qui ont été montré comme de bon proxy de l'environnement dans lequel a vécu un requin (Assemat et al. 2024; McCormack et al. 2022).

Cette étude aura ainsi participé à la caractérisation d'un moment clé de l'histoire des vertébrés, à savoir l'apparition de la mâchoire. La radiation évolutive putative associée à cet

événement reçoit ici un important soutien en venant confirmer l'existence de radiations évolutives à l'origine de la diversification des différents groupes de gnathostomes. En effet, selon Simpson (1953), une radiation évolutive est caractérisée par deux éléments principaux, à savoir une augmentation rapide du taux de diversification spécifique ainsi qu'une augmentation de la disparité morphologique et écologique des espèces. Avoir réussi à détecter un tel patron au sein de certains de nos groupes de gnathostomes, notamment chez les actinoptérygiens, les sarcoptérygiens et les chondrichthyens, nous permet d'avancer l'existence de radiations évolutives de type adaptatif chez ces groupes. Bien que nous n'ayons pas pu poursuivre cette recherche au sein des deux autres groupes de gnathostomes, à savoir les « acanthodiens » et les « placodermes », les résultats obtenus concernant les « placodermes » lors de l'analyse en écomorphologie semblent orienter vers une possible radiation adaptative chez ce groupe également. En effet, les « placodermes » étaient parmi les groupes les plus diversifiés lors du Dévonien et se répartissaient dans l'ensemble de notre espace fonctionnel, ce qui pourrait suggérer une grande disparité en termes d'écologie et ainsi soutenir la présence d'une radiation pour ce groupe.

Portée de l'étude, limites et perspectives

Cette étude aura permis de mieux comprendre un des processus clés du domaine de la biologie évolutive, à savoir les radiations évolutives. En effet, les radiations évolutives ont participé à façonner la biodiversité que l'on connaît aujourd'hui mais également celle qui jalonne notre registre fossile. Elles demeurent toutefois des événements complexes dont les mécanismes sous-jacents sont encore mal compris. Nous avons proposé ici une approche intégrative à l'échelle macroévolutive permettant de mieux caractériser ces événements, et qui pourra être utilisée dans l'étude d'autres groupes, autant fossiles qu'actuels. Dans une époque où l'intérêt pour la science moléculaire surpasse grandement celui pour les études paléontologiques, le registre fossile demeure une source d'information essentielle pour la compréhension du vivant. En effet, la paléontologie offre la possibilité de retracer l'évolution de la vie sur des millions d'années, permettant de mieux comprendre les dynamiques évolutives et les mécanismes encore à l'œuvre aujourd'hui.

Cette étude se concentrait sur une période géologique marquante de l'histoire de la Terre. Notre échelle temporelle comprenait l'une des cinq extinctions massives qui ont marqué son histoire, à savoir l'extinction de la fin du Dévonien (Kaiser et al. 2016; Carmichael et al. 2019). Pouvoir étudier le comportement de la diversité des espèces au travers de ce genre d'événements permet de mieux comprendre les mécanismes de récupération et de maintien de la diversité au travers d'une période critique. Considérant les changements globaux actuels, les connaissances apportées par les études paléontologiques quant aux mécanismes impliqués dans les événements d'extinction et de spéciation pourraient contribuer à l'établissement de modèles de prédictions plus précis.

Toutefois, comme nous l'avons vu ici, le registre fossile comporte également son lot de défis. Nous avons rencontré plusieurs problèmes liés à la préservation des fossiles surtout chez certains groupes tels que les chondrichthyens, dont la nature peu minéralisée de leur squelette de cartilage rend leur préservation plus difficile lors de la fossilisation. Ainsi, le registre fossile ne capture qu'une partie de la diversité du passé et les interprétations qui en découlent doivent être faites avec précaution. La majorité des espèces que nous avons étudiées provenaient de sites fossilifères du continent euraméricain, ce qui introduit un biais potentiel dans la représentativité de la diversité observée. En effet, les derniers siècles d'excavation se sont principalement concentrés sur ces sites et un effort d'échantillonnage plus important sur des sites en dehors pourrait révéler une diversité cryptique qui viendrait préciser les patrons que nous avons observés (Henderson et al. 2022).

Une autre limite imposée par le registre fossile concerne la précision anatomique que nous pouvons aller chercher. À l'exception de rares fossiles provenant de sites exceptionnels (Konzervat-Lagerstätte) conservés en trois dimensions, la plupart des spécimens sont fortement compressés et déformés. Cela limite grandement l'information morphologique que nous pouvons utiliser. Ainsi pour notre étude en disparité morphologique, plusieurs espèces ont dû être retirées de l'échantillonnage car trop incomplètes. Nous avons rencontré un problème similaire pour le chapitre 4 en écomorphologie. En effet, bien que l'utilisation de la morphologie comme proxy de l'écologie des espèces ait déjà fait ses preuves (Larouche et

al. 2020; Wainwright et Richard 1995; Chevrinais et al. 2017), la complexité des habitats aquatiques apporte un défi supplémentaire. Cela peut être dû à des contraintes fonctionnelles d'habitats différents qui aboutissent à des convergences morphologiques ; à la délimitation d'un habitat par rapport à un autre qui peut être compliquée par l'existence d'un continuum ; ou encore par l'utilisation de plus d'un seul habitat par une espèce. La précision morphologique que nous pouvons alors aller chercher dans l'état des différents caractères morphologiques sélectionnés est essentielle. La significativité des patrons que nous obtenons n'en est pas moins valide ; toutefois, il est important de considérer ces limitations lors de nos interprétations.

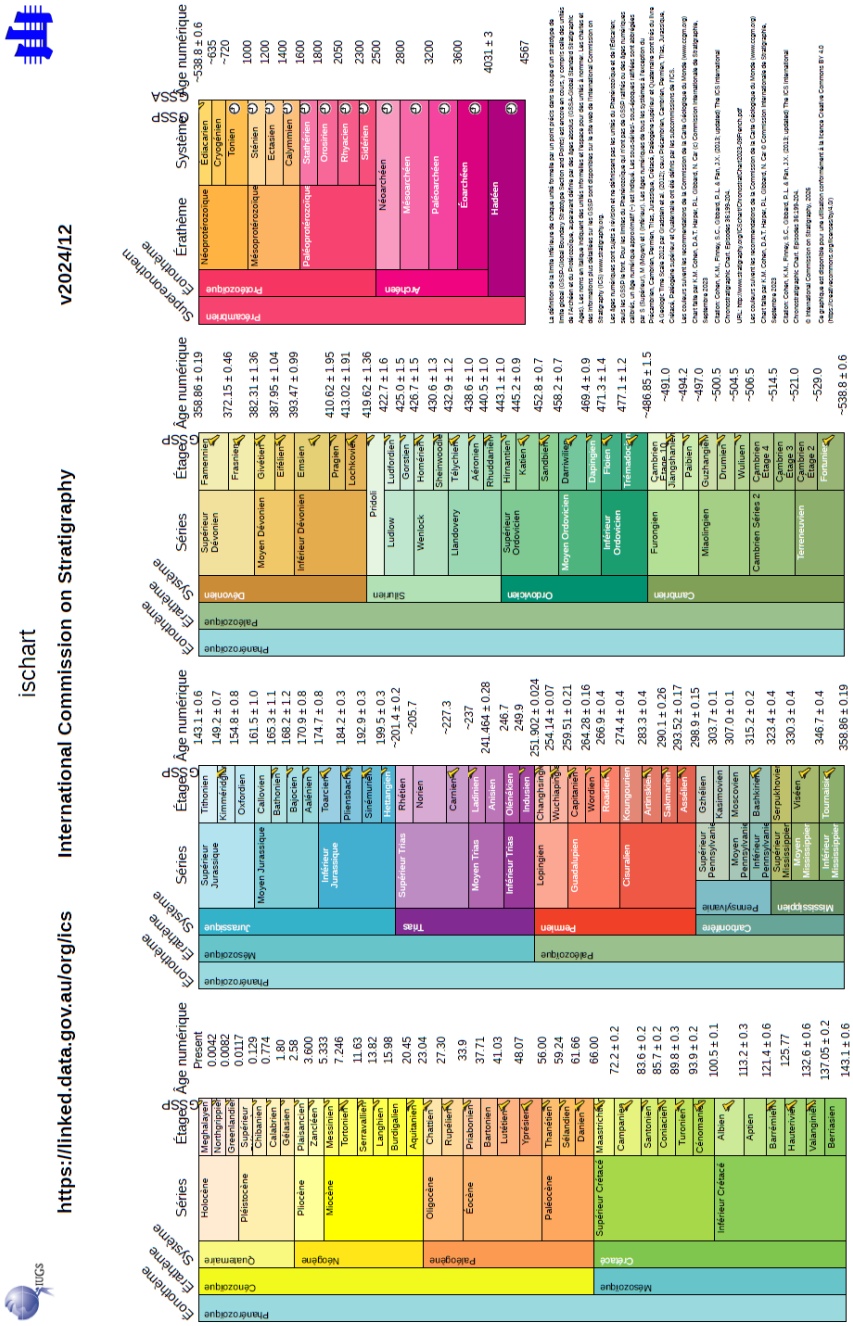
Nous pouvons également essayer de pallier ce manque d'informations de plusieurs façons, par exemple en utilisant des approches variées ayant une gestion des données manquantes différente. Dans notre cas nous avons utilisé deux types de descripteurs morphologiques différents : (1) la morphométrie géométrique, étant une mesure continue de la forme, elle apporte une information géométrique plus complète, mais est plus sensible aux données manquantes ; (2) les matrices morphométriques basées sur des caractères discrets et/ou continus, sont moins sensibles aux données manquantes mais perdent une partie de l'informatique géométrique. La précision des méthodes d'imputation des données manquantes telles qu'utilisées dans le dernier chapitre pourrait également être augmentée en venant incorporer manuellement à la matrice des estimations pour certains des codages manquants en nous basant sur l'expertise de chercheurs plutôt que seulement sur des modèles mathématiques. Ce genre de projets de grande échelle bénéficierait d'une importante collaboration entre chercheurs. En effet, la plupart des biologistes et paléontologues ont une expertise sans pareille concernant certains taxons ou certaines formations fossilifères qui dépassent de loin toutes les imputations mathématiques que l'on pourrait faire. La création de banques de données collaboratives multidisciplinaires pourrait grandement participer à pallier les limitations imposées par le registre fossile et permettre une étude intégrative de l'histoire de la Terre.

Pour ce qui est de la limitation dans la précision anatomique des fossiles, les nouvelles techniques d'imagerie non-destructives telles que la tomographie synchrotron ouvrent de nouvelles perspectives en donnant accès à une information dont la précision est encore inégalée, en permettant notamment des reconstructions en trois dimensions des fossiles.

Pour finir, cette étude se concentrait uniquement sur des patrons observables à l'échelle macroévolutive sur des espèces éteintes. Une des avenues intéressantes que nous pourrions maintenant emprunter serait de comparer ces patrons avec d'autres groupes plus récents afin de tester leur conservation au cours de l'évolution. Par exemple, le groupe des actinoptérygiens serait parfait pour cela. Son histoire est particulièrement riche, et il représente aujourd'hui le groupe de vertébrés le plus diversifié. Il serait donc intéressant de voir dans un premier temps si les patrons évolutifs associés à leur première radiation évolutive caractérisés ici pourraient être reconnus lors d'épisodes de diversification subséquents. Une période intéressante à étudier serait l'apparition des téléostéens durant le Jurassique (Arratia 1996), étant le groupe d'actinoptérygiens ayant connu le plus grand succès évolutif. De nombreuses études génétiques ont également été réalisées sur ce groupe (Ravi et Venkatesh 2008; Song et al. 2026; Reinar et al. 2023; Parey et al. 2023) ce qui permettrait de rajouter une dimension microévolutive à l'étude. La dimension microévolutive pourrait également être intéressante à rajouter dans l'étude des processus sous-jacents à la diversification tels que la modularité. Ainsi une étude sur des taxons actuels à une échelle moléculaire pourrait aider à mieux comprendre l'origine du caractère modulaire des organismes. Ainsi en alliant les connaissances macroévolutives apportées par la paléontologie à celles des études moléculaires, nous pourrions arriver à une meilleure compréhension générale des processus évolutifs du vivant à différentes échelles.

ANNEXE I

CHARTE CHRONOSTRATIGRAPHIQUE INTERNATIONALE (DEPUIS INTERNATIONAL COMMISSION ON STRATIGRAPHY, HTTPS://STRATIGRAPHY.ORG/CHART/)



ANNEXE II

SUPPLEMENTARY INFORMATION FOR CHAPTER 1: MORPHOLOGICAL DISPARITY AND EVOLUTIONARY RADIATION OF EARLY ACTINOPTERYGIANS THROUGH THE DEVONIAN-CARBONIFEROUS CRISIS

Table S1. List of the 197 basal actinopterygian species included in diversity analyses. FAD (first appearance datum) corresponds to the first time the species appears in the fossil record, and LAD (last appearance datum) to the last time it appears.

Species	Age	Formation/County	References	FAD	LAD
DEVONIAN					
MIDDLE DEVONIAN					
Austelliscus ferox	Givetian	Ponta Grossa, Paraná, Brazil	Figueroa, Weinschütz & Friedman 2021	387.7	386.03
Cheirolepis aleshkai	Eifelian	Narva Regional Stage, Lepel 1 borehole, Vitebsk region, Belarus	Plax 2020	393.3	391.43
Cheirolepis jonesi	Givetian	Mimerdalen subgroup, Fiskeløfta member, Spitsbergen, Svalbard, Norway	Newman *et al.* 2021	384.36	382.7
Cheirolepis schultzei	Givetian	Nevada, USA	Arratia & Cloutier 2004; Newman *et al.* 2021	384.36	379.2
Cheirolepis trailli	Eifelian	Old Red Sandstone, Orkney, Scotland	Pearson & Westoll 1979; Arratia & Cloutier 2004; Agassiz 1835	393.3	382.7
Donnrosenia schaefferi	Givetian	Aztec Siltstone of southern Victoria Land, Antarctica	Choo 2010; Long *et al.* 2008	387.7	382.7
Moythomasia lineata	Givetian	Bergisch Gladbach, Heiligenstock quarry, Germany	Choo 2015	384.36	379.2
Moythomasia nitida	Givetian	Bergisch Gladbach, Heiligenstock Quarry, Germany	Choo 2015; Gross 1953	384.36	379.2
Stegotrachelus finlayi	Givetian	Ness of Sound and Dunrossness, South-East Shetland, Old Red Sandstone, Scotland	Swartz 2009; Woodward & White, 1926	387.7	382.7
UPPER DEVONIAN					

Cheirolepis canadensis	Frasnian	Escuminac Formation, Miguasha, Quebec, Canada	Arratia & Cloutier 1996; Arratia *et al.* 2004; Whiteaves 1881	379.2	375.7
Cuneognathus gardineri	Famennian	Eastern Greenland, Obrutschew Bjerg Formation	Schultze *et al.* 2021; Friedman & Blom 2006	363.33	358.9
Elonichthys pulcherrimus	Famennian	Glencartholm, Dumfries and Galloway, Scotland; Borov and Rubchan Beds, Polese Regional Stage, Poland	Schultze *et al.* 2021; Moy-Thomas & Dyne 1938; Traquair 1881	363.33	336.16
Gogosardina coatesi	Frasnian	Gogo Formation, Australia	Choo *et al.* 2009	382.7	379.2
Howqualepis rostridens	Frasnian	Mt Howitt, Victoria, Australia	Long 1988	382.7	379.2
Kentuckia hlavini	Famennian	Cleveland Member, Ohio Shale, Ohio, USA	Dunkle 1964	363.33	358.9
Krasnoyarichthys jesseni	Famennian	Siberia, Russia	Prokofiev 2002	372.2	358.9
Limnomis delaneyi	Famennian	Catskill, Pennsylvania, USA	Daeschler 2000	363.33	358.9
Mimipiscis bartrami	Frasnian	Gogo Formation, Australia	Choo 2012	382.7	379.2
Mimipiscis toombsi	Frasnian	Gogo Formation, Australia	Choo 2012	382.7	379.2
Moythomasia durgaringa	Frasnian	Gogo Formation, Australia	Choo 2015; Gardiner & Bartram 1977	382.7	379.2
Osorioichthys marginis	Famennian	Famenne Formation, Belgium	Casier 1952; Taverne 1997; Schultze *et al.* 2021	372.2	367.76
Pickeringius acanthophorus	Frasnian	Gogo Formation, Australia	Choo *et al.* 2018	382.7	379.2
Raynerius splendens	Frasnian	Ferques Formation, Pas-de-Calais, France	Giles *et al.* 2015	379.2	375.7
Rhadinichthys macconochii	Famennian	East European platform, Russia; Glencartholm, Scotland	Traquair 1881	372.2	330.9
Rhadinichthys tuberculatus	Famennian	East European platform, Russia; Glencartholm, Scotland	Traquair 1881	372.2	330.9
Tegeolepis clarcki	Famennian	Cleveland shale, Ohio shale member, USA	Schultze *et al.* 2021; Miller 1892	363.33	358.9

CARBONIFEROUS					
MISSISSIPPIAN					
Acanthoniscus cracens	Serpukhovian	Heath Formation, Bear Gulch Limestone, Montana, USA	Schultze *et al.* 2021	325.76	323.2
Acrolepis ortholepis	Viséan	Glencartholm, Dumfries and Galloway, Scotland	Traquair 1884	341.43	336.16
Acrolepis wilsoni	Viséan	Coal Measures, Yoredale Rocks, Derbyshire, England	Traquair 1888	346.7	330.9
Adroichthys tuberculatus	Viséan	Upper Witteberg Series, Waaipoort Formation (Lake Mentz), Western Cape Province, South Africa	Schultze *et al.* 2021; Gardiner 1969	346.7	330.9
Apholidotos ossna	Serpukhovian	Heath Formation, Bear Gulch Limestone, Montana, USA	Lund 1991	325.76	323.2
Aesopichthys erinaceus	Serpukhovian	Heath Formation, Bear Gulch Limestone, Montana, USA	Poplin & Lund 2000	325.76	323.2
Aestuarichthys fulcratus	Viséan	Upper Witteberg Series, Waaipoort Formation (Lake Mentz), Western Cape Province, South Africa	Schultze *et al.* 2021; Gardiner 1969	346.7	330.9
Aetheretmon valentiacum	Tournaisian	Foulden, Scotland; east European platform, Turaŭ, Belarus	Schultze *et al.* 2021; White 1927	350.76	341.43
Atracauda lundi	Serpukhovian	Heath Formation, Bear Gulch Limestone, Montana, USA	Lowney 1991; Schultze *et al.* 2021	325.76	323.2
Australichthys longidorsalis	Viséan	Upper Witteberg Series, Waaipoort Formation (Lake Mentz), Western Cape Province, South Africa	Schultze *et al.* 2021; Gardiner 1969	346.7	330.9
Avonichthys manskyi	Tournaisian	Horton Bluff Formation, Nova Scotia, Canada	*Wilson et al.* 2018	358.9	350.76
Beagiascus pulcherrimus	Serpukhovian	Heath Formation, Bear Gulch	Mickle *et al.* 2009	325.76	323.2

		Limestone, Montana, USA			
Benedenius deneensis	Viséan	Molignée, Belgium	Mottequin *et al.* 2015; Traquair 1877	346.7	341.43
Benedenius soreili	Viséan	Molignée, Belgium	Mottequin *et al.* 2015; Fraipont 1890	346.7	341.43
Bishofia lucida	Tournaisian	Minusinsk, Russia	Kazantseva 1968	358.9	346.7
Blairolepis loanheadensis	Serpukhovian	Loanhead (Scotland)	Lowney 1983; Schultze *et al.* 2021	330.9	328.83
Bluefieldius mercerensis	Viséan	Bluefield Formation, West Virginia, USA	Mickle 2018	336.16	328.83
Bourbonnella jocelynae	Serpukhovian	Manning Canyon, Shale Formation, Utah, USA	Mickle 2011	330.9	320.53
Canobius elegantulus	Viséan	Glencartholm, Dumfries and Galloway, Scotland	Schultze *et al.* 2021; Moy-Thomas & Dyne 1938; Traquair 1881	341.43	336.16
Canobius modulus	Tournaisian	Albert Formation New Brunswick	Dawson 1877	358.9	346.7
Canobius ramsayi	Viséan	Glencartholm, Eksdale, Dumfries and Galloway, Scotland	Schultze *et al.* 2021; Moy-Thomas & Dyne 1938; Wood 1982; Traquair 1881	341.43	336.16
Cheirodopsis geikiei	Viséan	Glencartholm, Dumfries and Galloway, Scotland	Schultze *et al.* 2021; Moy-Thomas & Dyne 1938; Wood 1982; Traquair 1881	341.43	336.16
Cosmoptychius striatus	Viséan	Wardie, Scotland	Dineley et Metclaf 1999; Gardiner 1963; Watson 1928	335.5	333.5
Cryphiolepis striatus	Serpukhovian	Borough Lee Ironstone, Edge Coal Series, Loanhead locality, Scotland	Schultze *et al.* 2021; Traquair 1907; Traquair 1881	330.3	328.33
Cycloptychius bidens	Viséan	Glencartholm, Dumfries and Galloway, Scotland	Matveeva 1958	341.43	336.16
Cycloptychius concentricus	Viséan	Glencartholm, Dumfries and Galloway, Scotland	Schultze *et al.* 2021; Moy-Thomas & Dyne 1938; Traquair 1881	341.43	336.16

Cyranorhis bergeraci	Serpukhovian	Heath Formation, Bear Gulch Limestone, Montana, USA	Schultze *et al.* 2021; Lund & Poplin 1997	325.76	323.2
Discoserra pectinodon	Serpukhovian	Heath Formation, Bear Gulch Limestone, Montana, USA	Lund 2000	325.76	323.2
Drydenius insignis	Serpukhovian	Loanhead (Scotland)	Traquair 1890	330.3	328.33
Dwykia analensis	Viséan	Upper Witteberg Series, Soetendals Vlei, Eastern Cape province, South Africa	Gardiner 1969	346.7	330.9
Elonichthys browni	Tournaisian	Albert Formation New Brunswick	Goodarzi *et al.* 2019	358.9	346.7
Elonichthys robisoni	Viséan	Wardie Shales, Forth Bassin (Beds 2-7), Scotland	Schultze *et al.* 2021; Traquair 1901; Hibbert 1835	341.43	336.16
Elonichthys serratus	Viséan	Glencartholm, Dumfries and Galloway, Scotland	Schultze *et al.* 2021; Moy-Thomas & Dyne 1938; Traquair 1881	341.43	336.16
Enzichthys aizenvergi	Serpukhovian	Borehole 7854, Donetsk basin, Ukraine	Selezneva 1988	326.26	323.2
Fouldenia ischiptera	Tournaisian	Foulden Fish Bed, Foulden Burn, Berwickshire, Scotland	Schultze *et al.* 2021; Sallan 2013; Sallan & Coates 2013	350.76	346.7
Frederichthys musadentatus	Serpukhovian	Manse Burn Formation, Bearsden Scotland	Coates, 1993	330.9	328.33
Fubarichthys copiosus	Serpukhovian	Heath Formation, Bear Gulch Limestone, Montana USA	Lowney 1980; Schultze *et al.* 2021	325.76	323.2
Ganolepis gracilis	Tournaisian	Bystryanskaya Formation, Uzhur, Minusinsk (Russia)	Woodward 1893; Berg 1958; Schultze *et al.* 2021	358.9	346.7
Ganolepis longicauda	Tournaisian	Minusinsk, Russia	Matveeva 1958	358.9	346.7
Gonatodus punctatus	Viséan	Wardie, Scotland	Schultze *et al.* 2021; Gardiner 1967; Traquair 1877	335.5	333.5
Grassator bidens	Tournaisian	Minusinsk, Russia	Kazantseva 1968	358.9	346.7
Guildayichthys carnegiei	Serpukhovian	Heath Formation, Bear Gulch	Lund 2000	325.76	323.2

		Limestone Limestone, Montana, USA			
Guntherichthys lehiensis	Serpukhovian	Manning canyon, Shale Formation, Utah, USA	Mickle 2011	330.9	320.53
Gyrolepidotus microlepis	Tournaisian	Minusinsk, Russia	Berg 1958; Schultze *et al.* 2021	358.9	346.7
Gyrolepidotus schmidti	Tournaisian	Bystryanskaya Formation, Uzhur, Minusinsk (Russia)	Berg 1958; Schultze *et al.* 2021; Rohon 1889	358.9	346.7
Holurus parki	Viséan	Glencartholm, Dumfries and Galloway, Scotland	Moy-Thomas & Dyne 1938; Traquair 1881	341.43	336.16
Kalops diophrys	Serpukhovian	Heath Formation, Bear Gulch Limestone, Montana, USA	Schultze *et al.* 2021; Poplin & Lund 2002	325.76	323.2
Kalops monophrys	Serpukhovian	Heath Formation, Bear Gulch Limestone, Montana, USA	Schultze *et al.* 2021; Poplin & Lund 2002	325.76	323.2
Kansania eatoni	Kasimovian	Douglas Group, Lawrence Formation, Haskell Limestone Member, Douglas County, Kansas, USA	Poplin 1974; I.U.G.S. Subcommission on Carboniferous Stratigraphy 2006	304.8	303.7
Kentuckia deani	Tournaisian	New Providence Shale Member, Borden Formation, near Junction City, Kentucky	Rayner 1952	350.76	341.43
Lambeia pectinatus	Tournaisian	Albert Formation New Brunswick	Mickle 2017	358.9	346.7
Lineagruan judithi	Serpukhovian	Heath Formation, Bear Gulch Limestone, Montana, USA	Mickle *et al.* 2009	325.76	323.2
Lineagruan snowyi	Serpukhovian	Heath Formation, Bear Gulch Limestone, Montana, USA	Mickle *et al.* 2009	325.76	323.2
Mansfieldiscus sweeti	Tournaisian	Bridge creek, Australia	Schultze *et al.* 2021; Long 1988	358.9	350.76
Melanecta anneae	Serpukhovian	Shrimp member, Manse Burn Formation, Bearsden Scotland	Schultze *et al.* 2021; Coates 1998	330.9	328.33
Mentzichthys jubbi	Viséan	Upper Witteberg Series, Waaipoort Formation, Western	Schultze *et al.* 2021; Gardiner 1969	346.7	330.9

		Cape Province, South Africa			
Mentzichthys maraisi	Viséan	Upper Witteberg Series, Waaipoort Formation, Western Cape Province, South Africa	Schultze *et al.* 2021; Gardiner 1969	346.7	330.9
Mentzichthys theroni	Viséan	Upper Witteberg Series, Waaipoort Formation (Lake Mentz), Western Cape Province, South Africa	Schultze *et al.* 2021; Gardiner 1969	346.7	330.9
Mentzichthys walshi	Viséan	Upper Witteberg Series, Waaipoort Formation (Lake Mentz), Western Cape Province, South Africa	Jubb 1965	346.7	330.9
Mesonichthys aitkeni	Serpukhovian	Devonshire, England; Belgium, Northern France	Gardiner 1963	330.9	315.2
Mesopoma ardrossense	Viséan	Glencartholm volcanic member, Scotland	Moy-Thomas 1938	341.43	336.16
Mesopoma carriki	Serpukhovian	Shrimp member, Manse Burn Formation, Bearsden Scotland	Coates 1993	330.9	328.33
Mesopoma crassum	Viséan	Glencartholm volcanic member, Scotland	Schultze *et al.* 2021; Moy-Thomas & Dyne 1938; Traquair 1913	341.43	336.16
Mesopoma politum	Viséan	Glencartholm volcanic member, Scotland	Schultze *et al.* 2021; Traquair 1881	341.43	336.16
Mesopoma pulchellum	Viséan	Glencartholm volcanic member, Scotland	Schultze *et al.* 2021; Traquair 1881	341.43	336.16
Notacmon crenatus	Viséan	Shales Member of the Gullane Formation, Wardie, Scotland	Schultze *et al.* 2021; Friedman *et al.* 2018; Agassiz 1835	335.5	333.5
Novogonatodus kasantsevae	Tournaisian	Snowy plains Formation, Mansfield group, Australia	Holland *et al.*, 2004; Long 1988	358.9	350.76
Oxypteriscus minimus	Tournaisian	Minusinsk, Russia	Matveeva 1958	358.9	346.7
Paphosiscus circulocaudus	Serpukhovian	Heath Formation, Bear Gulch	Grogan & Lund 2015	325.76	323.2

		Limestone, Montana, USA			
Paphosiscus scalmocristus	Serpukhovian	Heath Formation, Bear Gulch Limestone, Montana, USA	Grogan & Lund 2015	325.76	323.2
Paramesolepis rhombus	Viséan	Glencartholm, Dumfries and Galloway, Scotland	Schultze *et al.* 2021; Moy-Thomas & Dyne 1938; Traquair 1890	341.43	336.16
Paramesolepis tuberculatus	Viséan	Glencartholm, Dumfries and Galloway, Scotland	Schultze *et al.* 2021; Moy-Thomas & Dyne 1938; Traquair 1890	341.43	336.16
Paratarrasius hibbardi	Serpukhovian	Heath Formation, Bear Gulch Limestone, Montana, USA	Lund & Poplin 2002; Lund & Melton 1982	325.76	323.2
Phanerosteon mirabile	Viséan	Glencartholm, Dumfries and Galloway, Scotland	Schultze *et al.* 2021; Traquair 1912; Traquair 1881	341.43	336.16
Phanerosteon ovensi	Tournaisian	Cementstones of Foulden, Scotland	White 1927; Gardiner 1985	358.9	344.5
Platysomus superbus	Viséan	Glencartholm, Dumfries and Galloway, Scotland	Schultze *et al.* 2021; Moy-Thomas & Dyne 1938; Traquair 1881	341.43	336.16
Proceramala montanensis	Serpukhovian	Heath Formation, Bear Gulch Limestone, Montana, USA	Poplin & Lund 2000	325.76	323.2
Proteurynotus traquairi	Viséan	Glencartholm, Dumfries and Galloway, Scotland	Moy-Thomas & Dyne 1938	341.43	336.16
Protohaplolepis scotica	Serpukhovian	Loanhead (Scotland)	Lowney 1983; Schultze *et al.* 2021	330.9	323.2
Pygopterus greenockii	Viséan	Wardie, Scotland; Belgium, Northern France	Traquair 1866	346.7	315.2
Rhadinichthys alberti	Tournaisian	Albert Formation New Brunswick	Lambe 1910	358.9	346.7
Rhadinichthys brevis	Viséan	Wardie Shales, Scotland	Traquair 1877	335.5	333.5
Rhadinichthys canobiensis	Viséan	Glencartholm, Dumfries and Galloway, Scotland	Schultze *et al.* 2021; Moy-Thomas & Dyne	341.43	336.16

			1938; Traquair 1909		
Rhadinichthys carinatus	Viséan	Wardie Shale, Scotland	Agassiz 1835	335.5	333.5
Rhadinichthys ferox	Viséan	Wardie Shale, Scotland	Traquair 1877	335.5	333.5
Rhadinichthys formosus	Viséan	Glencartholm, Dumfries and Galloway, Scotland	Traquair 1904	341.43	336.16
Rhadinichthys fusiformis	Viséan	Glencartholm, Dumfries and Galloway, Scotland	Moy-Thomas & Dyne 1938; Traquair 1881	341.43	336.16
Rhadinichthys ornatissimus	Viséan	Scotland: Dunnet shale (calciferous sandstone series) of Straiton	Schultze *et al.* 2021; Traquair 1911; Brindley & Spinner 1989; Agassiz 1835	346.7	330.9
Rhadinoniscus wrighti	Viséan	Adross Castle, Scotland	White 1937	336.16	330.9
Senekichthys hirundo	Tournaisian	Herbesskaya Formation, Senek Creek, Southwestern Siberia, Russia	Schultze *et al.* 2021; Prokofiev 2004	350.76	346.7
Soetendalichthys cromptoni	Viséan	Upper Witteberg Series, Soetendals Vlei, Eastern Cape province, South Africa	Gardiner 1969	346.7	330.9
Spinofacia pectinatus	Serpukhovian	Manning canyon, Shale Formation, Utah, USA	Mickle 2011	330.9	320.53
Strepheoschema fouldenensis	Tournaisian	Foulden, Scotland; Eastern European platform, Belarus	Schultze *et al.* 2021; White 1927	358.9	346.7
Styracopterus fulcratus	Viséan	Glencartholm, Dumfries and Galloway, Scotland; East European Platform, Russia	Schultze *et al.* 2021; Sallan and Coates 2013; Traquair 1881	339	337.5
Sundayichthys elegantulus	Viséan	Upper Witteberg Series, Waaipoort Formation, Western Cape Province, South Africa	Schultze *et al.* 2021; Gardiner 1969	346.7	330.9
Tanypterichthys pridensis	Serpukhovian	Bluestone Formation, Mauch Chunk Group, Virginia, USA	Weems & Windolph 1986	326.26	323.2
Tarrasius problematicus	Viséan	Calciferous Sandstone Series, Glencartholm, Dumfriesshire, Scotland	Lund & Poplin 2002; Traquair 1881	341.43	336.16

Trawdenia pancheni	Serpukhovian	Bearsden, Glasgow, Scotland	Coates 1993	330.9	328.83
Wardichthys cyclosoma	Viséan	Wardie, Scotland	Traquair 1875	335.5	333.5
Wendyichthys dicksoni	Serpukhovian	Heath Formation, Bear Gulch Limestone, Montana, USA	Schultze *et al.* 2021; Lund & Poplin 1997	325.76	323.2
Wendyichthys lautreci	Serpukhovian	Heath Formation, Bear Gulch Limestone, Montana, USA	Schultze *et al.* 2021; Lund & Poplin 1997	325.76	323.2
Willomorichthys striatulus	Viséan	Upper Witteberg Series, Waaipoort Formation, Western Cape Province, South Africa	Gardiner 1969	346.7	330.9
Woodichthys bearsdeni	Serpukhovian	Shrimp member, Manse Burn Formation, Bearsden Scotland	Schultze *et al.* 2021; Coates 1998	330.9	328.33
Yogoniscus gulo	Serpukhovian	Heath Formation, Bear Gulch Limestone, Montana, USA	Lowney 1991; Schultze *et al.* 2021	325.76	323.2
		PENNSYLVANIAN			
Acentrophorus dispersus	Gzhelian	Kounov, Czech Republic	Fritsch 1894	303.5	298.9
Acrolepis gigas	Gzhelian	Slany Formation, Central bohemia basin, Czech Republic	Stamberg 1991; Fritsch 1877	303.5	302.5
Andrewsolepis lochlani	Bashkirian	Lower Coal Measure, Wester Bracco, Scotland	Elliott 2018	317.86	312.46
Aeduella blainvillei	Kasimovian	Bassin d'Autun/Montceau-les-Mines, France	Poplin & Dutheil 2005; Heyler & Poplin 1983; Westoll 1937	307	303.7
Amphicentrum granulosum	Moscovian	Knowles Ironstone band of the Winghay Coal in Fenton Colliery, Fenton, Staffordshire, England	Schultze *et al.* 2021; Dyne 1939; Traquair 1880; Young 1866; Elliott 2018	314.75	310
Amphicentrum orbiculare	Moscovian	Francis Creek Shale Member, Carbondale Formation, Illinois, USA	Zidek 1992; Newberry & Worthen 1870	312.46	307
Amphicentrum jurgenai	Kasimovian	Kinney Quarry, New-Mexico, USA	Zidek 1992	307	304.8

Blairolepis wallacei	Bashkirian	Lower Coal Measure, Wester Bracco, Scotland	Elliott 2018	317.86	312.46
Blanzychthys prorobisoni	Kasimovian	Montceau-les-Mines, Buxières-les-mines, France	Heyler & Poplin 1994	307	303.7
Bourbonnella guilloti	Kasimovian	Montceau-les-Mines, Buxières-les-mines, France	Poplin & Dutheil 2005; Heyler 1967	307	303.7
Bourbonnella fourrieri	Kasimovian	Montceau-les-Mines, Buxières-les-mines, France	Poplin 2001	307	303.7
Braccohaplolepis fenestratum	Bashkirian	Lower Coal Measure, Wester Bracco, Scotland	Elliott 2018	317.86	312.46
Coccocephalus baldwinensis	Kasimovian	Douglas Group, Lawrence Formation, Haskell Limestone Member, Douglas County, Kansas, USA	Poplin 1974; I.U.G.S. Subcommission on Carboniferous Stratigraphy 2006	304.8	303.7
Coccocephalus wildi	Bashkirian	Mountain Fourfoot Mine of Trawden, Lancashire, England	Poplin & Véran 1996; Schultze *et al.* 2021; Watson 1925	317.86	312.46
Commentrya barroisi	Kasimovian	Saarland, Germany	Waterlot 1934	304.8	303.7
Commentrya traquairi	Gzhelian	Commentry, France	Schultze *et al.* 2021; Sauvage 1888	303.5	298.9
Cornuboniscus budensis	Bashkirian	Bude Formation, Cornwall, England	White 1939; Schultze *et al.* 2021	319.9	310.7
Decazella vetteri	Moscovian	Decazeville, France	Heyler 1969; Poplin & Dutheil 2005; Heyler 1964	307.5	298.9
Drydenius molyneuxi	Moscovian	Royaume-Uni, Belgium, Germany, France	Traquair 1888	315.2	307
Elonichthys germani	Gzhelian	Sachsen-Anhalt, Germany	Giebel 1848	302.5	298.9
Elonichthys hypsilepis	Moscovian	Carbondale Formation, Mazon Creek, Illinois, USA	Schultze & Bardack 1987; Hay 1900	312.46	307
Elonichthys krejcii	Gzhelian	Plzeň, Bohemia Czech Republic	Schultze *et al.* 2021; Stamberg 1991; Fritsch 1895	303.5	302.5
Elonichthys peltigerus	Moscovian	Carbondale Formation, Linton, Ohio, Mazon Creek, Illinois	Schultze & Bardack 1987; Newberry 1856	312.46	307
Gyrolepis speciosus	Gzhelian	Puertollano basin Spain	Fritsch 1877	302.84	302.5

Haplolepis corrugata	Moscovian	Linton, Ohio, USA	Schultze *et al.* 2021; Elliott 2014; Miller 1892	310	307.26
Huanghelepis pani	Bashkirian	Zhongwei, Ningxia, China	Lu 2002	323.2	315.2
Igornella comblei	Kasimovian	Montceau-les-Mines, Buxières-les-mines, France	Heyler & Poplin 1994	307	303.7
Illiniichthys cozarti	Moscovian	Mazon Creek, Illinois, USA	Schultze & Bardack 1987	310	309.09
Kansania eatoni	Kasimovian	Douglas Group, Lawrence Formation, Haskell Limestone Member, Douglas County, Kansas, USA	Poplin 1974; I.U.G.S. Subcommission on Carboniferous Stratigraphy 2006	304.8	303.7
Lanarkichthys gardineri	Bashkirian	Lower Coal Measures, Wester Bracco, Scotland	Elliott 2018	317.86	312.46
Lawrenciella schaefferi	Kasimovian	Douglas Group, Lawrence Formation, Haskell Limestone Member, Douglas county, near Lawrence, Kansas, USA	Poplin 1974; I.U.G.S. Subcomission on Carboniferous Stratigraphy 2006	304.8	303.7
Meisenheimichthys glanensis	Gzhelian	Basal Rotliegend, Remigiusberg and Altenglan Formation, Saar-Nahe basin, Germany	Schindler 2006	303.7	298.9
Mesolepis arabellae	Bashkirian	Upper Drumgray Coal shale, Wester Bracco, South Lanarkshire, Scotland	Elliott & Giles 2024	323.2	315.2
Mesolepis scalaris	Moscovian	Knowles Ironstone Member, Pennine Middle Coal Measures Formation, England	Schultze *et al.* 2021; Sallan and Coates 2013; Young 1866	315.2	307
Mesolepis wardi	Bashkirian	Knowles Ironstone Member, Pennine Middle Coal Measures Formation, England	Young 1866	317.86	312.46
Microhaplolepis ovoidea	Moscovian	Linton, Ohio, USA	Schultze *et al.* 2021; Lowney 1980; Newberry 1856	310	307.26
Microhaplolepis serrata	Moscovian	Linton, Ohio, USA; Upper Freeport Coal	Schultze *et al.* 2021; Lowney 1980; Newberry 1856	309.09	307.26

Ningxiaplatysomus parvus	Bashkirian	Tupo Formation, Daliushu Village, Zhongwei, Ningxia Hui Autonomous Region, China	Tan *et al.* 2015; Prokop & Ren 2007	323.2	315.2
Parahaplolepis tuberculata	Moscovian	Linton, Ohio, USA	Schultze *et al.* 2021; Westoll 1944; Newberry 1856	310	307.26
Paramblypterus comblei	Kasimovian	Autun basin, France	Heyler 1969	307	303.7
Paramblypterus decorus	Kasimovian	Bassin d'Autun/Montceau-les-Mines	Dietze 2000; Heyler & Poplin 1983; Blot 1966	307	303.7
Phanerorhynchus armatus	Moscovian	Middle Coal Measure, Lancashire England	Schultze *et al.* 2021; Moy-Thomas 1971; Gardiner 1967; Gill 1923	312.46	310.7
Platysella lallyi	Kasimovian	Montceau-les-Mines, Buxières-les-mines, France	Heyler & Poplin 1983	307	303.7
Protohaplolepis isabella	Bashkirian	Lower Coal Measure, Wester Bracco, Scotland	Elliott 2015	317.86	312.46
Protohaplolepis limnades	Bashkirian	Lower Coal Measure, Wester Bracco, Scotland	Elliott 2015	317.86	312.46
Protohaplolepis traquairi	Bashkirian	Lower Coal Measure, Wester Bracco, Scotland	Elliott 2015	317.86	312.46
Pseudogonatodus aurulentum	Bashkirian	Lower Coal Measure, Wester Bracco, Scotland	Elliott 2018	317.86	312.46
Pseudohaplolepis argentatum	Bashkirian	Lower Coal Measure, Wester Bracco, Scotland	Elliott 2018	317.86	312.46
Puertollanichthys ritchiei	Gzhelian	Puertollano basin Spain	Schultze *et al.* 2021; Poplin & Dutheil 2005; Forey & Young, 1985	302.84	302.5
Pyritocephalus lineatus	Moscovian	Linton and Five Points, Ohio, USA	Schultze *et al.* 2021; Westoll 1944; Newberry 1856	310	307.26
Pyritocephalus lowneyae	Kasimovian	Kinney Brick Quarry, New-Mexico, USA	Huber 1992	304.8	303.7
Pyritocephalus rudis	Bashkirian	Northumberland, England	Westoll 1944	317.86	315.2
Pyritocephalus sculptus	Moscovian	Nýřany, Bohemia, Czech Republic	Schultze *et al.* 2021; Westoll	309.73	305.9

			1944; Stamberg 2006; Fritsch 1875		
Pyritocephalus youngi	Bashkirian	Lower Coal Measure, Wester Bracco, Scotland	Elliott 2015	317.86	312.46
Rhadinichthys glabrolepis	Bashkirian	Lower Coal Measure, North Lanarkshire, Scotland	Elliott 2018	317.86	312.46
Rhadinichthys grossarti	Bashkirian	Lower Coal Measure, North Lanarkshire, Scotland	Elliott 2018	317.86	312.46
Rhadinichthys hancocki	Bashkirian	Northumberland, England; North Lanarkshire, Scotland	Atthey 1875	317.86	312.46
Rhadinichthys lerichei	Moscovian	Belgium; North of France	Pruvost 1919	310	307.26
Rhadinichthys monensis	Bashkirian	Scotland; Belgium; Northern France	Egerton 1850	317.86	312.46
Sceletophorus biserialis	Moscovian	Nýřany Member, Central western Bohemia	Schultze *et al.* 2021; Stamberg 1991, 2006; Fritsch 1894	309.73	305.9
Schizolepis manzanitaensis	Kasimovian	Kinney Quarry, New Mexico USA	Schultze *et al.* 2021; Gottfried 1993; Lucas et al. 2011	307	304.8
Setlikia bohemica	Gzhelian	Kroucova, Rakovnik district, Kladno-Rakovnik Basin, Bohemia, Czech Republic	Stamberg & Zajíc 1994	303.5	302.5
Sphaerolepis kounoviensis	Gzhelian	Kounov Basin, Bohemian Basin, Czech Republic	Schultze *et al.* 2021; Stamberg 1991; Fritsch 1877	303.5	298.9
Tanyrhinichthys mcallisteri	Kasimovian	Kinney Quarry, New Mexico, USA	Schultze *et al.* 2021; Stack *et al.* 2020; Lucas *et al.* 2011; Gottfried, 1987	307	304.8
Trawdenia planti	Bashkirian	Lancashire England	Coates & Tietjen 2018	317.86	312.46
Whiteichthys greenlandicus	Bashkirian	North Scoresby Land, Mester Vig Formation, East Greenland	Schultze *et al.* 2021; Moy-Thomas 1942; Milan *et al.* 2016	317.86	312.46
Zaborichthys fragmentalis	Gzhelian	Bohemia, Czech Republic	Stamberg 1989	303.5	302.5
Zhongweilepis macilentus	Bashkirian	Tupo Formation, Daliushu Village, Zhongwei, Ningxia Hui Autonomous Region, China	Tan 2017; Prokop & Ren 2007	323.2	315.2

Table S2. List of the 106 basal actinopterygian species included in disparity analyses and their respective actual GPS coordinates. For each species, we indicated in which analyses it was included.

Species	Age	Longitude	Latitude	Body shape	Skull (Lateral)
		DEVONIAN			
Cheirolepis canadensis	Frasnian	-66.34886	48.10338	**x**	**x**
Cheirolepis schultzei	Givetian	-115.7499	38.16952		**x**
Cheirolepis trailli	Eifelian	-3.30908	59.07727	**x**	**x**
Cuneognathus gardineri	Famennian	-23.335047	73.126333	**x**	**x**
Donnrosenia schaefferi	Givetian	160.4667	-77.78333		**x**
Elonichthys pulcherrimus	Famennian	-2.9767 and 30.97606	55.10371 and 52.43302	**x**	**x**
Gogosardina coatesi	Frasnian	126.5	-18.3		**x**
Howqualepis rostridens	Frasnian	146.64846	-37.17467	**x**	**x**
Limnomis delaneyi	Famennian	-77.64733	41.34038	**x**	**x**
Mimipiscis bartrami	Frasnian	126.5	-18.3		**x**
Mimipiscis toombsi	Frasnian	126.5	-18.3	**x**	**x**
Moythomasia durgaringa	Frasnian	126.5	-18.3	**x**	**x**
Moythomasia lineata	Givetian	7.15209546978796	50.992266341319	**x**	**x**
Moythomasia nitida	Givetian	7.15209546978796	50.992266341319	**x**	**x**
Osorioichthys marginis	Famennian	4.51843	50.09469		**x**
Pickeringius acanthophorus	Frasnian	126.5	-18.3		**x**
Stegotrachelus finlayi	Givetian	-1.15218 and -1.24615	60.13348 and 59.90058	**x**	**x**
Tegeolepis clarcki	Famennian	-83.6	39.4		**x**
		CARBONIFEROUS			
Acrolepis gigas	Gzhelian	13.31302	49.83998	x	
Adroichthys tuberculatus	Viséan	25.1819	-33.16435	x	x

Aeduella blainvillei	Kasimovian	4.36266	46.6744	x	
Aesopichthys erinaceus	Serpukhovian	-108.9235	46.9919	x	x
Aestuarichthys fulcratus	Viséan	25.1819	-33.16435		x
Aetheretmon valentiacum	Tournaisian	-2.10661 and 27.74177	55.79436 and 52.06715	x	x
Amphicentrum granulosum	Moscovian	-2.15727	52.99679	x	x
Australichthys longidorsalis	Viséan	25.1819	-33.16435		x
Beagiascus pulcherrimus	Serpukhovian	-108.9235	46.9919	x	x
Benedenius deneensis	Viséan	4.7522	50.3186	x	
Benedenius soreili	Viséan	4.7522	50.3186	x	
Bourbonnella guilloti	Kasimovian	2.9639	46.47002	x	x
Canobius elegantulus	Viséan	-3.06666	55.18998	x	x
Canobius ramsayi	Viséan	-3.06666	55.18998	x	x
Cheirodopsis geikiei	Viséan	-3.06666	55.18998	x	x
Coccocephalus wildi	Bashkirian	-2.13805	53.84377		x
Commentrya traquairi	Gzhelian	2.7412	46.28733	x	x
Cornuboniscus budensis	Bashkirian	-4.54385	50.8266	x	x
Cosmoptychius striatus	Viséan	-3.21109	55.9806		x
Cryphiolepis striatus	Serpukhovian	-3.15351	55.87596	x	
Cycloptychius concentricus	Viséan	-3.06666	55.18998	x	x
Cyranorhis bergeraci	Serpukhovian	-108.9235	46.9919	x	x
Discoserra pectinodon	Serpukhovian	-108.9235	46.9919	x	
Elonichthys browni	Tournaisian	-64.7	45.9	x	
Elonichthys hypsilepis	Moscovian	-88.34073	41.26115	x	

Elonichthys krejcii	Gzhelian	13.37152	49.73874	x	
Elonichthys peltigerus	Moscovian	-88.34073	41.26115	x	x
Elonichthys robisoni	Viséan	-3.21109	55.9806	x	
Elonichthys serratus	Viséan	-3.06666	55.18998	x	x
Fouldenia ischiptera	Tournaisian	-2.10661	55.79436	x	x
Frederichthys musadentatus	Serpukhovian	-4.2113 and -4.3537	55.5547 and 55.9298	x	
Fubarichthys copiosus	Serpukhovian	-108.2135	46.9919	x	x
Ganolepis gracilis	Tournaisian	89.8114	55.3841		x
Gonatodus punctatus	Viséan	-3.21109	55.9806	x	x
Guildayichthys carnegiei	Serpukhovian	-108.9235	46.9919	x	
Gyrolepidotus microlepis	Tournaisian	91.69309736192673	53.69950339913683		x
Gyrolepidotus schmidti	Tournaisian	89.8114	55.3841	x	x
Haplolepis corrugata	Moscovian	-80.70234	40.56789	x	x
Holurus parki	Viséan	-3.06666	55.18998	x	x
Kalops diophrys	Serpukhovian	-108.9235	46.9919	x	x
Kalops monophrys	Serpukhovian	-108.9235	46.9919	x	x
Lambeia pectinatus	Tournaisian	-64.7	45.9		x
Lineagruan judithi	Serpukhovian	-108.9235	46.9919	x	x
Lineagruan snowyi	Serpukhovian	-108.9235	46.9919	x	x
Mansfieldiscus sweeti	Tournaisian	146.224	-37.011	x	x
Melanecta anneae	Serpukhovian	4.2113 and -4.3537	55.5547 and 55.9298	x	x
Mentzichthys jubbi	Viséan	25.1819	-33.16435	x	x
Mesolepis scalaris	Moscovian	-2.1796	53.005	x	
Mesopoma carriki	Serpukhovian	-4.2113 and -4.3537	55.5547 and 55.9298	x	x
Mesopoma crassum	Viséan	-3.06666	55.18998	x	x
Mesopoma politum	Viséan	-3.06666	55.18998	x	
Mesopoma pulchellum	Viséan	-3.06666	55.18998	x	x

Microhaplolepis ovoidea	Moscovian	-80.70234	40.56789	x	x
Microhaplolepis serrata	Moscovian	-80.70234	40.56789	x	x
Notacmon crenatus	Viséan	-3.21109	55.9806	x	
Novogonatodus kasantsevae	Tournaisian	146.224	-37.011		x
Parahaplolepis tuberculata	Moscovian	-80.70234	40.56789	x	
Paramblypterus decorus	Kasimovian	4.366266	46.6744		x
Paramesolepis rhombus	Viséan	-3.06666	55.18998	x	x
Paramesolepis tuberculatus	Viséan	-3.06666	55.18998	x	x
Paratarrasius hibbardi	Serpukhovian	-108.9235	46.9919		x
Phanerorhynchus armatus	Moscovian	-2.15918	53.60898	x	x
Phanerosteon mirabile	Viséan	-3.06666	55.18998	x	
Phanerosteon ovensi	Tournaisian	-2.10661	55.79436	x	
Platysomus superbus	Viséan	3.06666	55.18998	x	x
Proceramala montanensis	Serpukhovian	-108.9235	46.9919	x	x
Protohaplolepis scotica	Serpukhovian	-3.1585543	55.870971		x
Puertollanichthys ritchiei	Gzhelian	-4.10623	38.68851	x	
Pyritocephalus lineatus	Moscovian	-80.70234 and -84.19231	40.56789 and 39.57062	x	x
Pyritocephalus sculptus	Moscovian	13.20083	49.71456	x	x
Rhadinichthys canobiensis	Viséan	-3.06666	55.18998	x	x
Rhadinichthys fusiformis	Viséan	-3.06666	55.18998	x	x
Rhadinichthys ornatissimus	Viséan	-3.16631	55.88428	x	x

Sceletophorus biserialis	Moscovian	13.20083	49.71456	x	x
Senekichthys hirundo	Tournaisian	91.2667	50.9667	x	
Sphaerolepis kounoviensis	Gzhelian	13.67517	50.21328	x	x
Strepheoschema fouldenensis	Tournaisian	-2.10661	55.79436		x
Styracopterus fulcratus	Viséan	-3.06666	55.18998	x	x
Sundayichthys elegantulus	Viséan	25.18190	- 33.16435		x
Tanyrhinichthys mcallisteri	Kasimovian	-106.33765	35.00104	x	x
Tarrasius problematicus	Viséan	-3.00034	55.15262		x
Trawdenia planti	Bashkirian	-2.13673	53.84366	x	x
Wendyichthys dicksoni	Serpukhovian	-108.9235	46.9919	x	x
Wendyichthys lautreci	Serpukhovian	-108.9235	46.9919	x	
Whiteichthys greenlandicus	Bashkirian	-23.9212	72.23257	x	x
Willomorichthys striatulus	Viséan	25.18190	- 33.16435		x
Woodichthys bearsdeni	Serpukhovian	-4.3537	55.9298	x	x
Yogoniscus gulo	Serpukhovian	-108.9235	46.9919	x	x

Table S3. Description of landmarks and semilandmarks for the body shape and skull analyses, respectively.

N°	Nature of the descriptor	Description
	Body shape	
1	Landmark	Most anterior tip of the snout
2	Landmark	Most anterior edge of the extrascapular
3	Landmark	Most ventral part of the pectoral girdle
4	Landmark	Most posterior tip of the jaw articulation
5	Landmark	Insertion of the first ray of the dorsal fin
6	Landmark	Insertion of the last ray of the dorsal fin
7	Landmark	Dorsal caudal peduncle point in front of landmarks 8
8	Landmark	Insertion of the first ray of the ventral lobe of the caudal fin
9	Landmark	Insertion of the first ray of the anal fin
10	Landmark	Insertion of the last ray of the anal fin
11	Landmark	Dorsal insertion of the first pectoral fin ray
12	Landmark	Ventral insertion of the last pectoral fin ray
13	Landmark	Most posterior tip of the caudal peduncle
14-43	Semi-landmarks	Dorsal body outline from landmark 2 to 7
44-81	Semi-landmarks	Dorsal fin web outline from landmark 5 to 6
82-111	Semi-landmarks	Ventral body outline from landmark 3 to 8
112-136	Semi-landmarks	Anal fin web outline from landmark 9 to 10
137-216	Semi-landmarks	Caudal fin web outline from landmark 7 to 8
	Lateral skull	
1	Landmark	Most anterior tip of the upper jaw
2	Landmark	Most anterior edge of the extrascapular
3	Landmark	Most posterior margin of the lower jaw
4	Landmark	Most dorsal margin of the orbit
5	Landmark	Most ventral margin of the orbit
6	Landmark	Most anterior margin of the orbit
7	Landmark	Most posterior margin of the orbit
8	Landmark	Tip of the anterior-dorsal angle of the operculum
9	Landmark	Posterior extremity of the operculum
10	Landmark	Tip of the anterior-ventral angle extremity of the operculum
11	Landmark	Tip of the anterior-ventral angle extremity of the suboperculum
12	Landmark	Tip of the posterior-ventral angle extremity of the suboperculum
13	Landmark	Tip of the posterior-dorsal angle of the preopercular
14	Landmark	Tip of the anterior-dorsal angle of the preopercular
15	Landmark	Tip of the anterior-ventral angle of the preopercular
16	Landmark	Tip of the posterior-ventral angle of the preopercular
17	Landmark	Most anterior-dorsal tip of the lower jaw
18	Landmark	Most anterior tip of the snout
19-43	Semi-landmarks	Dorsal skull outline from landmark 18 to 2
44-68	Semi-landmarks	Ventral outline of the lower jaw from landmark 17 to 3

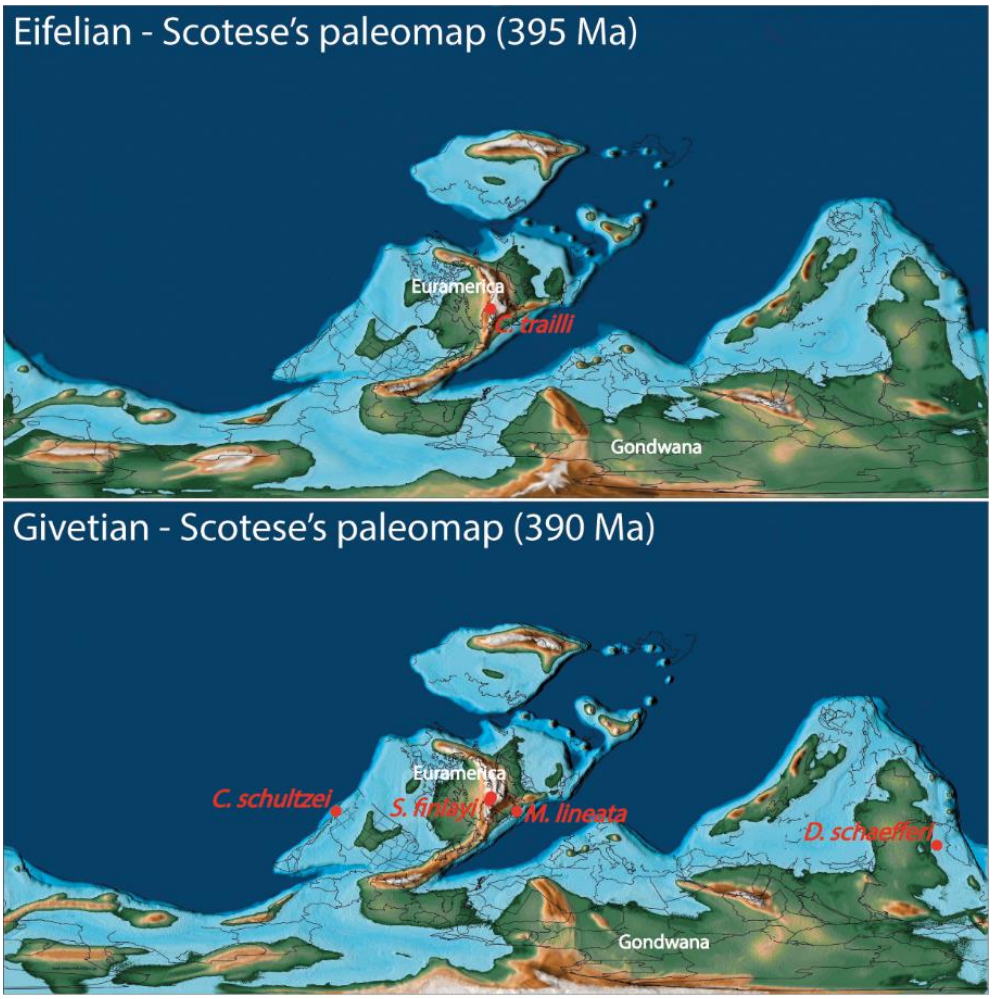


Figure S1. Palaeodistribution of the 18 Devonian actinopterygian species analysed based on their actual GPS coordinates. The background map used comes from the PALEOMAP PaleoAtlas [**Scotese 2016]** for Gplates available on *Earthbyte.org*. Species highlighted in these maps are: *Cheirolepis schultzei, Cheirolepis trailli, Donnrosenia schaefferi, Moythomasia lineata, Stegotrachelus finlayi.*

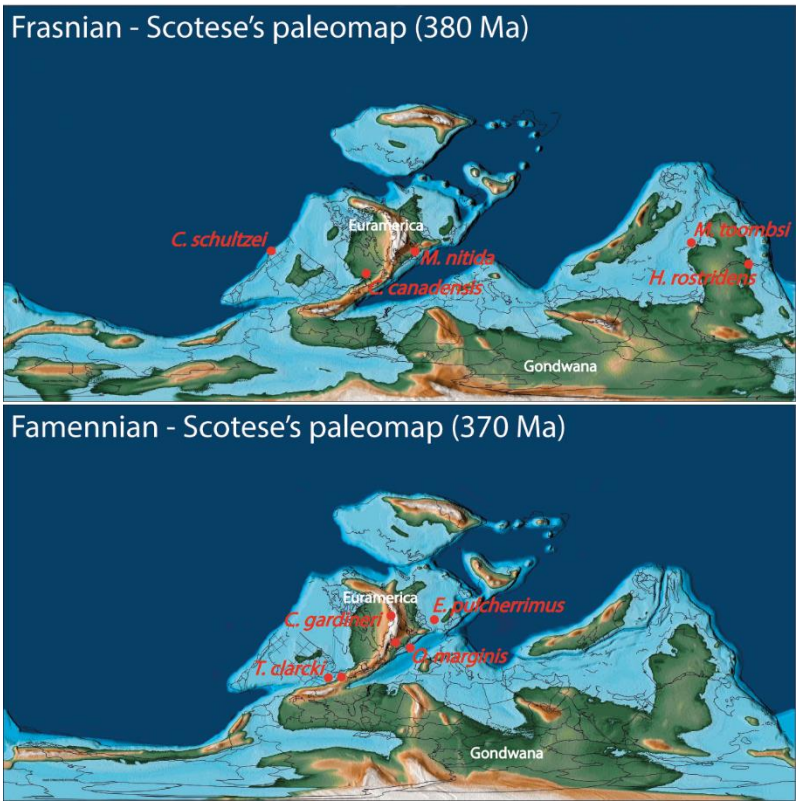


Figure S1. Palaeodistribution of the 18 Devonian actinopterygian species analysed based on their actual GPS coordinates. The background map used comes from the PALEOMAP PaleoAtlas **[Scotese 2016]** for Gplates available on *Earthbyte.org*. Species highlighted in these maps are: *Cheirolepis canadensis, Cheirolepis schultzei, Cuneognathus gardineri, Donnrosenia schaefferi, Elonichthys pulcherrimus, Howqualepis rostridens, Mimipiscis toombsi, Moythomasia nitida, Osorioichthys marginis, Tegeolepis clarcki.*

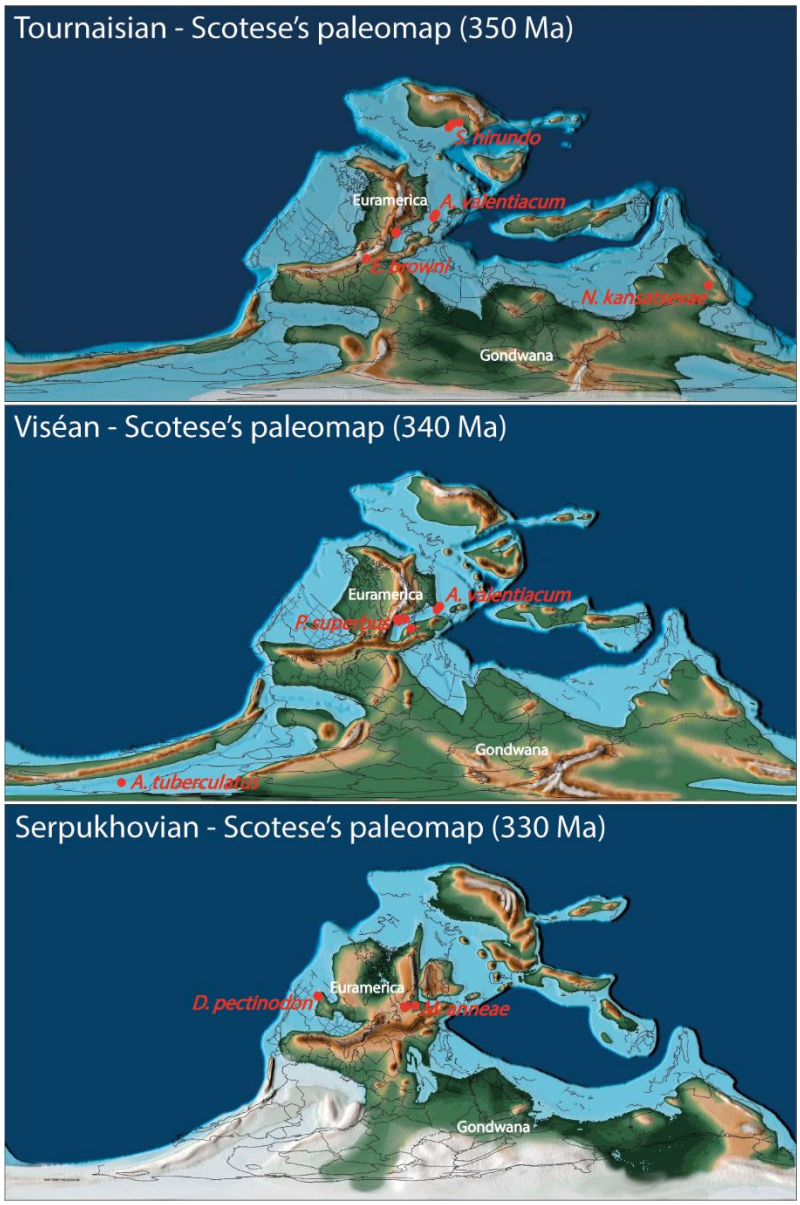


Figure S1. Palaeodistribution of the 50 Mississippian actinopterygian species analysed based on their actual GPS coordinates. The background map used comes from the PALEOMAP PaleoAtlas [**Scotese 2016]** for Gplates available on *Earthbyte.org*. Species highlighted in these maps are: *Adroichthys tuberculatus, Aetheretmon valentiacum, Discoserra pectinodon, Elonichthys browni, Melanecta anneae, Novogonatodus kansatsevae, Platysomus superbus, Senekichthys hirundo.*

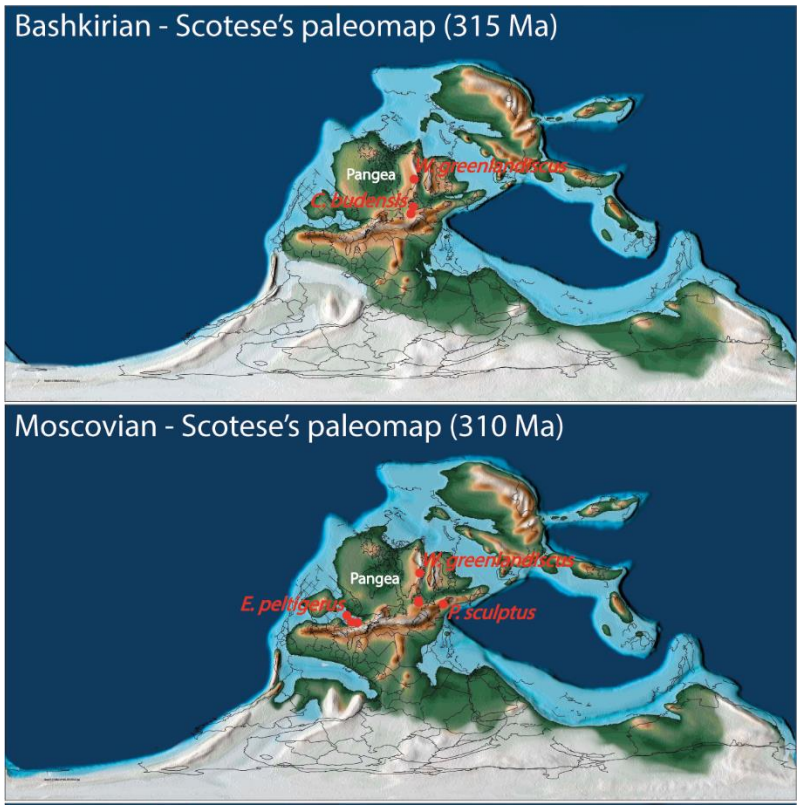


Figure S1. Palaeodistribution of the 18 Pennsylvanian actinopterygian species analysed based on their actual GPS coordinates. The background map used comes from the PALEOMAP PaleoAtlas [**Scotese 2016]** for Gplates available on *Earthbyte.org*. Species highlighted in these maps are: *Cornuboniscus budensis, Elonichthys peltigerus, Pyritocephalus sculptus, Whiteichthys greenlandiscus.*

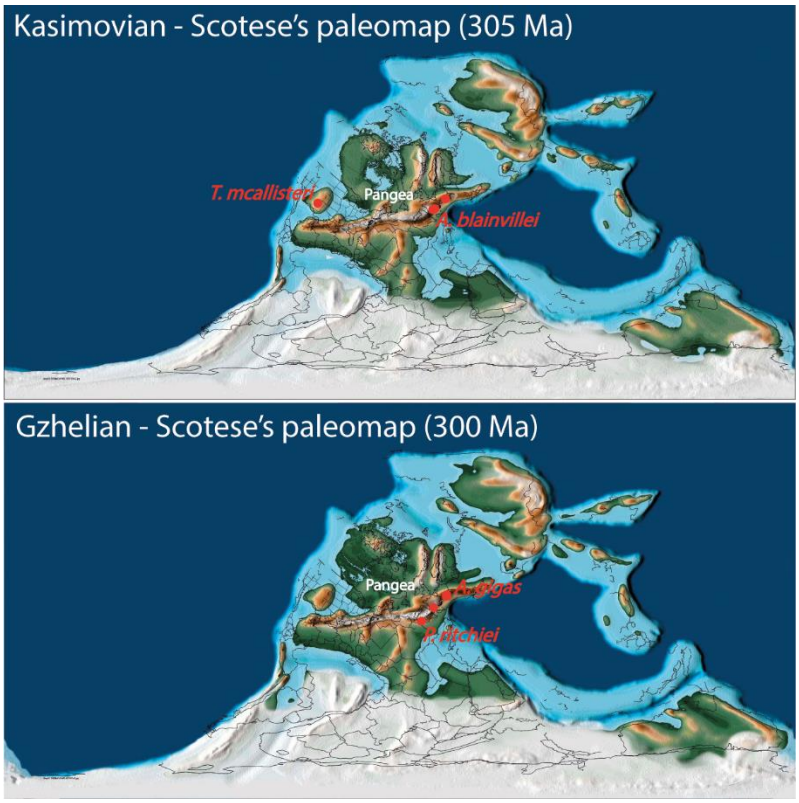


Figure S1. Palaeodistribution of the 18 Pennsylvanian actinopterygian species analysed based on their actual GPS coordinates. The background map used comes from the PALEOMAP PaleoAtlas **[Scotese 2016]** for Gplates available on *Earthbyte.org*. Species highlighted in these maps are: *Acrolepis gigas, Aeduella blainvillei, Puertollanichthys ritchiei, Tanyrhinichthys mcallisteri.*

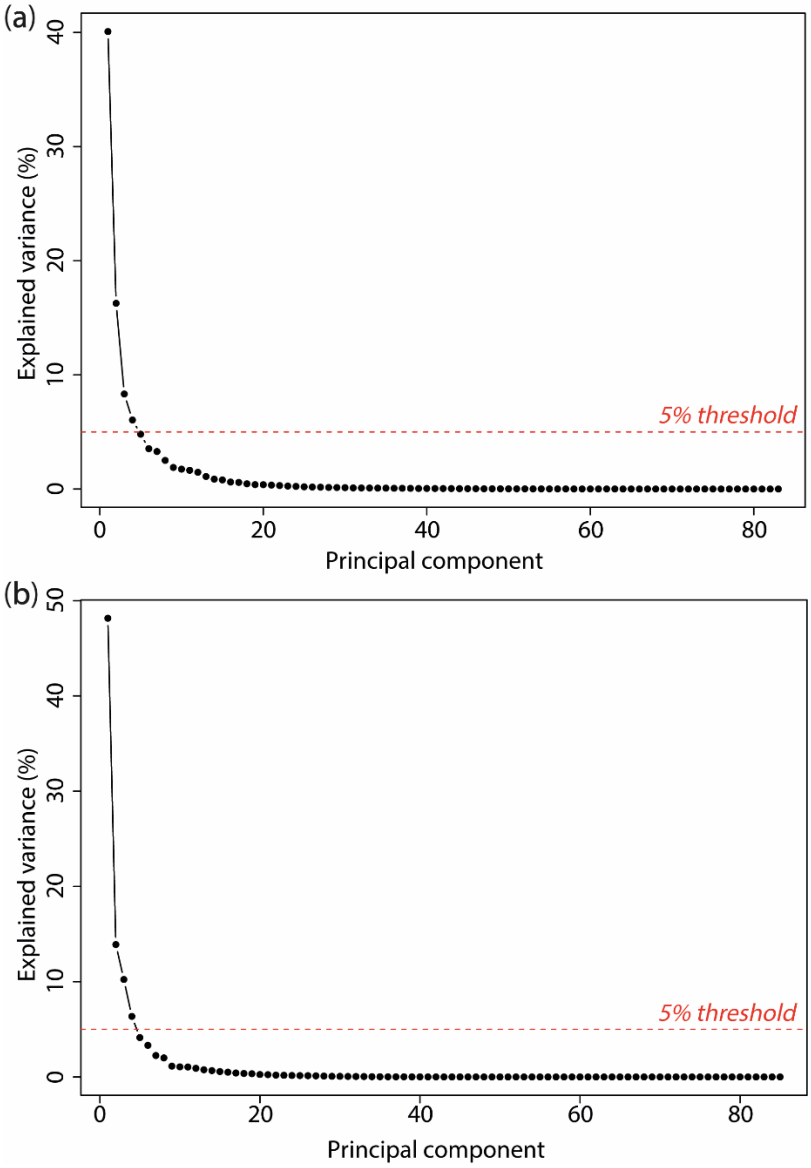


Figure S2. Scree plots. (a) Body shape PCA scree plot; (b) Lateral skull PCA scree plot. The dashed red line represents the 5% of explained variance.

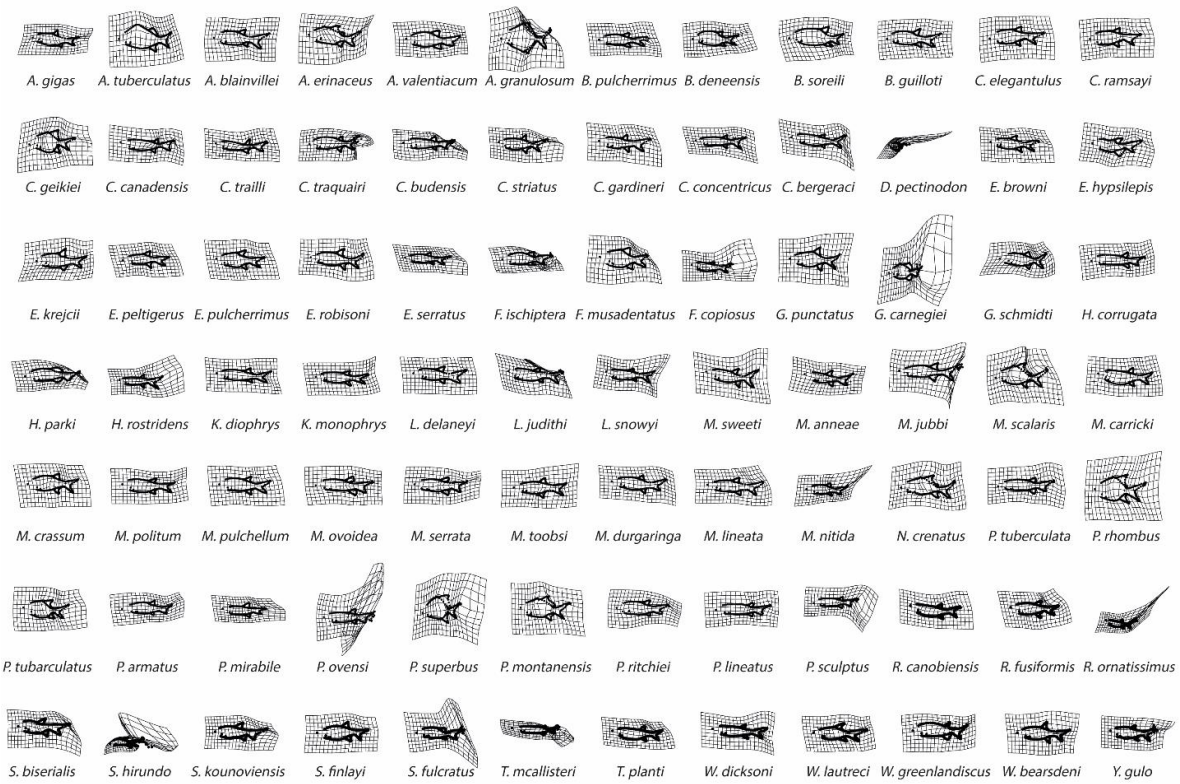


Figure S3. Deformation grids for each species compared to the mean body shape.

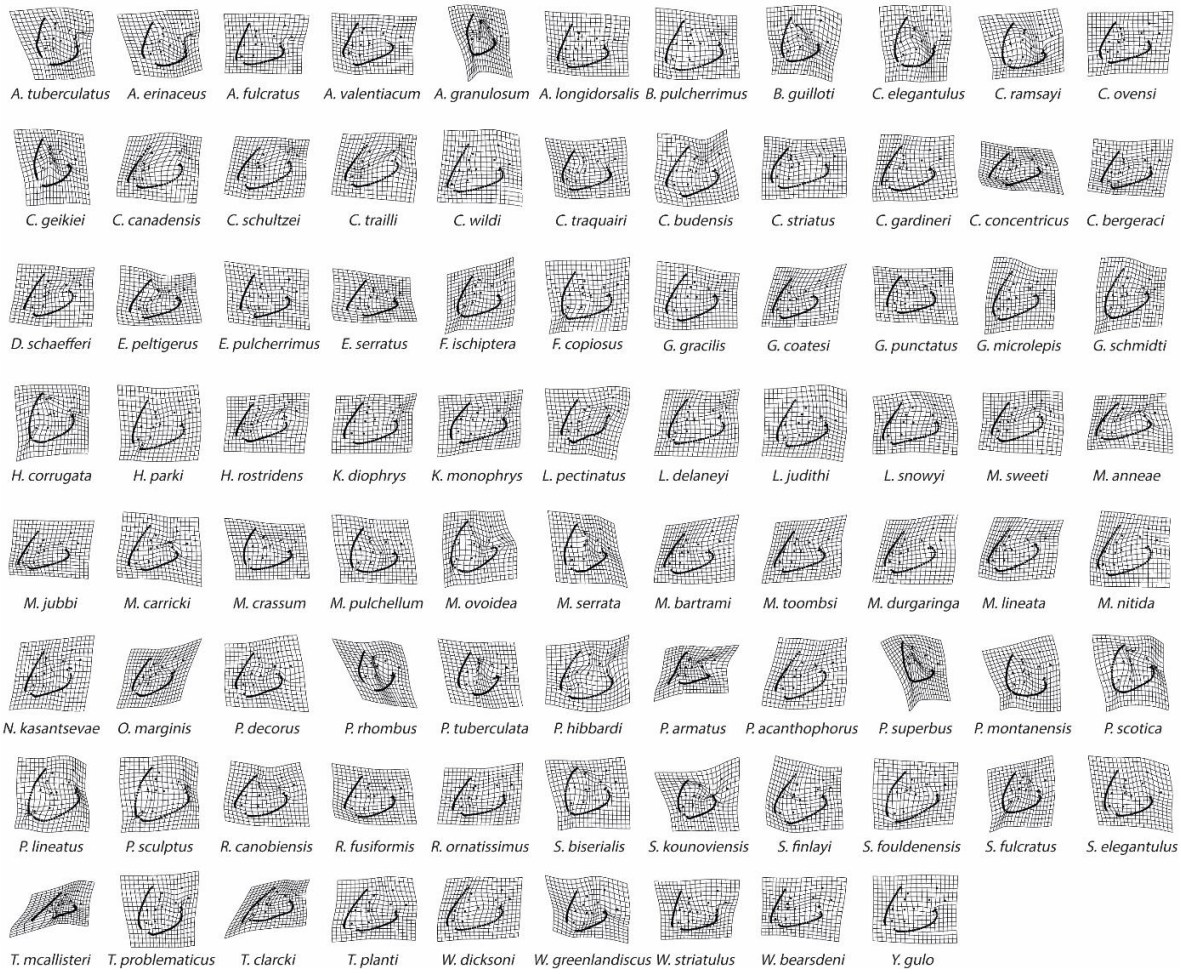


Figure S4. Deformation grids for each species compared to the mean skull shape.

Table S4. Convex hulls weighted surface area. Each surface area has been estimated for pairwise combination of the first five and first four PCs for the body and the skull, respectively, and weighted by the explained variance of each pair of axes. Two approaches have been used to calculate the weight of each pair of axes. The Simple Additive Weighting (SAW) estimates the weight of the pair of axes by calculating the average of the proportion of explained variance of each axis. The Weighted Sum of Pairwise Areas (WSPA) calculate the weight of each pair of axes by multiplying the proportion of variance explained by each. The N/A value corresponds to classes including two or less species, making the convex hull surface area estimation inapplicable.

	Class	Weighted surface area (SAW)		Weighted surface area (WSPA)		Number of species	
		Body shape	Lateral skull	Body shape	Lateral skull	Body shape	Lateral skull
Epoch	Middle Devonian	0.01064	0.00437	0.00149	0.00078	4	6
	Upper Devonian	0.01533	0.02979	0.00223	0.00479	7	12
	Mississippian	0.13236	0.11225	0.01686	0.01947	50	50
	Pennsylvanian	0.08361	0.06520	0.01237	0.01065	23	18
Stage	Eifelian	N/A	N/A	N/A	N/A	1	1
	Givetian	0.00225	0.00370	0.00025	0.00068	3	5
	Frasnian	0.00542	0.00557	0.00079	0.00090	4	7
	Famennian	0.00163	0.01997	0.00023	0.00326	3	5
	Tournaisian	0.02497	0.01429	0.00295	0.00251	7	10
	Viséan	0.08018	0.09629	0.01093	0.01662	24	24
	Serpukhovian	0.07328	0.03581	0.00963	0.00613	19	16
	Bashkirian	0.00247	0.00780	0.00029	0.00126	3	4
	Moscovian	0.05145	0.03228	0.00773	0.00558	12	9
	Kasimovian	0.00402	0.01138	0.00064	0.00164	3	3
	Gzhelian	0.01659	N/A	0.00209	N/A	5	2

Table S5. Morphological disparity analyses. The N/A values correspond to classes including only one species, making the variance estimation inapplicable.

Class		Procrustes variance		Proportion of total disparity (%)	
		Body shape	Lateral skull	Body shape	Lateral skull
Epoch	Middle Devonian	0.02017	0.00973	3.107	5.538
	Upper Devonian	0.02014	0.02068	5.330	12.537
	Mississippian	0.04327	0.03858	64.355	56.836
	Pennsylvanian	0.03809	0.04232	27.208	25.089
Stage	Eifelian	N/A	N/A	1.790	1.557
	Givetian	0.00819	0.00867**	1.317	3.981
	Frasnian	0.02037	0.01061**	3.718	6.604
	Famennian	0.00770	0.02996	1.612	5.933
	Tournaisian	0.03719	0.01778*	8.347	6.873
	Viséan	0.03927	0.04441	29.469	36.385
	Serpukhovian	0.04559	0.02750	26.539	13.578
	Bashkirian	0.01197	0.01694	2.239	2.532
	Moscovian	0.04139	0.03324	15.895	13.790
	Kasimovian	0.03644	0.06067	3.925	7.234
	Gzhelian	0.03023	0.01442	5.149	1.533

* difference statistically significant ($p < 0.05$) with the Viséan

** difference statistically significant ($p < 0.05$) with the Viséan and Kasimovian

References Annexe II :

Agassiz L. Recherches sur les poissons fossiles. 1833. Imprimerie de Petitpierre: Neuchatel: Switzerland. p890.

Arratia G. and Cloutier R. Reassessment of the morphology of *Cheirolepis canadensis* (Cheirolepididae: Actinopterygii). *In* Schultze H-P. and Cloutier R. (eds). Devonian Fishes and Plants of Miguasha, Quebec, Canada. 1996. Verlag Dr. Friedrich Pfeil: München, Germany. p165–97.

Arratia G. and Cloutier R. A new cheirolepidid fish from the Middle-Upper Devonian of Red Hill, Nevada, USA. *In* Arratia G., Wilson MVH. and Cloutier, R. (eds). Recent advances in the origin and early radiation of vertebrates. 2004. Verlag Dr. Friedrich Pfeil: München, Germany. p583–98.

Atthey T. XXXVIII.—On the articular bone and supposed vomerine teeth of *Ctenodus obliquus*; and on *Palæoniscus Hancocki*, n. sp., from the Low Main, Newsham, Northumberland. *Journal of Natural History*. 1875. 15(4):309–12.

Berg LS. Lower Carboniferous fish from the Achinsk region. *Voprosy Ikhtiol*. 1958. 11:142–53.

Blot J. Étude des palaeonisciformes du bassin houiller de Commentry (Allier, France). Cahiers de paléontologie: Paris. 1966. p99.

Brindley S. and Spinner E. Palynological assemblages from Lower Carboniferous deposits, Burntisland district, Fife, Scotland. *Proceedings of the Yorkshire Geological Society*. 1989. 47(3):215–31.

Casier EM. Contributions à l'étude des poissons fossiles de la Belgique. X. - Un Paléoniscoïde du Famennien inférieur de la Fagne: *Stereolepis marginis*, n. gen., n. sp. *Bulletin du Musée royal d'histoire naturelle de Belgique*. 1952. 28(47):1–17.

Choo B. Revision and description of the actinopterygian fishes of Devonian Eastern Gondwana. *Thesis.* Australian National University. 2010. Available from: http://hdl.handle.net/1885/150190

Choo B. Revision of the actinopterygian genus *Mimipiscis* (=*Mimia*) from the Upper Devonian Gogo Formation of Western Australia and the interrelationships of the early Actinopterygii. *Earth and Environmental Science Transactions of The Royal Society of Edinburgh*. 2012. 102(2):77–104.

Choo B. A new species of the Devonian actinopterygian *Moythomasia* from Bergisch Gladbach, Germany, and fresh observations on *M. durgaringa* from the Gogo Formation of Western Australia. *Journal of Vertebrate Paleontology*. 2015. 35(4):e952817.

Choo B, Long JA and Trinajstic K. A new genus and species of basal actinopterygian fish from the Upper Devonian Gogo Formation of Western Australia. *Acta Zoologica*. 2009. 90(1):194–210.

Choo B, Lu J, Giles S, Trinajstic K and Long JA. A new actinopterygian from the Late Devonian Gogo Formation, Western Australia. Papers in Palaeontology. 2019. 5(2):343–63.

Coates MI. Actinopterygians from the Namurian of Bearsden, Scotland, with comments on early actinopterygian neurocrania. *Zoological Journal of the Linnean Society*. 1998. 122:27–59.

Coates MI. New actinopterygian fish from the Namurian Manse Burn Formation of Bearsden, Scotland. *Palaeontology*. 1993. 36:123-146.

Coates MI. and Tietjen K. 'This strange little palaeoniscid': a new early actinopterygian genus, and commentary on pectoral fin conditions and function. *Earth and Environmental Science Transactions of The Royal Society of Edinburgh*. 2018. 109:15–31.

Daeschler EB. An early actinopterygian fish from the Catskill Formation (Late Devonian, Famennian) in Pennsylvania, U.S.A. *Proceedings of the Academy of Natural Sciences of Philadelphia*. 2000. 150:181–92.

Dawson JW. Lower Carboniferous fishes of New Brunswick. *Canadian Naturalist*. 1877. 2(8):337–40.

Dietze K. A revision of paramblypterid and amblypterid actinopterygians from Upper Carboniferous–Lower Permian lacustrine deposits of Central Europe. *Palaeontology*. 2000. 43(5):927–66.

Dineley DL. and Metclaf SJ. Fossil fishes of Great Britain. Geological Conservation Review Series, vol. 16. 1999. p.675

Dunkle DH. Preliminary description of a paleoniscid fish from the Upper Devonian Ohio Shale. *Scientific publications of the Cleveland Museum of Natural History*. 1964. 3(1):1–23.

Dyne MB. The skull of *Amphicentrum granulosum*. *Proceedings of the Zoological Society of London*. 1939. B109(2):195–210.

Egerton P. de MG. Palichthyologic notes No.3. On the Ganoidei Heterocerci. *Quarterly Journal of the Geological Society of London*. 1850. 6:1–10.

Elliott FM. A new haplolepid fauna (Osteichthyes: Actinopterygii) from the Lower Coal Measures of Scotland: Westphalian A; Langsettian, Carbonicola communis chronozone (Bashkirian). *Earth and Environmental Science Transactions of The Royal Society of Edinburgh*. 2014. 105(3):207–25.

Elliott FM. An early actinopterygian ichthyofauna from the Scottish Lower Coal Measures Formation: Westphalian A (Bashkirian). *Earth and Environmental Science Transactions of The Royal Society of Edinburgh*. 2018. 107(4):351–94.

Elliott FM. and Giles S. A new species of *Mesolepis* (Actinopterygii) from the Late Carboniferous of Scotland, with special reference to *Mesolepis wardi* Young. *Earth and Environmental Science Transactions of The Royal Society of Edinburgh*. 2024. 115(1–2):27–38.

Figueroa RT, Weinschütz LC. and Friedman M. The oldest Devonian circumpolar ray-finned fish? *Biology Letters*. 2021. 17(3):20200766.

Finlay TM, Woodward AS. and White EI. XII.—The Old Red Sandstone of Shetland. Part I. South-Eastern Area. With an account of the fossil fishes of the Old Red Sandstone of the Shetland Islands. *Earth and Environmental Science Transactions of The Royal Society of Edinburgh*. 1926. 54(3):553–72.

Forey PL. and Young VT. Acanthodian and coelacanth fish from the Dinantian of Foulden, Berwickshire, Scotland. *Earth and Environmental Science Transactions of The Royal Society of Edinburgh*. 1985. 76(1):53–9.

Frič A. Fauna der Gaskohle und der Kalksteine der Permformation Böhmens. 1889. Commission bei Fr. Rivnac: Prag. p318.

Friedman M. and Blom H. A new actinopterygian from the Famennian of East Greenland and the interrelationships of Devonian ray-finned fishes. *Journal of Paleontology*. 2006. 80(6):1186–204.

Friedman M, Pierce SE, Coates M. and Giles S. Feeding structures in the ray-finned fish *Eurynotus crenatus* (Actinopterygii: Eurynotiformes): implications for trophic diversification among Carboniferous actinopterygians. *Earth and Environmental Science Transactions of The Royal Society of Edinburgh*. 2018. 109(1–2):33–47.

Fritsch A. Über die Fauna der Gaskohle des Pilsner und Rakonitzer Beckens. *Sitzungsberichte der königl. böhmischen Gesellschaft der Wissenschaften*. 1875. 1875:70–9.

Gardiner BG. Certain palaeoniscoid fishes and the evolution of the snout in actinopterygians. *Bulletin of the British Museum (Natural History) Geology*. 1963. 8(6):237–325.

Gardiner BG. New palaeoniscoid fish from the Witteberg Series of South Africa. *Zoological Journal of the Linnean Society*. 1969. 48(4):423–52.

Gardiner BG. and Bartram AWH. The homologies of ventral cranial fissures in osteichthyans. *In* Andrews SM, Miles RS. and Walker AD. (eds). Problems in Vertebrate Evolution. 1977. Academic Press: London. p227–45.

Giebel C. Fauna der Vorwelt mit steter Berücksichtigung der lebenden Thiere. 1847. Leipzig: F.A. Brockhaus. p467.

Giles S, Darras L, Clément G, Blieck A. and Friedman M. An exceptionally preserved Late Devonian actinopterygian provides a new model for primitive cranial anatomy in ray-finned fishes. *Proceedings of the Royal Society B: Biological Sciences*. 2015. 282(1816):20151485.

Gill E. L. An undescribed fish from the Coal Measures of Lancashire. *Annals and Magazine of Natural History*. 1923. 11(9):465–71.

Goodarzi F, Haeri-Ardakani O, Gentzis T. and Pedersen PK. Organic petrology and geochemistry of Tournaisian-age Albert Formation oil shales, New Brunswick, Canada. *International Journal of Coal Geology*. 2019. 205:43–57.

Gottfried MD. A new long-snouted actinopterygian fish from the Pennsylvanian of north-central New Mexico. *New Mexico Journal of Science*. 1987. 27:7–19.

Gottfried MD. A subadult ‘palaeoniscoid’ (Actinopterygii, Osteichthyes) from the Upper Pennsylvanian of Kansas, U.S.A. *Pollichia-Buch*. 1993. 29:103–12.

Grogan ED. and Lund R. Two new Actinopterygii (Vertebrata, Osteichthyes) with cosmine from the Bear Gulch Limestone (Heath Fm., Serpukhovian, Mississippian) of Montana USA. *Academy of Natural Sciences*. 2015. 164(1):111–32.

Gross W. Devonische Palaeonisciden-Reste in Mittel-und Osteuropa. *Paläontologische Zeitschrift*. 1953. 27(1):85–112.

Hay OP. Descriptions of some vertebrates of the Carboniferous age. *Proceedings of the American Philosophical Society*. 1900. 39:96–123.

Heyler D. Quelques points nouveaux au sujet d’*Aeduella* Westoll. *Colloque International Centre National de la Recherche Scientifique*. 1967. 94:81–8.

Heyler D. and Poplin C. Les poissons stéphaniens du Bassin de Montceau-les-Mines. *In* Poplin C. and Heyler D. (eds). Quand le Massif central était sous l’équateur, un écosystème carbonifère à Montceau-les-Mines. 1994. CTHS : Paris. p328.

Heyler D. and Poplin C. Actinoptérygiens du Stéphanien de Montceau-les-Mines (Saône-et-Loire, France). *Palaeovertebrata*. 1983. 13(3):33–50.

Heyler D. À propos de quelques Vertébrés fossiles de l’Autunien (?) de Decazeville - L’Eduen. *Bulletin de la Société d'Histoire Naturelle d'Autun*. 1964. 31:6–14.

Heyler D. Vertébrés de l’Autunien de France - CNRS Éditions. Cahiers de paléontologie: Paris. 1969. p155.

Hibbert S. On the fossil fishes of the limestone of Burdiehouse. *Edinburgh New Philosophical Journal*. 1835. 18:383–4.

Holland T, Long J, Warren A. and Garvey J. Second specimen of the lower actinopterygian *Novogonatodus kasantsevae* Long 1988 from the Early Carboniferous of Mansfield, Victoria. *Proceedings of the Royal Society of Victoria*. 2004. 118:1–10.

Huber P. *Pyritocephalus lowneyae* n. sp., the youngest haplolepiform (Pisces: Actinopterygii) from the Pennsylvanian of central New Mexico. *New Mexico Bureau of Mines Bulletin*. 1992. p138.

Jubb RA. A new palaeoniscoid fish from the Witteberg series (Lower Carboniferous) of South Africa. *Annals of the South African Museum*. 1965. 48:267–72.

Kazantseva AA. Palaeoniscids of Bystraia Formation of the Minusinsk troughs. *In* Obruchev DV. (ed). Ocherki po filogenii I sistematike iskopaemykh ryb I bezcheliustnykh. Nauka Press: Moscow. 1968. p87–112.

Lambe LM. Palaeoniscid fishes from the Albert Shales of New Brunswick. *Geological Survey of Canada*. 1910. 3(5):7–35.

Lu LW. A new Namurian palaeoniscoid fish from Zhongwei, Ningxia. *Vertebrata Palasiatica*. 2023. 40(01):1.

Long JA. New palaeoniscoid fishes from the Late Devonian and Early Carboniferous of Victoria. *Australasian Palaeontological Memoirs*. 1988. (7):1–64.

Long J. New Palaeoniscoid fishes from the Late Devonian - Early Carboniferous of Victoria, Australia. *Memoirs of the Australasain Association of Palaeontologists*. 1988. 7:1–64.

Long JA, Choo B. and Young GC. A new basal actinopterygian fish from the Middle Devonian Aztec Siltstone of Antarctica. *Antarctic Science*. 2008. 20(4):393–412.

Lowney KA. A Revision of the Family Haplolepidae (Actinopterygii, Paleonisciformes) from Linton, Ohio (Westphalian D, Pennsylvanian). *Journal of Paleontology*. 1980. 54(5):942–53.

Lowney KA. The earliest known (Namurian A, E1) haplolepids (Osteichthyes: Actinopterygii). *Earth and Environmental Science Transactions of The Royal Society of Edinburgh*. 1983. 74(2):69–78.

Lowney KA. Certain Bear Gulch (Namurian A, Montana) actinopterygii (Osteichthyes) and a reevaluation of the evolution of the Paleozoic actinopterygians. *Thesis.* New York University. 1980. Available from: https://www.proquest.com/docview/303023402/abstract/88D69D8C504345ECPQ/1

Lucas S, Allen B, Krainer K, Barrick J, Vachard D, Schneider J, et al. Precise age and biostratigraphic significance of the Kinney Brick Quarry Lagerstätte, Pennsylvanian of New Mexico, USA. *Stratigraphy*. 2011. 8:7–27.

Lund R. and Melton WG. A new actinopterygian fish from the Mississipian Bear Gulch Limestone of Montana. *Palaeontology*. 1982. 25:485–98.

Lund R. The new Actinopterygian order Guildayichthyiformes from the Lower Carboniferous of Montana (USA). *Geodiversitas*. 2000. 22(2):171-206.

Lund R, Grogan ED. and Jacob A. *Apholidotus*, a highly specialized new actinopterygian from the Bear Gulch Limestone (Heath Formation, Serpukhovian, Upper Mississippian) of Montana, USA. *Annals of Carnegie Museum*. 2025. 91(1):39–54.

Lund R. and Poplin C. The Rhadinichthyids (paleoniscoid actinopterygians) from the Bear Gulch Limestone of Montana (USA, Lower Carboniferous). *Journal of Vertebrate Paleontology*. 1997. 17(3):466–86.

Lund R. and Poplin C. Cladistic analysis of the relationships of the tarrasiids (Lower Carboniferous actinopterygians). *Journal of Vertebrate Paleontology*. 2002. 22(3):480–6.

Matveeva AA. Palaeoniscids from the Izyk-chul' Horizon of the Minusinsk Depression. *Voprosy Ikhtiologiy*. 1958. 154–61.

Mickle KE. The lower actinopterygian fauna from the Lower Carboniferous Albert Shale Formation of New Brunswick, Canada: a review of previously described taxa and a description of a new genus and species. *Fossil Record*. 2017. 20(1):47–67.

Mickle KE. A new lower actinopterygian fish from the Upper Mississippian Bluefield Formation of West Virginia, USA. PeerJ. 2018. 6:e5533.

Mickle KE, Lund R. and Grogan ED. Three new palaeoniscoid fishes from the Bear Gulch Limestone (Serpukhovian, Mississippian) of Montana (USA) and the relationships of lower actinopterygians. *Geodiversitas*. 2009. 31(3):623–68.

Miller SA. North American geology for the use of amateurs, students, and scientists. 1892. Cincinnati, OH: Western Methodist Book Concern. p718.

Mosseichik Y. and Филимонов A. A new interpretation of *Cyclostigma*-like lepidophytes from the Lower Tournaisian of the Minusinsk Basin (Southern Siberia). *Lethaea rossica*. 2020. 20:1–18.

Mottequin B, Poty E. and Prestianni C. Catalogue of the types and illustrated specimens recovered from the 'black marble' of Denée, a marine conservation-Lagerstätte from the Mississippian of southern Belgium. *Geologica Belgica*. 2015. 18(1):1–14.

Moy-Thomas J. M. LXI.—Carboniferous Palæoniscids from East Greenland. *Journal of Natural History*. 1942. 9(11):737–59.

Moy-Thomas JA. and Dyne MB. XVII.—The Actinopterygian Fishes from the Lower Carboniferous of Glencartholm, Eskdale, Dumfriesshire. *Earth and Environmental Science Transactions of The Royal Society of Edinburgh*. 1938. 59(2):437–80.

Moy-Thomas JA. and Dyne MB. XVII.—The Actinopterygian Fishes from the Lower Carboniferous of Glencartholm, Eskdale, Dumfriesshire. *Earth and Environmental Science Transactions of The Royal Society of Edinburgh*. 1938. 59(2):437–80.

Moy-Thomas J. and Dyne M. XVII.—The actinopterygian fishes from the Lower Carboniferous of Glencartholm, Eskdale, Dumfriesshire. *Transactions of the Royal Society of Edinburgh*. 2012. 59:437–80.

Newberry JS. and Worthen AH. Geology and Palaeontology. Descriptions of fossil vertebrates. *Geological Survey of Illinois*. 1870. 4:343–74.

Newman M, Burrow C, den Blaauwen J. and Giles S. A new actinopterygian *Cheirolepis jonesi* nov. sp. from the Givetian of Spitsbergen, Svalbard. *Norwegian Journal of Geology*. 2021. 101(202103).

Pearson DM. and Westoll TS. The Devonian actinopterygian *Cheirolepis* Agassiz. *Earth and Environmental Science Transactions of The Royal Society of Edinburgh*. 1979. 70(13–14):337–99.

Plax D. A new species of the actinopterygian fish (Osteichthyes, Actinopterygii) from the Eifelian deposits of the Vileyka Buried Ridge (Belarus). *Lithosphere*. 2020. 1(52):68–74.

Poplin C. Étude de quelques Paléoniscidés pennsylvaniens du Kansas. Cahiers de paléontologie: Paris. 1974. p151.

Poplin C. Le genre *Bourbonella* (Actinopterygii, Aeduellidae): révision et description d'une nouvelle espèce du Stéphanien (Carbonifère supérieur) de Montceau-les-Mines (Massif Central, France). *Annales de Paléontologie*. 2001. 87(4):231–48.

Poplin CM. and Lund R. Two Carboniferous fine-eyed palaeoniscoids (Pisces, Actinopterygii) from Bear Gulch (USA). *Journal of Paleontology*. 2002. 76(6):1014–28.

Poplin C. and Véran M. A revision of the actinopterygian fish *Coccocephalus wildi* from the Upper Carboniferous of Lancashire. *Special Papers in Palaeontology*. 1996. 52:7–29.

Poplin C, Dutheil D. Les Aeduellidae (Pisces, Actinopterygii) carbonifères et permiens: systématique et étude phylogénétique préliminaire. *Geodiversitas*. 2005. 27:17–33.

Poplin C. and Lund R. Two new deep-bodied palaeoniscoid actinopterygians from Bear Gulch (Montana, USA, Lower Carboniferous). *Journal of Vertebrate Paleontology*. 2000. 20(3):428–49.

Prokofiev AM. First finding of an articulated actinopterygian skeleton from the Upper Devonian of Siberia and a reappraisal of the family Moythomasiidae Kazantseva, 1971 (Osteichthyes). *Paleontological Research*. 2002. 6(3):321–7.

Prokofiev AM. A remarkable new paleoniscoid fish (Osteichthyes: Actinopterygii) from the Lower Carboniferous of Tuva Republic (Russia). *Paleontological Research*. 2004. 8(2):109–14.

Prokop J. and Dong R. New significant fossil insects from the Upper Carboniferous of Ningxia in northern China (Palaeodictyoptera, Archaeorthoptera). *European Journal of Entomology*. 2007. 104(2):267-275.

Pruvost P. Comparaison entre le terrain houiller du Nord de la France et celui de Grande-Bretagne d'après la succession des faunes. *Comptes rendus de l'Académie des Sciences Paris*. 1919. 168:782–5.

Rayner DH. III.—On the Cranial Structure of an Early Palæoniscid, *Kentuckia*, gen. nov. *Earth and Environmental Science Transactions of The Royal Society of Edinburgh*. 1952. 62(1):53–83.

Rohon JV. Die Dendrodonten des devonischen Systems in Russland: paläontologische und vergleichend-anatomische Studie. 1889. Académie des sciences: St-Pétersbourg. p60.

Sallan LC. and Coates MI. Styracopterid (Actinopterygii) ontogeny and the multiple origins of post-Hangenberg deep-bodied fishes. *Zoological Journal of the Linnean Society*. 2013. 169(1):156–99.

Sauvage HE. Poissons du terrain houiller de Commentry. *In* Renault B. and Zeiller R. (eds). Études sur le terrain houiller de Commentry, Livre III : Faunes ichthyologique et entomologique. 1888. Imprimerie Théolier & Cie: Saint-Étienne. p. 39–120.

Schindler TG. Eine weitere Strahlenflosser-Art aus dem Saar-Nahe-Becken: *Meisenheimichthys glanensis* n.sp. (Osteichthyes): Actinopterygii; Permokarbon, SW-Deutschland. *Mitteilungen der Pollichia*. 2006. 92(166):1-4.

Schultze HP. and Bardack D. Diversity and size changes in palaeonisciform fishes (Actinopterygii, Pisces) from the Pennsylvanian Mazon Creek fauna, Illinois, U.S.A. *Journal of Vertebrate Paleontology*. 1987. 7(1):1–23.

Schultze HP, Mickle KE, Poplin C, Hilton EJ. and Grande L. Handbook of Paleoichthyology: Actinopterygii I Vol. 8A. 2021. Verlag Dr. Friedrich Pfeil: Münschen, Germany. p299.

Selezneva AA. A platysomid from the Doets Basin. *Paleontologicheskii Zhurnal*. 1988. 1988(1):117–20.

Stack J, Hodnett JP, Lucas S. and Sallan L. *Tanyrhinichthys mcallisteri*, a long-rostrumed Pennsylvanian ray-finned fish (Actinopterygii) and the simultaneous appearance of novel ecomorphologies in Late Palaeozoic fishes. *Zoological Journal of the Linnean Society*. 2020. 191(2):1–28.

Stamberg S. Actinopterygians of the Central Bohemian Carboniferous Basin. *Acta Musei Nationalis Pragae Series B Historia Naturalis*. 1991. 47:25–102.

Stamberg S. and Zajic J. *Setlikia bohemica* gen. et sp. nov., a new actinopterygian flsh (Actinopterygii, Igornichthyidae) from the Late Carboniferous of Bohemia. *Vestnik Ceskeho geologickeho ustavu*. 1994. 69(3):53–58.

Stamberg S. Scales and their utilisation for the determination of actinipterygian fishes (Actinopterygii) from Carboniferous basins of central Bohemia. *Casopis pro Mineralogii a Geologii*. 1989. 34(3):255–269.

Stamberg S. Carboniferous–Permian actinopterygian fishes of the continental basins of the Bohemian Massif, Czech Republic: an overview. *In* Lucas SG, Cassinis G. and Schneider JW. (eds). Non-Marine Permian Biostratigraphy and Biochronology. 2006. Geological Society of London. 265(1):1-14.

Swartz BA. Devonian actinopterygian phylogeny and evolution based on a redescription of *Stegotrachelus finlayi*. *Zoological Journal of the Linnean Society*. 2009. 156(4):750–784.

Tan K, Wang X. and Lu LW. A new Carboniferous platysomoid fish from Ningxia, Northwest China. *Acta Palaeotologica Sinica*. 2015. 54(2):174–183.

Taverne L. *Osorioichthys marginis*, 'Paléonisciforme' famennien de Belgique, et la phylogénie des actinoptéygiens dévoniens (Pisces). *Bulletin de l'Institut Royal des Sciences Naturelles de Belgique*. 1997. 67:57–78.

Traquair RH. XXXIV.—On some fossil fishes from the neighbourhood of Edinburgh. *Annals and Magazine of Natural History*. 1875. 15(4):258–68.

Traquair RH. XXXVI.—On the structure of *Amphicentrum granulosum*, Huxley. *Journal of Natural History*. 1875. 273–81.

Traquair RH. Faune du Calcaire Carbonifère de la Belgique. - Pt I. Poissons et genre *Nautilus*. *Annales du Musée Royal d'Histoire Naturelle de Belgique*. 1877. 2:1–152.

Traquair RH. Notice new fish remains from the Blackband Ironstone of Borough Lee near Edinburgh. *Geological Magazine*. 1881. 8(2):34–7.

Traquair RH. New Palaeoniscidae from the English Coal-Measures. *Geological Magazine*. 1888. 5(3):251–4.

Traquair RH. List of the fossil Dipnoi and Ganoidei of Fife and the Lothians. *Proceedings of the Royal Society of Edinburgh*. 1890. 17:385–400.

Traquair RH. Fossil fishes from the Carboniferous of Gullane, Haddingtonshire. *Summary of Progress of the Geological Survey of Great Britain*. 1904. 1903:121–3.

Traquair RH. The ganoid fishes of the British Carboniferous Formations, Pt. I, No. 5: Palaeoniscidae. *Monograph of the Palaeontographical Society*. 1911. 64:123–58.

Traquair RH. III.—Report on fossil fishes collected by the Geological Survey of Scotland in Eskdale and Liddesdale. Part I.—Ganoidei. *Earth and Environmental Science Transactions of The Royal Society of Edinburgh*. 1881. 30(1):15–71.

Traquair RH. The Ganoid Fishes of the British Carboniferous Formations. Part I. Palæoniscidæ. No. 3. Pages 87–106; Plates XIX–XXIII. *Monograph of the Palaeontographical Society*. 1907. 61(290):87–106.

Waterlot G. Bassin houiller de la Sarre et de la Lorraine Vol 2: Faune fossile. Lille. 1934. p317.

Watson DMS. The structure of certain palaeoniscoids and the relationships of that group with other bony fish. *Proceedings of the Zoological Society of London*. 1925. 1925:815–70.

Watson DMS. On some points in the structure of palaeoniscid and allied fish. *Proceedings of the Zoological Society of London*. 1928. 98(1):49-70.

Weems RE. and Windolph JFJ. A new actinopterygian fish (Paleonisciformes) from the Upper Mississippian Bluestone Formation of West Virginia. *Proceedings of the Biological Society of Washington*. 1986. 99(4):584–601.

Westoll TS. The Haplolepidae, a new family of late Carboniferous bony fishes: a study in taxonomy and evolution. 1944. *Bulletin of the AMNH*. 83: p138.

Westoll TS. LVII.—On a remarkable fish from the Lower Permian of Autun, France. *Annals and Magazine of Natural History*. 1937. 19(114):553–77.

White EI. A new type of palaoniscoid fish: 3. A new type of Palaeoniscoid fish, with remarks on the evolution of the actinopterygian pectoral fins. *Proceedings of the Zoological Society of London*. 1939. 109(1):41–61.

Whiteaves JF. On some remarkable fossil fishes from the Devonian Rocks of Scaumenac Bay, P. Q., with description of a new genus and three new species. *Canadian Naturalist*. 1881. 10:27–35.

Wilson CD, Pardo JD. and Anderson JS. A primitive actinopterygian braincase from the Tournaisian of Nova Scotia. *Royal Society Open Science*. 2018. 5(5):171727.

Wood SP. New basal Namurian (Upper Carboniferous) fishes and crustaceans found near Glasgow. *Nature*. 1982. 297(5867):574–7.

Woodward AS. Palaeoichthyological Notes. *Annals and Magazine of Natural History*. 1893. 11(6):281–7.

Young J. On the affinities of *Platysomus* and allied genera. *Quarterly journal of the Geological Society of London*. 1866. 22:301–17.

Young J. Collected papers. 1866. p56.

Zidek J. Late Pennsylvanian Chondrichthyes, Acanthodii, and deep-bodied Actinopterygii from the Kinney Quarry, Manzanita Mountains, New Mexico. *New Mexico Bureau of Mines and Mineral Resources Bulletin*. 1992. 138:145–182.

ANNEXE III

SUPPLEMENTARY INFORMATION FOR CHAPTER 2: EARLY SARCOPTERYGIAN MORPHOLOGICAL DISPARITY THROUGH THE DEVONIAN-CARBONIFEROUS CRISIS

Table S1. List of the 279 basal sarcopterygian species included in diversity analyses. FAD (first appearance datum) corresponds to the first time the species appears in the fossil record, and LAD (last appearance datum) to the last time it appears.

Species	Age	Formation/ Country	References	FAD	LAD
SILURIAN					
Guiyu oneiros	Ludfordian	Kuanti Formation, Qujing, Yunnan, China	Zhu *et al.* 2009	425.6	423
DEVONIAN					
LOWER DEVONIAN					
Diabolepis speratus	Lochkovian	Qujing, Yunnan, China	Chang & Yu 1984	413.6	409.73
Dipnorhynchus sussmilchi	Emsian	Taemas-Wee Jasper/Burrinjuck limestones of New South Wales, Australia	Clement *et al*. 2016; Etheridge 1906	407.6	393.3
Durialepis edentates	Emsian	Klerf Formation, Westphalia, Germany	Mondéjar-Fernández *et al*. 2021; Otto 2007	407.6	402.83
Euporosteus yunnanensis	Pragian	Posongchong Formation, Zhaotong, Yunnan Province, China	Zhu *et al*. 2012; Lu *et al*. 2012	408.66	407.6
Eoactinistia foreyi	Pragian	Fairy Formation, Buchan, Victoria, Australia	Johanson *et al*. 2006; Johanson *et al*. 2006	409.73	407.6
Heimenia ensis	Emsian	Verdalen Member, Wood bay Formation, Spitsbergen, Norway	Mondéjar-Fernández & Clément 2012; Ørvig 1969	407.6	402.83
Heimenia sp.	Emsian	Podlazie, Holy Cross Mountians, Poland	Wilk 2023; Wilk *et al.* 2022	402.83	393.3
Nasogaluakus chorni	Emsian	Bear Rock Formation, Anderson River, Northwest Territories, Canada	Schultze 2000	407.6	393.3
Porolepis brevis	Pragian	Spitsbergen, Norway	Mondéjar-Fernández *et al*. 2021; Jarvik 1937	410.8	407.6

Porolepis elongata	Pragian	Woodbay Formation, Spitsbergen, Norway	Jarvik 1942, 1972; Clément 2002	410.8	409.73
Porolepis foxi	Pragian	Mulga Downs Group, New South Wales, Australia	Johanson *et al*. 2013	408.67	387.7
Porolepis hefteri	Pragian	Siegen Formation, Rhenisch Massif, Germany	Gross 1935; Clément 2002	408.7	407.6
Porolepis kureikensis	Lochkovian	Kureika and Razvedochnaya Formation, Tareya river, Siberia, Russia	Vorobyeva 1963; Clément 2022	419.2	410.8
Porolepis siegenensis	Pragian	Siegen Formation, Rhenisch Massif, Germany	Gross 1936; Clément 2002	408.7	407.6
Porolepis spitsbergensis	Pragian	Woodbay Formation, Spitsbergen, Norway	Jarvik 1942, 1972; Clément 2002	410.8	409.73
Porolepis taimyrica	Lochkovian	Kureika and Razvedochnaya Formation, Tareya river, Siberia, Russia	Vorobyeva 1963; Clément 2022	419.2	410.8
Porolepis sp.	Emsian	Placoderm sandstone, Podlazie, Holy Cross Mountians, Poland	Wilk 2023	402.83	393.3
Styloichthys changae	Lochkovian	Xitun Formation, Qujing, East Yunnan, China	Zhu & Yu 2002; Friedman 2007; Zhao & Zhu 2010	413.6	410.8
Tungsenia paradoxa	Pragian	Posongchong Formation, Zhaotong, Yunnan Province, China	Lu *et al*. 2012	410.8	407.6
		MIDDLE DEVONIAN			
Aztecia mahalae	Givetian	Aztec Siltstone, Antarctica	Sallan & Coates 2010; Johanson & Ahlberg 2001	386.03	384.36
Bruehnopteron murphyi	Givetian	Red Hill, Northern Simpson Park Range, Nevada, USA	Schultze & Reed 2012	384.36	382.7
Cheirodipterus onawayensis	Givetian	Onaway Stone Quarry, Presque Isle County; Michigan, USA	Sallan & Coates 2010; Schultze 1982	386.03	384.36
Conchodus elkneri	Givetian	Gerolstein, Germany; Zone II, Wietrznia, Kadzielnia, Holy Cross Mountains, Poland	Sallan & Coates 2010; Gorisdro-Kulczyska 1950	387.7	363.33
Dictyonosteus arcticus	Givetian	West Spitzbergen, Norway	Forey 1998; Stensiö 1918	387.7	382.7

Diplocercides heiligenstockiensis	Givetian	Bergisch-Gladbach, Nordrhein-Westfalen, Germany	Jessen 1966; Schultze & Cloutier 1996	384.36	379.2
Dipterus calvani	Givetian	Cedar Valley Limestone, Milwaukee Formation, Iowa	Sallan & Coates 2010; Eastman 1900	384.36	375.7
Dipterus uddeni	Givetian	Cedar Valley Limestone, Milwaukee Formation, Iowa, USA	Sallan & Coates 2010; Eastman 1900	384.36	375.7
Dipterus valenciennesi	Eifelian	Achanarras fish beds, Caithness flagstone, Orcadian Basin, Scotland	Ahlberg & Trewin 1995 ; Challands 2015 ; Dineley & Metcalf 1999 (p171); Sedgwick & Murchison 1829	389.56	387.7
Eoctenodus sp.	Givetian	Aztec Siltstone, Antarctica	Sallan & Coates 2010; Hills 1929	386.03	384.36
Euporosteus eifeliensis	Givetian	Gerolstein, Germany	Gross 1950; Schultze & Cloutier 1996; Jaekel 1927	384.36	382.7
Glyptolepis baltica	Givetian	Amata Regional Stage, Luga river bassin, Leningrad Region, Russia; Gauja Regional Stage, Lode Quarry, Latvia	Gross 1936	384.36	379.2
Glyptolepis groenlandica	Eifelian	Canning Land, Vilddal Group, East Greenland	Jarvik 1972	389.56	386.03
Glyptolepis leptopterus	Eifelian	Lethen Bar and Tynet Burn, Nairn, Old Red Sandstone, Scotland	Agassiz 1844 ; Newman 2010 ; Dineley & Metcalf 1999 (p171)	389.56	387.7
Glyptolepis ?nessovi	Givetian	Aruküla Regional Stage, Luga river bassin, Leningrad Region, Russia		387.7	386.03
Glyptolepis paucidens	Givetian	Orcadian Basin, Scotland	Agassiz 1844	387.7	386.03
Glyptolepis quadrata	Eifelian	Narova Regional Stage, Luga river bassin, Leningrad Region, Russia	von Eichwald 1844; Ivanov & Lebedev 2011	393.3	387.7

Glyptolepis sp.	Eifelian	Narova Regional Stage, Luga river bassin, Leningrad Region, Russia	Ivanov & Lebedev 2012; Agassiz 1843	393.3	387.7
Glyptolepis sp.	Givetian	Aruküla Regional Stage, Luga river bassin, Leningrad Region, Russia	Ivanov & Lebedev 2012; Agassiz 1843	387.7	386.03
Griphognathus minutidens	Givetian	Lode Formation, Gauja, Latvia	Sallan & Coates 2010; Gross 1956	384.36	382.7
Griphognathus sculpta	Givetian	Upper Plattenkalk, Heiligenstock quarry, Bergisch-Gladbach, Germany	Friedman 2007; Schultze 1969	384.36	379.2
Grossipterus crassus	Givetian	Lode Formation, Gauja, Latvia	Sallan & Coates 2010; Gross 1933	384.36	382.7
Gyroptychius agassizi	Eifelian	Orcadian Basin, Scotland	Newman & Dean 2010 ; Dineley & Metcalf 1999 (p171); Traill 1841	389.56	387.7
Gyroptychius milleri	Eifelian	Caithness, Orcadian Basin, Scotland; Aruküla Formation, Estonia	Sallan & Coates 2010; Jarvik 1948	389.56	386.03
Hamodus lutkevitshi	Givetian	Karski outcrop, Harma substage, Estonia	Obruchev 1933	387.7	382.7
Holoptychius sp.	Givetian	Aruküla Regional Stage, Luga river bassin, Leningrad Region, Russia	Ivanov & Lebedev 2011; Agassiz 1839	387.7	386.03
Iowadipterus halli	Givetian	Cedar Valley Limestone, Milwaukee Formation, Iowa	Sallan & Coates 2010; Schultze 1992	384.36	375.7
Jemalongia ritchiei	Givetian	Hervey Group, Cloghnan Shale Formation, Jemalong Weir, Forbes, New South Wales, Australia	Young 2024	387.7	372.2
Kenichthys campbelli	Eifelian	Chuandong Fonnalion of Qujing, Yunnan, China	Chang & Zhu 1993	389.56	386.03
Koharalepis jarviki	Givetian	Mount Crean, Lashly Range, Antarctica	Young *et al*. 1992; Cloutier *et al*. 2020 (supp.)	386.03	384.36
Laccognathus grossi	Givetian	Gauja Formation, Latvia	Vorobyeva 2006	384.36	382.7

Laccognathus panderi	Givetian	Lode, Gauja Formation, Latvia	Vorobyeva 2006; Gross 1941	384.36	382.7
Latvius deckerti	Givetian	Upper Plattenkalk, Heiligenstock quarry, Bergisch-Gladbach near Cologne, Nordrhein-Westfalen (North Rhine-Westphalia), Germany	Jessen 1966	384.36	379.2
Latvius niger	Givetian	Bergish Gladbach, Oberer Plattenkalk, Germany	Sallan & Coates 2010; Jessen 1973	384.36	379.2
Livoniana multidentata	Givetian	Lode Formation, Gauja, Latvia	Sallan & Coates 2010; Ahlberg *et al*. 2000	384.36	382.7
Mahalalepis resima	Givetian	Aztec Siltstone, Antarctica	Sallan & Coates 2010; Young *et al*. 1992	387.7	382.7
Miguashaia grossi	Givetian	Gauja and Lode Formations, Latvia	Forey *et al*. 2000	384.36	382.7
Notorhizodon mackelveyi	Givetian	Mount Ritchie, Mount Crean, Mount Metschel, Mount Warren, Aztec Siltstone, Antarctica	Sallan & Coates 2010	387.7	382.7
Onychodus hopkinsi	Eifelian	Delaware Limestone, Ohio, USA	Newberry 1857	393.3	387.7
Onychodus sigmoides	Eifelian	Cedar Valley Limestone, Milwaukee Formation, Iowa, USA	Sallan & Coates 2010; Newberry 1857	393.3	387.7
Osteolepis macrolepidotus	Eifelian	Sandwick Fish Bed, Cruday Quarry, Orkney Mainland	Newman 2005; Agassiz 1835	389.56	387.7
Osteolepis panderi	Givetian	Spital Flagstone Formation, Upper Flagstone Group of the Middle Old Red Sandstone, Caithness	Hamilton & Trewin 1994 ; Dineley & Metcalf 1999 (p171); Pander 1860	387.7	386.03
Palaeospondylus gunni	Eifelian	Sandwick fish bed in Orkney, Orcadian basin, Scotland; Achanarras Quarry, Caithness, Scotland	Sallan & Coates 2010; Newman & den Blaauwen 2010; Traquair 1890	389.56	387.7
Panderichthys rhombolepis	Givetian	Lode Formation, Estonia	Boisvert *et al*. 2008 (supp.) ; Cloutier *et al*. 2020 (supp.); Gross 1930	384.36	382.7

Paraglyptolepis karksiensis	Givetian	Burnietki Regional Stage, Karksi, Estonia	Vorobyeva 1987	387.7	382.7
Pentlandia macroptera	Givetian	Last House Formation, John O'Groats Sandstone, Caithness, Scotland	Challands & den Blaauwen 2017; Traquair 1888	387.3	384.99
Pinnalongus saxoni	Eifelian	Brim Ness near Thurso, Caithness, Scotland	Newman & den Blaauwen 2007	391.43	389.56
Platyethmoidea antarctica	Givetian	Mount Ritchie and Mount Crean, Lashly Range, Aztec Siltstone, Antarctica	Sallan & Coates 2010; Young *et al*. 1992	386.03	384.36
Rhinodipterus secans	Givetian	Lode Formation, Gauja, Latvia	Sallan & Coates 2010; Gross 1956	384.36	382.7
Rhinodipterus sp.	Eifelian	Gerolstein, Germany	Sallan & Coates 2010; Gross 1956	389.56	386.03
Rhinodipterus ulrichi	Givetian	Upper Plattenkalk, Heiligenstock quarry, Bergisch-Gladbach, Germany	Friedman 2007; Schultze 1969	384.36	379.2
Shoshonia arctopteryx	Givetian	Beartooth Butte, Jefferson Formation, Wyoming, USA	Friedman *et al*. 2007	387.7	372.2
Straitonia sp.	Givetian	Cedar Valley Limestone, Milwaukee Formation, Iowa	Sallan & Coates 2010; Thomson 1966	384.36	375.7
Strunius walteri	Givetian	Upper Plattenkalk, Heiligenstock quarry, Bergisch-Gladbach near Cologne, Nordrhein-Westfalen (North Rhine-Westphalia), Germany	Upeniece 1995 ; Jessen dans Moy-Thomas 1971; Schultze & Cloutier 1996; Jessen 1966	384.36	379.2
Trackway 1	Eifelian	Greenland	Ahlberg 2024	393.3	391.43
Trackway 2	Givetian	Valentia Island, Ireland	Stössel 1995	387.7	382.7
Thursius macrolepidotus	Eifelian	Lybster Flagstone Formation, Westerdale Quarry, Orcadian Basin, Scotland	Newman & den Blaauwen 2007; Sedgwick & Murchison 1829	393.3	389.56
Thursius pholidotus	Eifelian	Orcadian Basin, Scotland	Traquair 1888	393.3	389.56
Tinirau clackae	Givetian	USA, Nevada, Simpson Park Mountains north of the Denay Valley,	Swartz 2012	384.36	382.7

		UCMP locality V74084			
Tristichopterus alatus	Givetian	Eday Flagstone/John O' Groats Sandstone Group of South Ronaldsay, Orkney	Newman 2005 ; Egerton 1861	386.03	384.36
Vorobjevaia dolonodon	Givetian	Mount Crean, Lashly Range, Antarctica	Young *et al*. 1992	386.03	384.36
		UPPER DEVONIAN			
Acanthostega gunarri	Famennian	Britta Dal Formation, Gauss Halvø, East Greenland	Coates 1996; Clack *et al*. 2012; Jarvik 1952	363.33	358.9
Adelargo schultzei	Famennian	Hunter Siltstone, Hervey Group, Grenfell, New South Wales, Australia	Sallan & Coates 2010; Johanson & Ritchie 2000; Young 1999	363.33	358.9
Andreyevichthys epitomus	Famennian	Andreyevka-2, Khovanshshina Beds, Zovalzkh Formation, Tula, Siberia, Russia	Sallan & Coates 2010; Lebedev *et al*. 2018; Krupina 1987	363.33	358.9
Barwickia downunda	Frasnian	Mt. Howitt, Victoria, Australia	Long & Clement 2009; Long 1992	382.7	379.2
Beelarongia patrichae	Frasnian	Mt. Howitt, Victoria, Australia	Long & Clement 2009; Long 1987	382.7	379.2
Cabonnichthys burnsi	Famennian	Mandagery Sandstone, Canowindra, New South Wales, Australia	Ahlberg & Johanson 1997	367.76	363.33
Canowindra grossi	Famennian	Mandagery Sandstone, Canowindra, New South Wales, Australia	Long 1985; Thomson 1973	367.76	363.33
Chagrinia enodis	Famennian	Chagrin shale, Ohio, USA	Schaeffer 1962; Schaeffer 1962	372.2	358.9
Chirodipterus australis	Frasnian	Gogo Formation, Australia	Sallan & Coates 2010; Miles 1977	382.7	379.2
Chirodipterus potteri	Famennian	MandagerySandstone , Canowindra, New South Wales, Australia	Sallan & Coates 2010; Kemp 2000	367.76	363.33
Chirodipterus wildungensis	Frasnian	Bad Wildungen, Germany	Sallan & Coates 2010; Gross 1933	375.7	372.2
Coelacanthus welleri	Famennian	Maple Mill Shale, Kinderhook Limestone Series, Burlington, Iowa, USA	Forey 1998; Eastman 1908	372.2	358.9
Conchodus jerofejewi	Frasnian	Stolbovo, Dubniki beds, Sargayevian region stage, Russia	Sallan & Coates 2010; Pander 1858	379.2	375.7

Conchodus ostreaformis	Frasnian	Scaat Craig beds, Upper Old Red Sandstone, Highland, Scotland	Sallan & Coates 2010; McCoy 1848	375.7	372.2
Conchodus parvulus	Famennian	Fossil Ridge, Parting Formation, Gunnison County, Colorado, USA	Sallan & Coates 2010; Bryant & Johnson 1936	363.33	358.9
Densignathus rowei	Famennian	Red Hill, Catskill Formation, Pennsylvania, USA	Sallan & Coates 2010; Daeschler 2000	363.33	358.9
Diplocercides jaekeli	Frasnian	Chagrin shale, Ohio, USA	Forey 1998; Stensio 1922	382.7	372.2
Diplocercides kayseri	Frasnian	Bad Wildungen, Germany; Kadzielnia Quarry and Wietrznia Quarry in Kielce, Poland	Schultze & Cloutier 1996; von Koenen 1895	375.7	363.33
Diplocercides sp.	Frasnian	Central Iran	Janvier 1974	382.7	372.2
Diplocercides sp.	Famennian	Kadzielnia Quarry, Kielce, Poland	Szrek 2007	367.76	363.33
Dipterus ithacensis	Frasnian	Rhinestreet shale, Portage Formation, New York, USA	Sallan & Coates 2010; Williams 1881	375.7	372.2
Dipterus johnsoni	Famennian	Fossil Ridge, Parting Formation, Chaffee Group, Gunnison County, Colorado, USA	Sallan & Coates 2010; Bryant & Johnson 1936	363.33	358.9
Dipterus murchisoni	Frasnian	Zone II, Wietrznia, Kadzielnia, Holy Cross Mountains, Poland	Sallan & Coates 2010	372.2	363.33
Dipterus nelsoni	Famennian	Chemung facies/Venago Formation, Warren, Pennsylvania, USA	Szrek 2007; Newberry 1889	363.33	358.9
Duffichthys mirabilis	Frasnian	Scat Craig Beds, Elgin, Scotland	Ahlberg 1992	375.7	372.2
Edenopteron keithcrooki	Famennian	Boyds Tower and Hegarty bay, New South Wales, Australia	Young *et al*. 2019; Young *et al*. 2013	363.33	358.9
Elginerpeton pancheni	Frasnian	Scaat Craig beds, Upper Old Red Sandstone, Scotland	Sallan & Coates 2010; Ahlberg 1995	375.7	372.2
Elpistostege watsoni	Frasnian	Escuminac Formation, Miguasha, Quebec, Canada	Cloutier *et al*. 2020; Westoll 1938	379.2	375.7

Eusthenodon gavini	Famennian	Hunter Siltstone, Hervey Group, New South Wales, Australia	Sallan & Coates 2010; Johanson & Ritchie 2000	363.33	358.9
Eusthenodon waengsjoei	Famennian	Britta Dal Formation on Gauss, East Greenland	Blom *et al*. 2007; Jarvik 1952	363.33	358.9
Eusthenopteron foordi	Frasnian	Escuminac Formation, Miguasha, Quebec, Canada	Schultze & Cloutier 1996; Whiteaves 1881	379.2	375.7
Eusthenopteron jenkinsi	Frasnian	Fram Formation, Nunavut Territory, Canada	Downs *et al*. 2018	382.7	379.2
Eusthenopteron kurshi	Frasnian	Lode, Gauja Formation, Latvia	Sallan & Coates 2010; Zupins 2008	382.7	379.2
Fleurantia denticulata	Frasnian	Escuminac Formation, Miguasha, Quebec, Canada	Cloutier 1996; Graham-Smith & Westoll 1937	379.2	375.7
Ganorhynchus sp.	Frasnian	Chemung facies/Venago Formation, Warren, Pennsylvania, USA	Sallan & Coates 2010; Traquair 1873	363.33	358.9
Gavinia syntrips	Frasnian	Avon River Group, Mount Howitt, Victoria, Australia	Long 1999	382.7	379.2
Glyptolaemus kinnairdi	Famennian	Dura Den, Upper Old Red Sandstone, Scotland	Cloutier (pers. Com); Huxley 1861	372.2	358.9
Glyptolepis ?dellei	Famennian	Plavsk Regional Stage, Russia		367.76	363.33
Glyptolepis sp.	Frasnian	Amata Regional Stage, Luga river bassin, Leningrad Region, Russia	Ivanov & Lebedev 2012; Agassiz 1843	382.7	379.2
Glyptolepis sp.	Frasnian	Plavinas Regional Stage, Luga river bassin, Leningrad Region, Russia	Ivanov & Lebedev 2012; Agassiz 1843	382.7	379.2
Glyptopomus bystrowi	Famennian	Ketleri Formation, Latvia; Turgenevo Formation of the Plavsk Regional Stage, Russia	Sallan & Coates 2010; Zupiņš 2009	363.33	358.9
Glyptopomus elginensis	Famennian	Rosebrae beds, Upper Old Red Sandstone, Morayshire, Scotland	Sallan & Coates 2010; Jarvik 1950	372.2	358.9
Gogodipterus paddyensis	Frasnian	Gogo Formation, Australia	Sallan & Coates 2010; Miles 1977	382.7	379.2

Gogonasus andrewsae	Frasnian	Gogo Formation, Australia	Hu *et al*. 2019; Long 1985	382.7	379.2
Gooloogongia loomesi	Famennian	Canowindra fish beds, New South Wales, Australia	Johanson & Ahlberg 1998 ; Cloutier *et al*. 2020 (supp.)	367.76	363.33
Griphognathus whitei	Frasnian	Gogo Formation, Australia	Campbell & Barwick 2002; Pridmore & Barwick 1993; Miles 1977	382.7	379.2
Heddleichthys dalgleisiensis	Famennian	Dura Den Formation, Midland Valley, Scotland	Snitting 2009; Anderson 1859	367.76	363.33
Heliodus lesleyi	Famennian	Chemung facies/Venago Formation, Warren, Pennsylvania, USA	Sallan & Coates 2010; Newberry 1875	363.33	358.9
Holodipterus elderae	Frasnian	Gogo Formation, Australia	Sallan & Coates 2010; Pridmore 1994	382.7	379.2
Holodipterus gogoensis	Frasnian	Gogo Formation, Australia	Sallan & Coates 2010; Miles 1977	382.7	379.2
Holodipterus kiprijanowi	Famennian	*Cheiloceras* beds, Holy Cross Mountains, Poland; Turgenevo Formation, Plavsk Regional Stage, Russia	Sallan & Coates 2010; P&er 1858	372.2	358.9
Holodipterus meemanae	Frasnian	Gogo Formation, Australia	Sallan & Coates 2010; Pridmore *et al*. 1994	382.7	379.2
Holopterygius nudus	Frasnian	Heiligenstock quarry, Bergisch-Gladbach, Germany	Hartkopf-Fröder *et al*. 2004 ; Friedman & Coates 2006; Jessen 1973	382.7	379.2
Holoptychius bergmanni	Frasnian	Fram Formation, Ellesmere Island, Nunavut, Canada	Downs *et al*. 2013	382.7	375.7
Holoptychius flemingi	Famennian	Dura Den Formation, Midland Valley, Scotland	Agassiz 1844; Cloutier & Schultze 1996	367.76	363.33
Holoptychius giganteus	Frasnian	Scaat Craig beds, Upper Old Red Sandstone, Highland, Scotland	Agassiz 1843, 1844, 1845	375.7	372.2
Holoptychius halli	Famennian	Catskill Formation, Delhi, New York, USA	Newberry 1889; Eastman 1908	363.33	358.9

Holoptychius jarviki	Frasnian	Escuminac Formation, Miguasha, Quebec, Canada	Cloutier & Schultze 1996	379.2	375.7
Holoptychius nobilissimus	Famennian	Dura Den, Upper Old Red Sandstone, Scotland	Dineley & Metcalf 1999; Agassiz 1839	367.76	363.33
Holoptychius sp.	Frasnian	Kap Kolthoff Group, Greenland	Jarvik 1942; Blom *et al*. 2007	382.7	379.2
Holoptychius sp.	Frasnian	Nadmeshi beds, Latvia	Mondéjar-Fernández & Meunier 2020; Agassiz 1839	382.7	372.2
Holoptychius sp.	Famennian	Khovanshchinian Regional Stage, Andreyevka-2 locality, Tula Region, Russia	Alekseev *et al*. 1994; Agassiz 1839	363.33	358.9
Holoptychius sp.	Famennian	Ketleri outcrop, Ketleri Formation, Venta River, Latvia	Lukševičs & Zupins 2004	363.33	358.9
Holoptychius sp.	Frasnian	Amata Regional Stage, Luga river bassin, Leningrad Region, Russia	Ivanov & Lebedev 2011; Agassiz 1839	382.7	379.2
Hongyu chowi	Famennian	Zhongning Formation, Quarry at Shixiagou, Qingtongxia, Ningxia, China	Zhu *et al*. 2017	372.2	358.9
Howidipterus donnae	Frasnian	Mt. Howitt, Victoria, Australia	Long & Clement 2009	382.7	379.2
Howidipterusus santacrucensis	Famennian	Zone II, Wietrznia, Kadzielnia, Holy Cross Mountains, Poland	Sallan & Coates 2010	367.76	363.33
Howittichthys warrenae	Frasnian	Mt Howitt, Victoria, Australia	Long & Holl& 2008	382.7	379.2
Hyneria lindae	Famennian	Red Hill, Duncannon Member, Catskill Formation, Hyner, Pennsylvania	Sallan & Coates 2010; Thompson 1968	363.33	358.9
Hynerpeton bassetti	Famennian	Red Hill, Duncannon Member, Catskill Formation, Hyner, Pennsylvania, USA	Sallan & Coates 2010; Daeschler *et al*. 1994	363.33	358.9
Ichthyostega eigili	Famennian	Britta Dal Formation, Celsius Bjerg Group, East Greenland	Sallan & Coates 2010; Säve-Söderbergh 1932	363.33	358.9
Ichthyostega stensioei	Famennian	East Greenland, Aina Dal Formation	Blom 2005; Säve-Söderbergh 1932	363.33	358.9

Iranorhynchus seyedemamii	Givetian	Kerman, Tabas Region, eastern Iran	Sallan & Coates 2010; Janvier & Martin 1978	384.36	379.2
Jakubsonia livnensis	Famennian	Gornostayevka quarry, SW of the Livny Town, Oryol Region, Russia	Sallan & Coates 2010; Lebedev 2004	372.2	367.76
Jarvikia arctica	Famennian	Aina Dal Formation and Britta Dal Formation, Celsius Bjerg Group, East Greenland	Sallan & Coates 2010; Lehman 1959	363.33	358.9
Jarvikia lebedevi	Famennian	Tugenevo beds/Dankoc-Lebedyan beds, Zadonckian/Plavsk Regional stage, central Devonian field, Oryol, Metsensk district, Russia	Sallan & Coates 2010; Krupina	372.2	358.9
Jarvikina wenjukowi	Frasnian	Upper Variegated Series, Yukhora village, Leningrad Oblast, Russia	Cloutier *et al*. 2020 (supp.); Rohon 1889	379.2	358.9
Laccognathus embryi	Frasnian	Fram Formation, Ellesmere Island, Nunavut, Canada	Downs *et al*. 2011	382.7	375.7
Langliera socqueti	Famennian	Evieux Formation, Famenne, Belgium	Sallan & Coates 2010; Clément *et al*. 2009	363.33	358.9
Latvius grewingki	Frasnian	Snetnaya Gora beds, Russia	Gross 1933; Trinajstic *et al*. 2019	382.7	379.2
Latvius obrutus	Famennian	Ketleri outcrop, Ketleri Formation, Venta River, Latvia	Sallan & Coates 2010; Vorobyeva 1977	363.33	358.9
Litoptychius bryanti	Famennian	Fossil Ridge, Parting Formation, Chaffee Group, Gunnison County, Colorado, USA	Sallan & Coates 2010; Denison 1951	363.33	358.9
Mandageria fairfaxi	Famennian	Mandagery Sandstone, Canowindra, New South Wale, Australia	Johanson & Ahlberg 1997	367.76	363.33
Marsdenichthys longioccipitus	Frasnian	Mt. Howitt, Victoria, Australia	Long 1985 ; Holland *et al*. 2010	382.7	379.2
Medoevia lata	Famennian	Unknown locality, Russia	Lebedev 1995	363.33	358.9

Megalichthys mullisoni	Famennian	Red Hill site, Duncannon Member, Catskill Formation, Clinton County, Pennsylvania, USA	Downs & Daeschler 2020	363.33	358.9
Miguashaia bureaui	Frasnian	Escuminac Formation, Miguasha, Quebec, Canada	Cloutier 1996; Schultze 1973	379.2	375.7
Ngamugawi wirngarri	Frasnian	Gogo Formation, Australia	Clement *et al*. 2024	382.7	379.2
Obruchevichthys gracilis	Famennian	Skujaine river, Tervete Formation, Latvia	Sallan & Coates 2010; Vorobyeva 1977	372.2	367.76
Oervigia nordica	Famennian	Britta Dal Formation, Celsius Bjerg Group, East Greenland	Sallan & Coates 2010; Lehman 1959	363.33	358.9
Onychodus jandemarrai	Frasnian	Gogo Formation, Australia	Andrews *et al*. 2006	382.7	379.2
Onychodus ortoni	Famennian	Ohio Shale, Huron Member, Ohio, USA; West Falls Group, New-York, USA	Newberry, 1889	372.2	358.9
Orlovichthys limnatus	Famennian	Tugenevo beds/Dankoc-Lebedyan beds, Zadonckian/Plavsk Regional stage, central Devonian field, Oryol, Metsensk district, Russia; Ketleri outcrop, Ketleri Formation, Venta River, Latvia	Sallan & Coates 2010; Krupina 1980	363.33	358.9
Panderichthys stolbowi	Frasnian	Schelonian beds at the river Siasj near Stolbovo, Russia	Vorobyeva 1960	382.7	372.2
Parapanderichthys stolbovi	Frasnian	Stolbovo, Syas River, Dubniki beds, Sargayevian region stage, Russia	Sallan & Coates 2010; Vorobyeva 1967	375.7	372.2
Parmastega aelidae	Famennian	Sosnogorsk Formation, Russia	Beznosov *et al*. 2019	372.2	367.76
Phaneropleuron andersoni	Famennian	Yellow Sandstone of Dura Den	Traquair 1871; Huxley 1859	367.76	363.33
Pillararhynchus longi	Frasnian	Gogo Formation, Australia	Sallan & Coates 2010; Campbell & Barwick 1990	382.7	379.2
Platycephalichthys bishoffi	Frasnian	Stolbovo, Syas River, Dubniki beds, Sargayevian region	Sallan & Coates 2010; Vorobyeva 1959	379.2	375.7

		stage, main Devonian field, northwestern Russia			
Platycephalichthys skuensis	Famennian	Skujaine river, Tervete Formation, Latvia	Sallan & Coates 2010	367.76	363.33
Porolepis posnaniensis	Emsian	Mimerdalen Subgroup, Spitzbergen, Norway; Placoderm sandstone, Podlazie, Holy Cross Mountains, Poland	Kade 1858; Clément 2002	402.83	358.9
Proceratodus wagneri	Famennian	Cleveland Shale Member, Ohio Shale, Cleveland, Ohio, USA	Sallan & Coates 2010; Newberry 1889	363.33	358.9
Pseudosauripterus anglicus	Frasnian	Brown Clee Hill, England	Ball *et al*. 1961; Woodward 1888	382.7	372.2
Quebecius quebecensis	Frasnian	Escuminac Formation, Miguasha, Quebec, Canada	Cloutier & Schultze 1996; Whiteaves 1889	379.2	375.7
Rhinodipterus stolbovi	Frasnian	Stolbovo, Syas River, Dubniki beds, Sargayevian region stage, Russia	Sallan & Coates 2010; Krupina 1995	379.2	375.7
Rhynchodipterus elginensis	Famennian	Rosebrae Beds, Elgin, Scotland	Ahlberg *et al*. 2001 ; Friedman 2007; Säve-Söderbergh 1937	372.2	358.9
Sauripterus anglicus	Famennian	Woodhill Bay Fish Bed, Upper Old Red Sandstone, Portishead, Avon, England	Sallan & Coates 2010; Woodward 1891	367.76	363.33
Sauripteris taylori	Famennian	Powys Curve, Catskill Formation, Pennsylvania, USA	Hall 1843	363.33	358.9
Scaumenacia curta	Frasnian	Escuminac Formation, Miguasha, Quebec, Canada	Cloutier 1996; Whiteaves 1881	379.2	375.7
Sengoerichthys ottoman	Frasnian	Armutgözlek Tepe, Kemer, Turkey	Janvier *et al*. 2007	382.7	372.2
Serenichthys kowiensis	Famennian	Witpoort Formation, South Africa	Gess & Coates 2015	363.33	358.9
Soederberghia groenlandica	Famennian	Aina Dal Formation, Celsius Bjerg Group, East Greenland	Sallan & Coates 2010; Lehman 1959	363.33	358.9
Soederberghia simpsoni	Famennian	Mandagery Sandstone, Canowindra, New	Ahlberg *et al*. 2001	367.76	363.33

		South Wales, Australia ; Aina Dal Formation East Greenland			
Spodichthys buetleri	Frasnian	Rodebjerg Formation/Snehvide Formation, Kap Kolthoff Group, Greenland	Sallan & Coates 2010; Jarvik 1985	382.7	379.2
Tetrapod indet. 1	Famennian	Greenland	Ahlberg 2024	363.33	358.9
Tetrapod indet. 2	Famennian	Greenland	Ahlberg 2024	363.33	358.9
Tetrapod indet. 3	Famennian	Greenland	Ahlberg 2024	363.33	358.9
Tetrapod indet. 4	Famennian	Greenland	Ahlberg 2024	363.33	358.9
Tetrapod indet. 5	Famennian	Greenland	Ahlberg 2024	363.33	358.9
Trackway 3	Frasnian	St. Finan's Sandstone Formation at Tooreen in St. Finan's Bay, Ireland	Higgs & Meere 2024	379.2	375.7
Trackway 4	Frasnian	Genoa River Beds, Victoria, Australia	Warren & Wakefield 1972	382.7	372.2
Thursius minor	Frasnian	Rodebjerg Formation/Snehvide Formation, Kap Kolthoff Group, Greenland	Sallan & Coates 2010; Jarvik 1985	382.7	375.7
Tiktaalik roseae	Frasnian	Okse Bay Group, middle part of the Fram Formation, Nunavut Territory, Canada	Daeschler *et al*. 2006 ; Shubin *et al*. 2013	382.7	379.2
Tulerpeton curtum	Famennian	Andreyevka-2, Khovanshshina Beds, Zovalzkh Formation, Tula, Siberia	Sallan & Coates 2010; Lebedev 1984	363.33	358.9
Ventalepis ketleriensis	Famennian	Lnyanaya Formation, Central-European Russia; Ketleri Formation, Varkali Member, Venta River, Latvia	Schultze 1980; Lebedev & Lukševičs 2018; Lukševičs & Zupins 2004	366.33	358.9
Ventastega curonica	Famennian	Ketleri outcrop, Ketleri Formation, Venta River, Latvia	Sallan & Coates 2010; Ahlberg *et al*. 1994	363.33	358.9
Yambira thomsoni	Famennian	Hunter Siltstone, Hervey Group, Grenfell, New South Wales, Australia	Sallan & Coates 2010; Johanson & Ritchie 2000	363.33	358.9
Ymeria denticulata	Famennian	South side of Celsius Bjerg, Ymer Ø, North-East Greenland; Celsius	Clack *et al*. 2012	372.2	358.9

		Bjerg Group, Greenland			
CARBONIFEROUS					
MISSISSIPPIAN					
Acheroniscus caledoniae	Serpukhovian	Burghlee Ironstone, Limestone Coal Group, Loanhead, Midlothian, Scotland	Sallan & Coates 2010; Carroll 1969	328.33	325.76
Adelogyrinus simorhynchus	Serpukhovian	Burghlee Ironstone, Limestone Coal Group, Loanhead, Midlothian, Scotland; Dora Bone Bed, Limestone Bone Bed, Cowdenbeath, Fife, Scotland	Sallan & Coates 2010; Watson 1929	328.33	323.2
Allenypterus montanus	Serpukhovian	Bear Gulch Limestone, Heath Formation, Montana, USA	Lund & Lund 1985; Melton 1969	325.76	323.2
Balanerpeton woodi	Viséan	East Kirkton, West Lothian, Scotland	Milner & Sequeira, 1993	330.9	330.3
Barameda decipiens	Tournaisian	Devil's Plain Formation, Mansfield group, Victoria, Australia	Long 1989 ; Cloutier *et al*. 2020 (supp.); Woodward 1906	358.9	354.83
Barameda mitchelli	Tournaisian	Broken river and Bridge Creek, Mansfield, Victoria, Australia	Long 1989 ; Jeffery 2012; Holl& *et al*. 2007	358.9	354.83
Caerorhachis bairdi	Serpukhovian	Burghlee Ironstone, Limestone Coal Group, Loanhead, Midlothian, Scotland	Sallan & Coates 2010; Holmes & Carroll 1977	328.33	325.76
Caridosuctor populosum	Serpukhovian	Bear Gulch Limestone, Heath Formation, Montana, USA	Lund & Lund 1984; Torino *et al*. 2021	325.76	323.2
Casineria kiddi	Viséan	Cheese Bay Shrimp Bed, Gullane Formation, Calciferous Sandstone Series, East Lothian, Scotland	Sallan & Coates 2010; Paton *et al*.1999	336.16	330.9
Claradosymblema narrienense	Viséan	Raymond Formation of the Officer Basin, Queensland, Australia	Clement *et al*. 2021; Fox *et al*. 1995	346.7	336.16
Coelacanthopsis curta	Viséan	Calciferous Sandstone Series, Scotland	Forey 1998; Traquair 1905	346.7	330.9

Coelacanthus abdenensis	Serpukhovian	Loanhead Ironstone, Edge Coal Group, Scotland	Traquair 1903	330.9	328.33
Coelacanthus hindi	Serpukhovian	England	Wellburn 1902	330.9	319.9
Coelacanthus spinatus	Serpukhovian	England	Wellburn 1902	330.9	319.9
Coelacanthus stensioei	Serpukhovian	Germany and Belgium	Aldinger 1931	330.9	328.33
Coelacanthus tuberculatus	Serpukhovian	England	Wellburn 1902	330.9	319.9
Coelacanthus woodwardia	Serpukhovian	England	Wellburn 1902	330.9	319.9
Crassigyrinus scoticus	Viséan	Gilmerton Blackband Ironstone, Scotland; Dora Bone Bed, Limestone Bone Bed, Fife, Scotland	Sallan & Coates 2010; Watson 1929	336.16	328.33
Ctenodus interruptus	Viséan	Powgree Burn, Ayrshire, Scotland; Broxburn Shale, Midlothian, Scotland; Loanhead No. 2 Ironstone and Burghlee Pit Ironstone, Midlothian, Scotland	Sallan & Coates 2010; Sharp & Clack 2013; Barkas 1869	341.43	328.33
Delatitia breviceps	Tournaisian	Broken River fish fauna, Devil's Plain Formation, Mansfield Group, Mansfield Basin, Victoria, Australia	Sallan & Coates 2010; Woodward 1906	358.9	354.83
Dolichopareias disjectins	Viséan	Burdiehouse limestone, Edinburgh, Scotland	Sallan & Coates 2010; Watson 1929	341.43	336.16
Doragnathus woodi	Viséan	Inchkeith, Upper Oil Shale Group, Firth of Forth, Fife, Scotland; Burghlee Ironstone, Limestone Coal Group, Loanhead, Midlothian, Scotland; Dora Bone Bed, Limestone Bone Bed, Cowdenbeath, Fife, Scotland	Sallan & Coates 2010; Smithson 1980	336.16	328.33
Eldeceeon rolferi	Viséan	East Kirkton Limestone, West Lothian Oil Shale Formation, Bathgate, Lothian, Scotland	Sallan & Coates 2010; Smithson 1993	336.16	330.9

Eoherpeton watsoni	Viséan	Gilmerton Blackband Ironstone, Scotland; Burghlee Ironstone, Limestone Coal Group, Loanhead, Midlothian, Scotland; Dora Bone Bed, Limestone Bone Bed, Cowdenbeath, Fife, Scotland	Sallan & Coates 2010; Panchen 1975	341.43	328.33
Eucritta melanolimnetes	Viséan	East Kirkton Limestone, West Lothian Oil Shale Formation, Bathgate, Lothian, Scotland	Sallan & Coates 2010; Clack 1998	336.16	330.9
Ganopristodus lobatus	Viséan	Burdiehouse limestone, Edinburgh, Scotland	Sallan & Coates 2010; Agassiz 1844	341.43	336.16
Ganopristodus splendens	Viséan	Gilmerton Blackband Ironstone, Gilmerton, Scotland; Burghlee Ironstone, Limestone Coal Group, Loanhead, Midlothian, Scotland	Sallan & Coates 2010; Traquair 1881	341.43	328.33
Hadronector donbairdi	Serpukhovian	Bear Gulch Limestone, Heath Formation, Montana, USA	Lund & Lund 1984; Torino *et al*. 2021	325.76	323.2
Latvius porosus	Tournaisian	Albert Formation, New Brunswick, Canada	Greiner 1977 ; Mickle 2017	358.9	346.7
Lethiscus stocki	Viséan	Wardie Shale, Lower Lothian Group, Scotland	Sallan & Coates 2010; Wellstead 1982	336.16	330.9
Letognathus hardingi	Tournaisian	Horton Bluff and Albert Formations, Bay of Fundy, Canada	Sallan & Coates 2010; Dawson 1868	358.9	350.76
Lochmocercus aciculodontus	Serpukhovian	Bear Gulch Limestone, Heath Formation, Montana, USA	Lund & Lund 1984; Torino *et al*. 2021	325.76	323.2
Loxomma allmanni	Viséan	Gilmerton Blackband Ironstone, Scotland	Sallan & Coates 2010; Huxley 1862	336.16	330.9
Megalichthys hibberti	Serpukhovian	Millstone Grit, Summit, Lancashire, England	Sallan & Coates 2010; Agassiz 1835	325.76	323.2
Megalichthys laticeps	Viséan	Burdiehouse limestone, Edinburgh, Scotland	Traquair 1884	341.43	336.16

Ophiderpeton kirktonense	Viséan	East Kirkton Limestone, West Lothian Oil Shale Formation, Scotland	Sallan & Coates 2010; Milner 1994	336.16	330.9
Ossinodus pueri	Viséan	Middle Paddock Tetrapod Unit, Ducabrook Formation, Drummond Basin, Queensland, Australia	Sallan & Coates 2010; Warren & Turner 2004	341.43	336.16
Papposaurus traquair	Serpukhovian	Burghlee Ironstone, Limestone Coal Group, Loanhead, Midlothian, Scotland	Sallan & Coates 2010; Watson 1914	328.33	325.76
Pholidogaster pisciformis	Viséan	Burdiehouse limestone, Edinburgh, Scotland	Sallan & Coates 2010; Huxley 1862	341.43	336.16
Polyosteorhynchus simplex	Serpukhovian	Bear Gulch Limestone, Heath Formation, Montana, USA	Lund & Lund 1984; Torino *et al*. 2021	325.76	323.2
Proterogyrinus sp.	Serpukhovian	Dora Bone Bed, Limestone Bone Bed, Cowdenbeath, Fife, Scotland	Sallan & Coates 2010; Romer 1970	325.76	323.2
Rhabdoderma alderingi	Serpukhovian	Clwyd, Wales	Forey 1998; Moy-Thomas 1937	330.9	323.2
Rhabdoderma ardrossense	Viséan	Calciferous Sandstone Series, Fifeshire, Scotland	Forey 1998; Moy-Thomas 1937	346.7	330.9
Rhabdoderma elegans	Serpukhovian	Linton, Ohio, USA	Forey 1998; Menning *et al*. 2001; Newberry 1856	330.9	307.26
Rhabdoderma huxleyi	Viséan	Calciferous Sandstone, Glencartholm Volcanic Group, Dumfrisshire, Scotland	Forey 1998; Traquair 1881	341.43	336.16
Rhizodus hibberti	Viséan	Strathclyde Group, Calciferous Sandstone Series from Crail, Fife, Scotland; Wardie shale, Scotland	Agassiz 1843	341.43	330.9
Sagenodus inequalis	Serpukhovian	Millstone Grit, Summit, Lancashire, England	Sallan & Coates 2010; Owen 1867	325.76	323.2
Sagenodus quinquecostatus	Serpukhovian	Gilmerton Blackband Ironstone, Gilmerton, Scotland; Burghlee	Sallan & Coates 2010; Traquair 1883	330.9	328.33

		Ironstone, Limestone Coal Group, Loanhead, Midlothian, Scotland			
Screbinodus ornatus	Viséan	Venturefair Pit near Gilmerton, Edinburgh	Jeffery 2012; Traquair 1878	336.16	330.9
Silvanerpeton miripedes	Viséan	East Kirkton Limestone, West Lothian Oil Shale Formation, Bathgate, Lothian, Scotland	Sallan & Coates 2010; Clack 1994	336.16	330.9
Spathicephalus mirus	Serpukhovian	Burghlee Ironstone, Limestone Coal Group, Loanhead, Midlothian, Scotland; Dora Bone Bed, Limestone Bone Bed, Cowdenbeath, Fife, Scotland	Sallan & Coates 2010; Watson 1929	328.33	323.2
Westlothiana lizziae	Viséan	East Kirkton Limestone, West Lothian Oil Shale Formation, Bathgate, Lothian, Scotland	Sallan & Coates 2010; Smithson & Rolfe 1990	336.16	330.9
		PENNSYLVANIAN			
Actiobates peabodyi	Kasimovian	Garnett Quarry of Kansas, USA	Schoch & Milner 2014	307	303.7
Adamanterpeton ohioensis	Moscovian	Linton, Ohio, USA	Milner & Sequeira 1998	310.7	307.5
Aemilia stellata	Gzhelian	Graham Formation, Texas, USA	Mondéjar-Fern&ez *et al*. (in review)	303.7	302.1
Anthracobamus fayoli	Gzhelian	Commentry, France	Werneburg 2019; Thevenin, 1906	303.5	298.9
Askerichthys heintzi	Bashkirian	Semsvik in Asker west of Oslo, Tanum Formation in the Asker Group, Norway	Borgen & Nakrem 2016	317.86	307
Baphetes bohemicus	Moscovian	Nýřany, Czech Republic	Miller *et al*. 2009; Fritsch 1889	310.7	307.5
Coelacanthus sp.	Gzhelian	Ukraine	Chabakov 1927	303.5	302.5
Coelacanthus sp.	N/A	Coal Measures, Nova Scotia, Canada	Fetcher 1884	323.2	298.9
Gephyrostegus bohemicus	Moscovian	Plattenkohle of Humboldt Mine, Nýřany, Plzeň-Manětín Basin, Czech Republic	Jaekel 1902; Klembara *et al*. 2014	309.73	307
Megalichthys intermedius	Moscovian	Coal Measures, Knowles Ironstone shale, Fenton,	Woodward 1891; Borgen & Nakrem 2016	315.2	307

		Staffordshire, England			
Microbrachis pelikani	Moscovian	Nýřany, Czech Republic	Fritsch 1875	309.73	307
Rhabdoderma exiguum	Moscovian	Francis Creek Shale, Mazon Creek, Illinois, USA	Clements *et al*. 2019; Eastman 1902	309.73	307
Rhabdoderma newelli	Kasimovian	Stanton Formation, Rock Lake Shale Member, Garnett, Kansas, USA	Echols 1963; Schultze 1995; Hibbard 1933	307	303.7
Rhabdoderma tinglyense	Bashkirian	Yorkshire, England	Forey 1998; Davis 1884	317.86	310.7
Rhizodopsis rankini	Bashkirian	Upper Drumgray Coal shale, Wester Bracco, South Lanarkshire, Scotland	Elliott 2023	323.2	315.2
Sagenodus copeanus	Kasimovian	Montceau-les-mines, France ; Hamilton Quarry, Kansas, USA	Olive *et al*. 2012; Williston 1899	307	303.7
Strepsodus sauroides	Moscovian	Hannah Pit, Newsham, Northumberland, England	Binney 1841; Jeffery 2004	312.46	309.73
Tuditanus punctulatus	Moscovian	Linton, Ohio, USA	Cope 1875	310.7	307.5

Table S2. List of the 70 basal sarcopterygian species included in disparity analyses. For each species, we indicated in which analyses it was included.

Species	Group	Age	Aquatic habitat	Precise palaeo-environment	Full body	Cheek	Skull roof
DEVONIAN							
LOWER DEVONIAN							
Dipnorhynchus sussmilchi	Dipnoi	Emsian	Marine	Reef			x
Durialepis edentatus	Porolepiformes	Emsian	Marine	Coastal marine		x	x
Heimenia ensis	Porolepiformes	Emsian	Freshwater	Alluvial plain	x		
Porolepis brevis	Porolepiformes	Pragian	Freshwater	Alluvial plain	x	x	
MIDDLE DEVONIAN							
Bruehnopteron murphyi	'Osteolepiformes'	Givetian	Marine	Other marine		x	
Diplocercides heiligenstockiensis	Actinistia	Givetian	Marine	Lagoon		x	
Dipterus valenciennesi	Dipnoi	Eifelian	Freshwater	Calm freshwater lake	x		x
Glyptolepis groenlandica	Porolepiformes	Eifelian	Freshwater	Alluvial plain		x	
Glyptolepis leptopterus	Porolepiformes	Eifelian	Freshwater	Calm freshwater lake	x		
Griphognathus sculpta	Dipnoi	Givetian	Freshwater	Lagoon	x		x
Gyroptychius agassizi	'Osteolepiformes'	Eifelian	Freshwater	Calm freshwater lake	x	x	x
Koharalepis jarviki	'Osteolepiformes'	Givetian	Freshwater	Alluvial plain		x	x
Laccognathus panderi	Porolepiformes	Givetian	Freshwater	Lagoon		x	x
Osteolepis macrolepidotus	'Osteolepiformes'	Eifelian	Freshwater	Calm freshwater lake	x	x	x
Osteolepis panderi	'Osteolepiformes'	Givetian	Freshwater	Calm freshwater lake	x		
Panderichthys rhombolepis	'Elpistostegalia'	Givetian	Freshwater	Lagoon		x	x
Pentlandia macroptera	Dipnoi	Givetian	Freshwater	Calm freshwater lake	x		x
Pinnalongus saxoni	Dipnoi	Eifelian	Marine	Other marine	x		
Strunius walteri	Onychodontida	Givetian	Marine	Lagoon	x	x	x
Thursius macrolepidotus	'Osteolepiformes'	Eifelian	Freshwater	Calm freshwater lake	x	x	

Tristichopterus alatus	'Osteolepiformes'	Givetian	Freshwater	Calm freshwater lake	x	x	
UPPER DEVONIAN							
Acanthostega gunarri	Tetrapoda	Famennian	Freshwater	Alluvial plain			x
Barwickia downunda	Dipnoi	Frasnian	Freshwater	Other freshwater	x		x
Beelarongia patrichae	'Osteolepiformes'	Frasnian	Freshwater	Other freshwater		x	
Cabonnichthys burnsi	'Osteolepiformes'	Famennian	Freshwater	Oxbow lake/ meandering river	x	x	x
Canowindra grossi	'Osteolepiformes'	Famennian	Freshwater	Oxbow lake/ meandering river		x	x
Edenopteron keithcrooki	'Osteolepiformes'	Famennian	Marine	Other marine		x	x
Elpistostege watsoni	Tetrapoda	Frasnian	Estuary	Estuary			x
Eusthenodon waengsjoei	'Osteolepiformes'	Famennian	Freshwater	Alluvial plain		x	x
Eusthenopteron foordi	'Osteolepiformes'	Frasnian	Estuary	Estuary	x	x	x
Fleurantia denticulata	Dipnoi	Frasnian	Estuary	Estuary	x		x
Gavinia syntrips	Actinistia	Frasnian	Freshwater	Other freshwater		x	
Glyptolaemus kinnairdi	'Osteolepiformes'	Famennian	Freshwater	Dynamic freshwater lake	x		
Gogonasus andrewsae	'Osteolepiformes'	Frasnian	Marine	Reef			x
Gooloogongia loomesi	Rhizodontida	Famennian	Freshwater	Oxbow lake/ meandering river	x		x
Griphognathus whitei	Dipnoi	Frasnian	Marine	Reef			x
Heddleichthys dalgleisiensis	'Osteolepiformes'	Famennian	Freshwater	Dynamic freshwater lake	x	x	
Holoptychius jarviki	Porolepiformes	Frasnian	Estuary	Estuary	x	x	x
Holoptychius nobilissimus	Porolepiformes	Famennian	Freshwater	Dynamic freshwater lake	x		
Howidipterus donnae	Dipnoi	Frasnian	Freshwater	Other freshwater	x		x
Ichthyostega stensioei	Tetrapoda	Famennian	Freshwater	Alluvial plain			x
Jarvikina wenjukowi	'Osteolepiformes'	Frasnian	Estuary	Estuary		x	
Mandageria fairfaxi	'Osteolepiformes'	Famennian	Freshwater	Oxbow lake/ meandering river	x	x	
Marsdenichthys longioccipitus	'Osteolepiformes'	Frasnian	Freshwater	Other freshwater		x	x
Miguashaia bureaui	Actinistia	Frasnian	Estuary	Estuary	x	x	x
Ngamugawi wirngarri	Actinistia	Frasnian	Marine	Reef		x	x

Onychodus jandemarrai	Onychodontida	Frasnian	Marine	Reef		x	x
Parmastega aelidae	Tetrapoda	Famennian	Freshwater	Lagoon			x
Quebecius quebecensis	Porolepiformes	Frasnian	Estuary	Estuary	x	x	x
Rhynchodipterus elginensis	Dipnoi	Famennian	Freshwater	Dynamic freshwater lake	x		
Scaumenacia curta	Dipnoi	Frasnian	Estuary	Estuary	x		x
Serenichthys kowiensis	Actinistia	Famennian	Estuary	Estuary	x	x	
Soederberghia simpsoni	Dipnoi	Famennian	Freshwater	Oxbow lake/ meandering river			x
Tiktaalik roseae	'Elpistostegalia'	Frasnian	Freshwater	Oxbow lake/ meandering river			x
CARBONIFEROUS							
MISSISSIPPIAN							
Allenypterus montanus	Actinistia	Serpukhovian	Marine	Bay	x	x	x
Balanerpeton woodi	Tetrapoda	Viséan	Freshwater	Calm freshwater lake			x
Barameda decipiens	Rhizodontida	Tournaisian	Freshwater	Other freshwater		x	x
Barameda mitchelli	Rhizodontida	Tournaisian	Freshwater	Other freshwater		x	x
Caridosuctor populosum	Actinistia	Serpukhovian	Marine	Bay	x	x	x
Claradosymblema narrienense	'Osteolepiformes'	Viséan	Freshwater	Lagoon		x	x
Hadronector donbairdi	Actinistia	Serpukhovian	Marine	Bay	x	x	x
Latvius porosus	'Osteolepiformes'	Tournaisian	Freshwater	Calm freshwater lake		x	
Lochmocercus aciculodontus	Actinistia	Serpukhovian	Marine	Bay	x		
Polyosteorhynchus simplex	Actinistia	Serpukhovian	Marine	Bay	x	x	x
Rhabdoderma elegans	Actinistia	Serpukhovian	Freshwater	Oxbow lake/ meandering river	x		x
Screbinodus ornatus	Rhizodontida	Viséan	Freshwater	Other freshwater		x	
PENNSYLVANIAN							
Anthracobamus fayoli	Tetrapoda	Gzhelian	Freshwater	Calm freshwater lake			x
Baphetes bohemicus	Tetrapoda	Moscovian	Freshwater	Calm freshwater lake			x
Rhabdoderma exiguum	Actinistia	Moscovian	Freshwater	Delta	x		

Rhizodopsis rankini	'Osteolepiformes'	Bashkirian	Freshwater	Other freshwater	x	x

Table S3. Description of landmarks and semilandmarks for the body shape, cheek region, and skull roof analyses respectively. (L) and (R) indicates the landmarks on the left or right side of the fish when paired landmarks have been digitised.

No.	Nature of the descriptor	Description
		Body shape
1	Landmark	Most anterior edge of the extrascapular
2	Landmark	Insertion of the first ray of the posterior (second) dorsal fin
3	Landmark	Insertion of the last ray of the posterior (second) dorsal fin
4	Landmark	Insertion of the first ray of the dorsal lobe of the caudal fin
5	Landmark	Most posterior tip of the caudal peduncle
6	Landmark	Insertion of the first ray of the ventral lobe of the caudal fin
7	Landmark	Insertion of the first ray of the anal fin
8	Landmark	Insertion of the last ray of the anal fin
9	Landmark	Anterior insertion of the pelvic fins
10	Landmark	Dorsal insertion of the pectoral fins
11	Landmark	Most ventral part of the pectoral girdle
12-31	Semilandmarks	Dorsal body outline from landmark 1 to 2
32-67	Semilandmarks	Posterior dorsal fin web outline from landmark 2 to 3
68-87	Semilandmarks	Ventral body outline from landmark 11 to 9
88-97	Semilandmarks	Ventral body outline from landmark 9 to 7
98-207	Semilandmarks	Caudal fin web outline from landmark 4 to 6

Table S3. Description of landmarks and semilandmarks for the body shape, cheek region, and skull roof analyses respectively. (L) and (R) indicates the landmarks on the left or right side of the fish when paired landmarks have been digitised.

No.	Nature of the descriptor	Description
		Cheek region
1	Landmark	Most anterior-dorsal margin of the lacrimal (or lacrimojugal if fused)
2	Landmark	Most anterior-ventral margin of the lacrimal (or lacrimojugal if fused)
3	Landmark	Most posterior-dorsal margin of the jugal (or lacrimojugal if fused)
4	Landmark	Most posterior-ventral margin of the jugal (or lacrimojugal if fused)
5	Landmark	Most dorsal tip of the anterior margin of the post-orbital
6	Landmark	Most ventral tip of the anterior margin of the post-orbital
7	Landmark	Tip of the anterior-dorsal angle of the squamosal
8	Landmark	Tip of the anterior-ventral angle of the squamosal
9	Landmark	Tip of the posterior-ventral angle of the squamosal
10	Landmark	Tip of the anterior-dorsal angle of the operculum
11	Landmark	Posterior extremity of the operculum
12	Landmark	Tip of the anterior-ventral angle extremity of the operculum
13	Landmark	Tip of the anterior-dorsal angle of the preopercular
14	Landmark	Tip of the posterior-dorsal angle of the preopercular
15	Landmark	Tip of the anterior-ventral angle of the preopercular
16	Landmark	Tip of the posterior-ventral angle of the preopercular
		Skull roof
1	Landmark	Anterior median extremity of the parietal (L)
2	Landmark	Anterior median extremity of the parietal (R)
3	Landmark	Posterior lateral extremity of the parietal (L)
4	Landmark	Posterior lateral extremity of the parietal (R)
5	Landmark	Posterior median extremity of the parietal (L)
6	Landmark	Posterior median extremity of the parietal (R)
7	Landmark	Anterior median extremity of the postparietal (L)
8	Landmark	Anterior median extremity of the postparietal (R)
9	Landmark	Posterior lateral extremity of the postparietal (L)
10	Landmark	Posterior lateral extremity of the postparietal (R)
11	Landmark	Posterior median extremity of the postparietal (L)
12	Landmark	Posterior median extremity of the postparietal (R)
13	Landmark	Most anterior extremity of the snout
14	Landmark	Most anterior junction between the tabular and the postparietal (R)
15	Landmark	Anterior lateral extremity of the tabular (R)
16	Landmark	Most anterior junction between the tabular and the postparietal (L)
17	Landmark	Anterior lateral extremity of the tabular (L)
18	Landmark	Anterior margin of the orbit (R)
19	Landmark	Posterior margin of the orbit (R)
20	Landmark	Dorsal margin of the orbit (R)
21	Landmark	Anterior margin of the orbit (L)
22	Landmark	Posterior margin of the orbit (L)
23	Landmark	Dorsal margin of the orbit (L)

Table S4. Convex hulls surface area. The N/A value corresponds to classes including two or less species, making the convex hull surface area estimation inapplicable.

	Class	Surface area			Number of species		
		Body shape	Cheek	Skull roof	Body shape	Cheek	Skull roof
Epoch	Lower Devonian	N/A	N/A	N/A	2	2	2
	Middle Devonian	0.0384	0.1451	0.1217	11	11	9
	Upper Devonian	0.0690	0.1431	0.1786	16	17	24
	Mississippian	0.0195	0.0581	0.0675	6	8	9
	Pennsylvanian	N/A	N/A	0.0422	1	1	3
Aquatic habitat	Estuary	0.0258	0.0680	0.1369	7	6	7
	Freshwater	0.0743	0.0403	0.1632	22	22	28
	Marine	0.0314	0.2776	0.1453	7	11	12
More precise palaeo-environment	Alluvial plain	N/A	0.0044	0.0141	2	4	4
	Bay	0.0223	0.0265	0.0081	5	4	4
	Calm freshwater lake	0.0179	0.0028	0.0534	8	5	7
	Coastal marine	-	N/A	N/A	0	1	1
	Dynamic freshwater lake	0.0017	N/A	-	4	1	0
	Estuary	0.0371	0.0730	0.1368	7	6	7
	Fluvial delta	N/A	-	-	1	0	0
	Lagoon	N/A	0.1465	0.0842	2	5	6
	Oxbow lake/meandering river	0.0135	0.0005	0.0633	4	3	6
	Reef	-	N/A	0.1001	0	2	5
Group of early sarcopterygians	Actinistia	0.0334	0.1099	0.0304	9	9	7
	Dipnoi	0.0094	-	0.0163	9	0	10
	“Elpistostegalia”	-	N/A	N/A	0	1	2
	Onychodontida	N/A	N/A	N/A	1	2	2
	“Osteolepiformes”	0.0095	0.0262	0.0228	10	19	12
	Porolepiformes	0.0160	0.0128	0.0108	6	6	4
	Rhizodontida	N/A	N/A	0.0002	1	2	3
	Tetrapoda	-	-	0.0382	0	0	7

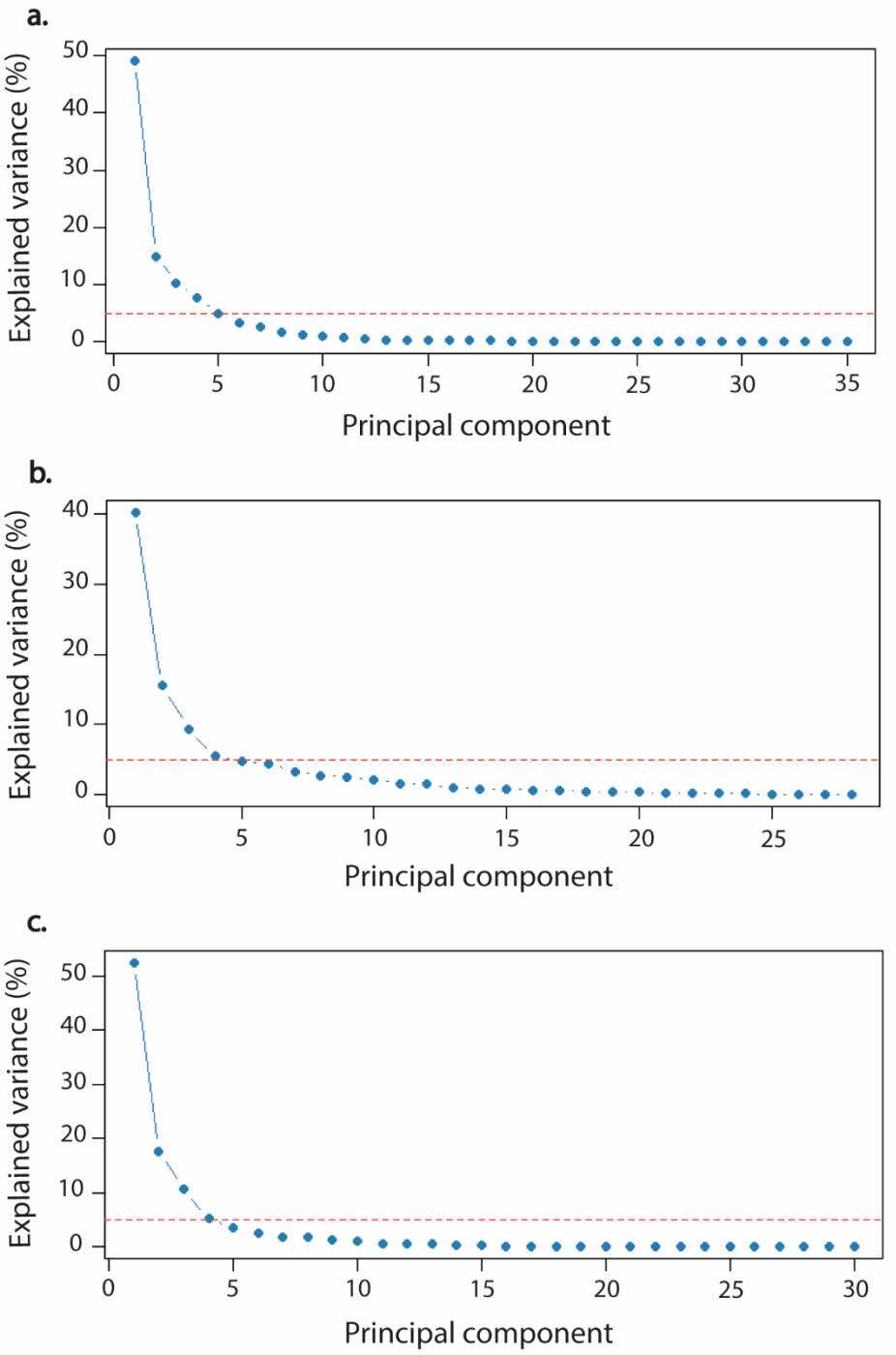


Figure S1. Scree plots. (**a**) Body shape PCA scree plot; (**b**) Cheek PCA scree plot; (**c**) Skull roof PCA scree plot. The dashed red line represents the 5% of explained variance.

Table S5. Convex hulls weighted surface area. Each surface area has been estimated for pairwise combination of the first five PCs and weighted by the explained variance of each pair of axes. The Simple Additive Weighting (SAW) has been used to calculate the weight of each pair of axes. The weight of the pair of axes is calculated by the average of the proportion of explained variance of each axis. The N/A value corresponds to classes including two or less species, making the convex hull surface area estimation inapplicable.

	Class	Weighted surface area (SAW)			Number of species		
		Body shape	Cheek	Skull roof	Body shape	Cheek	Skull roof
Epoch	Lower Devonian	N/A	N/A	N/A	2	2	2
	Middle Devonian	0.0468	0.1112	0.1123	11	11	9
	Upper Devonian	0.0794	0.1366	0.1693	16	17	24
	Mississippian	0.0199	0.0896	0.0722	6	8	9
	Pennsylvanian	N/A	N/A	0.0358	1	1	3
Aquatic habitat	Estuary	0.0411	0.0636	0.0899	7	6	7
	Freshwater	0.0821	0.0640	0.1792	22	22	28
	Marine	0.0449	0.2046	0.1484	7	11	12
More precise palaeoenvironment	Alluvial plain	N/A	0.0071	0.0165	2	4	4
	Bay	0.0175	0.0308	0.0115	5	4	4
	Calm freshwater lake	0.0260	0.0038	0.0644	8	5	7
	Coastal marine	-	N/A	N/A	0	1	1
	Dynamic freshwater lake	0.0046	N/A	-	4	1	0
	Estuary	0.0447	0.0837	0.0869	7	6	7
	Fluvial delta	N/A	-	-	1	0	0
	Lagoon	N/A	0.0830	0.1020	2	5	6
	Oxbow lake/meandering river	0.0108	0.0005	0.0677	4	3	6
	Reef	-	N/A	0.0809	0	2	5
Group of early sarcopterygians	Actinistia	0.0448	0.1123	0.0380	9	9	7
	Dipnoi	0.0247	-	0.0199	9	0	10
	“Elpistostegalia”	-	N/A	N/A	0	1	2
	Onychodontida	N/A	N/A	N/A	1	2	2
	“Osteolepiformes”	0.0169	0.0349	0.0231	10	19	12
	Porolepiformes	0.0152	0.0168	0.0149	6	6	4
	Rhizodontida	N/A	N/A	0.0003	1	2	3
	Tetrapoda	-	-	0.0430	0	0	7

Table S6. Convex hulls weighted surface area. Each surface area has been estimated for pairwise combination of the first five PCs and weighted by the explained variance of each pair of axes. The Weighted Sum of Pairwise Areas (WSPA) has been used to calculate the weight of each pair of axes. The weight of each pair of axes is calculated by multiplying the proportion of variance explained by each. The N/A value corresponds to classes including two or less species, making the convex hull surface area estimation inapplicable.

Class		Weighted surface area (WSPA)			Number of species		
		Body shape	Cheek	Skull roof	Body shape	Cheek	Skull roof
Epoch	Lower Devonian	N/A	N/A	N/A	2	2	2
	Middle Devonian	0.0070	0.0166	0.0199	11	11	9
	Upper Devonian	0.0122	0.0189	0.0288	16	17	24
	Mississippian	0.0030	0.0120	0.0128	6	8	9
	Pennsylvanian	N/A	N/A	0.0061	1	1	3
Aquatic habitat	Estuary	0.0062	0.0095	0.0171	7	6	7
	Freshwater	0.0124	0.0076	0.0286	22	22	28
	Marine	0.0066	0.0314	0.0265	7	11	12
More precise palaeo-environment	Alluvial plain	N/A	0.0009	0.0028	2	4	4
	Bay	0.0029	0.0044	0.0019	5	4	4
	Calm freshwater lake	0.0036	0.0005	0.0100	8	5	7
	Coastal marine	-	N/A	N/A	0	1	1
	Dynamic freshwater lake	0.0005	N/A	-	4	1	0
	Estuary	0.0070	0.0113	0.0171	7	6	7
	Fluvial delta	N/A	-	-	1	0	0
	Lagoon	N/A	0.0134	0.0175	2	5	6
	Oxbow lake/meandering river	0.0017	0.0001	0.0111	4	3	6
	Reef	-	N/A	0.0151	0	2	5
Group of early sarcopterygians	Actinistia	0.0066	0.0157	0.0063	9	9	7
	Dipnoi	0.0031	-	0.0029	9	0	10
	“Elpistostegalia”	-	N/A	N/A	0	1	2
	Onychodontida	N/A	N/A	N/A	1	2	2
	“Osteolepiformes”	0.0023	0.0044	0.0039	10	19	12
	Porolepiformes	0.0023	0.0020	0.0024	6	6	4
	Rhizodontida	N/A	N/A	0.0000	1	2	3
	Tetrapoda	-	-	0.0073	0	0	7

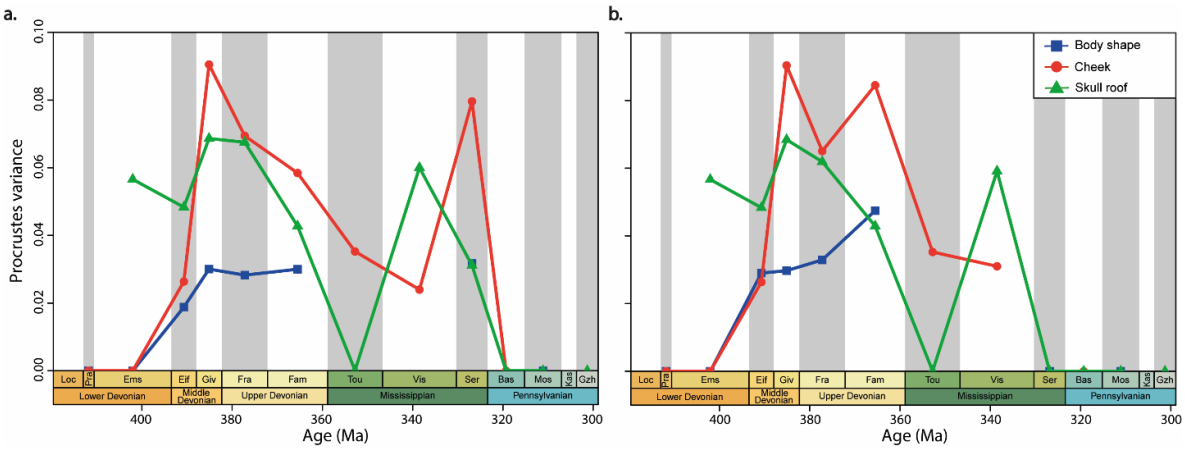


Figure S2. Lagerstätte effect. (**a**) Procrustes variances for each age for the complete dataset; (**b**) Procrustes variances for each age without Bear Gulch species.

Table S7. Morphological disparity analyses. The N/A values correspond to the class including only one species, making the variance estimation inapplicable.

	Class	Procrustes variance			Proportion of total disparity (%)		
		Body shape	**Cheek**	**Skull roof**	**Body shape**	**Cheek**	**Skull roof**
Epoch	Lower Devonian	0.0122	0.0082	0.0566	4.574	2.661	5.091
	Middle Devonian	0.0251	0.0714	0.0633	18.658	25.081	19.762
	Upper Devonian	0.0350	0.0702	0.0607	37.998	37.107	48.628
	Mississippian	0.0318	0.1003	0.0456	35.529	32.222	16.920
	Pennsylvanian	N/A	N/A	0.0846	3.241	2.929	9.599
Aquatic habitat	Estuary	0.0305	0.0828	0.0656	14.670	15.681	15.603
	Freshwater	0.0320	0.0397	0.0614	49.045	31.593	57.557
	Marine	0.0444	0.1297	0.0639	36.285	52.726	26.840
More precise palaeo-environment	Alluvial plain	0.0118	0.0328	0.0303	5.184	7.063	5.861
	Bay	0.0365	0.0797	0.0303	33.539	30.340	7.774
	Calm freshwater lake	0.0198	0.0154	0.0523	13.879	5.651	19.761
	Coastal marine	-	N/A	N/A	-	1.675	2.107
	Dynamic freshwater lake	0.0180	N/A	-	8.415	1.141	-
	Estuary	0.0350	0.0830	0.0656	16.212	18.406	18.222
	Fluvial delta	N/A	-	-	3.355	-	-
	Lagoon	0.0274	0.1129	0.0769	5.170	21.131	18.067
	Oxbow lake/meandering river	0.0381	0.0069	0.0474	14.246	4.925	12.270
	Reef	-	0.0771	0.0800	-	9.668	15.938
Group of early sarcopterygians	Actinistia	0.0323	0.0961	0.0327	43.890	47.927	12.329
	Dipnoi	0.0267	-	0.0193	22.945	-	28.850
	“Elpistostegalia”	-	N/A	0.0107	-	3.248	3.567
	Onychodontida	N/A	0.0241	0.0333	2.518	11.349	8.501
	“Osteolepiformes”	0.0131	0.0278	0.0180	16.966	24.257	14.436
	Porolepiformes	0.0135	0.0347	0.0247	9.710	10.374	8.662
	Rhizodontida	N/A	0.0210	0.0087	3.971	2.845	5.282
	Tetrapoda	-	-	0.0365	-	-	18.373

ANNEXE IV

SUPPLEMENTARY INFORMATION FOR CHAPTER 3: VARIATIONAL MODULARITY OF EARLY ACTINOPTERYGIANS: THE BUILDING BLOCKS OF THE PALAEOZOIC FISH HEAD

Table S1. List of the 197 basal actinopterygian species included in diversity analyses. Species included in modularity analyses are indicated with an asterisk (*). FAD (first appearance datum) corresponds to the first time the species appears in the fossil record, and LAD (last appearance datum) to the last time it appears.

Species	Age	Formation/County	References	FAD	LAD
DEVONIAN					
MIDDLE DEVONIAN					
Austelliscus ferox	Givetian	Ponta Grossa, Paraná, Brazil	Figueroa, Weinschütz & Friedman 2021	387.7	386.03
Cheirolepis aleshkai	Eifelian	Narva Regional Stage, Lepel 1 borehole, Vitebsk region, Belarus	Plax 2020	393.3	391.43
Cheirolepis jonesi	Givetian	Mimerdalen subgroup, Fiskeløfta member, Spitsbergen, Svalbard, Norway	Newman *et al.* 2021	384.36	382.7
*Cheirolepis schultzei**	Givetian	Nevada, USA	Arratia & Cloutier 2004; Newman *et al.* 2021	384.36	379.2
*Cheirolepis trailli**	Eifelian	Old Red Sandstone, Orkney, Scotland	Pearson & Westoll 1979; Arratia & Cloutier 2004; Agassiz 1835	393.3	382.7
*Donnrosenia schaefferi**	Givetian	Aztec Siltstone of southern Victoria Land, Antarctica	Choo 2010; Long *et al.* 2008	387.7	382.7
*Moythomasia lineata**	Givetian	Bergisch Gladbach, Heiligenstock quarry, Germany	Choo 2015	384.36	379.2
*Moythomasia nitida**	Givetian	Bergisch Gladbach, Heiligenstock Quarry, Germany	Choo 2015; Gross 1953	384.36	379.2
*Stegotrachelus finlayi**	Givetian	Ness of Sound and Dunrossness, South-East Shetland, Old Red Sandstone, Scotland	Swartz 2009; Woodward & White, 1926	387.7	382.7
UPPER DEVONIAN					

*Cheirolepis canadensis**	Frasnian	Escuminac Formation, Miguasha, Quebec, Canada	Arratia & Cloutier 1996; Arratia *et al.* 2004; Whiteaves 1881	379.2	375.7
*Cuneognathus gardineri**	Famennian	Eastern Greenland, Obrutschew Bjerg Formation	Schultze *et al.* 2021; Friedman & Blom 2006	363.33	358.9
Elonichthys pulcherrimus	Famennian	Glencartholm, Dumfries and Galloway, Scotland; Borov and Rubchan Beds, Polese Regional Stage, Poland	Schultze *et al.* 2021; Moy-Thomas & Dyne 1938; Traquair 1881	363.33	336.16
*Gogosardina coatesi**	Frasnian	Gogo Formation, Australia	Choo *et al.* 2009	382.7	379.2
*Howqualepis rostridens**	Frasnian	Mt Howitt, Victoria, Australia	Long 1988	382.7	379.2
Kentuckia hlavini	Famennian	Cleveland Member, Ohio Shale, Ohio, USA	Dunkle 1964	363.33	358.9
Krasnoyarichthys jesseni	Famennian	Siberia, Russia	Prokofiev 2002	372.2	358.9
*Limnomis delaneyi**	Famennian	Catskill, Pennsylvania, USA	Daeschler 2000	363.33	358.9
*Mimipiscis bartrami**	Frasnian	Gogo Formation, Australia	Choo 2012	382.7	379.2
*Mimipiscis toombsi**	Frasnian	Gogo Formation, Australia	Choo 2012	382.7	379.2
*Moythomasia durgaringa**	Frasnian	Gogo Formation, Australia	Choo 2015; Gardiner & Bartram 1977	382.7	379.2
*Osorioichthys marginis**	Famennian	Famenne Formation, Belgium	Casier 1952; Taverne 1997; Schultze *et al.* 2021	372.2	367.76
*Pickeringius acanthophorus**	Frasnian	Gogo Formation, Australia	Choo *et al.* 2018	382.7	379.2
Raynerius splendens	Frasnian	Ferques Formation, Pas-de-Calais, France	Giles *et al.* 2015	379.2	375.7
Rhadinichthys macconochii	Famennian	East European platform, Russia; Glencartholm, Scotland	Traquair 1881	372.2	330.9
Rhadinichthys tuberculatus	Famennian	East European platform, Russia; Glencartholm, Scotland	Traquair 1881	372.2	330.9
*Tegeolepis clarcki**	Famennian	Cleveland shale, Ohio shale member, USA	Schultze *et al.* 2021; Miller 1892	363.33	358.9

CARBONIFEROUS					
MISSISSIPPIAN					
Acanthoniscus cracens	Serpukhovian	Heath Formation, Bear Gulch Limestone, Montana, USA	Schultze *et al.* 2021	325.76	323.2
Acrolepis ortholepis	Viséan	Glencartholm, Dumfries and Galloway, Scotland	Traquair 1884	341.43	336.16
Acrolepis wilsoni	Viséan	Coal Measures, Yoredale Rocks, Derbyshire, England	Traquair 1888	346.7	330.9
*Adroichthys tuberculatus**	Viséan	Upper Witteberg Series, Waaipoort Formation (Lake Mentz), Western Cape Province, South Africa	Schultze *et al.* 2021; Gardiner 1969	346.7	330.9
Apholidotos ossna	Serpukhovian	Heath Formation, Bear Gulch Limestone, Montana, USA	Lund 1991	325.76	323.2
Aesopichthys erinaceus	Serpukhovian	Heath Formation, Bear Gulch Limestone, Montana, USA	Poplin & Lund 2000	325.76	323.2
Aestuarichthys fulcratus	Viséan	Upper Witteberg Series, Waaipoort Formation (Lake Mentz), Western Cape Province, South Africa	Schultze *et al.* 2021; Gardiner 1969	346.7	330.9
Aetheretmon valentiacum	Tournaisian	Foulden, Scotland; east European platform, Turaŭ, Belarus	Schultze *et al.* 2021; White 1927	350.76	341.43
Atracauda lundi	Serpukhovian	Heath Formation, Bear Gulch Limestone, Montana, USA	Lowney 1991; Schultze *et al.* 2021	325.76	323.2
Australichthys longidorsalis	Viséan	Upper Witteberg Series, Waaipoort Formation (Lake Mentz), Western Cape Province, South Africa	Schultze *et al.* 2021; Gardiner 1969	346.7	330.9
Avonichthys manskyi	Tournaisian	Horton Bluff Formation, Nova Scotia, Canada	*Wilson et al.* 2018	358.9	350.76
*Beagiascus pulcherrimus**	Serpukhovian	Heath Formation, Bear Gulch	Mickle *et al.* 2009	325.76	323.2

		Limestone, Montana, USA			
Benedenius deneensis	Viséan	Molignée, Belgium	Mottequin *et al.* 2015; Traquair 1877	346.7	341.43
Benedenius soreili	Viséan	Molignée, Belgium	Mottequin *et al.* 2015; Fraipont 1890	346.7	341.43
Bishofia lucida	Tournaisian	Minusinsk, Russia	Kazantseva 1968	358.9	346.7
Blairolepis loanheadensis	Serpukhovian	Loanhead (Scotland)	Lowney 1983; Schultze *et al.* 2021	330.9	328.83
Bluefieldius mercerensis	Viséan	Bluefield Formation, West Virginia, USA	Mickle 2018	336.16	328.83
Bourbonnella jocelynae	Serpukhovian	Manning Canyon, Shale Formation, Utah, USA	Mickle 2011	330.9	320.53
*Canobius elegantulus**	Viséan	Glencartholm, Dumfries and Galloway, Scotland	Schultze *et al.* 2021; Moy-Thomas & Dyne 1938; Traquair 1881	341.43	336.16
Canobius modulus	Tournaisian	Albert Formation New Brunswick	Dawson 1877	358.9	346.7
*Canobius ramsayi**	Viséan	Glencartholm, Eksdale, Dumfries and Galloway, Scotland	Schultze *et al.* 2021; Moy-Thomas & Dyne 1938; Wood 1982; Traquair 1881	341.43	336.16
*Cheirodopsis geikiei**	Viséan	Glencartholm, Dumfries and Galloway, Scotland	Schultze *et al.* 2021; Moy-Thomas & Dyne 1938; Wood 1982; Traquair 1881	341.43	336.16
*Cosmoptychius striatus**	Viséan	Wardie, Scotland	Dineley et Metclaf 1999; Gardiner 1963; Watson 1928	335.5	333.5
Cryphiolepis striatus	Serpukhovian	Borough Lee Ironstone, Edge Coal Series, Loanhead locality, Scotland	Schultze *et al.* 2021; Traquair 1907; Traquair 1881	330.3	328.33
Cycloptychius bidens	Viséan	Glencartholm, Dumfries and Galloway, Scotland	Matveeva 1958	341.43	336.16
*Cycloptychius concentricus**	Viséan	Glencartholm, Dumfries and Galloway, Scotland	Schultze *et al.* 2021; Moy-Thomas & Dyne 1938; Traquair 1881	341.43	336.16

Cyranorhis bergeraci	Serpukhovian	Heath Formation, Bear Gulch Limestone, Montana, USA	Schultze *et al.* 2021; Lund & Poplin 1997	325.76	323.2
Discoserra pectinodon	Serpukhovian	Heath Formation, Bear Gulch Limestone, Montana, USA	Lund 2000	325.76	323.2
Drydenius insignis	Serpukhovian	Loanhead (Scotland)	Traquair 1890	330.3	328.33
Dwykia analensis	Viséan	Upper Witteberg Series, Soetendals Vlei, Eastern Cape province, South Africa	Gardiner 1969	346.7	330.9
Elonichthys browni	Tournaisian	Albert Formation New Brunswick	Goodarzi *et al.* 2019	358.9	346.7
Elonichthys robisoni	Viséan	Wardie Shales, Forth Bassin (Beds 2-7), Scotland	Schultze *et al.* 2021; Traquair 1901; Hibbert 1835	341.43	336.16
Elonichthys serratus	Viséan	Glencartholm, Dumfries and Galloway, Scotland	Schultze *et al.* 2021; Moy-Thomas & Dyne 1938; Traquair 1881	341.43	336.16
Enzichthys aizenvergi	Serpukhovian	Borehole 7854, Donetsk basin, Ukraine	Selezneva 1988	326.26	323.2
*Fouldenia ischiptera**	Tournaisian	Foulden Fish Bed, Foulden Burn, Berwickshire, Scotland	Schultze *et al.* 2021; Sallan 2013; Sallan & Coates 2013	350.76	346.7
Frederichthys musadentatus	Serpukhovian	Manse Burn Formation, Bearsden Scotland	Coates, 1993	330.9	328.33
Fubarichthys copiosus	Serpukhovian	Heath Formation, Bear Gulch Limestone, Montana USA	Lowney 1980; Schultze *et al.* 2021	325.76	323.2
*Ganolepis gracilis**	Tournaisian	Bystryanskaya Formation, Uzhur, Minusinsk (Russia)	Woodward 1893; Berg 1958; Schultze *et al.* 2021	358.9	346.7
Ganolepis longicauda	Tournaisian	Minusinsk, Russia	Matveeva 1958	358.9	346.7
*Gonatodus punctatus**	Viséan	Wardie, Scotland	Schultze *et al.* 2021; Gardiner 1967; Traquair 1877	335.5	333.5
Grassator bidens	Tournaisian	Minusinsk, Russia	Kazantseva 1968	358.9	346.7
Guildayichthys carnegiei	Serpukhovian	Heath Formation, Bear Gulch	Lund 2000	325.76	323.2

		Limestone Limestone, Montana, USA			
Guntherichthys lehiensis	Serpukhovian	Manning canyon, Shale Formation, Utah, USA	Mickle 2011	330.9	320.53
*Gyrolepidotus microlepis**	Tournaisian	Minusinsk, Russia	Berg 1958; Schultze *et al.* 2021	358.9	346.7
*Gyrolepidotus schmidti**	Tournaisian	Bystryanskaya Formation, Uzhur, Minusinsk (Russia)	Berg 1958; Schultze *et al.* 2021; Rohon 1889	358.9	346.7
Holurus parki	Viséan	Glencartholm, Dumfries and Galloway, Scotland	Moy-Thomas & Dyne 1938; Traquair 1881	341.43	336.16
*Kalops diophrys**	Serpukhovian	Heath Formation, Bear Gulch Limestone, Montana, USA	Schultze *et al.* 2021; Poplin & Lund 2002	325.76	323.2
*Kalops monophrys**	Serpukhovian	Heath Formation, Bear Gulch Limestone, Montana, USA	Schultze *et al.* 2021; Poplin & Lund 2002	325.76	323.2
Kansania eatoni	Kasimovian	Douglas Group, Lawrence Formation, Haskell Limestone Member, Douglas County, Kansas, USA	Poplin 1974; I.U.G.S. Subcommission on Carboniferous Stratigraphy 2006	304.8	303.7
Kentuckia deani	Tournaisian	New Providence Shale Member, Borden Formation, near Junction City, Kentucky	Rayner 1952	350.76	341.43
*Lambeia pectinatus**	Tournaisian	Albert Formation New Brunswick	Mickle 2017	358.9	346.7
*Lineagruan judithi**	Serpukhovian	Heath Formation, Bear Gulch Limestone, Montana, USA	Mickle *et al.* 2009	325.76	323.2
*Lineagruan snowyi**	Serpukhovian	Heath Formation, Bear Gulch Limestone, Montana, USA	Mickle *et al.* 2009	325.76	323.2
*Mansfieldiscus sweeti**	Tournaisian	Bridge creek, Australia	Schultze *et al.* 2021; Long 1988	358.9	350.76
Melanecta anneae	Serpukhovian	Shrimp member, Manse Burn Formation, Bearsden Scotland	Schultze *et al.* 2021; Coates 1998	330.9	328.33
Mentzichthys jubbi	Viséan	Upper Witteberg Series, Waaipoort Formation, Western	Schultze *et al.* 2021; Gardiner 1969	346.7	330.9

		Cape Province, South Africa			
Mentzichthys maraisi	Viséan	Upper Witteberg Series, Waaipoort Formation, Western Cape Province, South Africa	Schultze *et al.* 2021; Gardiner 1969	346.7	330.9
Mentzichthys theroni	Viséan	Upper Witteberg Series, Waaipoort Formation (Lake Mentz), Western Cape Province, South Africa	Schultze *et al.* 2021; Gardiner 1969	346.7	330.9
Mentzichthys walshi	Viséan	Upper Witteberg Series, Waaipoort Formation (Lake Mentz), Western Cape Province, South Africa	Jubb 1965	346.7	330.9
Mesonichthys aitkeni	Serpukhovian	Devonshire, England; Belgium, Northern France	Gardiner 1963	330.9	315.2
Mesopoma ardrossense	Viséan	Glencartholm volcanic member, Scotland	Moy-Thomas 1938	341.43	336.16
*Mesopoma carriki**	Serpukhovian	Shrimp member, Manse Burn Formation, Bearsden Scotland	Coates 1993	330.9	328.33
Mesopoma crassum	Viséan	Glencartholm volcanic member, Scotland	Schultze *et al.* 2021; Moy-Thomas & Dyne 1938; Traquair 1913	341.43	336.16
Mesopoma politum	Viséan	Glencartholm volcanic member, Scotland	Schultze *et al.* 2021; Traquair 1881	341.43	336.16
Mesopoma pulchellum	Viséan	Glencartholm volcanic member, Scotland	Schultze *et al.* 2021; Traquair 1881	341.43	336.16
Notacmon crenatus	Viséan	Shales Member of the Gullane Formation, Wardie, Scotland	Schultze *et al.* 2021; Friedman *et al.* 2018; Agassiz 1835	335.5	333.5
*Novogonatodus kasantsevae**	Tournaisian	Snowy plains Formation, Mansfield group, Australia	Holland *et al.*, 2004; Long 1988	358.9	350.76
Oxypteriscus minimus	Tournaisian	Minusinsk, Russia	Matveeva 1958	358.9	346.7
Paphosiscus circulocaudus	Serpukhovian	Heath Formation, Bear Gulch	Grogan & Lund 2015	325.76	323.2

		Limestone, Montana, USA			
Paphosiscus scalmocristus	Serpukhovian	Heath Formation, Bear Gulch Limestone, Montana, USA	Grogan & Lund 2015	325.76	323.2
Paramesolepis rhombus	Viséan	Glencartholm, Dumfries and Galloway, Scotland	Schultze *et al.* 2021; Moy-Thomas & Dyne 1938; Traquair 1890	341.43	336.16
*Paramesolepis tuberculatus**	Viséan	Glencartholm, Dumfries and Galloway, Scotland	Schultze *et al.* 2021; Moy-Thomas & Dyne 1938; Traquair 1890	341.43	336.16
*Paratarrasius hibbardi**	Serpukhovian	Heath Formation, Bear Gulch Limestone, Montana, USA	Lund & Poplin 2002; Lund & Melton 1982	325.76	323.2
Phanerosteon mirabile	Viséan	Glencartholm, Dumfries and Galloway, Scotland	Schultze *et al.* 2021; Traquair 1912; Traquair 1881	341.43	336.16
Phanerosteon ovensi	Tournaisian	Cementstones of Foulden, Scotland	White 1927; Gardiner 1985	358.9	344.5
Platysomus superbus	Viséan	Glencartholm, Dumfries and Galloway, Scotland	Schultze *et al.* 2021; Moy-Thomas & Dyne 1938; Traquair 1881	341.43	336.16
Proceramala montanensis	Serpukhovian	Heath Formation, Bear Gulch Limestone, Montana, USA	Poplin & Lund 2000	325.76	323.2
Proteurynotus traquairi	Viséan	Glencartholm, Dumfries and Galloway, Scotland	Moy-Thomas & Dyne 1938	341.43	336.16
Protohaplolepis scotica	Serpukhovian	Loanhead (Scotland)	Lowney 1983; Schultze *et al.* 2021	330.9	323.2
Pygopterus greenockii	Viséan	Wardie, Scotland; Belgium, Northern France	Traquair 1866	346.7	315.2
Rhadinichthys alberti	Tournaisian	Albert Formation New Brunswick	Lambe 1910	358.9	346.7
Rhadinichthys brevis	Viséan	Wardie Shales, Scotland	Traquair 1877	335.5	333.5
*Rhadinichthys canobiensis**	Viséan	Glencartholm, Dumfries and Galloway, Scotland	Schultze *et al.* 2021; Moy-Thomas & Dyne	341.43	336.16

			1938; Traquair 1909		
Rhadinichthys carinatus	Viséan	Wardie Shale, Scotland	Agassiz 1835	335.5	333.5
Rhadinichthys ferox	Viséan	Wardie Shale, Scotland	Traquair 1877	335.5	333.5
Rhadinichthys formosus	Viséan	Glencartholm, Dumfries and Galloway, Scotland	Traquair 1904	341.43	336.16
*Rhadinichthys fusiformis**	Viséan	Glencartholm, Dumfries and Galloway, Scotland	Moy-Thomas & Dyne 1938; Traquair 1881	341.43	336.16
Rhadinichthys ornatissimus	Viséan	Scotland: Dunnet shale (calciferous sandstone series) of Straiton	Schultze *et al.* 2021; Traquair 1911; Brindley & Spinner 1989; Agassiz 1835	346.7	330.9
Rhadinoniscus wrighti	Viséan	Adross Castle, Scotland	White 1937	336.16	330.9
Senekichthys hirundo	Tournaisian	Herbesskaya Formation, Senek Creek, Southwestern Siberia, Russia	Schultze *et al.* 2021; Prokofiev 2004	350.76	346.7
Soetendalichthys cromptoni	Viséan	Upper Witteberg Series, Soetendals Vlei, Eastern Cape province, South Africa	Gardiner 1969	346.7	330.9
Spinofacia pectinatus	Serpukhovian	Manning canyon, Shale Formation, Utah, USA	Mickle 2011	330.9	320.53
*Strepheoschema fouldenensis**	Tournaisian	Foulden, Scotland; Eastern European platform, Belarus	Schultze *et al.* 2021; White 1927	358.9	346.7
*Styracopterus fulcratus**	Viséan	Glencartholm, Dumfries and Galloway, Scotland; East European Platform, Russia	Schultze *et al.* 2021; Sallan and Coates 2013; Traquair 1881	339	337.5
Sundayichthys elegantulus	Viséan	Upper Witteberg Series, Waaipoort Formation, Western Cape Province, South Africa	Schultze *et al.* 2021; Gardiner 1969	346.7	330.9
Tanypterichthys pridensis	Serpukhovian	Bluestone Formation, Mauch Chunk Group, Virginia, USA	Weems & Windolph 1986	326.26	323.2
*Tarrasius problematicus**	Viséan	Calciferous Sandstone Series, Glencartholm, Dumfriesshire, Scotland	Lund & Poplin 2002; Traquair 1881	341.43	336.16

Trawdenia pancheni	Serpukhovian	Bearsden, Glasgow, Scotland	Coates 1993	330.9	328.83
Wardichthys cyclosoma	Viséan	Wardie, Scotland	Traquair 1875	335.5	333.5
Wendyichthys dicksoni	Serpukhovian	Heath Formation, Bear Gulch Limestone, Montana, USA	Schultze *et al.* 2021; Lund & Poplin 1997	325.76	323.2
Wendyichthys lautreci	Serpukhovian	Heath Formation, Bear Gulch Limestone, Montana, USA	Schultze *et al.* 2021; Lund & Poplin 1997	325.76	323.2
*Willomorichthys striatulus**	Viséan	Upper Witteberg Series, Waaipoort Formation, Western Cape Province, South Africa	Gardiner 1969	346.7	330.9
*Woodichthys bearsdeni**	Serpukhovian	Shrimp member, Manse Burn Formation, Bearsden Scotland	Schultze *et al.* 2021; Coates 1998	330.9	328.33
*Yogoniscus gulo**	Serpukhovian	Heath Formation, Bear Gulch Limestone, Montana, USA	Lowney 1991; Schultze *et al.* 2021	325.76	323.2
PENNSYLVANIAN					
Acentrophorus dispersus	Gzhelian	Kounov, Czech Republic	Fritsch 1894	303.5	298.9
Acrolepis gigas	Gzhelian	Slany Formation, Central bohemia basin, Czech Republic	Stamberg 1991; Fritsch 1877	303.5	302.5
Andrewsolepis lochlani	Bashkirian	Lower Coal Measure, Wester Bracco, Scotland	Elliott 2018	317.86	312.46
Aeduella blainvillei	Kasimovian	Bassin d'Autun/Montceau-les-Mines, France	Poplin & Dutheil 2005; Heyler & Poplin 1983; Westoll 1937	307	303.7
*Amphicentrum granulosum**	Moscovian	Knowles Ironstone band of the Winghay Coal in Fenton Colliery, Fenton, Staffordshire, England	Schultze *et al.* 2021; Dyne 1939; Traquair 1880; Young 1866; Elliott 2018	314.75	310
Amphicentrum orbiculare	Moscovian	Francis Creek Shale Member, Carbondale Formation, Illinois, USA	Zidek 1992; Newberry & Worthen 1870	312.46	307
Amphicentrum jurgenai	Kasimovian	Kinney Quarry, New-Mexico, USA	Zidek 1992	307	304.8

Blairolepis wallacei	Bashkirian	Lower Coal Measure, Wester Bracco, Scotland	Elliott 2018	317.86	312.46
Blanzychthys prorobisoni	Kasimovian	Montceau-les-Mines, Buxières-les-mines, France	Heyler & Poplin 1994	307	303.7
Bourbonnella guilloti	Kasimovian	Montceau-les-Mines, Buxières-les-mines, France	Poplin & Dutheil 2005; Heyler 1967	307	303.7
Bourbonnella fourrieri	Kasimovian	Montceau-les-Mines, Buxières-les-mines, France	Poplin 2001	307	303.7
Braccohaplolepis fenestratum	Bashkirian	Lower Coal Measure, Wester Bracco, Scotland	Elliott 2018	317.86	312.46
Coccocephalus baldwinensis	Kasimovian	Douglas Group, Lawrence Formation, Haskell Limestone Member, Douglas County, Kansas, USA	Poplin 1974; I.U.G.S. Subcommission on Carboniferous Stratigraphy 2006	304.8	303.7
*Coccocephalus wildi**	Bashkirian	Mountain Fourfoot Mine of Trawden, Lancashire, England	Poplin & Véran 1996; Schultze *et al.* 2021; Watson 1925	317.86	312.46
Commentrya barroisi	Kasimovian	Saarland, Germany	Waterlot 1934	304.8	303.7
*Commentrya traquairi**	Gzhelian	Commentry, France	Schultze *et al.* 2021; Sauvage 1888	303.5	298.9
Cornuboniscus budensis	Bashkirian	Bude Formation, Cornwall, England	White 1939; Schultze *et al.* 2021	319.9	310.7
Decazella vetteri	Moscovian	Decazeville, France	Heyler 1969; Poplin & Dutheil 2005; Heyler 1964	307.5	298.9
Drydenius molyneuxi	Moscovian	Royaume-Uni, Belgium, Germany, France	Traquair 1888	315.2	307
Elonichthys germani	Gzhelian	Sachsen-Anhalt, Germany	Giebel 1848	302.5	298.9
Elonichthys hypsilepis	Moscovian	Carbondale Formation, Mazon Creek, Illinois, USA	Schultze & Bardack 1987; Hay 1900	312.46	307
Elonichthys krejcii	Gzhelian	Plzeň, Bohemia Czech Republic	Schultze *et al.* 2021; Stamberg 1991; Fritsch 1895	303.5	302.5
Elonichthys peltigerus	Moscovian	Carbondale Formation, Linton, Ohio, Mazon Creek, Illinois	Schultze & Bardack 1987; Newberry 1856	312.46	307
Gyrolepis speciosus	Gzhelian	Puertollano basin Spain	Fritsch 1877	302.84	302.5

Haplolepis corrugata	Moscovian	Linton, Ohio, USA	Schultze *et al.* 2021; Elliott 2014; Miller 1892	310	307.26
Huanghelepis pani	Bashkirian	Zhongwei, Ningxia, China	Lu 2002	323.2	315.2
Igornella comblei	Kasimovian	Montceau-les-Mines, Buxières-les-mines, France	Heyler & Poplin 1994	307	303.7
Illiniichthys cozarti	Moscovian	Mazon Creek, Illinois, USA	Schultze & Bardack 1987	310	309.09
Kansania eatoni	Kasimovian	Douglas Group, Lawrence Formation, Haskell Limestone Member, Douglas County, Kansas, USA	Poplin 1974; I.U.G.S. Subcommission on Carboniferous Stratigraphy 2006	304.8	303.7
Lanarkichthys gardineri	Bashkirian	Lower Coal Measures, Wester Bracco, Scotland	Elliott 2018	317.86	312.46
Lawrenciella schaefferi	Kasimovian	Douglas Group, Lawrence Formation, Haskell Limestone Member, Douglas county, near Lawrence, Kansas, USA	Poplin 1974; I.U.G.S. Subcomission on Carboniferous Stratigraphy 2006	304.8	303.7
Meisenheimichthys glanensis	Gzhelian	Basal Rotliegend, Remigiusberg and Altenglan Formation, Saar-Nahe basin, Germany	Schindler 2006	303.7	298.9
Mesolepis arabellae	Bashkirian	Upper Drumgray Coal shale, Wester Bracco, South Lanarkshire, Scotland	Elliott & Giles 2024	323.2	315.2
*Mesolepis scalaris**	Moscovian	Knowles Ironstone Member, Pennine Middle Coal Measures Formation, England	Schultze *et al.* 2021; Sallan and Coates 2013; Young 1866	315.2	307
Mesolepis wardi	Bashkirian	Knowles Ironstone Member, Pennine Middle Coal Measures Formation, England	Young 1866	317.86	312.46
Microhaplolepis ovoidea	Moscovian	Linton, Ohio, USA	Schultze *et al.* 2021; Lowney 1980; Newberry 1856	310	307.26
Microhaplolepis serrata	Moscovian	Linton, Ohio, USA; Upper Freeport Coal	Schultze *et al.* 2021; Lowney 1980; Newberry 1856	309.09	307.26

Ningxiaplatysomus parvus	Bashkirian	Tupo Formation, Daliushu Village, Zhongwei, Ningxia Hui Autonomous Region, China	Tan *et al.* 2015; Prokop & Ren 2007	323.2	315.2
*Parahaplolepis tuberculata**	Moscovian	Linton, Ohio, USA	Schultze *et al.* 2021; Westoll 1944; Newberry 1856	310	307.26
Paramblypterus comblei	Kasimovian	Autun basin, France	Heyler 1969	307	303.7
Paramblypterus decorus	Kasimovian	Bassin d'Autun/Montceau-les-Mines	Dietze 2000; Heyler & Poplin 1983; Blot 1966	307	303.7
Phanerorhynchus armatus	Moscovian	Middle Coal Measure, Lancashire England	Schultze *et al.* 2021; Moy-Thomas 1971; Gardiner 1967; Gill 1923	312.46	310.7
Platysella lallyi	Kasimovian	Montceau-les-Mines, Buxières-les-mines, France	Heyler & Poplin 1983	307	303.7
Protohaplolepis isabella	Bashkirian	Lower Coal Measure, Wester Bracco, Scotland	Elliott 2015	317.86	312.46
Protohaplolepis limnades	Bashkirian	Lower Coal Measure, Wester Bracco, Scotland	Elliott 2015	317.86	312.46
Protohaplolepis traquairi	Bashkirian	Lower Coal Measure, Wester Bracco, Scotland	Elliott 2015	317.86	312.46
Pseudogonatodus aurulentum	Bashkirian	Lower Coal Measure, Wester Bracco, Scotland	Elliott 2018	317.86	312.46
Pseudohaplolepis argentatum	Bashkirian	Lower Coal Measure, Wester Bracco, Scotland	Elliott 2018	317.86	312.46
Puertollanichthys ritchiei	Gzhelian	Puertollano basin Spain	Schultze *et al.* 2021; Poplin & Dutheil 2005; Forey & Young, 1985	302.84	302.5
Pyritocephalus lineatus	Moscovian	Linton and Five Points, Ohio, USA	Schultze *et al.* 2021; Westoll 1944; Newberry 1856	310	307.26
Pyritocephalus lowneyae	Kasimovian	Kinney Brick Quarry, New-Mexico, USA	Huber 1992	304.8	303.7
Pyritocephalus rudis	Bashkirian	Northumberland, England	Westoll 1944	317.86	315.2
Pyritocephalus sculptus	Moscovian	Nýřany, Bohemia, Czech Republic	Schultze *et al.* 2021; Westoll	309.73	305.9

			1944; Stamberg 2006; Fritsch 1875		
Pyritocephalus youngi	Bashkirian	Lower Coal Measure, Wester Bracco, Scotland	Elliott 2015	317.86	312.46
Rhadinichthys glabrolepis	Bashkirian	Lower Coal Measure, North Lanarkshire, Scotland	Elliott 2018	317.86	312.46
Rhadinichthys grossarti	Bashkirian	Lower Coal Measure, North Lanarkshire, Scotland	Elliott 2018	317.86	312.46
Rhadinichthys hancocki	Bashkirian	Northumberland, England; North Lanarkshire, Scotland	Atthey 1875	317.86	312.46
Rhadinichthys lerichei	Moscovian	Belgium; North of France	Pruvost 1919	310	307.26
Rhadinichthys monensis	Bashkirian	Scotland; Belgium; Northern France	Egerton 1850	317.86	312.46
Sceletophorus biserialis	Moscovian	Nýřany Member, Central western Bohemia	Schultze *et al.* 2021; Stamberg 1991, 2006; Fritsch 1894	309.73	305.9
Schizolepis manzanitaensis	Kasimovian	Kinney Quarry, New Mexico USA	Schultze *et al.* 2021; Gottfried 1993; Lucas *et al.* 2011	307	304.8
Setlikia bohemica	Gzhelian	Kroucova, Rakovnik district, Kladno-Rakovnik Basin, Bohemia, Czech Republic	Stamberg & Zajíc 1994	303.5	302.5
*Sphaerolepis kounoviensis**	Gzhelian	Kounov Basin, Bohemian Basin, Czech Republic	Schultze *et al.* 2021; Stamberg 1991; Fritsch 1877	303.5	298.9
*Tanyrhinichthys mcallisteri**	Kasimovian	Kinney Quarry, New Mexico, USA	Schultze *et al.* 2021; Stack *et al.* 2020; Lucas *et al.* 2011; Gottfried, 1987	307	304.8
*Trawdenia planti**	Bashkirian	Lancashire England	Coates & Tietjen 2018	317.86	312.46
Whiteichthys greenlandicus	Bashkirian	North Scoresby Land, Mester Vig Formation, East Greenland	Schultze *et al.* 2021; Moy-Thomas 1942; Milan *et al.* 2016	317.86	312.46
Zaborichthys fragmentalis	Gzhelian	Bohemia, Czech Republic	Stamberg 1989	303.5	302.5
Zhongweilepis macilentus	Bashkirian	Tupo Formation, Daliushu Village, Zhongwei, Ningxia Hui Autonomous Region, China	Tan 2017; Prokop & Ren 2007	323.2	315.2

Table S2. Description of landmarks and semilandmarks for the skull analyses.

N°	Nature of the descriptor	Description
		Body shape
1	Landmark	Most dorsal anterior margin of the nasal
2	Landmark	Most ventral anterior margin of the nasal
3	Landmark	Most anterior margin of the orbit
4	Landmark	Most anterior ventral margin of the dermosphenotic
5	Landmark	Most anterior dorsal tip of the premaxillary
6	Landmark	Most anterior ventral tip of the maxillary
7	Landmark	Most anterior dorsal tip of the dentary
8	Landmark	Most anterior dorsal tip of the maxillary
9	Landmark	Most anterior dorsal extremity of the jugal
10	Landmark	Most anterior ventral extremity of the jugal
11	Landmark	Most posterior margin of the orbit
12	Landmark	Most ventral extremity of the dermosphenotic behind the orbit
13	Landmark	Tip of the anterior-dorsal angle of the preopercular
14	Landmark	Tip of the anterior-ventral angle of the preopercular
15	Landmark	Tip of the anterior-dorsal angle of the operculum
16	Landmark	Tip of the anterior-ventral angle extremity of the operculum
17	Landmark	Posterior extremity of the operculum
18	Landmark	Tip of the posterior-ventral angle of the preopercular
19	Landmark	Tip of the anterior-ventral angle of the preopercular
20	Landmark	Tip of the anterior-ventral angle extremity of the suboperculum
21	Landmark	Tip of the posterior-ventral angle extremity of the suboperculum
22	Landmark	Most posterior ventral extremity of the maxillary
23	Landmark	Most posterior dorsal extremity of the dentary
24-53	Semi-landmarks	Dorsal opercular outline from landmark 15 to 17
54-73	Semi-landmarks	Dorsal preopercular outline from landmark 13 to 18
74-113	Semi-landmarks	Dorsal maxillary outline from landmark 8 to 19
114-143	Semi-landmarks	Ventral dentary outline from landmark 7 to 23
144-163	Semi-landmarks	Anterior nasal outline from landmark 2 to 1
164-173	Semi-landmarks	Dorsal orbit outline from landmark 3 to 11

Modularity *a priori* hypotheses

Jaw constituted a major innovation in the history of vertebrates (Khaner, 2007; Mallatt, 1996; Miyashita, 2016). Extant fishes show high disparity in jaw morphology, which tends to correlate with their feeding mechanics (Albertson et al. 2003; Konow et al. 2008; Wainwright et al., 2004; Wainwright and Richard, 1995). Furthermore, gnathostome jaws showed recurrent modifications in their anatomy such as the progressive complexification of the dermal bones associated with the lower jaws of "placoderms" (Young, 2010; Zhu et al. 2019), the variation of jaw musculature in actinopterygians (Datovo and Rizzato, 2018; Friel

and Wainwright, 1999; Wainwright et al. 2015; Westneat, 2004), and the variation of jaw kinematics in aquatic vertebrates (Bellwood et al. 2015; Hulsey et al. 2005; Wainwright et al. 2015). Early history of jawed vertebrates is marked by the rapid reach of a maximum functional diversity in jaw morphology during the Devonian, mostly within "placoderms" and sarcopterygians (Anderson et al., 2011) with some extreme forms such as *Alienacanthus* (Jobbins et al. 2024). All these functional properties of the jaw anatomy constitute evidence that the jaw could be a variational module.

Vision and more broadly eye positioning and diameter are closely related to habitats and feeding behaviors in fishes (Goatley and Bellwood, 2009; Ingram and Shurin, 2009; Warrant and Locket, 2004). Furthermore, Cooper et al. (2010) proposed the preorbital region as a module related to trophic biomechanics that has strong association with the radiations of the African Rift-Lake cichlids. At least for teleosts, the modularity of this region is also supported by craniofacial variation in zebrafish mutants for which the length of the snout is modified (Albertson and Yelick, 2007; Cooper et al. 2013; LeClair et al. 2009). These ecological, functional and developmental arguments support the hypothesis of the preorbital region being a variational module.

The opercular series and cheek bones, plays a key role in the breathing and the feeding behavior of fishes and exhibits great diversity within both extant and extinct fishes (Ascarrunz et al. 2019; Lauder, 1980; Schultze et al. 2008; Wainwright and Bellwood, 2002; Zhu et al., 1999). Despite the disparity of this region among the species, the functional property of the opercular series could beneficiate from the morphological integration of its structures which could support this region as a hypothesized variational module.

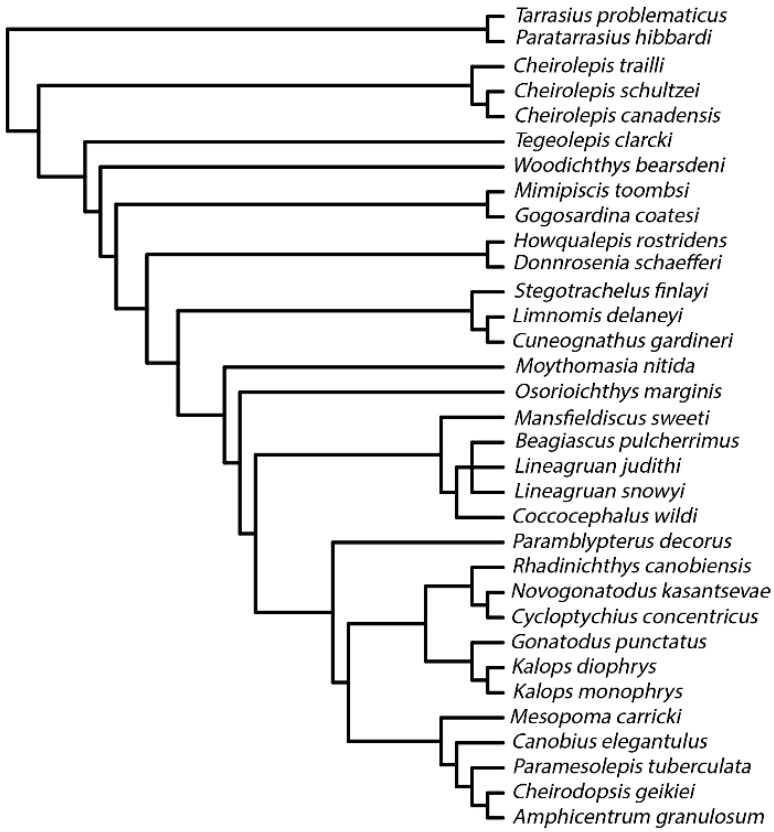


Figure S1. Phylogenetic relationships among 33 species of early actinopterygians. The topology is based on the parsimony analysis performed by Mickle (2012).

Table S3. Results of modularity testing on 33 species using the CR metric and morphological integration using PLS analyses. The bold results correspond to the phylogenetic constrained analyses.

Hypothesis	CR coefficient			Morphological integration	
	CR	*p-value*	Z_{CR}	PLS	p-value
1	0.871	0.001	-18.47	0.900	0.001
	0.750	**0.001**	**-14.52**	**0.819**	**0.001**
2	0.859	0.001	-16.61	0.883	0.001
	0.745	**0.001**	**-12.44**	**0.791**	**0.001**
3	0.928	0.001	-14.49	0.951	0.001
	0.843	**0.001**	**-12.93**	**0.895**	**0.001**
4	0.931	0.001	-12.99	0.958	0.001
	0.883	**0.001**	**-12.18**	**0.92**	**0.001**

References Annexe IV

Albertson, R. C., J. T. Streelman, and T. D. Kocher. 2003. 'Directional selection has shaped the oral jaws of lake malawi cichlid fishes'. Proceedings of the National Academy of Sciences 100 (9): 5252–57.

Albertson, R. C., and P. C. Yelick. 2007. '*Fgf8* haploinsufficiency results in distinct craniofacial defects in adult zebrafish'. Developmental Biology 306 (2): 505–15.

Anderson, P. S. L., M. Friedman, M. D. Brazeau, and E. J. Rayfield. 2011. 'Initial radiation of jaws demonstrated stability despite faunal and environmental change'. Nature 476 (7359): 206–9.

Ascarrunz, E., M. R. Sánchez-Villagra, R. Betancur-R, and M. Laurin. 2019. 'On trends and patterns in macroevolution: Williston's law and the branchiostegal series of extant and extinct osteichthyans'. BMC Evolutionary Biology 19 (1): 117.

Bellwood, D. R., C. H. R. Goatley, O. Bellwood, D. J. Delbarre, and M. Friedman. 2015. 'The rise of jaw protrusion in spiny-rayed fishes closes the gap on elusive prey'. Current Biology 25 (20): 2696–700.

Cooper, W. J., K. Parsons, A. McIntyre, B. Kern, A. McGee-Moore, and R. C. Albertson. 2010. 'Bentho-pelagic divergence of cichlid feeding architecture was prodigious and

consistent during multiple adaptive radiations within African Rift-Lakes'. PLOS One 5 (3): e9551.

Cooper, W. J., R. M. Wirgau, E. M. Sweet, and R. C. Albertson. 2013. 'Deficiency of zebrafish *fgf20a* results in aberrant skull remodeling that mimics both human cranial disease and evolutionarily important fish skull morphologies'. Evolution & Development 15 (6): 426–41.

Datovo, A., and P. P. Rizzato. 2018. 'Evolution of the facial musculature in basal ray-finned fishes'. Frontiers in Zoology 15 (1): e40.

Friel, J. P., and P. C. Wainwright. 1999. 'Evolution of complexity in motor patterns and jaw musculature of tetraodontiform fishes'. Journal of Experimental Biology 202 (7): 867–80.

Goatley, C. H. R., and D. R. Bellwood. 2009. 'Morphological structure in a reef fish assemblage'. Coral Reefs 28 (2): 449–57.

Hulsey, C. D., G. J. Fraser, and J. T. Streelman. 2005. 'Evolution and development of complex biomechanical systems: 300 million years of fish jaws'. Zebrafish 2 (4): 243–57.

Ingram, T., and J. B. Shurin. 2009. 'Trait-based assembly and phylogenetic structure in northeast pacific rockfish assemblages'. Ecology 90 (9): 2444–53.

Jobbins, M., M. Rücklin, M. R. Sánchez Villagra, et al. 2024. 'Extreme lower jaw elongation in a placoderm reflects high disparity and modularity in early vertebrate evolution'. Royal Society Open Science 11 (1): e231747.

Khaner, O.. 2007. 'Evolutionary innovations of the vertebrates'. Integrative Zoology 2 (2): 60–67.

Konow, N., D. R. Bellwood, P. C. Wainwright, and A. M. Kerr. 2008. 'Evolution of novel jaw joints promote trophic diversity in coral reef fishes'. Biological Journal of the Linnean Society 93 (3): 545–55.

Lauder, G. V. 1982. 'Patterns of evolution in the feeding mechanism of actinopterygian fishes'. American Zoologist 22 (2): 275–85.

LeClair, E. E., Stephanie R. M., A. Huang, J. M. Topczewska, and J. Topczewski. 2009. 'Craniofacial skeletal defects of adult zebrafish *glypican 4* (*knypek*) mutants'. Developmental Dynamics 238 (10): 2550–63.

Mallat, J. 1996. 'Ventilation and the origin of jawed vertebrates: a new mouth'. Zoological Journal of the Linnean Society 117 (4): 329–404.

Mickle, K. E. 2012. ‘Unraveling the systematics of palaeoniscoid fishes--lower actinopterygians in need of a complete phylogenetic revision’. University of Kansas. Thesis.

Miyashita, T. 2016. ‘Fishing for jaws in early vertebrate evolution: a new hypothesis of mandibular confinement’. Biological Reviews 91 (3): 611–57.

Wainwright, P. C., D. R. Bellwood, M. W. Westneat, J. R. Grubich, and A. S. Hoey. 2004. ‘A functional morphospace for the skull of labrid fishes: patterns of diversity in a complex biomechanical system’. Biological Journal of the Linnean Society 82 (1): 1–25.

Wainwright, P. C., M. D. McGee, S. J. Longo, and L. P. Hernandez. 2015. ‘Origins, innovations, and diversification of suction feeding in vertebrates’. Integrative and Comparative Biology 55 (1): 134–45.

Wainwright, P. C., and B. A. Richard. 1995. ‘Predicting patterns of prey use from morphology of fishes’. Environmental Biology of Fishes 44 (1): 97–113.

Westneat, M.. W. 2005. ‘Skull biomechanics and suction feeding in fishes’. Fish Physiology 23: 29-75.

Young, G. C. 2010. ‘Placoderms (armored fish): dominant vertebrates of the Devonian period’. Annual Review of Earth and Planetary Sciences 38: 523–50.

Zhu, Y.-A., P. A. Ahlberg, and M. Zhu. 2019. ‘The evolution of vertebrate dermal jaw bones in the light of maxillate placoderms’. Evolution and Development of Fishes 1: 71-86.

ANNEXE V

SUPPLEMENTARY INFORMATION FOR CHAPTER 4: ECOMORPHOLOGY OF JAWED VERTEBRATES DURING THE SILURIAN-CARBONIFEROUS AND THE DYNAMICS OF SHARED AND INNOVATIVE ECOMORPHOSPACES

Table S1. List of the 374 gnathostome species included in analyses. Species with more than 60% of missing data are indicated with an asterisk (*). FAD (first appearance datum) corresponds to the first time the species appears in the fossil record, and LAD (last appearance datum) to the last time it appears.

Species	Class	Period	FAD	LAD	References
Albula vulpes	Actinopterygii	Extant	*NA*	*NA*	Fishbase
Balistapus undulatus	Actinopterygii	Extant	*NA*	*NA*	Fishbase
Callorhinchus milii	Chondrichthyes	Extant	*NA*	*NA*	Fishbase
Carcharhinus melanopterus	Chondrichthyes	Extant	*NA*	*NA*	Fishbase
Cottus gobio	Actinopterygii	Extant	*NA*	*NA*	Fishbase
Cryptobranchus alleganiensis	Sarcopterygii	Extant	*NA*	*NA*	Fishbase
Ctenochaetus striatus	Actinopterygii	Extant	*NA*	*NA*	Fishbase
Gnathodentex aureolineatus	Actinopterygii	Extant	*NA*	*NA*	Fishbase
Labrus bergylta	Actinopterygii	Extant	*NA*	*NA*	Fishbase
Poroderma africanum	Chondrichthyes	Extant	*NA*	*NA*	Fishbase
Protopterus annectens	Sarcopterygii	Extant	*NA*	*NA*	Fishbase
Raja montagui	Chondrichthyes	Extant	*NA*	*NA*	Fishbase
Spectrunculus grandis	Actinopterygii	Extant	*NA*	*NA*	Fishbase
Squalus acanthias	Chondrichthyes	Extant	*NA*	*NA*	Fishbase
Trachurus trachurus	Actinopterygii	Extant	*NA*	*NA*	Fishbase
Zebrasoma velifer	Actinopterygii	Extant	*NA*	*NA*	Fishbase
Acanthodes bridgei	'Acanthodii'	Carboniferous	303.7	298.9	Zidek 1976
Acanthodes lopatini	'Acanthodii'	Carboniferous	358.9	354.83	Beznosov 2009; Rohon 1989
Acanthostega gunarri	Sarcopterygii	Devonian	363.33	358.9	Coates 1996; Clack *et al.*2012; Jarvik 1952
Acrolepis gigas	Actinopterygii	Carboniferous	303.5	302.5	Stamberg 1991; Fritsch 1877
Adroichthys tuberculatus	Actinopterygii	Carboniferous	346.7	330.9	Schultze *et al.*2021; Gardiner 1969
Aeduella blainvillei	Actinopterygii	Carboniferous	307	303.7	Poplin and Dutheil 2005; Heyler and Poplin 1983; Westoll 1937
Aesopichthys erinaceus	Actinopterygii	Carboniferous	325.76	323.2	Poplin and Lund 2000
Aestuarichthys fulcratus	Actinopterygii	Carboniferous	346.7	330.9	Schultze *et al.* 2021; Gardiner 1969

Aetheretmon valentiacum	Actinopterygii	Carboniferous	350.76	341.43	Schultze *et al.* 2021; White 1927
Africanaspis doryssa	'Placodermi'	Devonian	363.33	358.9	Gess and Trinajstic 2017; Long *et al.* 1997
Africanaspis edmountaini	'Placodermi'	Devonian	363.33	358.9	Gess and Trinajstic 2017
Akmonistion zangerli	Chondrichthyes	Carboniferous	330.9	328.33	Coates and Sequeira 2001
*Aleosteus eganensis**	'Placodermi'	Devonian	398.06	393.3	Johnson *et al.* 2000
*Alienacanthus malkowskii**	'Placodermi'	Devonian	367.76	363.33	Kulczycki 1957; Jobbins *et al.* 2024
Allenypterus montanus	Sarcopterygii	Carboniferous	325.76	323.2	Lund and Lund 1985; Melton 1969
Amazichthys trinajsticas	'Placodermi'	Devonian	367.76	363.33	Jobbins *et al.* 2022
Amphicentrum granulosum	Actinopterygii	Carboniferous	314.75	310	Schultze *et al.* 2021; Dyne 1939; Traquair 1880; Young 1866; Elliott 2018
Antarctilamna ultima	Chondrichthyes	Devonian	363.33	358.9	Gess and Coates 2015
Anthracobamus fayoli	Sarcopterygii	Carboniferous	303.5	298.9	Werneburg 2019; Thevenin, 1906
*Arctolepis decipiens**	'Placodermi'	Devonian	407.6	393.3	Goujet 1984; Woodward 1891
*Asterolepis maxima**	'Placodermi'	Devonian	384.36	372.2	Olive 2015; Agassiz 1844; Newman and den Blaauwen 2018
Asterolepis ornata	'Placodermi'	Devonian	384.36	379.2	Moloshnikov 2012; Eichwald 1840; Carr 1995
Australichthys longidorsalis	Actinopterygii	Carboniferous	346.7	330.9	Schultze *et al.* 2021; Gardiner 1969
Austrophyllolepis ritchiei	'Placodermi'	Devonian	382.7	379.2	Long 1983
Austrophyllolepis youngi	'Placodermi'	Devonian	382.7	379.2	Long 1983
Balanerpeton woodi	Sarcopterygii	Carboniferous	330.9	330.3	Miner and Sequeira 1993
Bandringa herdinae	Chondrichthyes	Carboniferous	309.73	307	Zangerl 1979; Sallan and Coates 2014; Zangerl 1969
Bandringa rayi	Chondrichthyes	Carboniferous	309.73	307	Zangerl 1969; Sallan and Coates 2014; Zangerl 1969
*Baphetes bohemicus**	Sarcopterygii	Carboniferous	310.7	307.5	Miller *et al.*2009; Fritsch 1889
Barameda decipiens	Sarcopterygii	Carboniferous	358.9	354.83	Long 1989; Cloutier *et al.* 2020 (supp.); Woodward 1906
Barameda mitchelli	Sarcopterygii	Carboniferous	358.9	354.83	Long 1989; Jeffery 2012; Holland *et al.* 2007
Barwickia dowunda	Sarcopterygii	Devonian	382.7	379.2	Long and Clement 2009; Long 1992

Beagiascus pulcherrimus	Actinopterygii	Carboniferous	325.76	323.2	Mickle *et al.* 2009
Bealbonn rogaire	Chondrichthyes	Carboniferous	325.76	323.2	Lund and Grogan 2004 in Arratia *et al.* 2004
*Beelarongia patrichae**	Sarcopterygii	Devonian	382.7	379.2	Long and Clement 2009; Long 1987
Belantsea montana	Chondrichthyes	Carboniferous	325.76	323.2	Lund 1989
Benedenius deneensis	Actinopterygii	Carboniferous	346.7	341.43	Mottequin *et al.* 2015; Traquair 1877
Benedenius soreili	Actinopterygii	Carboniferous	346.7	341.43	Mottequin *et al.* 2015; Fraipont 1890
Bollandaspis woschmidti	'Placodermi'	Devonian	407.6	402.83	Schmidt 1976
Bothriolepis africana	'Placodermi'	Devonian	363.33	358.9	Long *et al.* 1997
Bothriolepis canadensis	'Placodermi'	Devonian	379.2	375.7	Béchard *et al.* 2014; Whiteaves 1980
Bothriolepis cullodenensis	'Placodermi'	Devonian	382.7	379.2	Long and Werdelin 1986; Long 1983
Bothriolepis evaldi	'Placodermi'	Devonian	379.2	375.7	Lukševičs 2001; Lyarskaja 1986
Bothriolepis fergusoni	'Placodermi'	Devonian	382.7	379.2	Long and Werdelin 1986; Long 1983
Bothriolepis gippslandiensis	'Placodermi'	Devonian	382.7	379.2	Long and Werdelin 1986; Hills 1929
Bourbonnella guilloti	Actinopterygii	Carboniferous	307	303.7	Poplin and Dutheil 2005; Heyler 1967
Brachyacanthus scutiger	'Acanthodii'	Devonian	419.2	416.4	Watson 1937 in Denison 1979; Egerton 1860
Brachydeirus grandis	'Placodermi'	Devonian	375.7	372.2	
Brachyosteus dietrichi	'Placodermi'	Devonian	375.7	372.2	Gross 1932; Denison 1978
Brochoadmones milesi	'Acanthodii'	Devonian	416.4	413.6	Hanke *et al.* 2006; Bernacsek and Dineley 1977
*Bruehnopteron murphyi**	Sarcopterygii	Devonian	384.36	382.7	Schultze and Reed 2012
Bungartius perissus	'Placodermi'	Devonian	363.33	358.9	Dunkle 1947; Denison 1978
Byssacanthus dilatatus	'Placodermi'	Devonian	398.06	386.03	Eichwald 1844
Cabonnichthys burnsi	Sarcopterygii	Devonian	367.76	363.33	Ahlberg and Johanson 1997
Canobius elegantulus	Actinopterygii	Carboniferous	341.43	336.16	Schultze *et al.* 2021; Moy-Thomas and Dyne 1938; Wood 1982; Traquair 1881
Canobius ramsayi	Actinopterygii	Carboniferous	341.43	336.16	Schultze *et al.* 2021; Moy-Thomas and Dyne 1938; Wood 1982; Traquair 1881
Canowindra grossi	Sarcopterygii	Devonian	367.76	363.33	Long 1985; Thomson 1973

Caridosuctor populosum	Sarcopterygii	Carboniferous	325.76	323.2	Lund and Lund 1984; Torino *et al.* 2021
Caseodus basalis	Chondrichthyes	Carboniferous	309.73	307	Zangerl 1981; Cope 1894
Cassidiceps vermiculatus	‘Acanthodii’	Devonian	416.4	413.6	Gagnier and Wilson 1996
Cervifurca nasuta	Chondrichthyes	Carboniferous	310	309.09	Zangerl 1997
Cheiracanthus grandispinus	‘Acanthodii’	Devonian	389.56	386.03	McCoy 1948; Newman 2010
Cheiracanthus latus	‘Acanthodii’	Devonian	398.06	384.36	Watson 1937 in Denison 1979; Egerton 1861
Cheiracanthus murchisoni	‘Acanthodii’	Devonian	389.56	387.7	Agassiz 1835
Cheiracanthus peachi	‘Acanthodii’	Devonian	389.56	386.03	Den Blaauwen *et al.* 2019
Cheirodopsis geikiei	Actinopterygii	Carboniferous	341.43	336.16	Schultze *et al.* 2021; Moy-Thomas and Dyne 1938; Wood 1982; Traquair 1881
Cheirolepis canadensis	Actinopterygii	Devonian	379.2	375.7	Arratia and Cloutier 1996; Arratia *et al.* 2004; Whiteaves 1881
Cheirolepis schultzei	Actinopterygii	Devonian	384.36	379.2	Arratia and Cloutier 2004; Newman *et al.* 2021
Cheirolepis trailli	Actinopterygii	Devonian	393.3	382.7	Pearson and Westoll 1979; Arratia and Cloutier 2004; Agassiz 1835
Chondrenchelys problematica	Chondrichthyes	Carboniferous	341.43	336.16	Lund 1982; Finarelli and Coates 2014; Traquair 1888
Cladoselache fyleri	Chondrichthyes	Devonian	363.33	358.9	Moy-Thomas and Miles 1971; Newberry 1889
Claradosymblema narrienense	Sarcopterygii	Carboniferous	346.7	336.16	Clement *et al.* 2021; Fox *et al.* 1995
Climatius reticulatus	‘Acanthodii’	Devonian	419.2	410.8	Watson 1937 in Denison 1979; Agassiz 1845; Burrow *et al.* 2015
Cobelodus aculeatus	Chondrichthyes	Carboniferous	310	309.09	Zangerl and Case 1976; Cope 1894
*Coccocephalus wildi**	Actinopterygii	Carboniferous	317.86	312.46	Poplin and Véran 1996; Schultze *et al.* 2021; Watson 1925
Coccosteus cuspidatus	‘Placodermi’	Devonian	389.56	387.7	Miles and Westoll 1968; Miller 1841
Commentrya traquairi	Actinopterygii	Carboniferous	303.5	298.9	Schultze *et al.* 2021; Sauvage 1888

Compagopiscis croucheri	'Placodermi'	Devonian	382.7	379.2	Gardiner and Miller 1994
Cornuboniscus budensis	Actinopterygii	Carboniferous	319.9	310.7	White 1939; Schultze *et al.* 2021
Cosmoptychius striatus	Actinopterygii	Carboniferous	335.5	333.5	Dineley et Metclaf 1999; Gardiner 1963; Watson 1928
Cryphiolepis striatus	Actinopterygii	Carboniferous	330.3	328.33	Schultze *et al.* 2021; Traquair 1907; Traquair 1881
Ctenacanthus costellatus	Chondrichthyes	Carboniferous	341.43	336.16	Moy-Thomas 1936; Brough 1935
Ctenurella gladbachensis	'Placodermi'	Devonian	384.36	379.2	Carr 1995; Ørvig 1960
Culmacanthus stewarti	'Acanthodii'	Devonian	382.7	379.2	Long 1983
Cuneognathus gardineri	Actinopterygii	Devonian	363.33	358.9	Schultze *et al.* 2021; Friedman and Blom 2006
Cycloptychius concentricus	Actinopterygii	Carboniferous	341.43	336.16	Schultze *et al.* 2021; Moy-Thomas and Dyne 1938; Traquair 1881
Cyranorhis bergeraci	Actinopterygii	Carboniferous	325.76	323.2	Schultze *et al.* 2021; Lund and Poplin 1997
*Dabasacanthus inskasi**	Chondrichthyes	Carboniferous	309.73	307	Zangerl 1979
Damocles serratus	Chondrichthyes	Carboniferous	325.76	323.2	Lund 1986
Dayaoshania youngi	'Placodermi'	Devonian	407.6	393.3	Ritchie *et al.* 1992; Wang 1992
Debeerius ellefseni	Chondrichthyes	Carboniferous	325.76	323.2	Grogan and Lund, 2000
Decazella vetteri	Actinopterygii	Carboniferous	307.5	298.9	Heyler 1969; Poplin and Dutheil 2005; Heyler 1964
Deltoptychius armigerus	Chondrichthyes	Carboniferous	350.76	323.2	Traquair 1888; Patterson 1965
*Denaea fournieri**	Chondrichthyes	Carboniferous	346.7	341.43	Maisey 2008 from Fournier and Pruvost 1928; Pruvost 1922
Diademodus hydei	Chondrichthyes	Devonian	363.33	358.9	Harris 1951; Zangerl 1981
Dicksonosteus arcticus	'Placodermi'	Devonian	410.8	407.6	Goujet 1975
Diplacanthus crassisimus	'Acanthodii'	Devonian	393.3	386.03	Miles 1973 in Burrow *et al.*, 2016; Duff 1842
Diplacanthus ellsi	'Acanthodii'	Devonian	379.2	375.7	Gagnier 1996
Diplacanthus horridus	'Acanthodii'	Devonian	379.2	375.7	Cloutier *et al.* 2009; Woodward 1892
Diplacanthus tenuistriatus	'Acanthodii'	Devonian	389.56	384.36	Traquair 1894
Diplocercides heiligenstockiensis	Sarcopterygii	Devonian	384.36	379.2	Jessen 1966; Schultze and Cloutier 1996
Diplodoselache woodi	Chondrichthyes	Carboniferous	335.5	333.5	Dick 1981
Dipterus valenciennesi	Sarcopterygii	Devonian	389.56	387.7	Ahlberg and Trewin 1995; Challands 2015;

					Dineley and Metcalf 1999 (p 171); Sedgwick and Murchison 1829
Discoserra pectinodon	Actinopterygii	Carboniferous	325.76	323.2	Lund 2000
Donnrosenia schaefferi	Actinopterygii	Devonian	387.7	382.7	Schultze *et al.* 2021; Choo 2010; Long *et al.* 2008
Dracopristis hoffmanorum	Chondrichthyes	Carboniferous	307	304.8	Lund *et al.* 2021
Dunkleosteus terrelli	'Placodermi'	Devonian	363.33	358.9	Ferron *et al.* 2017; Newberry 1873
Durialepis edentatus	Sarcopterygii	Devonian	407.6	402.83	Mondéjar-Fernández *et al.* 2021; Otto 2007
Eastmanosteus pustulosus	'Placodermi'	Devonian	382.7	379.2	Boylan 1973
Echinochimaera meltoni	Chondrichthyes	Carboniferous	325.76	323.2	Lund 1977 and 1988
Echinochimaera snyderi	Chondrichthyes	Carboniferous	325.76	323.2	Lund 1988
*Edenopteron keithcrooki**	Sarcopterygii	Devonian	363.33	358.9	Young *et al.* 2019; Young *et al.* 2013
Elonichthys brownii	Actinopterygii	Carboniferous	358.9	346.7	Goodarzi *et al.* 2019
Elonichthys hypsilepis	Actinopterygii	Carboniferous	312.46	307	Schultze and Bardack 1987; Hay 1900
Elonichthys krejcii	Actinopterygii	Carboniferous	303.5	302.5	Schultze *et al.* 2021; Stamberg 1991; Fritsch 1895
Elonichthys peltigerus	Actinopterygii	Carboniferous	312.46	307	Schultze and Bardack 1987; Newberry 1856
Elonichthys pulcherrimus	Actinopterygii	Devonian	363.33	336.16	Schultze *et al.* 2021; Moy-Thomas and Dyne 1938; Traquair 1881
Elonichthys robisoni	Actinopterygii	Carboniferous	341.43	336.16	Schultze *et al.* 2021; Traquair 1901; Hibbert 1835
Elonichthys serratus	Actinopterygii	Carboniferous	341.43	336.16	Schultze *et al.* 2021; Moy-Thomas and Dyne 1938; Traquair 1881
Elpistostege watsoni	Sarcopterygii	Devonian	379.2	375.7	Cloutier *et al.* 2020; Westoll 1938
Entelognathus primordialis	'Placodermi'	Silurian	425.6	419.2	Zhu *et al.* 2013; Cui *et al.* 2023
Erromenosteus concavus	'Placodermi'	Devonian	375.7	372.2	Gross 1932; Denison 1978
Erromenosteus inflatus	'Placodermi'	Devonian	375.7	372.2	Stensiö 1963; Denison 1978
*Eusthenodon waengsjoei**	Sarcopterygii	Devonian	363.33	358.9	Blom *et al.* 2007; Jarvik 1952
Eusthenopteron foordi	Sarcopterygii	Devonian	379.2	375.7	Schultze and Cloutier 1996; Whiteaves 1881

Euthacanthus macnicoli	'Acanthodii'	Devonian	419.2	416.4	Bernacsek and Dineley 1977 (in Denison 1979); Powrie 1864
Falcatus falcatus	Chondrichthyes	Carboniferous	325.76	323.2	Lund 1985; St. John and Worthen 1883
Fallocosteus turneri	'Placodermi'	Devonian	382.7	379.2	Long 1990
Fallodentus davidsoni	'Acanthodii'	Devonian	387.7	386.03	Newman *et al.* 2020
Fleurentia denticulata	Sarcopterygii	Devonian	379.2	375.7	Cloutier 1996; Graham-Mith and Westoll 1937
Fouldenia ischiptera	Actinopterygii	Carboniferous	350.76	346.7	Schultze et al. 2021; Sallan 2013; Sallan and Coates 2013
Frederichthys musadentatus	Actinopterygii	Carboniferous	330.9	328.33	Coates, 1993
Fubarichthys copiosus	Actinopterygii	Carboniferous	325.76	323.2	Lowney 1980; Schultze *et al.* 2021
Ganolepis gracilis	Actinopterygii	Carboniferous	358.9	346.7	Woodward 1893; Berg 1958; Schultze *et al.* 2021; Moseychik and Filimonov
Gavinia syntrips	Sarcopterygii	Devonian	382.7	379.2	Long 1999
Gemuendina stuertzi	'Placodermi'	Devonian	407.6	402.83	Carr 1995; Traquair 1903
*Gerdalepis rhenana**	'Placodermi'	Devonian	391.43	389.56	Beyrich 1877
Gladiobranchus probaton	'Acanthodii'	Devonian	419.2	410.8	Hanke and Davis 2008; Bernacsek and Dineley 1977
Glyptoleamus kinnairdi	Sarcopterygii	Devonian	372.2	358.9	Cloutier (Pers.Com); Huxley 1861
Glyptolepis groenlandica	Sarcopterygii	Devonian	389.56	386.03	Jarvik 1972
Glyptolepis leptopterus	Sarcopterygii	Devonian	389.56	387.7	Agassiz 1844; Newman 2010; Dineley and Metcalf 1999 (p 171)
Gogonasus andrewsae	Sarcopterygii	Devonian	382.7	379.2	Hu *et al.* 2019; Long 1985
Gogopiscis gracilis	'Placodermi'	Devonian	382.7	379.2	Gardiner and Miles, 1994
Gogosardina coatesi	Actinopterygii	Devonian	382.7	379.2	Choo *et al.* 2009
Gogosteus sarahae	'Placodermi'	Devonian	382.7	379.2	Long, 1994
Gonatodus punctatus	Actinopterygii	Carboniferous	335.5	333.5	Schultze *et al.* 2021; Gardiner 1967; Traquair 1877
Goodrichthys eskdalensis	Chondrichthyes	Carboniferous	341.43	336.16	Moy-Thomas 1936
Gooloogongia loomesi	Sarcopterygii	Devonian	367.76	363.33	Johanson and Ahlberg 1998; Cloutier et al. 2020 (supp.)
Gregorius rexi	Chondrichthyes	Carboniferous	325.76	323.2	Lund and Grogan 2004 in Arratia *et al.* 2004
Grenfellaspis branagani	'Placodermi'	Devonian	363.33	358.9	Ritchie *et al.* 1992; Young 1999

Griphognathus sculpta	Sarcopterygii	Devonian	384.36	379.2	Friedman 2007; Schultze 1969
Griphognathus whitei	Sarcopterygii	Devonian	382.7	379.2	Campbell and Barwick 2002; Pridmore and Barwick 1993; Miles 1977
*Groenlandaspis riniensis**	'Placodermi'	Devonian	363.33	358.9	Long *et al.* 1997
Grossilepis rikiki	'Placodermi'	Devonian	363.33	358.9	Olive *et al.* 2016
*Grossilepis tuberculata**	'Placodermi'	Devonian	382.7	379.2	Olive 2015; Gross 1941
Guildayichthys carnegiei	Actinopterygii	Carboniferous	325.76	323.2	Lund 2000
Guiyu oneiros	Sarcopterygii	Silurian	425.6	423	Zhu *et al.* 2009
Gutturensis neilsoni	Chondrichthyes	Carboniferous	330.9	328.33	Sequeira and Coates 2000; Traquair 1998
Gymnotrachelus hydei	'Placodermi'	Devonian	363.33	358.9	Carr 1994; Dunkle and Bungart 1939
Gyracanthides hawkinsi	'Acanthodii'	Carboniferous	341.43	336.16	Turner *et al.* 2005
Gyracanthides murrayi	'Acanthodii'	Carboniferous	358.9	346.7	Warren *et al.* 2000; Woodward 1906
Gyrolepidotus schmidti	Actinopterygii	Carboniferous	358.9	346.7	Berg 1958; Schultze *et al.* 2021; Rohon 1889
Gyroptychius agassizi	Sarcopterygii	Devonian	389.56	387.7	Newman and Dean 2010; Dineley and Metcalf 1999 (p 171); Traill 1841
Hadronector donbairdi	Sarcopterygii	Carboniferous	325.76	323.2	Lund and Lund 1984; Torino *et al.* 2021
Hamiltonichthys mapesi	Chondrichthyes	Carboniferous	302.1	300.5	Maisey 1989
Haplolepis corrugata	Actinopterygii	Carboniferous	310	307.26	Schultze *et al.* 2021; Elliott 2014; Miller 1892
Harpacanthus fimbriatus	Chondrichthyes	Carboniferous	336.16	323.2	Lund and Grogan in Arratia *et al.* 2004; Stock 1883
Harpagofututor volsellorhinus	Chondrichthyes	Carboniferous	325.76	323.2	Lund 1982 and 1990
Harrytoombsia elegans	'Placodermi'	Devonian	382.7	379.2	Miles and Dennis 1979
Heddleichthys dalgleisiensis	Sarcopterygii	Devonian	367.76	363.33	Snitting 2009; Anderson 1859
Heimenia ensis	Sarcopterygii	Devonian	407.6	402.83	Mondéjar-Fernåndez and Clément 2012; Ørvig 1969
Heintzichthys gouldii	'Placodermi'	Devonian	363.33	358.9	Carr 1991; Newberry 1885
Helodus simplex	Chondrichthyes	Carboniferous	315.2	307	Moy-Thomas 1936; Agassiz 1838
Heteropetalus elegantulus	Chondrichthyes	Carboniferous	325.76	323.2	Lund 1977
Holonema westolli	'Placodermi'	Devonian	382.7	379.2	Miles 1971; Trinajstic 1999
Holopterygius nudus	Sarcopterygii	Devonian	382.7	379.2	Hartkopf-Fröder *et al.* 2004; Friedman and

					Coates 2006; Jessen 1973
Holoptychius jarviki	Sarcopterygii	Devonian	379.2	375.7	Cloutier and schultze 1996
Holoptychius nobilissimus	Sarcopterygii	Devonian	367.76	363.33	Dineley and Metcalf 1999; Agassiz
Holurus parki	Actinopterygii	Carboniferous	341.43	336.16	Schultze *et al.* 2021; Moy-Thomas and Dyne 1938; Traquair 1881
Homalacanthus concinnus	'Acanthodii'	Devonian	379.2	375.7	Gagnier 1996; Whiteaves 1887
Howidipterus donnae	Sarcopterygii	Devonian	382.7	379.2	Long and Clément 2009
Howittacanthus kentoni	'Acanthodii'	Devonian	382.7	379.2	Long 1986
Howqualepis rostridens	Actinopterygii	Devonian	382.7	379.2	Long 1988
Ichthyostega stensioei	Sarcopterygii	Devonian	363.33	358.9	Blom 2005; Säve-Söderbergh 1932
Incisoscutum ritchiei	'Placodermi'	Devonian	382.7	379.2	Dennis and Miles 1981
*Iniopera richardsoni**	Chondrichthyes	Carboniferous	307	298.9	Zangerl and Case 1973
Iniopteryx rushlaui	Chondrichthyes	Carboniferous	315.2	303.7	Stahl 1980; Zangerl and Case 1973
Ischnacanthus gracilis	'Acanthodii'	Devonian	419.2	410.8	Watson in Moy-Thomas and Miles 1971; Egerton 1861
*Jarvikina wenjukowi**	Sarcopterygii	Devonian	379.2	358.9	Cloutier *et al.* 2020 (supp.); Rohon 1889
Kalops diophrys	Actinopterygii	Carboniferous	325.76	323.2	Schultze *et al.* 2021; Poplin and Lund 2002
Kalops monophrys	Actinopterygii	Carboniferous	325.76	323.2	Schultze *et al.* 2021; Poplin and Lund 2002
Kathemacanthus rosulentus	Chondrichthyes	Devonian	416.4	413.6	Hanke and Wilson 2010; Gagnier and Wilson 1996
*Kentuckia deani**	Actinopterygii	Carboniferous	350.76	341.43	Rayner 1951
Koharalepis jarviki	Sarcopterygii	Devonian	386.03	384.36	Young *et al.* 1992; Cloutier *et al.* 2020 (supp.)
*Laccognathus panderi**	Sarcopterygii	Devonian	384.36	382.7	Vorobyeva 2006; Gross 1941
Lambeia pectinatus	Actinopterygii	Carboniferous	358.9	346.7	Mickle 2017
*Latocamurus coulthardi**	'Placodermi'	Devonian	382.7	379.2	Long 1988
*Latvius porosus**	Sarcopterygii	Carboniferous	358.9	346.7	Greiner 1977; Mickle 2017
Limnomis delaneyi	Actinopterygii	Devonian	363.33	358.9	Daeschler 2000
Lineagruan judithi	Actinopterygii	Carboniferous	325.76	323.2	Mickle *et al.* 2009
Lineagruan snowyi	Actinopterygii	Carboniferous	325.76	323.2	Mickle *et al.* 2009
Liujiangolepis suni	'Placodermi'	Devonian	410.8	407.6	Wang 1987
Lochmocercus aciculodontus	Sarcopterygii	Carboniferous	325.76	323.2	Lund and Lund 1984; Torino *et al.* 2021

Lodeacanthus gaujicus	‘Acanthodii’	Devonian	384.36	382.7	Upeniece 2011; Upeniece 1996
Lunaspis broilii	‘Placodermi’	Devonian	408.66	402.83	Moy-Thomas and Miles 1971; Gross 1937
Lupopsyroides macracanthus	‘Acanthodii’	Devonian	416.4	413.6	Hanke and Wilson 2004 in Arratia *et al.* 2004
Lupopsyrus pygmaeus	‘Acanthodii’	Devonian	416.4	413.6	Hanke and Davis 2012; Bernacsek and Dineley, 1977
Maghriboselache mohamezanei	Chondrichthyes	Devonian	369.2	366.2	Klug *et al.* 2023
Mandageria fairfaxi	Sarcopterygii	Devonian	367.76	363.33	Johanson and Ahlberg 1997
Mansfieldiscus sweeti	Actinopterygii	Carboniferous	358.9	350.76	Schultze *et al.* 2021; Long 1988
*Marsdenichthys longioccipitus**	Sarcopterygii	Devonian	382.7	379.2	Long 1985; Holland *et al.* 2010
Mcnamaraspis kaprios	‘Placodermi’	Devonian	382.7	379.2	Long 1995
Melanecta anneae	Actinopterygii	Carboniferous	330.9	328.33	Schultze *et al.* 2021; Coates 1998
Melanoacanthus minutus	‘Acanthodii’	Devonian	407.6	393.3	Cuumba and Schultze 2002
Mentzichthys jubbi	Actinopterygii	Carboniferous	346.7	330.9	Schultze *et al.* 2021; Gardiner 1969
Mesacanthus mitchelli	‘Acanthodii’	Devonian	410.8	407.6	Watson 1937 in Denison 1979; Egerton 1861
Mesolepis arabellae	Actinopterygii	Carboniferous	323.2	315.2	Elliott and Giles 2024
Mesolepis scalaris	Actinopterygii	Carboniferous	315.2	307	Schultze *et al.* 2021; Sallan 2013; Young 1866
Mesolepis wardi	Actinopterygii	Carboniferous	317.86	312.46	Young 1866
Mesopoma carricki	Actinopterygii	Carboniferous	330.9	328.33	Coates 1993
Mesopoma crassum	Actinopterygii	Carboniferous	341.43	336.16	Schultze *et al.* 2021; Moy-Thomas and Dyne 1938; Traquair 1913
Mesopoma politum	Actinopterygii	Carboniferous	341.43	336.16	Schultze *et al.* 2021; Traquair 1881
Mesopoma pulchellum	Actinopterygii	Carboniferous	341.43	336.16	Schultze *et al.* 2021; Traquair 1881
Microbrachius dicki	‘Placodermi’	Devonian	386.03	384.36	Long *et al.* 2014; Traquair 1888
Microhaplolepis ovoidea	Actinopterygii	Carboniferous	310	307.26	Schultze *et al.* 2021; Lowney 1980; Newberry 1856
Microhaplolepis serrata	Actinopterygii	Carboniferous	309.09	307.26	Schultze *et al.* 2021; lowney 1980; Newberry 1856

Miguashaia bureaui	Sarcopterygii	Devonian	379.2	375.7	Cloutier 1996; Schultze 1973
Milesacanthus antarctica	'Acanthodii'	Devonian	387.7	382.7	Young and Burrow 2004
Millerosteus minor	'Placodermi'	Devonian	387.7	386.03	Desmond 1974; Miller 1858
Mimipiscis bartrami	Actinopterygii	Devonian	382.7	379.2	Choo 2011
Mimipiscis toombsi	Actinopterygii	Devonian	382.7	379.2	Choo 2011
Moythomasia durgaringa	Actinopterygii	Devonian	382.7	379.2	Choo 2015; Gardiner and Bartram 1977
Moythomasia lineata	Actinopterygii	Devonian	384.36	379.2	Choo 2015
Moythomasia nitida	Actinopterygii	Devonian	384.36	379.2	Choo 2015; Gross 1953
*Ngamugawi wirngarrii**	Sarcopterygii	Devonian	382.7	379.2	Clement *et al.* 2024
Notacmon crenatus	Actinopterygii	Carboniferous	335.5	333.5	Schultze *et al.* 2021; Friedman *et al.* 2018; Agassiz 1835
Novogonatodus kasantsevae	Actinopterygii	Carboniferous	358.9	350.76	Holland et al. 2004; Long 1988
Obtusacanthus corroconis	'Acanthodii'	Devonian	416.4	413.6	Hanke and Wilson 2004 in Arratia *et al.* 2004
Onychodus jandemarrai	Sarcopterygii	Devonian	382.7	379.2	Andrews *et al.* 2006
Onycoselache traquairi	Chondrichthyes	Carboniferous	341.43	336.16	Coates and Gess 2007; Dick 1978
Orodus micropterygius	Chondrichthyes	Carboniferous	330.9	323.2	Zangerl 1981
Orthacanthus bohemicus	Chondrichthyes	Carboniferous	310	305.9	Soler-Gijon 2004 in Arratia *et al.* 2004; Fritsch 1889
Osorioichthys marginis	Actinopterygii	Devonian	372.2	367.76	Casier 1952; Taverne 1997; Schultze *et al.* 2021
Osteolepis macrolepidotus	Sarcopterygii	Devonian	389.56	387.7	Newman 2005; Agassiz 1835
Osteolepis panderi	Sarcopterygii	Devonian	387.7	386.03	Hamilton and Trewin 1994; Dineley and Metcalf 1999 (p171); Pander 1860
*Oxyosteus rostratus**	'Placodermi'	Devonian	375.7	372.2	Moy-Thomas and Miles 1971; Denison 1978; Gross 1932
Panderichthys rhombolepis	Sarcopterygii	Devonian	384.36	382.7	Boisvert *et al.* 2008 (supp.); Cloutier *et al.* 2020 (supp.); Gross 1930
Papilionichthys stahlae	Chondrichthyes	Carboniferous	325.76	323.2	Grogan and Lund, 2009
*Parabelosteus acuticeps**	'Placodermi'	Devonian	375.7	372.2	Groos 1932; Denison 1978

Parahaplolepis tuberculata	Actinopterygii	Carboniferous	310	307.26	Schultze *et al.* 2021; Westoll 1944; Newberry 1856
Paramblyterus decorus	Actinopterygii	Carboniferous	307	303.7	Dietze 2000; Heyler and Poplin 1983; Blot 1966
Paramesolepis rhombus	Actinopterygii	Carboniferous	341.43	336.16	Schultze *et al.* 2021; Moy-Thomas and Dyne 1938; Traquair 1890
Paramesolepis tuberculatus	Actinopterygii	Carboniferous	341.43	336.16	Schultze *et al.* 2021; Moy-Thomas and Dyne 1938; Traquair 1890
Paratarrasius hibbardi	Actinopterygii	Carboniferous	325.76	323.2	Lund and Poplin 2002; Lund and Melton 1982
Parayunnanolepis xitunensis	'Placodermi'	Devonian	413.6	410.8	Zhu *et al.* 2012; Zhang *et al.* 2001
Parexus recurvus	'Acanthodii'	Devonian	419.2	410.8	Watson 1937 in Denison 1979; Agassiz 1845; Burrow *et al.* 2013
Parmastega aelidae	Sarcopterygii	Devonian	372.2	367.76	Beznosov *et al.* 2019
Paucicanthus vanelsti	'Acanthodii'	Devonian	416.4	413.6	Hanke 2008
Pentlandia macroptera	Sarcopterygii	Devonian	387.3	384.99	Challands and den Blaauwen 2017; Traquair 1888
Phaneropleuron andersoni	Sarcopterygii	Devonian	367.76	363.33	Traquair 1871; Huxley 1859
Phanerorhynchus armatus	Actinopterygii	Carboniferous	312.46	310.7	Schultze *et al.* 2021; Moy-Thomas 1971; Gardiner 1967; Gill 1923
Phanerosteon mirabile	Actinopterygii	Carboniferous	341.43	336.16	Schultze *et al.* 2021; Traquair 1912; Traquair 1881
Phanerosteon ovensi	Actinopterygii	Carboniferous	358.9	344.5	White 1927; Gardiner 1985
Phoebodus saidselachus	Chondrichthyes	Devonian	367.76	363.33	Frey *et al.* 2019
*Pholidosteus friedeli**	'Placodermi'	Devonian	375.7	372.2	Jaekel 1907; Denison 1978
Phymolepis cuifengshanensis	'Placodermi'	Devonian	416.4	410.8	Wang and Zhu 2018
Pickeringius acanthophorus	Actinopterygii	Devonian	382.7	379.2	Choo *et al.* 2018
Pinnalongus saxoni	Sarcopterygii	Devonian	391.43	389.56	Newman and den Blaauwen 2007
Platysomus superbus	Actinopterygii	Carboniferous	341.43	336.16	Schultze *et al.* 2021; Moy-Thomas and Dyne 1938; Traquair 1881
Plourdosteus canadensis	'Placodermi'	Devonian	379.2	375.7	Vézina 1990; Woodward 1892

Polymerolepis whitei	Chondrichthyes	Devonian	419.2	413.6	Hanke *et al.* 2013; Karatajütè-Talimaa 1968
Polyosteorhynchus simplex	Sarcopterygii	Carboniferous	325.76	323.2	Lund and Lund 1984; Torino *et al.* 2021
Polysentor gorbairdi	Chondrichthyes	Carboniferous	311.82	309.09	Zangerl 1979
Porolepis brevis	Sarcopterygii	Devonian	410.8	407.6	Mondéjar-Fernåndez *et al.* 2021; Jarvik 1937
Proceramala montanensis	Actinopterygii	Carboniferous	325.76	323.2	Poplin and Lund 2000
Promesacanthus eppleri	'Acanthodii'	Devonian	416.4	413.6	Hanke 2008
Promexyele peyeri	Chondrichthyes	Carboniferous	310	309.9	Stahl 1980; Zangerl and Case 1973
Protogonacanthus juergeni	'Acanthodii'	Devonian	382.7	379.2	Miles 1966 in Denison 1979
Protohaplolepis scotica	Actinopterygii	Carboniferous	330.9	323.2	Lowney 1983; Schultze *et al.* 2021
*Pseudopetalichthys problematica**	'Placodermi'	Devonian	408.66	402.83	Gross 1962 in Moy-Thomas and Miles 1971; Moy-Thomas 1939
Pterichthyodes milleri	'Placodermi'	Devonian	393.3	387.7	Moloshnikov 2012; Burrow *et al.* 2020; Miller and Agassiz 1841
Ptomacanthus anglicus	'Acanthodii'	Devonian	413.6	410.8	Brazeau 2012; Miles 1973
Puertollanichthys ritchiei	Actinopterygii	Carboniferous	302.84	302.5	Schultze *et al.* 2021; Poplin and Dutheil 2005; Forey and Young 1985
Pyritocephalus lineatus	Actinopterygii	Carboniferous	310	307.26	Schultze *et al.* 2021; Westoll 1944; Newberry 1856
Pyritocephalus sculptus	Actinopterygii	Carboniferous	309.73	305.9	Schultze *et al.* 2021; Westoll 1944; Stamberg 2006; Fritsch 1875
Quebecius quebecensis	Sarcopterygii	Devonian	379.2	375.7	Cloutier and Schultze 1996; Whiteaves 1889
Rainerichthys zangerli	Chondrichthyes	Carboniferous	325.76	323.2	Grogan and Lund 2009
*Remigolepis durnalensis**	'Placodermi'	Devonian	363.33	358.9	Olive 2015
Remigolepis walkeri	'Placodermi'	Devonian	367.76	363.33	Johanson 1997
Rhabdoderma elegans	Sarcopterygii	Carboniferous	330.9	307.26	Forey 1998; Cloutier and Candilier 1995; Menning *et al.* 2001
Rhabdoderma exiguum	Sarcopterygii	Carboniferous	309.73	307	Clement *et al.* 2019; Eastman 1902
Rhadinacanthus longispinus	'Acanthodii'	Devonian	391.43	384.36	Burrow *et al.* 2016; Agassiz 1844
Rhadinichthys canobiensis	Actinopterygii	Carboniferous	341.43	336.16	Schultze *et al.* 2021; Moy-Thomas and

					Dyne 1938; Traquair 1909
Rhadinichthys fusiformis	Actinopterygii	Carboniferous	341.43	336.16	Moy-Thomas and Dyne 1938; Traquair 1881
Rhadinichthys ornatissimus	Actinopterygii	Carboniferous	346.7	330.9	Schultze *et al.* 2021; Traquair 1911; Brindley and Spinner 1989; Agassiz
Rhamphodopsis threiplandi	'Placodermi'	Devonian	389.56	387.7	Miles 1967; Watson 1934
*Rhinosteus parvulus**	'Placodermi'	Devonian	375.7	372.2	Gross 1932; Denison 1978
Rhizodopsis rankini	Sarcopterygii	Carboniferous	323.2	315.2	Elliott 2023
Rhynchodipterus elginensis	Sarcopterygii	Carboniferous	372.2	358.9	Ahlberg *et al.* 2001; Friedman 2007; Säve-Söderbergh 1937
Rolfosteus canningensis	'Placodermi'	Devonian	382.7	379.2	Dennis and Miles 1979
Romerodus orodontus	Chondrichthyes	Carboniferous	310	307.26	Zangerl 1981
Sagenodus copeanus	Sarcopterygii	Carboniferous	307	303.7	Olive *et al.* 2012; Williston 1899
Scaumenacia curta	Sarcopterygii	Devonian	379.2	375.7	Cloutier 1996; Whiteaves 1881
Sceletophorus biserialis	Actinopterygii	Carboniferous	309.73	305.9	Schultze *et al.* 2021; Stamberg 1991,2006; Fritsch 1894
Schizolepis manzanitaensis	Actinopterygii	Carboniferous	307	304.8	Schultze *et al.* 2021; Gottfried 1993; Lucas *et al.* 2011
Screbinodus ornatus	Sarcopterygii	Carboniferous	336.16	330.9	Jeffery 2012; Traquair 1878
Senekichthys hirundo	Actinopterygii	Carboniferous	350.76	346.7	Schultze *et al.* 2021; Prokofiev 2004
Serenichthys kowiensis	Sarcopterygii	Devonian	363.33	358.9	Gess and Coates 2015
Sherbonaspis hillsi	'Placodermi'	Devonian	393.3	387.7	Young and Guorui 1992; Young and Gorter 1981
Sibyrhynchus denisoni	Chondrichthyes	Carboniferous	310	307.26	Zangerl and Case 1973
*Sigaspis lepidophora**	'Placodermi'	Devonian	410.8	409.73	Goujet 1973; Schultze *et al.* 1978
Soederberghia simpsoni	Sarcopterygii	Devonian	367.76	363.33	Ahlberg *et al.* 2001
Sphaerolepis kounoviensis	Actinopterygii	Carboniferous	303.5	298.9	Schultze *et al.* 2021; Stamberg 1991; Fritsch 1877
*Squatinactis caudispinatus**	Chondrichthyes	Carboniferous	325.76	323.2	Lund and Zangerl 1974
Srianta dawsoni	Chondrichthyes	Carboniferous	325.76	323.2	Lund and Grogan 2004 in Arratia *et al.* 2004
Srianta srianta	Chondrichthyes	Carboniferous	325.76	323.2	Lund and Grogan 2004 in Arratia *et al.* 2004

Stegotrachelus finlayi	Actinopterygii	Devonian	387.7	382.7	Swartz 2009; Woodward and White, 1926
Stensioella heintzi	'Placodermi'	Devonian	408.66	402.83	Denison 1983; Broili 1933
Stethacanthus altonensis	Chondrichthyes	Devonian	363.33	298.9	Zangerl 1984; St. John and Worthen 1875
Strepheoschema fouldenensis	Actinopterygii	Carboniferous	358.9	346.7	Schultze *et al.* 2021; White 1927
Strunius walteri	Sarcopterygii	Devonian	384.36	379.2	Upeniece 1995; Jessen in Moy-Thomas 1971; Schultze and Cloutier 1996; Jessen 1966
Styracopterus fulcratus	Actinopterygii	Carboniferous	339	337.5	Schultze *et al.* 2021; Sallan 2013; Traquair 1881
Sundayichthys elegantulus	Actinopterygii	Carboniferous	346.7	330.9	Schultze *et al.* 2021; Gardiner 1969
Symmorium reniforme	Chondrichthyes	Carboniferous	309.73	307	Zangerl 2004; Cope 1893
Tanyrhinichthys mcallisteri	Actinopterygii	Carboniferous	307	304.8	Schultze *et al.* 2021; Stack *et al.* 2020; Lucas *et al.* 2011; Gottfried 1987
*Tapinosteus heintzi**	'Placodermi'	Devonian	375.7	372.2	Stensiö 1963; Denison 1978
Tarrasius problematicus	Actinopterygii	Carboniferous	341.43	336.16	Lund and Poplin 2002; Traquair 1881
Tegeolpeis clarcki	Actinopterygii	Devonian	363.33	358.9	Schultze *et al.* 2021; Miller 1892
Tetanopsyrus breviacanthias	'Acanthodii'	Devonian	416.4	413.6	Hanke *et al.* 2001
Tetanopsyrus lindoei	'Acanthodii'	Devonian	416.4	413.6	Gagnier *et al.* 1999
Thrinacoselache gracia	Chondrichthyes	Carboniferous	325.76	323.2	Grogan and Lund 2008
Thursius macrolepidotus	Sarcopterygii	Devonian	393.3	389.56	Newman and den Blaauwen 2007; Sedgwick and Murchison 1829
Tiktaalik roseae	Sarcopterygii	Devonian	382.7	379.2	Daeschler *et al.* 2006; Schubin *et al.* 2013
Tinirau clackae	Sarcopterygii	Devonian	384.36	382.7	Swartz 2012
Titanichthys clarki	'Placodermi'	Devonian	363.33	358.9	Boyle and Rayan 2017; Newberry 1887
Torosteus tuberculatus	'Placodermi'	Devonian	382.7	379.2	Gardiner and Miles, 1990
Traquairius agkistrocephalus	Chondrichthyes	Carboniferous	325.76	323.2	Lund and Grogan 1997; Carrier *et al.* 2004
Trawdenia planti	Actinopterygii	Carboniferous	317.86	312.46	Coates and Tietjen 2018
Triazeugacanthus affinis	'Acanthodii'	Devonian	379.2	375.7	Chevrinais *et al.* 2017; Whiteaves 1887

Triodus carinatus	Chondrichthyes	Carboniferous	323.2	315.2	Fritsch 1890
Triodus sessilis	Chondrichthyes	Carboniferous	307	298.9	
Tristichopterus alatus	Sarcopterygii	Devonian	386.03	384.36	Newman 2005; Egerton 1861
Tristychius arcuatus	Chondrichthyes	Carboniferous	336.16	328.83	Dick 1978; Agassiz 1837
Tubonasus lennardensis	'Placodermi'	Devonian	382.7	379.2	Dennis and Miles, 1979
Uraniacanthus curtus	'Acanthodii'	Devonian	419.2	410.8	Powrie 1870 in Newman and Davidson 2010
Utahacanthus guntheri	'Acanthodii'	Carboniferous	330.9	320.53	Schultze 1990; Ahern *et al.* 2021
Vernicomacanthus uncinatus	'Acanthodii'	Devonian	419.2	410.8	Dearden *et al.* 2021; Powrie 1864
Vernicomacanthus waynensis	'Acanthodii'	Devonian	413.6	410.8	Miles 1973 in Denison 1979
Wendyichthys dicksoni	Actinopterygii	Carboniferous	325.76	323.2	Schultze *et al.* 2021; Lund and Poplin 1997
Wendyichthys lautreci	Actinopterygii	Carboniferous	325.76	323.2	Schultze *et al.* 2021; Lund and Poplin 1997
Whiteichthys greenlandicus	Actinopterygii	Carboniferous	317.86	312.46	Schultze *et al.* 2021; Moy-Thomas 1942; Milan *et al.* 2016
Willomorichthys striatulus	Actinopterygii	Carboniferous	346.7	330.9	Gardiner 1969
Woodichthys bearsdeni	Actinopterygii	Carboniferous	330.9	328.33	Schultze *et al.* 2021; Coates 1998
Xenacanthus gaudryi	Chondrichthyes	Carboniferous	303.5	298.9	Brongniart and Sauvage, 1888
Xenacanthus parallelus	Chondrichthyes	Carboniferous	310	305.9	Soler-Gijon 2004 in Arratia *et al.* 2004; Fritsch 1890
Xichonolepis qujingensis	'Placodermi'	Devonian	387.7	382.7	Ritchie et al. 1992; P'an & Wang 1992
*Xiushanosteus mirabilis**	'Placodermi'	Silurian	436.8	433.4	Zhu *et al.* 2022
Yogoniscus gulo	Actinopterygii	Carboniferous	325.76	323.2	Lowney 1991; Schultze *et al.* 2021

*species with more than 60% of missing data removed from the analyses

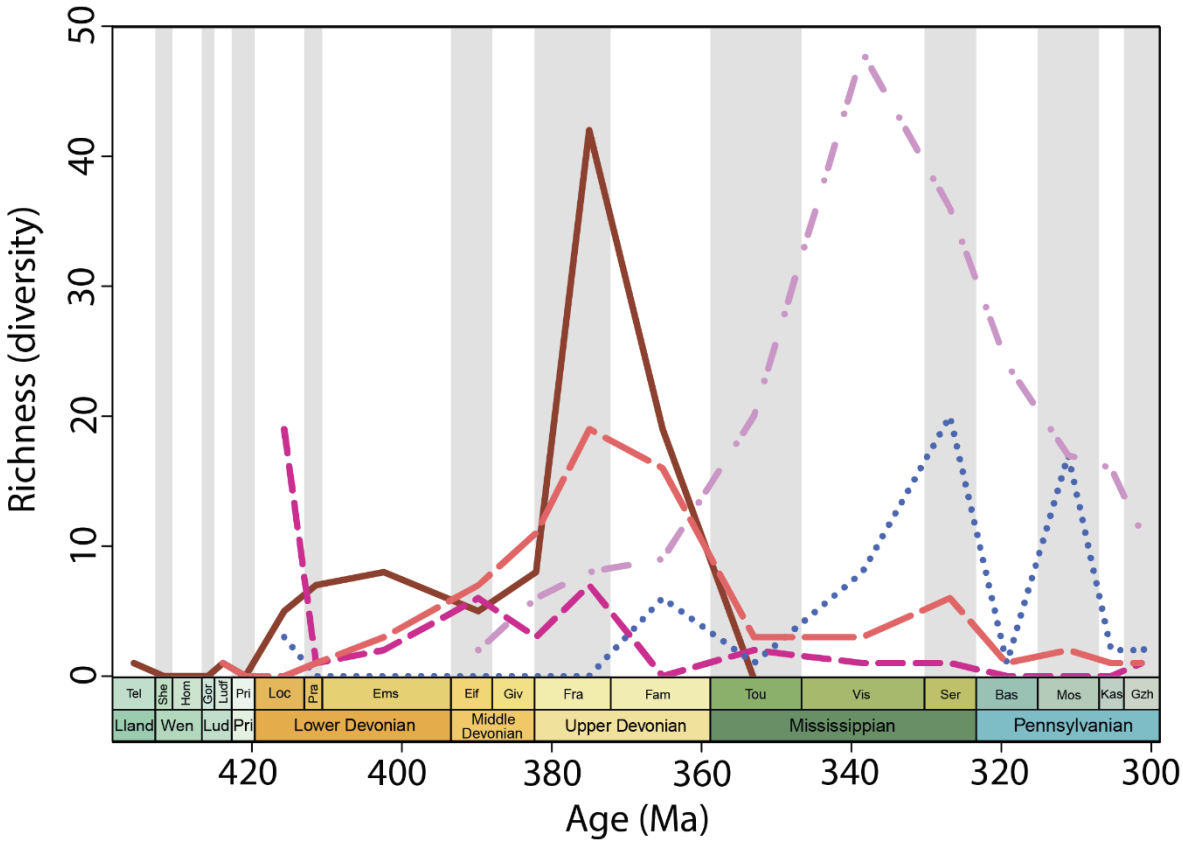


Figure S1. Taxonomic diversity (richness) through time, including 471 early gnathostome species. "Placoderms" (n=73; brown line), "acanthodians" (n=43; dark pink, short-dashed line), chondrichthyan (n=58; blue dotted line), actinopterygians (n=110; light violet dash dotted line), and sarcopterygians (n=74; red dashed line). Bas: Bashkirian; Eif: Eifelian; Ems: Emsian; Fam: Famennian; Fra: Frasnian; Giv: Givetian; Gor: Gorstian; Gzh: Gzhelian; Hom: Homerian; Kas: Kasimovian; Lland: Llandovery; Loc: Lochkovian; Lud: Ludlow; Ludf: Ludfordian; Mos: Moscovian; Pra: Pragian; Pri: Pridoli; Ser: Serpukhovian; She: Sheinwoodian; Tel: Telychian; Tou: Tournaisian; and Vis: Viséan; Wen: Wenlock.

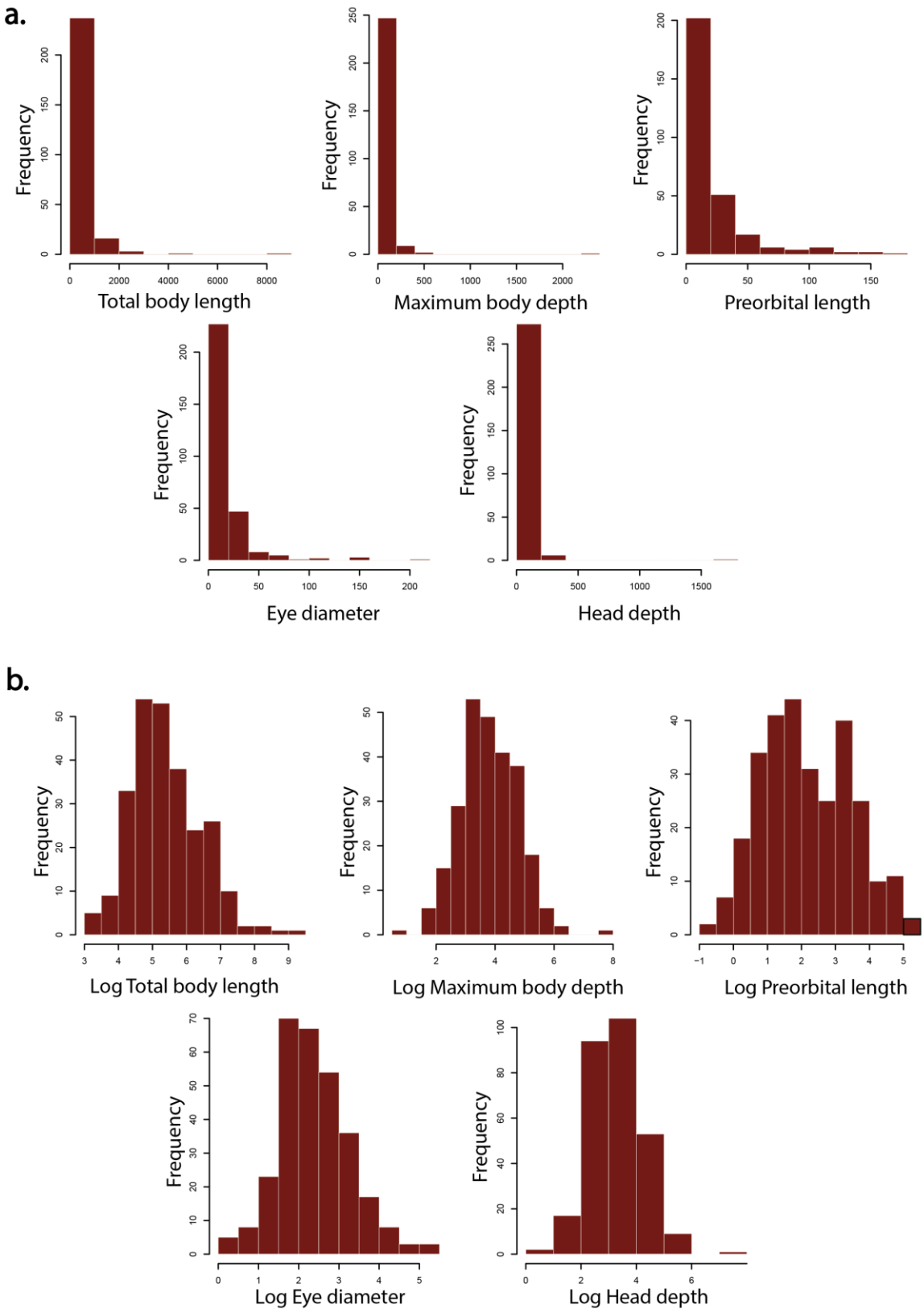

a.
Frequency
Total body length
Maximum body depth
Preorbital length
Eye diameter
Head depth
b.
Log Total body length
Log Maximum body depth
Log Preorbital length
Log Eye diameter
Log Head depth

Figure S2. Distributions of the continuous characters of (**a.**) raw data, and (**b.**) after log transformations.

C.

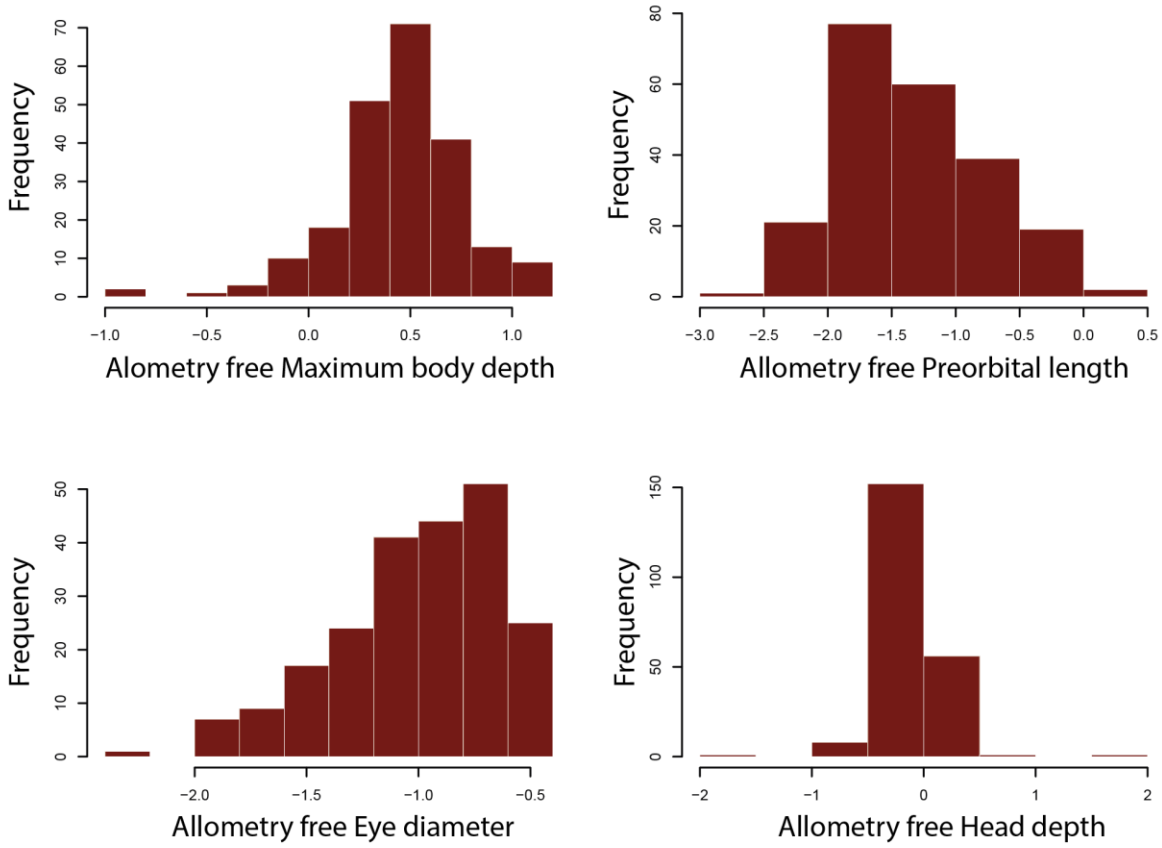
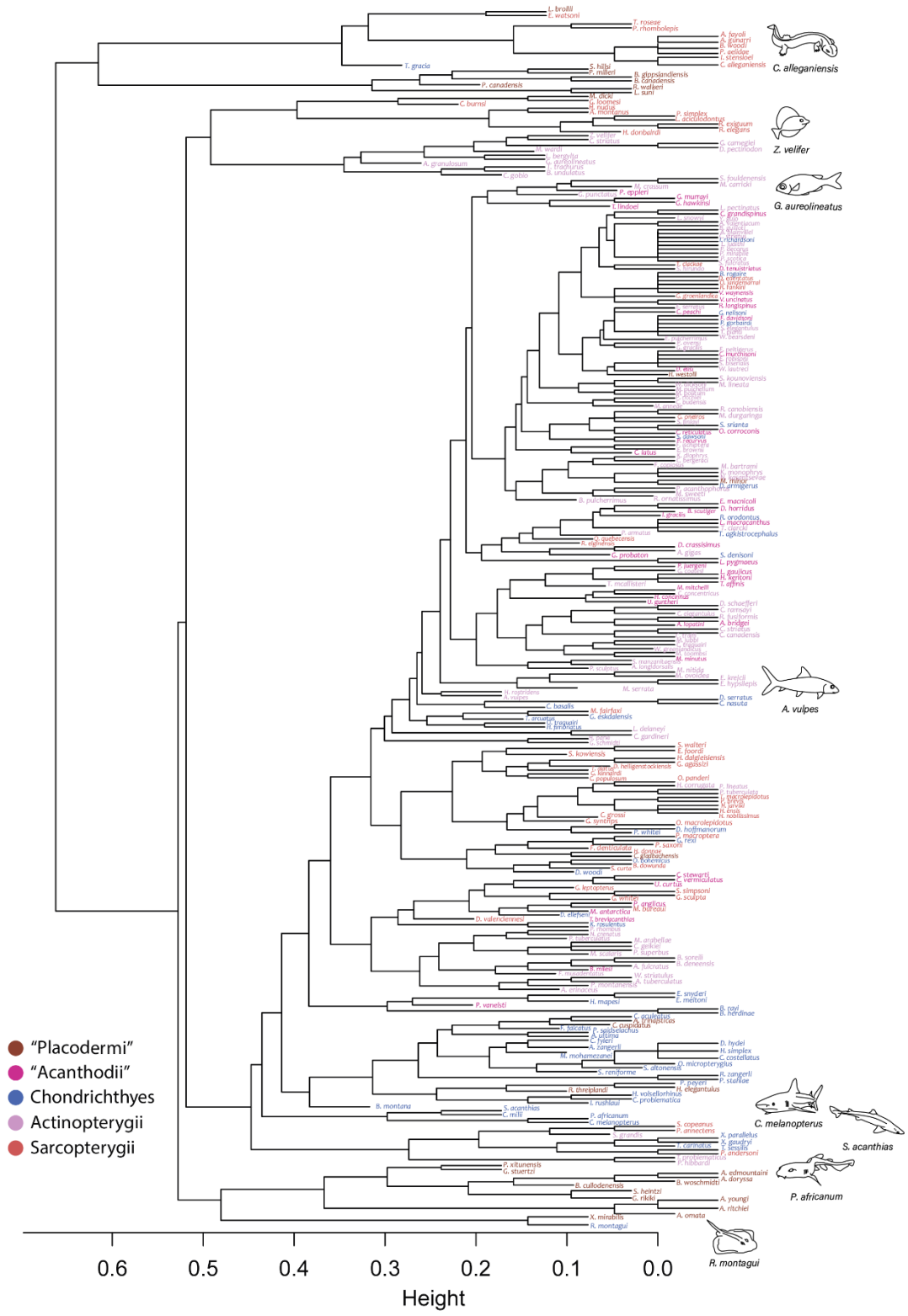


Figure S2. Distributions of the continuous characters (**c.**) after allometry correction with the Mosimann approach.



UPGMA based on Gower distances

Figure S3. Unweighted Pair Group Method with Arithmetic mean (UPGMA) based on Gower distances for the 374 species included in the ecomorphological matrix. Different colors indicated different classes of early gnathostomes. Silhouettes represent shapes of extant species included in the analysis.

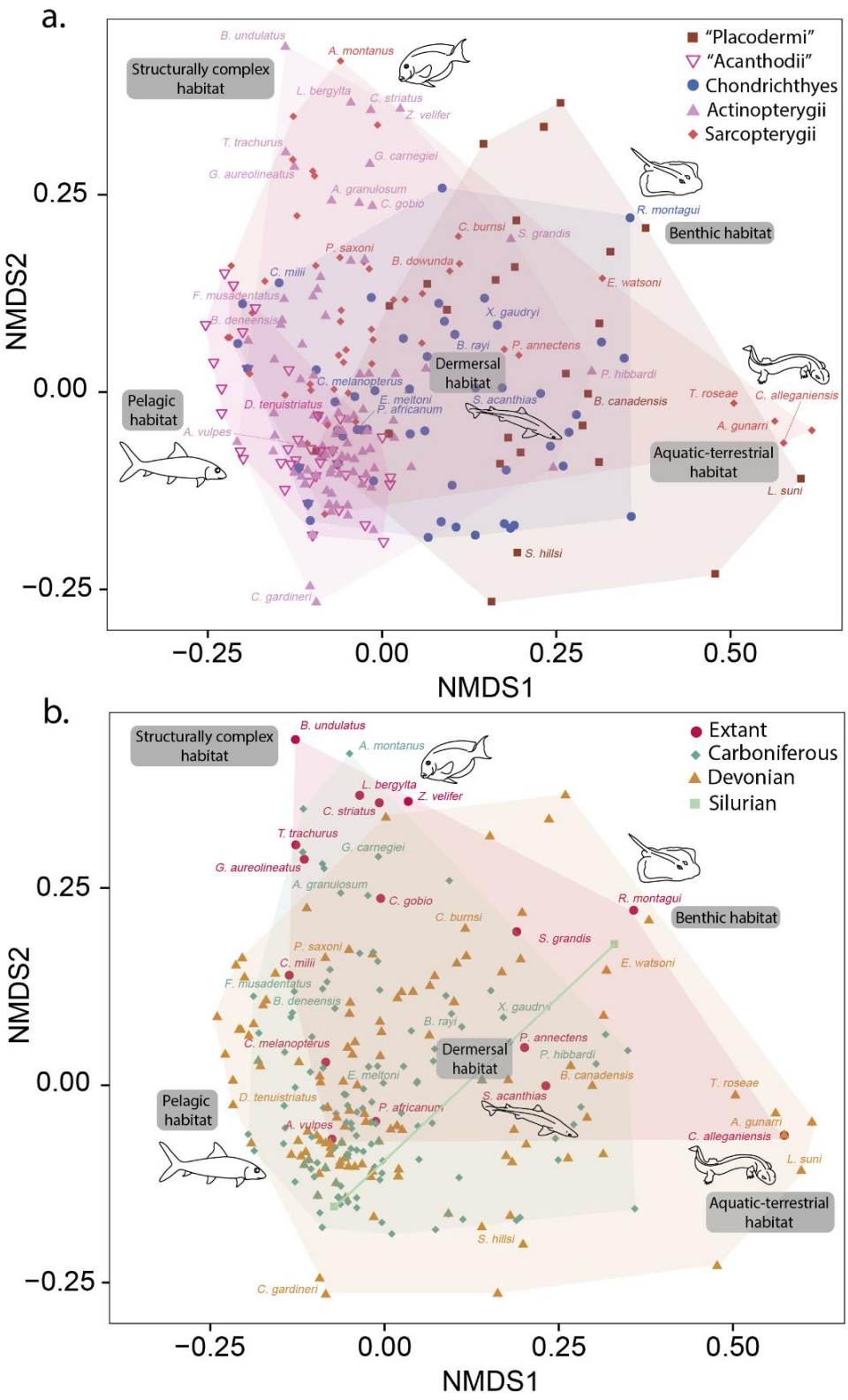

a.
"Placodermi"
"Acanthodii"
Chondrichthyes
Actinopterygii
Sarcopterygii
Structurally complex habitat
Benthic habitat
Dermersal habitat
Pelagic habitat
Aquatic-terrestrial habitat
B. undulatus
A. montanus
L. bergylta
C. striatus
Z. velifer
T. trachurus
G. carnegiei
G. aureolineatus
A. granulosum
C. gobio
R. montagui
C. burnsi
S. grandis
P. saxoni
B. dowunda
C. milii
E. watsoni
F. musadentatus
X. gaudryi
B. deneensis
B. rayi
P. annectens
P. hibbardi
C. melanopterus
E. meltoni
P. africanum
S. acanthias
B. canadensis
T. roseae
C. alleganiensis
A. gunarri
D. tenuistriatus
A. vulpes
L. suni
S. hillsi
C. gardineri
NMDS2
NMDS1
0.25
0.00
−0.25
−0.25
0.00
0.25
0.50
b.
Extant
Carboniferous
Devonian
Silurian
Structurally complex habitat
Benthic habitat
Dermersal habitat
Pelagic habitat
Aquatic-terrestrial habitat
B. undulatus
A. montanus
L. bergylta
Z. velifer
C. striatus
T. trachurus
G. carnegiei
G. aureolineatus
A. granulosum
C. gobio
R. montagui
C. burnsi
S. grandis
P. saxoni
C. milii
E. watsoni
F. musadentatus
B. deneensis
X. gaudryi
B. rayi
P. annectens
P. hibbardi
C. melanopterus
E. meltoni
B. canadensis
S. acanthias
T. roseae
D. tenuistriatus
P. africanum
A. gunarri
A. vulpes
C. alleganiensis
L. suni
S. hillsi
C. gardineri
NMDS2
NMDS1
0.25
0.00
−0.25
−0.25
0.00
0.25
0.50

Figure S4. Ecomorphospace (**a.**) per taxonomic class and (**b.**) per geological period for 325 early gnathostomes and 16 extant species based on the first two axes of the NMDS based on Gower distances (k=2, stress = 0.17). 21 discrete characters were included. Silhouettes represent the shape of extant species used to polarize the ecomorphological matrix.

Table S2. Presentation of the five aquatic habitats. A brief description and some common morphological adaptations are given for each habitat. Based on Lund *et al.* (2015) and personal observations.

Habitats	Description	Most common morphological adaptations
Benthic zone Burrowing	• High interaction with the bottom substrate • Anoxic zone • Low temperature • Relatively dark environment • High competition	• Depressiform (dorso-ventrally flattened) • Terminal/Superior mouth • Both eyes on the same side/Both eyes on the top of the head • Rounded/Truncate/Filiform caudal fin • Lobed ventro-lateral/Flattened and extended pectoral fins
Demersal zone	• Anoxic zone • Low temperature • Relatively dark environment • High competition	• Depressiform/Tadpole-shaped • Subterminal mouth • One eye one each side/Both eyes on the top of the head • Forked/Rounded caudal fin • Lobed ventro-lateral/ Flattened and extended pectoral fins
Pelagic zone	• Variation in the temperature, light absorption, and pressure depending on the depth • Currents and water masses influenced by wind and surface circulation • Indirect and minimal influence of the benthic community • Vertical migration	• Fusiform/Sagittiform/Anguiliform • Terminal mouth • One eye on each side • Lunate-shaped/heterocercal caudal fin • Lobed dorso-vertical pectoral fins • Thoracic/Jugular pelvic fins
Complex habitats (Algae forest, Mangrove swamp, Coral reef)	• High productivity • Dynamic ecosystem influenced by complex 3D physical structure • Most diverse ecosystems	• Compressiform (laterally compressed) • Terminal/Superior mouth • Emarginate/Rounded/Truncate caudal fin • Extended dorsal fin • One eye on each side • Lobed dorso-vertical pectoral fins

Aquatic-terrestrial transitional habitats	• Physical constraints associated with the difference in medium (gravity, friction)	• Elongated body • Dorso-ventrally flattened skull • Mix between fish-like features and tetrapod-like features

List of characters included in the ecomorphological matrix. The matrix includes 5 continuous characters and 27 discrete characters.

1. **Lateral body shape –** Discrete 6 levels
   0 Eel-like
   1 Deep
   2 Elongated
   3 Fusiform
   4 Compact deep-bodied
   5 Other

Description: Describes the global lateral shape of the organism.
The lateral body shape is based on the ratio of the standard length over the maximum height of the body.
If the ratio is inferior to 2, the shape is considered deep.
If the ratio is included between 2 and 3, the shape is considered compact deep-bodied.
If the ratio is included between 3 and 6, the shape is considered fusiform.
If the ratio is superior to 6, the shape is considered elongated.

2. **Transversal body shape –** Discrete 4 levels
   0 Circular
   1 Triangular
   2 Ventrally-flattened
   3 Laterally-flattened

Description: Describes the global transversal shape of the organism.

3. **Dermal plates** – Discrete 2 levels
   0 Absent
   1 Present

4. **Spines at the insertion of fins** – Discrete 2 levels
   0 Absent
   1 Present

5. **Dorsal fin** – Discrete 2 levels
   0 Absent
   1 Present

6. **Anterior dorsal fin** – Discrete 2 levels
    0 Absent
    1 Present

Description: The anterior dorsal fin is considered as a second dorsal fin. When only one dorsal fin is present, it is considered as a posterior dorsal fin.

7. **Shape of the dorsal fin**
    0 Triangular
    1 Rounded
    2 Trapezoid
    3 Fused

Description: Describes the shape of the dorsal fin web.

8. **Proportion of the dorsal fin**
    0 Small
    1 Equal
    2 Large

Description: Describes the proportion of the fin related to the ratio between the base and the height of the fin.
If the ratio is larger than 1.05 it is considered small.
If the ratio is between 0.95 and 1.05 it is considered equal.
If the ratio is between 0 and 0.95 it is considered large.

9. **Position of the posterior dorsal fin –** Discrete 3 levels
    0 Anterior to the pelvic fins insertion
    1 Between the insertion of the pelvic fins and the insertion of the anal fin
    2 Posterior to the insertion of the anal fin

Description: Describes the positioning of the posterior dorsal fin along the anteroposterior axis of the organism.

10. **Anal fin –** Discrete 2 levels
    0 Absent
    1 Present

11. **Shape of the anal fin –** Discrete 4 levels
    0 Triangular
    1 Rounded
    2 Trapezoid
    3 Fused

Description: Describes the shape of the anal fin web.

12. **Proportion of the anal fin –** Discrete 3 levels
    0 Small
    1 Equal

2 Large

Description: Describes the proportion of the fin related to the ratio between the base and the height of the fin.
If the ratio is larger than 1.05 it is considered small.
If the ratio is between 0.95 and 1.05 it is considered equal.
If the ratio is between 0 and 0.95 it is considered large.

13. **Pelvic appendages –** Discrete 2 levels
    0 Absent
    1 Present

14. **Nature of the pelvic appendages –** Discrete 2 levels
    0 Fin
    1 Limb

15. **Position of the pelvic fins –** Discrete 3 levels
    0 Abdominal
    1 Thoracic
    2 Jugular

Description: Describes the positioning of the pelvic fins along the anteroposterior axis of the organism.

16. **Nature of the pectoral appendages –** Discrete 2 levels
    0 Fin
    1 Limb

17. **Position of the pectoral appendages –** Discrete 2 levels
    0 Ventral
    1 Lateral

Description: Describes the positioning of the pectoral appendages along the dorsoventral axis of the organism.

18. **Type of caudal fin –** Discrete 4 levels
    0 Hypocercal
    1 Heterocercal
    2 Diphycercal
    3 Homocercal

Description: Characterizes the type of caudal fin.

19. **Caudal fin shape –** Discrete 5 levels
    0 Filiform
    1 Rounded
    2 Truncate
    3 Forked
    4 Forked unevently

20. **Fulcra –** Discrete 2 levels
    0 Absent
    1 Present

Description: Present or absence of modified fused scales on the body.

21. **Total body length –** Continuous

Description: Straight-line distance between the anterior tip of the snout and the end of the tail. In millimeters.

22. **Maximum body depth –** Continuous

Description: Greatest depth as measured by a straight-line distance from dorsal to ventral surfaces of the body (posterior to the operculum and anterior to the caudal peduncle). In millimeters.

23. **Lateral shape of the head –** Discrete 3 levels
    0 Triangular/beak-like
    1 Rounded
    2 Elongated

Description: Describes the global lateral shape of the head.
The lateral shape of the head is based on the ratio of the length of the head from the top of the snout to the posterior part of the opercular over the maximum height.
If the ratio is inferior to 2 it is considered rounded.
If the ratio is superior to 2 it is considered elongated.

24. **Transversal shape of the head –** Discrete 3 levels
    0 Rounded
    1 Ventrally-flattened
    2 Laterally-flattened

Description: Describes the global transversal shape of the head.

25. **Position of the eyes –** Discrete 3 levels
    0 Lateral
    1 Dorsal
    2 Anterior

26. **Preorbital length –** Continuous

Description: Straight-line distance between the anterior tip of the snout and the anterior margin of the orbit. In millimeters.

27. **Eye diameter –** Continuous

Description: Diameter of the orbit. In millimeters.

28. **Position of the mouth –** Discrete 4 levels
    0 Ventral
    1 Subterminal

2 Terminal
3 Supraterminal

29. **Teeth** – Discrete 2 levels
    0 Absent
    1 Present

30. **Shape of the teeth –** Discrete 6 levels
    0 Pointy/conical
    1 Tumid
    2 Rounded
    3 Posteriorly recurved
    4 Spiral
    5 Other

Description: Describes the shape of the teeth.

31. **Spiracle** – Discrete 2 levels
    0 Absent
    1 Present

32. **Head depth** – Continuous

Description: Vertical distance from the dorsal to the ventral surface of the head passing through the center of the eye. In millimeters.

RÉFÉRENCES BIBLIOGRAPHIQUES

Adams, D. C., et M. L. Collyer. 2016. ‘On the comparison of the strength of morphological integration across morphometric datasets’. Evolution 70 (11): 2623–31.

Adams, D. C., et M. L. Collyer. 2019. ‘Phylogenetic comparative methods and the evolution of multivariate phenotypes’. Annual Review of Ecology, Evolution, and Systematics 50: 405–25.

Ahlberg, P. E. 2018. ‘Follow the footprints and mind the gaps: a new look at the origin of tetrapods’. Earth and Environmental Science Transactions of the Royal Society of Edinburgh 109 (1–2): 115–37.

Ahlberg, P. E., et J. A. Clack. 2020. ‘The smallest known Devonian tetrapod shows unexpectedly derived features’. Royal Society Open Science 7 (4): e192117.

Albertson, R. C., J. T. Streelman, et T. D. Kocher. 2003. ‘Directional selection has shaped the oral jaws of Lake Malawi cichlid fishes’. Proceedings of the National Academy of Sciences 100 (9): 5252–57.

Algeo, T. J., S. E. Scheckler, et J. B. Maynard. 2001. ‘Effects of the middle to Late Devonian spread of vascular land plants on weathering regimes, marine biotas, and global climate’. *Dans* Plants invade the land: evolutionary and environmental perspectives, P. G. Gensel et D. Edwards (eds). New York: Columbia University Press. 213-236.

Anderson, P. S. L., M. Friedman, M. D. Brazeau, et E. J. Rayfield. 2011. ‘Initial radiation of jaws demonstrated stability despite faunal and environmental change’. Nature 476 (7359): 206–9.

Andreev, P. S., M. I. Coates, R. M. Shelton, P. R. Cooper, M. P. Smith, I. J. Sansom, et Z. Johanson. 2015. ‘Upper Ordovician chondrichthyan-like scales from North America. Palaeontology’. Philosophical Transactions of the Royal Society B 58, 691–704.

Andreev, P. S., W. Zhao, N.-Z. Wang, et al. 2020. ‘Early Silurian chondrichthyans from the Tarim Basin (Xinjiang, China)’. PLOS One 15 (2): e0228589.

Andreev P. S., I. J. Sansom, Q. Li, W. Zhao, J. Wang, C. C. Wang, L. Peng, L. Jia, T. Qiao, et M. Zhu. 2022. ‘The oldest gnathostome teeth’. Nature. 609 (7929): 964–968.

Aretz, M., C. Corradini, et J. Denayer. 2021. ‘The Devonian–Carboniferous boundary around the globe: a complement’. Palaeobiodiversity and Palaeoenvironments 101 (2): 633–62.

Armbruster, W. S. 1997. ‘Exaptations link evolution of plant–herbivore and plant–pollinator interactions: a phylogenetic inquiry’. Ecology 78 (6): 1661–72.

Arratia, G. 1996. ‘The Jurassic and the early history of teleosts’. *Dans* Mesozoic Fishes - Systematics and Paleoecology, G. Arratia et G. Viohl (eds). München: Verlag Dr. Friedrich Pfeil. 243–259.

Arratia, G., et R. Cloutier. 1996. ‘Reassessment of the morphology of *Cheirolepis canadensis* (Actinopterygii)’. *Dans* Devonian Fishes and Plants of Miguasha, Quebec, Canada, H.-P. Schultze et R. Cloutier (eds). München: Verlag Dr. Friedrich Pfeil. 165-197.

Assemat, A., S. Adnet, K. Bayez, A. Hassler, F. Arnaud-Godet, F. H. Mollen, C. Girard, J. E. Martin. 2024. ‘Exploring diet shifts and ecology in modern sharks using calcium isotopes and trace metal records of their teeth’. Journal of Fish Biology 105 (5): 1469-81.

Bambach, R. K., A. H. Knoll, et S. C. Wang. 2004. ‘Origination, extinction, and mass depletions of marine diversity’. Paleobiology 30 (4): 522–42.

Béchard, I., F. Arsenault, R. Cloutier, et J. Kerr. 2014. ‘The Devonian placoderm fish *Bothriolepis canadensis* revisited with three-dimensional digital imagery’. Palaeontologia Electronica: 1–9.

Boisvert, C. A., E. Mark-Kurik, et P. E. Ahlberg. 2008. ‘The pectoral fin of *Panderichthys* and the origin of digits’. Nature 456 (7222): 636–38.

Bookstein, F. L. 1991. Morphometric Tools for Landmark Data: Geometry and Biology. Cambridge: Cambridge University Press. 456p.

Boyle, J., et M. J. Ryan. 2017. ‘New information on *Titanichthys* (Placodermi, Arthrodira) from the Cleveland Shale (Upper Devonian) of Ohio, USA’. Journal of Paleontology 91 (2): 318–36.

Brandon, R. N. 2005. ‘Evolutionary Modules: Conceptual Analyses and Empirical Hypotheses’. *Dans* Modularity: understanding the development and evolution of natural complex systems, W. Callebaut et D. Rasskin-Gutman (eds). Cambridge, Mass: MIT Press. 51-60.

Brazeau, M. D. 2009. ‘The braincase and jaws of a Devonian “acanthodian” and modern gnathostome origins’. Nature 457 (7227): 305–8.

Brazeau, M. D., et M. Friedman. 2014. ‘The characters of Paleozoic jawed vertebrates’. Zoological Journal of the Linnean Society 170 (4): 779–821.

Brazeau, M. D., et M. Friedman. 2015. ‘The origin and early phylogenetic history of jawed vertebrates’. Nature 520 (7548): 490–97.

Brazeau, M. D., S. Giles, R. P. Dearden, et al. 2020. ‘Endochondral bone in an Early Devonian “placoderm” from Mongolia’. Nature Ecology & Evolution 4 (11): 1477–84.

Brazeau, M. D., et V. de Winter. 2015. ‘The hyoid arch and braincase anatomy of *Acanthodes* support chondrichthyan affinity of “acanthodians”’. Proceedings of the Royal Society B: Biological Sciences 282 (1821): e20152210.

Bridge, T. C. L., A. H. Baird, J. M. Pandolfi, M. J. McWilliam, et M. K. Zapalski. 2022. ‘Functional consequences of Palaeozoic reef collapse’. Scientific Reports 12 (1): e1386.

Buatois, L. A., N. S. Davies, M. R. Gibling, et al. 2022. ‘The invasion of the land in deep time: integrating Paleozoic records of paleobiology, ichnology, sedimentology, and geomorphology’. Integrative and Comparative Biology 62 (2): 297–331.

Buggisch, W. 1991. ‘The global Frasnian–Famennian “Kellwasser Event”’. Geologische Rundschau 80 (1): 49–72.

Burrow, C. J., M. J. Newman, R. G. Davidson, et J. L. den Blaauwen. 2013. ‘Redescription of *Parexus recurvus*, an Early Devonian acanthodian from the Midland Valley of Scotland’. Alcheringa 37 (3): 392–414.

Burrow, C. J., et D. Rudkin. 2014. ‘Oldest near-complete acanthodian: the first vertebrate from the Silurian Bertie Formation Konservat-Lagerstätte, Ontario’. PLOS One 9 (8): e104171.

Carmichael, S. K., J. A. Waters, P. Königshof, T. J. Suttner, et E. Kido. 2019. ‘Paleogeography and paleoenvironments of the Late Devonian Kellwasser Event: a review of its sedimentological and geochemical expression’. Global and Planetary Change 183: e102984.

Carr, R. 2010. ‘Paleoecology of *Dunkleosteus terrelli* (Placodermi: Arthrodira)’. Kirtlandia Cleveland, Ohio, Cleveland Museum of Natural History 57: 36–45.

Carr, R. K. 1994. ‘Placoderm systematics, diversity, and evolution’. Ph.D. thesis. University of Michigan.

Chen, B., X. Ma, B. J. W. Mills, et al. 2021. ‘Devonian paleoclimate and its drivers: a reassessment based on a new conodont $\delta^{18}O$ record from South China’. Earth-Science Reviews 222: e103814.

Cheverud, J. M. 1982. ‘Phenotypic, genetic, and environmental morphological integration in the cranium’. Evolution 36 (3): 499–516.

Cheverud, J. M. 1996. ‘Developmental integration and the evolution of pleiotropy’. American Zoologist 36 (1): 44–50.

Chevrinais, M., C. Jacquet, et R. Cloutier. 2017. ‘Early establishment of vertebrate trophic interactions: food web structure in Middle to Late Devonian fish assemblages with exceptional fossilization’. Bulletin of Geosciences 31: 491–510.

Chevrinais, M., E. Balan, et R. Cloutier. 2016. ‘New insights in the ontogeny and taphonomy of the Devonian acanthodian *Triazeugacanthus affinis* from the Miguasha Fossil-Lagerstätte, eastern Canada’. Minerals 6 (1): e1.

Chevrinais, M., J.-Y. Sire, et R. Cloutier. 2017. ‘From body scale ontogeny to species ontogeny: histological and morphological assessment of the Late Devonian acanthodian *Triazeugacanthus affinis* from Miguasha, Canada’. PLOS One 12 (4): e0174655.

Choo, B., J. Lu, S. Giles, K. Trinajstic, et J. A. Long. 2019. ‘A new actinopterygian from the Late Devonian Gogo Formation, Western Australia’. Papers in Palaeontology 5 (2): 343–63.

Ciampaglio, C. N., M. Kemp, et D. W. McShea. 2001. ‘Detecting changes in morphospace occupation patterns in the fossil record: characterization and analysis of measures of disparity’. Paleobiology 27 (4): 695–715.

Clement, A. M., R. Cloutier, M. S. Y. Lee, et al. 2024. ‘A Late Devonian coelacanth reconfigures actinistian phylogeny, disparity, and evolutionary dynamics’. Nature Communications 15 (1): e7529.

Cloutier, R. 1997. ‘Morphologie et variations du toit crânien du dipneuste *Scaumenacia curta* (Whiteaves) (Sarcopterygii), du Dévonien Supérieur du Québec’. Geodiversitas 19: 59–105.

Cloutier, R. 2010. ‘The fossil record of fish ontogenies: insights into developmental patterns and processes’. Seminars in Cell & Developmental Biology 21 (4): 400–413.

Cloutier, R., et P. Ahlberg. 1996. ‘Morphology, characters, and the interrelationships of basal sarcopterygians’. *Dans* Interrelationships of fishes, M. L. J. Stiassny, L. R. Parenti et G.D. Johnson (eds). Academic Press. 445–480.

Cloutier, R., et G. Arratia. 2004. ‘Early diversification of actinopterygians’. *Dans* Recent advances in the origin and early radiation of vertebrates, G. Arratia, M. V. H. Wilson et R. Cloutier (eds). München: Verlag Dr. Friedrich Pfeil. 217–270.

Cloutier, R., J.-N. Proust, et B. Tessier. 2011. ‘The Miguasha Fossil-Fish-Lagerstätte: a consequence of the Devonian land–sea interactions’. Palaeobiodiversity and Palaeoenvironments 91: 293–323.

Cloutier, R., A. M. Clement, M. S. Y. Lee, et al. 2020. ‘*Elpistostege* and the origin of the vertebrate hand’. Nature 579 (7800): 549–54.

Coates, M. I. 2009. ‘Beyond the age of fishes’. Nature 458 (7237): 413–14.

Coatham, S. J., J. Vinther, E. J. Rayfield, et C. Klug. 2020. ‘Was the Devonian placoderm *Titanichthys* a suspension feeder?’ Royal Society Open Science 7 (5): e200272.

Copper, P. 1994. ‘Ancient reef ecosystem expansion and collapse’. Coral Reefs 13 (1): 3–11.

Copper, P. 2002. ‘Reef development at the Frasnian/Famennian mass extinction boundary’. Palaeogeography, Palaeoclimatology, Palaeoecology 181 (1): 27–65.

Cooper, J. A., J. R. Hutchinson, D. C. Bernvi, G. Cliff, R. P. Wilson, M. L. Dicken, J. Menzel, S. Wroe, J. Pirlo, et C. Pimiento. 2022. ‘The extinct shark Otodus megalodon was a transoceanic superpredator: Inferences from 3D modelling’. Science Advances 8: eabm9424.

Cui, X., Q. Qu, P. S. Andreev, Q. Li, H. Mai, et M. Zhu. 2021. ‘Modeling scale morphogenesis in a Devonian chondrichthyan and scale growth patterns in crown gnathostomes’. Journal of Vertebrate Paleontology 41 (2): e1930018.

Czekanski-Moir, J. E., et R. J. Rundell. 2019. ‘The ecology of nonecological speciation and nonadaptive radiations’. Trends in Ecology & Evolution 34 (5): 400–415.

Davis, S. P., J. A. Finarelli, et M. I. Coates. 2012. ‘*Acanthodes* and shark-like conditions in the last common ancestor of modern gnathostomes’. Nature 486 (7402): 247–50.

Dearden, R. P., J. L. den Blaauwen, I. J. Sansom, et al. 2021. ‘A revision of *Vernicomacanthus miles* with comments on the characters of stem-group chondrichthyans’. Papers in Palaeontology 7 (4): 1949–76.

Dellinger, A. S., S. Artuso, S. Pamperl, et al. 2019. ‘Modularity increases rate of floral evolution and adaptive success for functionally specialized pollination systems’. Communications Biology 2 (1): e453.

Denison, R. 1978. Handbook of Paleoichthyology 2 – Placodermi. H.-P. Schultze (eds). Stuttgart, New York: Gustav Fischer Verlag. 94p.

Denison, R. 1979. Handbook of Paleoichthyology 5 – Acanthodii. H.-P. Schultze (eds). München: Gustav Fischer Verlag. 117p.

Dupret, V., S. Sanchez, D. Goujet, P. Tafforeau, et P. E. Ahlberg. 2014. ‘A primitive placoderm sheds light on the origin of the jawed vertebrate face’. Nature 507 (7493): 500–503.

Esteve-Altava, B. 2017. ‘Challenges in identifying and interpreting organizational modules in morphology’. Journal of Morphology 278 (7): 960–74.

Evans, K. M., O. Larouche, S.-J. Watson, S. Farina, M. L. Habegger, et M. Friedman. 2021. ‘Integration drives rapid phenotypic evolution in flatfishes’. Proceedings of the National Academy of Sciences 118 (18): e2101330118.

Flannery-Sutherland, J. T., S. Henderson, S. A. Fasey, et S. Giles. 2025. ‘Diversification dynamics of the Palaeozoic actinopterygian radiation’. Proceedings of the Royal Society B: Biological Sciences 292 (2061): e20252732.

Foote, M. 1993. ‘Discordance and concordance between morphological and taxonomic diversity’. Paleobiology 19 (2): 185–204.

Foote, M. 1997. ‘The evolution of morphological diversity’. Annual Review of Ecology, Evolution, and Systematics 28: 129–52.

Foote, M. 1999. ‘Morphological diversity in the evolutionary radiation of Paleozoic and post-Paleozoic crinoids’. Paleobiology 25 (S2): 1–115.

Frey, L., M. Coates, M. Ginter, et al. 2019. ‘The early elasmobranch *Phoebodus*: phylogenetic relationships, ecomorphology and a new time-scale for shark evolution’. Proceedings of the Royal Society B: Biological Sciences 286 (1912): e20191336.

Fricke, R. 2021. ‘Eschmeyer’s catalog of fishes: genera/species by family/subfamily’. Electronic version.

Friedman, M. 2015. ‘The early evolution of ray-finned fishes’. Palaeontology 58 (2): 213–28.

Gartner, S. M., O. Larouche, K. M. Evans, et M. W. Westneat. 2023. ‘Evolutionary patterns of modularity in the linkage systems of the skull in wrasses and parrotfishes’. Integrative Organismal Biology 5 (1): obad035.

Gavrilets, S., et J. B. Losos. 2009. ‘Adaptive radiation: contrasting theory with data’. Science 323 (5915): 732–37.

George, D., et A. Blieck. 2011. ‘Rise of the earliest tetrapods: an Early Devonian origin from marine environment’. PLOS One 6 (7): e22136.

Gerber, S. 2019. ‘Use and misuse of discrete character data for morphospace and disparity analyses’. Palaeontology 62 (2): 305–19.

Golonka, J., et D. Ford. 2000. ‘Pangean (Late Carboniferous–Middle Jurassic) paleoenvironment and lithofacies’. Palaeogeography, Palaeoclimatology, Palaeoecology 161 (1): 1–34.

Golonka, J. 2020. ‘Late Devonian paleogeography in the framework of global plate tectonics’. Global and Planetary Change 186: e103129.

Goujet, D., et G. Young. 2004. ‘Placoderm anatomy and phylogeny: new insights’. *Dans* Recent Advances in the Origin and Early Radiation of Vertebrates, G. Arratia, M. V. H. Wilson et R. Cloutier (eds). München: Verlag Dr. Friedrich Pfeil. 109–126.

Gould, S. J. 1991. ‘The disparity of the Burgess Shale arthropod fauna and the limits of cladistic analysis: why we must strive to quantify morphospace’. Paleobiology 17 (4): 411–23.

Grant, P. R., et B. R. Grant. 2020. How and why species multiply: the radiation of Darwin’s finches. Princeton University Press. 272p.

Griffin, B. W., J. N. Keating, P. S. Milla Carmona, Z. Johanson, R. P. Dearden, P. C. J. Donoghue, et E. J. Rayfield. 2026. ‘Evolution of chondrichthyan jaw morphology, from ecological generalists to specialists’. Paleobiology 52: 131–144.

Grogan, E. D., et R. Lund. 2002. ‘The geological and biological environment of the Bear Gulch Limestone (Mississippian of Montana, USA) and a model for its deposition’. Geodiversitas 24 (2) : 295-315

Guillam, E., et M.-B. Forel. 2025. ‘Marine ostracod faunas through the Late Devonian extinction events. Part II: the Hangenberg Event’. Earth-Science Reviews 268: e105172.

Harmon, L. J., J. A. Schulte, A. Larson, et J. B. Losos. 2003. ‘Tempo and mode of evolutionary radiation in iguanian lizards’. Science 301 (5635): 961–64.

Hartenfels, S. 2024. ‘Upper Devonian to Mississippian global environmental change and impact on conodonts’. Palaeobiodiversity and Palaeoenvironments 104 (3): 629–82.

Henderson, S., E. M. Dunne, et S. Giles. 2022. ‘Sampling biases obscure the early diversification of the largest living vertebrate group’. Proceedings of the Royal Society B: Biological Sciences 289 (1985): e20220916.

Hetherington, A. J., E. Sherratt, M. Ruta, M. Wilkinson, B. Deline, et P. C. J. Donoghue. 2015. ‘Do cladistic and morphometric data capture common patterns of morphological disparity?’ Palaeontology 58 (3): 393–99.

Hopkins, M. J., et S. Gerber. 2017. ‘Morphological disparity’. *Dans* Evolutionary developmental biology, L. Nuño de la Rosa et G. B. Müller (eds). Springer, Cham. 1-12.

Jobbins, M., M. Rücklin, M. R. Sánchez Villagra, et al. 2024. ‘Extreme lower jaw elongation in a placoderm reflects high disparity and modularity in early vertebrate evolution’. Royal Society Open Science 11 (1): e231747.

Johanson, Z. 2002. ‘Vascularization of the Osteostracan and Antiarch (Placodermi) pectoral fin: similarities, and implications for placoderm relationships’. Lethaia 35 (2): 169–86.

Johanson, Z., C. Underwood, et M. Richter. 2019. Evolution and Development of Fishes. Cambridge University Press. 280p.

Jurina, A. L. 2024. ‘First Devonian forests on Earth: appearance, composition of plants, types of forest ecosystems, and their distribution’. Moscow University Geology Bulletin 79 (2): 233–42.

Kaiser, S. I., M. Aretz, et R. T. Becker. 2016. ‘The global Hangenberg crisis (Devonian–Carboniferous transition): review of a first-order mass extinction’. *Dans* Devonian climate, sea level and evolutionary events, R. T. Becker, P. Königshof, et C. E. Brett (eds). Geological Society of London. 387-437.

Kershaw, S., et J. Jeon. 2024. ‘Stromatoporoids and extinctions: a review’. Earth-Science Reviews 252: e104721.

Kidwell, S. M., et S. M. Holland. 2002. ‘The quality of the fossil record: implications for evolutionary analyses’. Annual Review of Ecology, Evolution, and Systematics 33: 561–88.

King, B., T. Qiao, M. S. Y. Lee, M. Zhu, et J. A. Long. 2017. ‘Bayesian morphological clock methods resurrect placoderm monophyly and reveal rapid early evolution in jawed vertebrates’. Systematic Biology 66 (4): 499–516.

King, B., et M. Rücklin. 2020. ‘A Bayesian approach to dynamic homology of morphological characters and the ancestral phenotype of jawed vertebrates’. eLife 9: e62374.

Kirschner, M., et J. Gerhart. 1998. ‘Evolvability’. Proceedings of the National Academy of Sciences 95 (15): 8420–27.

Klingenberg, C. P. 2008. ‘Morphological integration and developmental modularity’. Annual Review of Ecology, Evolution, and Systematics 39: 115–32.

Klingenberg, C. P. 2010. ‘Evolution and development of shape: integrating quantitative approaches’. Nature Reviews Genetics 11 (9): 623–35.

Klingenberg, C. P. 2014. ‘Studying morphological integration and modularity at multiple levels: concepts and analysis’. Philosophical Transactions of the Royal Society B: Biological Sciences 369 (1649): e20130249.

Klug, C., Kröger, B., Kiessling, W., Mullins, et al. (2010). The Devonian nekton revolution. Lethaia, 43(4), 465-477.

Königshof, P., et W. Buggisch. 2005. ‘The Late Devonian Kellwasser crisis: evidence from conodonts and stable isotopes’. Facies 51 (1): 1–15.

Lakin, J. A., J. E. A. Marshall, I. Troth, et I. C. Harding. 2016. ‘Greenhouse to icehouse: a biostratigraphic review of latest Devonian–Mississippian glaciations and their global effects’. *Dans* Devonian climate, sea level and evolutionary events, R. T. Becker, P. Königshof, et C. E. Brett (eds). Geological Society of London. 439-64.

Lamsdell, J. C., et S. T. F. Littlewood. 2023. ‘The evolution of disparity in ancient arthropods’. Biological Reviews 98 (2): 456–72.

Larouche, O., M. L. Zelditch, et R. Cloutier. 2017. ‘Fin modules: an evolutionary perspective on appendage disparity in basal vertebrates’. BMC Biology 15 (1): e32.

Larouche, O., M. L. Zelditch, et R. Cloutier. 2019. ‘A critical appraisal of appendage disparity and homology in fishes’. Fish and Fisheries 20 (6): 1138–75.

Larouche, O., K. M. Evans, et M. Friedman. 2020. ‘Integration and modularity in fishes: implications for morphological evolution’. Proceedings of the Royal Society B: Biological Sciences 287 (1927): e20201685.

Lee, M. S. Y., et A. F. Hugall. 2006. ‘Phylogeny of placental mammals and the origin of the placental trophoblast’. Nature 444 (7121): 851–56.

Lee, M. S. Y., et al. 2015. ‘Morphological support for fossil calibrations of molecular phylogenies’. Nature 522 (7557): 92–95.

Lehmann, O. E. R., M. D. Ezcurra, R. J. Butler, et G. T. Lloyd. 2019. ‘Biases with the generalized Euclidean distance measure in disparity analyses with high levels of missing data’. Palaeontology 62 (5): 837–49.

Lieberman, B. S. 2012. ‘Adaptive radiations in the context of macroevolutionary theory: a paleontological perspective’. Evolutionary Biology 39 (2): 181–91

Liu, Y., et al. 2023. ‘Early vertebrate evolution and the origin of jaws revisited’. Nature Ecology & Evolution 7 (3): 345–56.

Lloyd, G. T. 2016. ‘Estimating morphological diversity and tempo with discrete character-taxon matrices: implementation, challenges, progress, and future directions’. Biological Journal of the Linnean Society 118 (1): 131–51.

Long, J. A. 1986. ‘New Ischnacanthid acanthodians from the Early Devonian of Australia, with comments on acanthodian interrelationships’. Zoological Journal of the Linnean Society 87 (4): 321–39.

Long, J. A. 1995. The Rise of Fishes: 500 Million Years of Evolution. Johns Hopkins University Press. 304p.

Long, J. A. 2011. ‘The rise of fishes: evolution and diversification’. Annual Review of Earth and Planetary Sciences 39: 1–26.

Long, J. A., B. Choo, et A. Clement. 2019. ‘The evolution of fishes through geological time’. *Dans* Evolution and development of fishes, C. Underwood, M. Richter, et Z. Johanson (eds). Cambridge University Press. 3-29.

Long, J. A., K. Trinajstic, et Zerina Johanson. 2009. ‘Devonian arthrodire embryos and the origin of internal fertilization in vertebrates’. Nature 457 (7233): 1124–27.

Long, J. A., K. Trinajstic, G. C. Young, et T. Senden. 2008. ‘Live birth in the Devonian period’. Nature 453 (7195): 650–52.

López-Arbarello, A. 2012. ‘Phylogenetic interrelationships of Ginglymodian fishes (Actinopterygii)’. Zoological Journal of the Linnean Society 166 (3): 496–536.

Losos, J. B. 2010. ‘Adaptive Radiation, Ecological Opportunity, and Evolutionary Determinism’. The American Naturalists 175 (6): 623-639.

Losos, J. B. 2011. ‘Convergence, adaptation, and constraint’. Evolution 65 (7): 1827–40.

Lu, J., et M. Zhu. 2009. ‘An onychodont fish (Osteichthyes, Sarcopterygii) from the Early Devonian of China, and the evolution of the Onychodontiformes’. Proceedings of the Royal Society B: Biological Sciences 277 (1679): 293–99.

Lu, M., Y. Sun, G. Duan, T. Ikejiri, N. Liu, Q. Luo, D. Lv, R. Carroll, and Y. Lu. 2026. ‘Massive wildfires followed oceanic anoxic events during the Late Devonian Frasnian- Famennian mass extinction’. Science Advances 12: eady4534.

Lund, R., E. Greenfest-Allen, et E. D. Grogan. 2012. ‘Habitat and diversity of the Bear Gulch fish: life in a 318 million year old marine Mississippian Bay’. Palaeogeography, Palaeoclimatology, Palaeoecology 342: 1–16.

Lund, R., E. Greenfest-Allen, et Eileen D. Grogan. 2015. ‘Ecomorphology of the Mississippian fishes of the Bear Gulch Limestone (Heath Formation, Montana, USA)’. Environmental Biology of Fishes 98 (2): 739–54.

Ma, K., L. Hinnov, Z. Wang, et al. 2025. ‘Astronomically forced dynamics of Late Devonian (Famennian) sea level and biotic recovery in western Junggar, northwest China’. Global and Planetary Change 245: e104677.

MacArthur, R. H., et E. O. Wilson. 1967. The Theory of Island Biogeography. Princeton University Press. 224p.

Maguire, K. C., et A. L. Stigall. 2008. ‘Paleobiogeography of Miocene equinae of North America: a phylogenetic biogeographic analysis of the relative roles of climate, vicariance, and dispersal’. Palaeogeography, Palaeoclimatology, Palaeoecology 267 (3): 175–84.

Mahler, D. L., T. Ingram, L. J. Revell, et J. B. Losos. 2013. ‘Exceptional convergence on the macroevolutionary landscape in island lizard radiations’. Science 341 (6143): 292–95.

Mann, A., D. Rudkin, D. C. Evans, et M. Laflamme. 2017. ‘A large Onychodontiform (Osteichthyes: Sarcopterygii) apex predator from the Eifelian-aged Dundee Formation of Ontario, Canada’. Canadian Journal of Earth Sciences 54 (3): 233–41.

Mannolini, F., et al. 2024. ‘Devonian fish assemblages and environmental drivers of disparity’. Palaeogeography, Palaeoclimatology, Palaeoecology 630: e111849.

Marques, D. A., F. C. Jones, F. Di Palma, D. M. Kingsley, et T. E. Reimchen. 2018. ‘Experimental evidence for rapid genomic adaptation to a new niche in an adaptive radiation’. Nature Ecology & Evolution 2 (7): 1128–38.

Märss, T., et P.-Y. Gagnier. 2001. ‘A new chondrichthyan from the Wenlock, Lower Silurian, of Baillie-Hamilton Island, the Canadian Arctic’. Journal of Vertebrate Paleontology 21 (4): 693–701.

Marx, F. G., et M. Uhen. 2010. ‘Climate, critters, and cetaceans: Cenozoic evolutionary patterns’. Proceedings of the Royal Society B: Biological Sciences 277 (1680): 165–73.

Matsubayashi, K. W., et R. Yamaguchi. 2022. ‘The speciation view: disentangling multiple causes of adaptive and non-adaptive radiation in terms of speciation’. Population Ecology 64 (2): 95–107.

Maynard Smith, J. 1983. ‘The genetics of stasis and punctuations’. Annual Review of Genetics 17: 11–25.

McCormack, J., M. L. Griffiths, S. L. Kim, et al. 2022. ‘Trophic position of *Otodus megalodon* and great white sharks through time revealed by zinc isotopes’. Nature Communications 13, e2980.

McGhee, G. R. 1999. Theoretical Morphology: the Concept and its Applications. Columbia University Press. 316p.

McMillan, W. O., et S. R. Palumbi. 1995. ‘Concordant evolutionary patterns among Indo-West Pacific butterflyfishes’. Proceedings of the Royal Society B: Biological Sciences 260 (1358): 229–36.

McGhee, G. R. 2007. The Geometry of Evolution: Adaptive Landscapes and Theoretical Morphospaces. Cambridge University Press. 212p.

McShea, D. W. 1996. ‘Metazoan complexity and evolution: is there a trend?’ Evolution 50 (2): 477–92.

McShea, D. W., et B. Simpson. 2011. ‘The evolution of morphological complexity’. Proceedings of the National Academy of Sciences 108 (Supplement 3): 201–6.

Meyer, A. 1993. ‘Phylogenetic relationships and evolutionary processes in East African cichlid fishes’. Trends in Ecology & Evolution 8 (8): 272–76.

Miller, R. F., R. Cloutier, et S. Turner. 2003. ‘The oldest articulated chondrichthyan from the Early Devonian period’. Nature 425 (6957): 501–4.

Mitteroecker, P., et P. Gunz. 2009. ‘Advances in geometric morphometrics’. Evolutionary Biology 36 (2): 235–47.

Mitteroecker, P., et al. 2013. ‘Modularity and integration in cranial morphology’. Evolution 67 (12): 3541–52.

Mitteroecker, P., et al. 2016. ‘Evolutionary developmental biology and the evolution of morphological integration’. Philosophical Transactions of the Royal Society B: Biological Sciences 371 (1699): e20150467.

Moczek, A. P. 2008. ‘On the origins of novelty in development and evolution’. BioEssays 30 (5): 431–47.

Mondéjar-Fernández, J., M. Friedman, et S. Giles. 2021. ‘Redescription of the cranial skeleton of the Early Devonian (Emsian) sarcopterygian *Durialepis edentatus* Otto (Dipnomorpha, porolepiforms)’. Papers in Palaeontology 7 (2): 789–806.

Monteiro, L. R., et A. F. Reis. 1999. ‘Principles of morphometric analysis in biology’. Revista Brasileira de Zoologia 16 (2): 287–93.

Morris, J. L., J. R. Leake, W. E. Stein, et al. 2015. ‘Investigating Devonian trees as geo-engineers of past climates: linking palaeosols to palaeobotany and experimental geobiology’. Palaeontology 58 (5): 787–801.

Muller, G. B., et S. A. Newman. 2003. Origination of Organismal Form: Beyond the Gene in Developmental and Evolutionary Biology. MIT Press. 342p.

Nabavizadeh, A. 2016. ‘Development and evolution of the skull in early tetrapods’. Journal of Anatomy 229 (2): 196–210.

Nardelli, M. J., et al. 2019. ‘Morphological disparity in early vertebrates’. Paleobiology 45 (3): 400–16.

Near, T. J., et M. F. Benard. 2004. ‘Rapid allopatric speciation in logperch darters (Percidae: Percina)’. Evolution 58 (12): 2798–808.

Neige, P. 2003. ‘Le débat macroévolutif : apports de la disparité morphologique’. Comptes Rendus Palevol 2 (6): 423–33.

Nelson, J. S., T. C. Grande, et M. V. H. Wilson. 2016. Fishes of the World. John Wiley & Sons. 752p.

Newman, M. J., J. den Blaauwen, C. Burrow, et R. Jones. 2021. 'Earliest vertebrate embryos in the fossil record (Middle Devonian, Givetian)'. Palaeontology 64 (1): 21–30.

Nudds, J., et P. Selden. 2008. 'Fossil–Lagerstätten'. Geology Today 24 (4): 153–58.

Oliver, W. A. 1990. 'Extinctions and migrations of Devonian rugose corals in the eastern Americas realm'. Lethaia 23 (2): 167–78.

Olson, E. C. 1961. Fauna of the Edgewood Group. University of Chicago Press. 154p.

Owen, R. 1840. On the Archetype and Homologies of the Vertebrate Skeleton. London: John Van Voorst. 203p.

Paradis, E. 2012. Analysis of Phylogenetics and Evolution with R. Springer. 211p.

Paradis, E., J. Claude, et K. Strimmer. 2004. 'APE: analyses of phylogenetics and evolution in R language'. Bioinformatics 20 (2): 289–90.

Patterson, C. 1977. 'Cartilage bones, dermal bones and membrane bones, or the exoskeleton versus the endoskeleton'. *Dans* Problems in Vertebrate Evolution, S. M. Andrews et al. (eds). Linnean Society of London. Academic Press. 77-122.

Patterson, C. 1982. 'Morphological characters and homology'. Dans Problems of Phylogenetic Reconstruction, K. A. Joysey et A. E. Friday (eds). Academic Press. 21-74.

Pavlinov, I. Y. 2021. 'Modularity in evolution: concepts and approaches'. Biology Bulletin Reviews 11 (5): 455–72.

Pinto, G., D. L. Mahler, L. Harmon, et J. Losos. 2008. 'Testing the island effect in adaptive radiation: rates and patterns of morphological diversification in Caribbean and mainland *Anolis* lizards'. Proceedings. Biological Sciences 275: 2749–57.

Plotnick, R. E. 1999. 'Habitat engineering by animals and plants'. Paleobiology 25 (S2): 96–104.

Polly, P. D. 2008. 'Developmental dynamics and evolutionary disparity'. Evolutionary Biology 35: 1–13.

Pradel, A., et al. 2010. 'Skull morphology and braincase anatomy of a Carboniferous shark'. Nature 463 (7277): 364–67.

Prum, R. O., et al. 2015. 'A comprehensive phylogeny of birds (Aves) using targeted next-generation DNA sequencing'. Nature 526 (7574): 569–73.

Purnell, M. A., P. J. C. Donoghue, S. E. Gabbott, M. E. McNamara, D. J. E. Murdock, et R. S. Sansom. 2018. 'Experimental analysis of soft-tissue fossilization: opening the black box'. Palaeontology 61 (3): 317–23.

Qiao, T., B. King, J. A. Long, P. E. Ahlberg, et M. Zhu. 2016. 'Early gnathostome phylogeny revisited: multiple method consensus'. PLOS One 11 (9): e0163157.

Qu, Q.-M., M. Zhu, et W.-J. Zhao. 2010. 'Silurian atmospheric O_2 changes and the early radiation of gnathostomes'. Palaeoworld 19 (1): 146–59.

Rabosky, D. L., et I. J. Lovette. 2008. 'Explosive evolutionary radiations: decreasing speciation or increasing extinction through time?' Evolution 62 (8): 1866–75.

Raup, D. M. 1966. 'Geometric analysis of shell coiling: general problems'. Journal of Paleontology 40 (5): 1178–90.

Reif, W.-E. 1985. 'Functions of scales and evolution of scale morphology in fishes'. Zoological Journal of the Linnean Society 84 (1): 1–23.

Revell, L. J. 2012. 'phytools: an R package for phylogenetic comparative biology (and other things)'. Methods in Ecology and Evolution 3 (2): 217–23.

Richards K. R., J. E. Sherwin, T. R. Smithson, R. F. Bennion, S. J. Davies, J. E. A. Marshall, et J. A. Clack. 2017. 'Diverse and durophagous: early Carboniferous chondrichthyans from the Scottish borders'. Earth and Environmental Science Transactions of the Royal Society of Edinburgh 108: 67–87.

Ritchie, A. 1987. 'Placoderms from the Devonian of Australia'. Memoirs of the Queensland Museum 25 (1): 1–60.

Rohlf, F. J., et L. F. Marcus. 1993. 'A revolution in morphometrics'. Trends in Ecology & Evolution 8 (4): 129–32.

Rolfe, W. D. I., et J. D. Lawson. 1997. 'Early terrestrial arthropods: a fragmentary record'. Philosophical Transactions of the Royal Society of London. B, Biological Sciences 309 (1138): 207–18.

Rücklin, M., B. King, J. A. Cunningham, Z. Johanson, F. Marone, et P. C. J. Donoghue. 2021. 'Acanthodian dental development and the origin of gnathostome dentitions'. Nature Ecology & Evolution 5 (7): 919–26.

Rundell, R. J. 2011. 'Snails on an evolutionary tree: Gulick, speciation, and isolation'. American Malacological Bulletin 29 (1/2): 145–57.

Rundell, R. J., et T. D. Price. 2009. 'Adaptive radiation, nonadaptive radiation, ecological speciation and nonecological speciation'. Trends in Ecology & Evolution 24 (7): 394–99.

Ruta, M., et M. I. Coates. 2007. ‘Dates, nodes and character conflict: addressing the lissamphibian origin problem’. Journal of Systematic Palaeontology 5 (1): 61–80.

Ruta, M., M. I. Coates, et D. L. J. Quicke. 2003. ‘Early tetrapod relationships revisited’. Biological Reviews 78 (2): 251–345.

Sallan, L. Cole, et M. I. Coates. 2010. ‘End-Devonian extinction and a bottleneck in the early evolution of modern jawed vertebrates’. Proceedings of the National Academy of Sciences 107 (22): 10131–35.

Sallan, L. Cole, et M. I. Coates. 2013. ‘Styracopterid (Actinopterygii) ontogeny and the multiple origins of post-Hangenberg deep-bodied fishes’. Zoological Journal of the Linnean Society 169 (1): 156–99.

Sallan, L. C., et M. Friedman. 2012. ‘Heads or tails: staged diversification in vertebrate evolutionary radiations’. Proceedings of the Royal Society B: Biological Sciences 279 (1748): 2025–32.

Sandberg, C. A., R. C. Gutschick, J. G. Johnson, F. G. Poole, et W. J. Sando. 1982. ‘Middle Devonian to Late Mississippian Geologic History of the Overthrust Belt Region, Western United States’. Annales - Société Géologique de Belgique 2 : 691-719.

Sansom, I. J., N. S. Davies, M. I. Coates, R. S. Nicoll, et A. Ritchie. 2012. ‘Chondrichthyan-like scales from the Middle Ordovician of Australia’. Palaeontology 55 (2): 243–47.

Sansom, I. J., et M. I. Coates. 2013. ‘The origin of jaws and teeth’. Biological Reviews 88 (3): 1–15.

Savoy, Lauret E. 1992. ‘Environmental record of Devonian-Mississippian carbonate and low-oxygen facies transitions, southernmost Canadian Rocky Mountains and northwesternmost Montana’. GSA Bulletin 104 (11): 1412–32.

Schaeffer, J., M. J. Benton, E. J. Rayfield, et T. L. Stubbs. 2020. ‘Morphological disparity in theropod jaws: comparing discrete characters and geometric morphometrics’. Palaeontology 63 (2): 283–99.

Schluter, D. 2000. The Ecology of Adaptive Radiation. Oxford: Oxford University Press. 288p.

Schnetz L., E. M. Dunne, I. Feichtinger, R. J. Butler, M. I. Coates, et I. J. Sansom. 2024. ‘Rise and diversification of chondrichthyans in the Paleozoic’. Paleobiology 50: 271–284.

Schopf, J. M. 1975. ‘Modes of fossil preservation’. Review of Palaeobotany and Palynology 20 (1): 27–53.

Schultze, H.-P., et R. Cloutier. 1996. Devonian Fishes and Plants of Miguasha, Québec, Canada. München: Verlag Dr. Friedrich Pfeil. 374p.

Seilacher, A., W.-E.. Reif, et F. Westphal. 1985. ‘Sedimentological, ecological and temporal patterns of fossil Lagerstätten’. Philosophical Transactions of the Royal Society of London. B, Biological Sciences 311 (1148): 5–24.

Sepkoski, J. J. 1981. ‘A factor analytic description of the Phanerozoic marine fossil record’. Paleobiology 7 (1): 36–53.

Sepkoski, J. J. 1997. ‘Biodiversity: past, present, and future’. Journal of Paleontology 71 (4): 533–39.

Sepkoski, J. J. 2002. ‘A compendium of fossil marine animal genera’. Bulletins of American Paleontology 363: 1-560.

Sereno, P. C. 1999. ‘The evolution of dinosaurs’. Science 284 (5423): 2137–47.

Shubin, N. H., E. B. Daeschler, et F. A. Jenkins Jr. 2006. ‘The pectoral fin of *Tiktaalik roseae* and the origin of the tetrapod limb’. Nature 440 (7085): 764–71.

Simões, M., L. Breitkreuz, M. Alvarado, et al. 2016. ‘The evolving theory of evolutionary radiations’. Trends in Ecology & Evolution 31 (1): 27–34.

Simpson, G. G. 1944. Tempo and Mode in Evolution. Columbia University Press. 237p.

Simpson, G. G. 1953. The Major Features of Evolution. Columbia University Press. 434p.

Smith, M. M., et I. J. Sansom. 1997. ‘Exoskeletal micro-remains of an Ordovician fish from the Harding Sandstone of Colorado’. Palaeontology 40, 645–658.

Soulebeau, A., X. Aubriot, M. Gaudeul, et al. 2015. ‘The hypothesis of adaptive radiation in evolutionary biology: hard facts about a hazy concept’. Organisms Diversity & Evolution 15 (4): 747–61.

Spiegelhalter, D. J., N. G. Best, B. P. Carlin, et A. Van Der Linde. 2002. ‘Bayesian measures of model complexity and fit’. Journal of the Royal Statistical Society: Series B (Statistical Methodology) 64 (4): 583–639.

Stampfli, G. M. 2013. ‘Response to the comments on “The formation of Pangea” by D.A. Ruban’. Tectonophysics 608: 1445–47.

Starck, J. M., J. R. Stewart, et D. G. Blackburn. 2021. ‘Phylogeny and evolutionary history of the amniote egg’. Journal of Morphology 282 (7): 1080–122.

Stayton, C. T. 2015. ‘The definition, recognition, and interpretation of evolutionary novelty’. Biological Reviews 90 (2): 535–56.

Stayton, C. T. 2019. ‘What does convergence mean? The interpretation of convergence in evolutionary biology’. Evolution 73 (3): 577–89.

Stebbins, G. L. 1974. Flowering Plants: Evolution Above the Species Level. Harvard University Press. 480p.

Stewart, T. A., J. B. Lemberg, A. Daly, E. B. Daeschler, et N. H. Shubin. 2022. ‘A new elpistostegalian from the Late Devonian of the Canadian Arctic’. Nature 608: 563–568

Stiefel, K. M. 2021. ‘Evolutionary trends in large pelagic filter-feeders’. Historical Biology 33 (9): 1477–88.

Stockley, P., et al. 2005. ‘Evolution of the vertebrate head’. Nature 434 (7030): 941–44.

Swofford, D. L. 2003. PAUP: Phylogenetic Analysis Using Parsimony (and Other Methods). Sinauer Associates.

Thompson, D. W. 1917. On Growth and Form. Cambridge University Press. 793p.

Tillyard, R. J. 1918. The Biology of Dragonflies (Odonata). Cambridge University Press. 396p.

Turner, C. F., et al. 2020. ‘Morphological disparity and ecological diversification in early vertebrates’. Evolution 74 (6): 1234–50.

Uyeda, J. C., D. S. Caetano, et M. W. Pennell. 2015. ‘Comparative analysis of principal components can be misleading’. Systematic Biology 64 (4): 677–89.

Valentine, J. W. 2004. On the Origin of Phyla. University of Chicago Press. 614p.

Van Valen, L. 1973. ‘A new evolutionary law’. Evolutionary Theory 1: 1–30.

Wagner, G. P. 1996. ‘Homologues, natural kinds and the evolution of modularity’. American Zoologist 36 (1): 36–43.

Wagner, G. P., et L. Altenberg. 1996. ‘Complex adaptations and the evolution of evolvability’. Evolution 50 (3): 967–76.

Wagner, G. P., M. Pavlicev, et J. M. Cheverud. 2007. ‘The road to modularity’. Nature Reviews Genetics 8 (12): 921–31.

Wagner, P. J., et M. Foote. 2001. ‘On the relationship between the completeness of the fossil record and the number of taxa’. Paleobiology 27 (2): 324–38.

Wainwright, P. C., et S. M. Reilly. 1994. Ecological Morphology: Integrative Organismal Biology. University of Chicago Press. 376p.

Wang, J. 1991. ‘The Antiarchi from Early Silurian of Hunan’. Vertebrata Palasiatica 29 (3): 240–44.

Watson, D. M. S. 1937. ‘The acanthodian fishes’. Philosophical Transactions of the Royal Society of London. 228: 49–146.

Webster, M., et H. D. Sheets. 2010. ‘A practical introduction to landmark-based geometric morphometrics’. The Paleontological Society Papers 16: 163–88.

Wellenreuther, M., et R. A. Sánchez-Guillén. 2016. ‘Nonadaptive radiation in damselflies’. Evolutionary Applications 9 (1): 103–18.

Westneat, M. W. 2004. ‘Evolution of levers and linkages in the feeding mechanisms of fishes’. Integrative and Comparative Biology 44 (5): 378–89.

Whitenack, L. B., et P. J. Motta. 2010. ‘Performance of Shark Teeth During Puncture and Draw: Implications for the Mechanics of Cutting’. Biological Journal of the Linnean Society 100 (2): 271–286.

Wills, M. A., D. E. G. Briggs, et R. A. Fortey. 1994. ‘Disparity as an evolutionary index: a comparison of Cambrian and Recent arthropods’. Paleobiology 20 (2): 172–95.

Wills, M. A. 2001. ‘Morphological disparity: a primer’. *Dans* Fossils, Phylogeny, and Form, J. M. Adrain, G. D. Edgecombe et B. S. Lieberman (eds). Yale University Press. 55-144.

Wilson, E. O. 1992. The Diversity of Life. Cambridge: Harvard University Press. 432p.

Wiens, J. J. 2005. ‘Can incomplete taxa resolve the tree of life?’ Systematic Biology 54 (5): 705–18.

Wilkinson, M. 1995. ‘A comparison of two methods of character construction’. Cladistics 11 (3): 241–57.

Winther, R. G. 2001. ‘Varieties of modules: kinds, levels, origins, and behaviors’. Journal of Experimental Zoology 291 (2): 116–29.

Yao, L., M. Aretz, P. B. Wignall, J. Chen, D. Vachard, Y. Qi, S. Shen, X. Wang. 2020. ‘The longest delay: re-emergence of coral reef ecosystems after the Late Devonian extinctions’. Earth-Science Review 203: 103060.

Yoder, J. B., E. Clancey, S. Des Roches, et al. 2010. ‘Ecological opportunity and the origin of adaptive radiations’. Journal of Evolutionary Biology 23 (8): 1581–96.

Young, G. C. 2008. ‘The relationships of antiarchs (Devonian placoderm fishes)—evidence supporting placoderm monophyly’. Journal of Vertebrate Paleontology 28 (3): 626–36.

Young, G. C. 2010. ‘Placoderms (armored fish): dominant vertebrates of the Devonian period’. Annual Review of Earth and Planetary Sciences 38: 523–50.

Zelditch, M. L., D. L. Swiderski, H. D. Sheets, et W. L. Fink. 2004. Geometric Morphometrics for Biologists: A Primer. Elsevier Academic Press. 489p.

Zelditch, M. L., et al. 2012. ‘Morphological integration in evolutionary biology’. Annual Review of Ecology, Evolution, and Systematics 43: 347–69.

Zelditch, M. L., et al. 2017. ‘Evolutionary biology and modularity’. Biological Journal of the Linnean Society 122 (2): 185–97.

Zhang, G.-R., S.-T. Wang, J.-Q. Wang, N.-Z. Wang, et M. Zhu. 2010. ‘A basal Antiarch (Placoderm Fish) from the Silurian of Qujing, Yunnan, China’. Palaeoworld 19 (1): 129–35.

Zhao, W.-J., et M. Zhu. 2007. ‘Diversification and faunal shift of Siluro-Devonian vertebrates of China’. Geological Journal 42 (3–4): 351–69.

Zhu, M., P. E. Ahlberg, Z. Pan, et al. 2016. ‘A Silurian maxillate Placoderm illuminates jaw evolution’. Science 354 (6310): 334–36.

Zhu, M., et P. Janvier. 1996. ‘A small antiarch, *Minicrania lirouyii* gen. et sp. nov., from the Early Devonian of Qujing, Yunnan (China), with remarks on Antiarch phylogeny’. Journal of Vertebrate Paleontology 16 (1): 1–15.

Zhu, M., X. Yu, P. E. Ahlberg, et al. 2013. ‘A Silurian placoderm with osteichthyan-like marginal jaw bones’. Nature 502 (7470): 188–93.

Zhu, M, X. Yu, B. Choo, et al. 2012. ‘Fossil fishes from China provide first evidence of dermal pelvic girdles in osteichthyans’. PLOS One 7 (4): e35103.

Zhu, M., W. Zhao, L. Jia, J. Lu, T. Qiao, et Q. Qu. 2009. ‘The oldest articulated osteichthyan reveals mosaic gnathostome characters’. Nature 458 (7237): 469–74.

Zhu, Y.-A., S. Giles, G. C. Young, et al. 2021. ‘Endocast and bony labyrinth of a Devonian “placoderm” challenges stem gnathostome phylogeny’. Current Biology 31 (5): 1112–1118.e4.